UNIVERSIDAD COMPLUTENSE DE MADRID

FACULTAD DE CIENCIAS MATEMÁTICAS

Departamento de Estadística e Investigación Operativa I

STOCHASTIC MODELS FOR TWO INTERACTIG POPULATIONS : COMPETITION AND HOST-PARASITE INTERACTIONS

MEMORIA PARA OPTAR AL GRADO DE DOCTOR
PRESENTADA POR

Martín López García

Bajo la dirección del doctor

Antonio Gómez-Corral

MADRID, 2013

Complutense University of Madrid
Faculty of Mathematics
Department of Statistics and Operations Research I

Stochastic Models for Two Interacting Populations: Competition and Host-parasite Interactions

PhD Thesis

Martín López García

Supervised by
Dr. Antonio Gómez-Corral

Madrid, May 2013

ANTONIO GÓMEZ CORRAL, Profesor Titular del Departamento de Estadística e Investigación Operativa I de la Universidad Complutense de Madrid

CERTIFICA:

Que la presente memoria titulada

Stochastic Models for Two Interacting Populations: Competition and Host-parasite Interactions

(Modelos Estocásticos para la Interacción de Dos Poblaciones: Competición e Interacción Receptor-parásito)

ha sido realizada bajo mi dirección por D. Martín López García, Licenciado en Matemáticas por la Universidad de Alicante, y constituye su Tesis para optar al Grado de Doctor en Ciencias Matemáticas.

Y para que conste, en cumplimiento de la legislación vigente y a los efectos oportunos, firmo la presente en Madrid a nueve de mayo de dos mil trece.

Fdo. Dr. Antonio Gómez Corral

Agradecimientos

En primer lugar, debo expresar mi agradecimiento al Ministerio de Economía y Competitividad, que por medio de la beca FPI de referencia **BES-2009-018747** y los proyectos **MTM2008-01121** y **MTM2011-23864** ha financiado esta investigación. Sin dicha financiación, esta tesis doctoral no habría sido posible. También quiero dar las gracias a todas aquellas personas que no están en estas líneas posiblemente por mi propensión infinita al despiste, pero que me han ayudado en todos estos años de trabajo.

Es de justicia agradecer, en primer lugar, a mi director, Antonio, todo el trabajo realizado para que esta tesis viera la luz. Agradecer no sólo su guía y consejos, sus esfuerzos por introducirme en el mundo de la investigación, sino también las innumerables horas dedicadas al preciso chequeo de cada una de mis notas que pasaban por sus manos. Sé que fue una gran labor de paciencia. También a Jesús quiero agradecer su apoyo durante estos años, y su confianza en mí al incorporarme a los proyectos de investigación. Además, quiero agradecer en estas líneas a Antonis y Poly su hospitalidad en mi visita a Atenas, consiguiendo que me sintiera casi como en casa estando tan lejos del hogar.

No deben faltar en estas líneas mis compañeros y amigos Grego, Tingo, Rosa, Karina, Paola y Javi, a los que quiero agradecer su apoyo en todo momento tanto en la facultad como fuera de ella. Porque sin los desayunos, comidas y reuniones nocturnas mi estancia en Madrid no hubiera sido la misma. Los que venimos de fuera de Madrid a realizar la tesis, sabemos que este apoyo es inestimable en muchas ocasiones. Por ello, gracias.

Gracias a mi familia, a mis hermanos Pilar, Ana y José, y a mis padres. Gracias por haber conseguido que no notase tanto su ausencia al venir a Madrid para realizar la tesis. Porque estando en la distancia puedes notar su apoyo, su preocupación al hablar por teléfono si les cuentas algún problema, si les dices que estás enfermo. Porque puedes visitarles un fin de semana y sentirte como si nunca te hubieras ido.

Y por último pero no menos importante, sino al contrario, le doy las gracias a Nuria, porque sin ella mis días en Madrid hubieran sido muy diferentes, o no hubieran sido. Porque ante cualquier problema ella estaba allí para sacarme una sonrisa, para ofrecerme una solución, para enseñarme el lado positivo o, simplemente, para mostrarme de nuevo el camino. *Gracias.*

Madrid,
Mayo 2013 *Martín López García*

A mis padres y mis hermanos,
y a Nuria, sin cuyo apoyo este
trabajo no habría sido posible

Contents

List of Figures

List of Tables

Glossary of Notation

$\mathbb{N}$: Set of natural numbers $\{1, 2, \dots\}$.

$\mathbb{N}_0$: $\mathbb{N} \cup \{0\}$.

$\delta_{i,j}$: Kronecker's delta, which is equal to 1 if $i = j$, and to 0 otherwise.

$[x]$: Integer part of a number x.

$\mathbf{A}, \mathbf{B}, \dots$: Matrices.

$\mathbf{A} = \text{diag}(a_1, a_2, \dots)$: Diagonal matrix with elements $a_1, a_2, \dots$ in the diagonal, and zeros elsewhere.

$\mathbf{A} = \text{diag}(\mathbf{B}_1, \mathbf{B}_2, \dots)$: Diagonal matrix by blocks, that is, blocks $\mathbf{B}_1, \mathbf{B}_2, \dots$ in the diagonal, and zeros elsewhere.

$\mathbf{A}^T$: Transpose of the matrix $\mathbf{A}$.

$\mathbf{I}_p$: Identity matrix of order p.

$\mathbf{I}$: Identity matrix of infinite dimension.

$\mathbf{0}_{p \times q}$: Null matrix of dimension $p \times q$.

$\mathbf{0}$: Null matrix with an infinite number of rows and/or columns.

$\exp\{\mathbf{V}\}$: Matrix exponential of the square matrix $\mathbf{V}$, that is, $\exp\{\mathbf{V}\} = \sum_{k=0}^{\infty} \mathbf{V}^k/k!$.

$\mathbf{A} \otimes \mathbf{B}$: Kronecker product of two matrices $\mathbf{A}$ and $\mathbf{B}$.

$\mathbf{A} \oplus \mathbf{B}$: Kronecker sum of two matrices $\mathbf{A}$ and $\mathbf{B}$.

$[\mathbf{U}, \mathbf{V}]$: Commutator of the matrices $\mathbf{U}$ and $\mathbf{V}$, that is, $\mathbf{UV} - \mathbf{VU}$.

$||\mathbf{W}||_S$: Spectral norm of the matrix $\mathbf{W}$.

$||\mathbf{W}||_\infty$: Maximum row sum norm of the matrix $\mathbf{W}$.

$\mu_\infty(\mathbf{W})$: Logarithmic norm of the matrix $\mathbf{W}$.

$\mathbf{a}, \boldsymbol{\pi}, \ldots$: Vectors.

$\mathbf{e}_p$: Column vector of order p of 1s.

$\mathbf{e}_p(j)$: Column vector of order p such that all entries equal 0, except for the jth one which is equal to 1.

$\mathbf{e}$: Column vector of infinite dimension of 1s.

$\mathbf{e}(j)$: Column vector of infinite dimension such that all entries equal 0, except for the jth one which is equal to 1.

$\mathbf{0}_p$: Column vector of order p of 0s.

$||\mathbf{w}||_2$: Euclidean norm of the vector $\mathbf{w}$.

$c.v.(\cdot)$: Coefficient of variation of a random variable.

$\rho(\cdot, \cdot)$: Coefficient of correlation between two random variables.

BSDE: Block-structured state-dependent methodology.

CTMC: Continuous-time Markov chain.

DTMC: Discrete-time Markov chain.

MAP: Markovian arrival process.

MMAP: Marked Markovian arrival process.

PH: Phase-type distribution or random variable.

QBD: Quasi-birth-death process.

1

Introduction

1.1 Interspecific relations for biological and ecological models

Competition processes, as discussed by Iglehart [67] and Reuter [105], have been frequently used in biology to describe the dynamics of population models involving some kind of interaction among various species. Several types of interaction arise in a variety of biological problems, such as competition between two species for a limited food supply, or a prey-predator relationship in which one of the species becomes part of the food supply of the second one.

In the paper by Reuter [105], a general stochastic framework is first presented in order to reflect interaction between two species in terms of a time-homogeneous continuous-time Markov chain (CTMC) $\mathcal{X} = \{X(t) = (M(t), N(t)) : t \geq 0\}$ on the state space $\mathcal{S} = \mathbb{N}_0 \times \mathbb{N}_0$, where $M(t)$ and $N(t)$ are defined as the population sizes of two species coexisting in an ecosystem. Possible jumps of $\mathcal{X}$ from a given state (m, n) are only permitted to adjacent states (m', n') with $(m', n') \in \{(m+1, n), (m, n+1), (m-1, n), (m, n-1), (m-1, n+1), (m+1, n-1)\}$, and they are governed by the following transitions rates:

$$q_{(m,n),(m',n')} = \begin{cases} a_{(m,n)}, & \text{if } (m', n') = (m+1, n), \\ b_{(m,n)}, & \text{if } (m', n') = (m, n+1), \\ c_{(m,n)}, & \text{if } (m', n') = (m-1, n), \\ d_{(m,n)}, & \text{if } (m', n') = (m, n-1), \\ e_{(m,n)}, & \text{if } (m', n') = (m-1, n+1), \\ f_{(m,n)}, & \text{if } (m', n') = (m+1, n-1), \end{cases} \tag{1.1}$$

where $a_{(m,n)}$, $b_{(m,n)}$, $c_{(m,n)}$, $d_{(m,n)}$, $e_{(m,n)}$ and $f_{(m,n)}$ are non-negative constants for $(m,n) \in \mathcal{S}$. Moreover, the condition

$$\begin{aligned} q_{(m,n)} &= -q_{(m,n),(m,n)} \\ &= a_{(m,n)} + b_{(m,n)} + c_{(m,n)} + d_{(m,n)} + e_{(m,n)} + f_{(m,n)} \end{aligned}$$

results in a conservative infinitesimal generator $\mathbf{Q}$; see Figure 1.1 for a graphical representation of the possible transitions in the competition process of [105].

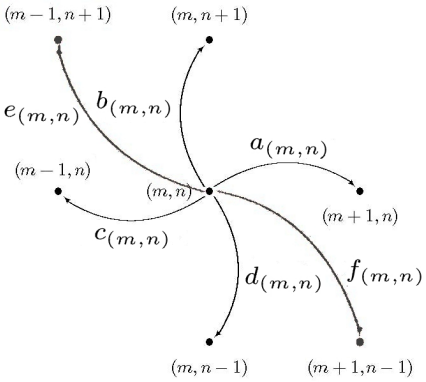

Fig. 1.1. Transitions among states in the competition process $\mathcal{X}$

In [105], the following classification is presented for some competition processes of interest:

Type I: A competition process given by (1.1) is termed *Type I* if both of the following conditions hold:

(i) States in the axes are absorbing states, that is, $a_{(m,n)} = b_{(m,n)} = c_{(m,n)} = d_{(m,n)} = e_{(m,n)} = f_{(m,n)} = 0$ for states $(m,n) \in \mathcal{C}_0 = l(\cdot,0) \cup l(0,\cdot)$, with $l(\cdot,0) = \{(m,0) : m \geq 0\}$ and $l(0,\cdot) = \{(0,n) : n \geq 0\}$.

(ii) For states $(m,n) \in \mathbb{N}\times\mathbb{N}$, it is verified that $a_{(m,n)}+b_{(m,n)} > 0$ and $c_{(m,n)} + d_{(m,n)} > 0$, so that $\mathcal{C} = \mathbb{N} \times \mathbb{N}$ is an irreducible class of transient states, and the class $\mathcal{C}_0$ of states is accessible from $\mathcal{C}$.

Type II: A competition process given by (1.1) is termed *Type II* if $\mathbf{Q}$ is irreducible, so that there are no absorbing states.

Most widely studied two-species interactions include the two-species competition, prey-predator relationship, host-parasite interaction and epidemic models. We show here how concrete specifications of the transition rates (1.1) yield processes covering these interactions; for applications of CTMCs to epidemic, competition, predation and genetics processes, we refer the reader to the books by Allen [5, Chapter 7], and Anderson [10, Chapter 9].

(A) Competition between two species: A two-species competition process is presented by Reuter [105, Example 1] as an example of Type I process. In this model, transition rates are defined by

$$\begin{aligned} a_{(m,n)} &= \alpha m, \quad b_{(m,n)} = \beta n, \quad c_{(m,n)} = \gamma mn, \\ d_{(m,n)} &= \delta mn, \quad e_{(m,n)} = 0, \quad f_{(m,n)} = 0, \end{aligned} \tag{1.2}$$

where α, β, γ and δ are strictly positive constants. Although this specification does not lead us to a Type I process (since states of the form $(m,0)$ and $(0,n)$ are not absorbing), it is suggested in [105] to *freeze* states $(m,0)$ and $(0,n)$ by making $q_{(m,0),(m',n')} = 0$ and $q_{(0,n),(m',n')} = 0$, for $(m',n') \in \mathcal{S}$ and $m,n \geq 0$. This means that the state space becomes $\mathcal{S} = \mathbb{N}_0 \times \mathbb{N}_0 - \{(0,0)\}$, since the state $(0,0)$ is accessible only from the positive axes. When the process becomes absorbed into (m',n') with $m' = 0$ or $n' = 0$, it is suggested in [105] to study the dynamics of the surviving species by means of a one-dimensional birth and death process.

This two-species competition process was widely studied by Ridler-Rowe [108], and is related to an ecosystem where individuals of two different species compete either directly or indirectly for common resources. As the total size of the ecosystem increases, the maintenance of stable growth conditions becomes unsustainable because of the *environmental pressure* (by overcrowding) and, consequently, births and deaths in both species depend strongly on the population sizes of one or both of the species. Note that the ecosystem in [108] is closed, in the sense that no immigration or emigration is supposed to take place, that is, $e_{(m,n)} = f_{(m,n)} = 0$. More details on this model are given in Section 1.2 and Chapter 2.

(B) Prey-predator models: A prey-predator model, presented by Hitchcock [62, Model 2] and analyzed later by Ridler-Rowe [109], is obtained by specifying

$$\begin{aligned} a_{(m,n)} &= \alpha mn, \quad b_{(m,n)} = \lambda n, \quad c_{(m,n)} = \beta m, \\ d_{(m,n)} &= \mu mn, \quad e_{(m,n)} = 0, \quad f_{(m,n)} = 0, \end{aligned} \tag{1.3}$$

where α, β, μ and λ are strictly positive constants. States of the form $(m, 0)$ and $(0, n)$ are assumed to be absorbing states, so that the process is of Type I.

The process described by (1.3) reflects a prey-predator interaction, where $M(t)$ and $N(t)$ amount to the numbers of predators and preys alive at time t, respectively. The number of predators (respectively, preys) increases (respectively, decreases) as a function of the number of encounters between the predator and its prey.

(C) Host-parasite models: A process modeling host-parasite interaction is presented by Hitchcock [62, Model 1] by using the transition rates

$$\begin{aligned} a_{(m,n)} &= 0, \quad b_{(m,n)} = \lambda n, \quad c_{(m,n)} = \beta m, \\ d_{(m,n)} &= 0, \quad e_{(m,n)} = 0, \quad f_{(m,n)} = \alpha mn, \end{aligned} \tag{1.4}$$

where α, β and λ are strictly positive constants, and transition rates $q_{(m,0),(m',n')} = q_{(0,n),(m',n')} = 0$, which means that the process is of Type I. We may observe that the state space here becomes $\mathcal{S} = \mathbb{N}_0 \times \mathbb{N}_0 - \{(0,0),(1,0)\}$, since states $(0,0)$ and $(1,0)$ are not accessible.

Host-parasite models can be seen as a specific class of prey-predator system, where parasites play the role of predators, and hosts play the role of preys. Thus, if $M(t)$ and $N(t)$ denote the numbers of parasites and hosts at time t, respectively, then the interspecific interaction described in [62, Model 1] by (1.4) belongs to a special subclass of host-parasite models where parasites are called *parasitoids*, since hosts that are successfully parasitized die. In (1.4), the parasitism transition is related to the rate $f_{(m,n)} = \alpha mn$. As an example of host-parasitoid interaction, we recall the motivation in [62], where parasitoids encounter hosts at random in such a way that, as an encounter occurs, one egg is laid in the host. The egg then develops into a new parasitoid and the

host dies. Therefore, transitions from a given state (m, n) to state (m', n') with $(m', n') = (m-1, n)$, $(m, n+1)$ and $(m+1, n-1)$ amount to the death of a parasite, birth of a host, and parasitism, respectively. In this thesis, we shall focus on this host-parasitoid model in Section 1.3 and Chapter 3. An individual-based model for the host-parasite interaction, where the interest is in a population of parasites infecting a single host, is presented in Section 1.4 and later studied in Chapter 4.

(D) Epidemic models: A basic epidemic process is presented by Bartlett [24] and later studied by Reuter [105, Example 2], and it corresponds to the transition rates

$$\begin{aligned} a_{(m,n)} &= \alpha, \quad & b_{(m,n)} &= \beta, \quad & c_{(m,n)} &= \gamma m, \\ d_{(m,n)} &= \delta n, \quad & e_{(m,n)} &= \epsilon mn, \quad & f_{(m,n)} &= 0. \end{aligned}$$

Note that in the case $\alpha + \beta > 0$, there are no absorbing states and we have a Type II process. Otherwise, the positive axes become absorbing sets and, as the process hits states (m', n') with m' or n' equal to zero, it becomes absorbed into this state or it behaves as a pure death process.

In SIS epidemic models, we deal with a population of individuals, where each individual passes from being susceptible to turning infected, to becoming again susceptible, thus allowing for a bidirectional transition between the two possible states. Let $M(t)$ and $N(t)$ denote the numbers of susceptible individuals and infected individuals, respectively, at time t. Then, increments in the number $N(t)$ of infected individuals due to the spread of the disease directly depend on incidental random encounters between susceptible and infected individuals, so that $e_{(m,n)} = \epsilon mn$. Ridler-Rowe [107] studied the special case $\gamma = 0$; more concretely, he investigated the asymptotic behavior of the mean duration of the epidemic. The particularization $\alpha = \beta = \gamma = 0$ yields the *general stochastic epidemic model*, which was studied by Bailey [17].

Multivariate versions of processes (A)-(D) can be constructed as a generalization of the two-dimensional competition process in [105] to higher dimensions. Such a generalization for $d \geq 2$ species was first introduced by Iglehart [67] who assumed that transitions

are only related to the birth and death of single individuals within each species, as well as to immigration between species.

Stochastic models presented in this work are closely related to their deterministic counterparts. The fundamental difference between deterministic and stochastic models is that, whereas the stochastic model predicts the probability of an outcome, the deterministic analogue provides an outcome with absolute certainty. This means that, in the deterministic case, the dynamics of the process depend crucially on the initial condition. On the contrary, in the stochastic case, it will be possible for one species or the other to survive under identical initial conditions. In a population model is often used the deterministic version when the population size is sufficiently large. However, if the population sizes are small or even moderate, then population extinction may occur and the stochastic option becomes more realistic, since random variations associated with demography and environment can be included; see [5, 16].

The two-species competition process given by (1.2) is particularly related to one subclass of mutual competition, namely the *two-species autonomous competitive model* [80, 130, 136], which yields the deterministic equations

$$\frac{dx_1(t)}{dt} = x_1(t)\left(b_1 - a_{12}x_2(t)\right), \tag{1.5}$$

$$\frac{dx_2(t)}{dt} = x_2(t)\left(b_2 - a_{21}x_1(t)\right), \tag{1.6}$$

where $x_i(t)$ is the population size of the ith species at time t, for $i \in \{1, 2\}$. The mutual interspecific competition between species dictates that a_{12} and a_{21} are strictly positive. This model can also incorporate intraspecific competition (that is, competition between members of the same species) by including the terms $-a_{11}x_1^2(t)$ and $-a_{22}x_2^2(t)$ in Equations (1.5) and (1.6), respectively. We refer the reader to [3] for Lotka-Volterra competition models with diffusion and spatial variation in some coefficients; see also [80, 130] for the pioneering work on the deterministic two-species competition model.

Prey-predator models have received much attention since the seminal work [80, 130] by Lotka and Volterra, and all contemporary biology/ecology texts give a lot of coverage to the subject;

see the monographs by Bartlett [25], Edelstein-Keshet [47], May and McLean [84], and Murray [88], among others; see also the survey article [134]. The Lotka-Volterra prey-predator model, as an analogue of the process defined by (1.3), has the form

$$\begin{aligned} \frac{dx_1(t)}{dt} &= x_1(t)\left(b_1 - a_{12}x_2(t)\right), \\ \frac{dx_2(t)}{dt} &= x_2(t)\left(a_{21}x_1(t) - b_2\right). \end{aligned} \tag{1.7}$$

The host-parasite model defined by (1.4), which can be seen as an special case of the prey-predator interaction, is presented by Hitchcock [62, Model 1] as a stochastic analogue of the prey-predator process defined by (1.7) for the concrete specification $a_{12} = a_{21}$. Details on the deterministic model are briefly given by Bailey [16, Chapter 5] with a more extensive treatment given by Bartlett [25, Chapters 4 and 5]. There is an extensive literature dealing with prey-predator models analyzed in the deterministic framework; for example, we can cite the work of Bhattacharya and Martcheva [28], Hsu and Hubbell [64], Hsu [65], and Loman [79], who analyze a variety of prey-predator models under various assumptions, such as the assumption of nonterritorial and territorial predators [79] or a specialist predator in size-structured models [28]. In other cases, modeling aspects incorporate two predators that compete for a single, limited prey [65] or two predators competing for two prey species [64]. In [5, Sections 7.6 and 7.7] we find a review of the main results for deterministic and stochastic models of interacting biological populations; as a related work, see the paper by Roozen [110].

1.2 Two-species competition models

The two-species competition interaction [134] is one of the basic interspecific relations for biological, ecological and social models, and it is also the key of more complicated structures. Unlike a prey-predator relationship in which one species is part of the food supply of the second one, in a competition relationship two species compete either directly or indirectly for a limited food supply and, as a consequence, an increase in the density of one species results in

a decrease in the other species that is proportional to the product of both species.

In this thesis, our interest is in the stochastic version of the two-species competition process given by (1.2). This process was first analyzed by Reuter [105], who showed that the underlying CTMC may be specified uniquely by its transition rates, that the extinction of one or other of the species is certain, and that the expectation of the time at which this species becomes extinct is finite. The results of Reuter [105] were later extended by Iglehart [67] to the multivariate case; in particular, Iglehart [67] obtained sufficient conditions for a multivariate competition process to be regular, positive recurrent, absorbed with certainty, and to have finite mean absorption time. Billard [29] considered a simplified version in which each species can only decrease in number because of deaths caused, for instance, by starvation, overcrowding, or removal in some form. Instead of working with the resulting differential equation, Billard [29] transformed the related differential-difference equations into a system of equations whose matrix of coefficients is lower triangular. A particular partitioning of this matrix allows the population size probabilities and moments to be derived with relative ease.

In a more general setting, Allen [4] used stochastic differential equations and difference equations for the population dynamics and the persistence time, respectively, of two interacting populations, and showed applications of these equations to a model with possible movement of individuals between populations, an SIS epidemic model and several variants of the standard Lotka-Volterra prey-predator model. The Lotka-Volterra equations for two competing species are studied in [42] under the assumption that the coefficients are periodic functions of a common period; as a related work, see [89]. Sufficient conditions are given in [48] for convergence to stationary distributions in the case of some models of two species competing in a randomly varying environment. In [65], a resource-based ecological competition model with interference is defined from the Lotka-Volterra dynamics with two predators that compete for a single, limited prey. An application of the two-species competition model to microbial growth on two essential limiting resources can be found in [78]. The model in

[78] is defined to incorporate internal resource variables, which serve the direct connection between species growth, and external resource availability. A recent graphical method complementing that of Tilman [125] is given in [18] for determining the outcome of two-species competition for two resources. While Tilman's method deals with information at potential coexistence equilibria, Ballyk and Wolkowicz [18] first introduce a feasible set where the resource concentrations of any equilibrium solution must be found, they then locate the single species equilibria on the boundary of this set and the coexistence equilibria inside the set, and they finally determine the competitive outcomes based on the position of the single species equilibria. Other models of competition include the studies of Gopalsamy [54], Kostova et al. [74], and Li and Smith [77], where processes are studied under different assumptions, such as the assumption of age-dependent mortality and fertility functions [54], age-structured models [74] or a model where four species coexist in competition for three essential resources [77].

The Ridler-Rowe process [108] amounts to a time-homogeneous CTMC defined on the quarter plane $\mathbb{N}_0 \times \mathbb{N}_0$, where transitions given by (1.2) are only allowed to neighboring states and the positive axes constitute the subset of absorbing states. In analyzing the extinction time and the size of the surviving species, the quadratic terms in the transition rates (see [108, Section 2]) of the process make the solution intractable from an analytical point of view. One way of analyzing the process is to approximate its behavior, as the initial population sizes become large, by an essentially deterministic motion with a random diffusion of smaller order superimposed upon it. The techniques used by Ridler-Rowe [108] yield the asymptotic distribution of the position at which the process first hits the subset of absorbing states, and a limit result for the probability that a given species should survive the other. In Chapter 2 of this thesis, our interest is in an approximating model based on the use of a process defined on a finite space of states. We use the underlying quasi-stationary distribution, which serves the role of approximating the state of the process, provided that the process has been going on for a long time, and that extinction has not occurred.

The theory of quasi-stationary distributions and their applications seem to have begun in 1956 with a paper by Bartlett [24] (see also [25]), which influenced the early theoretical work by Darroch and Seneta [43, 44]. The importance of quasi-stationarity in stochastic population models is suitably remarked in the monograph by Nisbet and Gurney [93], where an iterative method for determining the quasi-stationary distribution is presented. The contribution in [93] is continued by Renshaw [104], who emphasizes the importance of the concept of quasi-stationarity in modeling biological populations and derives relations between the time to extinction and the quasi-stationary distribution. As a related work, see [101] for an application to the stochastic logistic model.

An extensive bibliography of work on quasi-stationary distributions is maintained by Pollett, and can be found at the website `www.maths.uq.edu.au/~pkp/papers/qsds/qsds.html`. The reference by van Doorn and Pollet [131] is an excellent paper containing a survey of results related to quasi-stationary distributions for CTMCs over a finite or countably infinite state space. The reader can also find in [58, Chapter 8] appropriate remarks to an extensive bibliography on quasi-stationarity and applications to biological, risk, and applied probability models, among others. A modern presentation of the theory is given in textbook form by Kijima [72]. See e.g. [26, 27] for details on the quasi-stationary behavior of structured Markov chains.

Recently, Gyllenberg and Silvestrov [58] use new methods of asymptotic analysis for non-linearly perturbed stochastic systems, which are based on asymptotic expansions for the perturbed renewal equation and recurrence algorithms in the case of Markovian processes with absorption. In particular, asymptotic expansions for absorption times are given in terms of large deviations for a variety of absorbing processes, such as perturbed regenerative processes, semi-Markov processes, and Markov chains. We refer the reader to [58, Chapter 6] for specific applications to birth-and-death processes, epidemic and population dynamic models, and metapopulation dynamic models. Further results on limit theorems for birth, death and catastrophe processes on the sets of non-extinction and of extinction can be found in the papers [34, 95, 96, 97, 98]. Renewal theory and perturbation results for finite CTMCs are used in

[57] to describe the asymptotic behavior of a stochastic metapopulation model exhibiting first order interactions between pairs of local populations. The underlying Markov chain model in [57] takes the spatial distribution of patches explicitly into account, keeps track of which patches are occupied and which are empty, and allows for variable patch size.

1.3 Host-parasite models

Parasitism is one of the factors believed to have a major impact on competitive interactions, but parasites might exhibit a wide degree of variability between species in the level of harm or damage they cause to their hosts. A parasite may spend a long period of its life with one or more host species or, alternatively, it may spend short periods with its host and then adopt a free-living mode for the majority of its developmental cycle. The host-parasite association is commonly seen as obligatory for the parasite because, during the parasitic phase of its life cycle, the parasite should depend upon its host for the synthesis of nutrients essential for its own metabolism. In host-parasitoid associations, the term parasitoid refers to a parasite which is free-living as an adult and whose adult females lay their eggs in the larvae or pupae of its host species. Those hosts that are not parasitized give rise to their own progeny. Hosts that are successfully parasitized die, but the eggs laid by parasitoids may survive to be the next generation of parasitoids.

Parasitoids and their hosts usually have synchronized life cycles and the first descriptions of their dynamics used difference equations. The application of the discrete-time methods to host-parasitoid models was pioneered by Thompson [124] in 1924. In 1935, Nicholson and Bailey [92] applied a modified version of Thompson's model to the parasitoid *Encarsia formosa*, and the host *Trialeurodes vaporarioum*. The Thompson model and the Nicholson-Bailey model do not permit equilibrium coexistence of hosts and parasitoids; specifically, the former admits no positive equilibrium, and the positive equilibrium in the latter is unstable. The book by Edelstein-Keshet [47, Chapter 3] gives an appropriate coverage to modifications of the Nicholson-Bailey model by using nonlinear difference equations.

Among other mechanisms for stable coexistence, we may mention the aggregation of parasitoid attacks, host density dependence, density dependent sex ratios, and coevolution in spatially heterogeneous environments; see the reference [33] for an interesting review on stabilizing effects in spatial host-parasitoid models. In [83], the individual behavior is used to stabilize the Nicholson-Bailey dynamics. Tang et al. [122] investigate how the incorporation of parasitoid intergenerational survival rates, the periodicity of insecticide spraying and the augmentation of natural enemies influence on the dynamics of the Nicholson-Bailey model. In the recent paper by Schreiber [113], the interest is in a generalization of Thompson's model including host density dependence and aggregation of parasitoid attacks. An interesting application of host-parasitoid dynamics to the forest tent caterpillar can be found in [37], where the community of parasitoids is assumed to differ among geographical regions. Cobbold et al. [37] present an integrodifference host-parasitoid model, which is discrete in time and continuous in space, to study how the critical habitat-size necessary for parasitoid survival changes in response to parasitoid life history traits, such as emergence time. As a related work, see the reference [38] where the focus is on host-parasitoid population dynamics by allowing competitive mortality of parasitized hosts. Although the qualitative host-parasitoid dynamics are mainly based on deterministic models, stochastic assumptions are also applied to host-parasitoid interactions; see e.g. [111], and references therein, where the use of simulation models allows to incorporate important features missing from simple deterministic models, such as spatial structure with local interactions, and genetical and behavioral differences among individual hosts.

In this thesis, our interest is in the Hitchcock process [62], which is uniquely specified in terms of its transition rates $q_{(m,n),(m',n')}$ given by (1.4), and where time delays are ignored. The process is modeled by a time-homogeneous CTMC $\mathcal{X} = \{X(t) = (M(t), N(t)) : t \geq 0\}$ defined on $\mathcal{S} = \mathbb{N}_0 \times \mathbb{N}_0 - \{(0,0),(1,0)\}$, where $M(t)$ and $N(t)$ record the numbers of parasitoids and hosts alive at time t, respectively. By using criteria developed by Reuter [105], Hitchcock [62] showed that ultimate extinction of either parasitoids or hosts is certain and that, given initial numbers of m

parasitoids and n hosts, the expected time $\tau_{(m,n)}$ to the first extinction is always finite. Based on the general epidemic model [17] where $M(t)$ and $N(t)$ amount to the numbers of infected and susceptible individuals alive at time t, respectively, an exact expression is derived in [62, Section 3] for the probability that the parasitoid population is the first to become extinct in the special case $\lambda = 0$. These probabilities are then used to derive power series approximations to extinction probabilities when the host birth rate λ is strictly positive, and a similar method of approximation is applied to estimate the mean number of events before the first extinction occurs; see [62, Sections 4 and 5]. By means of an alternative construction – using Reuter's criterion [105] together a simple minimization result – Ridler-Rowe [109] proved that the mean extinction time $\tau_{(m,n)}$ tends to zero as the combined initial population of parasitoids and hosts $m+n$ becomes large. A similar procedure can be applied to other related models; see e.g. [107] for an epidemic model, and [109, Section 4] for a prey-predator model where a predator birth is not directly associated with a prey death.

1.4 Individual-based models of host-macroparasite interaction

Parasites are usually classified (see e.g. [135]) in two groups: microparasites, such as viruses, bacteria or protozoa; and macroparasites (helminths). The main difference between them is that microparasites multiply directly within their host, whereas macroparasites grow within their host but multiply by producing infective stages which are released into the environment to infect new hosts. For macroparasites, the burden of worms in an individual host is the unit of study.

Recently, Herbert and Isham [61] contribute to the discussion of causes and effects of aggregation of macroparasite counts, with special emphasis on clumped infections and parasite-induced host mortality. Herbert and Isham [61] use a fully stochastic approach enabling the investigation of a wide range of distributional properties of interest, in a nonlinear stochastic model for the evolution of the parasite load of a single host. A simpler version of such a model was previously investigated by Isham [68]. In [61],

the model of Isham [68] is extended to incorporate three parasite stages (larval, mature and offspring), general clumped infections, parasite-induced host mortality, and to allow durations of the parasite stages to be non-exponentially distributed. Between-host heterogeneities and disease control are also discussed in [61]. Exact algebraic results are obtained in [61, 68] on the distribution of parasite load and on host survival. In the setting of macroparasites coexisting in individual hosts, important results have been obtained by Anderson et al. [8], Bottomley et al. [32], and Rosà et al. [111]; as a related work, see [9]. The paper by Cornell [41] is an excellent reference where stochastic helminth population models are discussed. More particularly, Cornell [41] demonstrates the mathematical techniques that can help to analyze these models, starting with the infection dynamics within a single host and finishing with the full parasite lifecycle among a population of hosts, as well as the insights into host-parasite biology that these stochastic models can bring.

In Chapter 4 of this thesis, our interest is in host-macroparasite interactions that can be modeled by birth and death processes with killing with rates varying throughout time. We shall consider a time-inhomogeneous CTMC $\mathcal{X} = \{M(t) : 0 \leq t \leq \tau\}$ where $M(t)$ amounts to the number of parasites within the host (for practical use, the infection level of the host, which is caused by the presence of parasites), and τ might amount to the periodic occurrence of a certain event, such as an annual inspection. The CTMC $\mathcal{X}$ is defined on $\{-1\} \cup \mathcal{S}$ with $\mathcal{S} = \{0, \ldots, M_0\}$, where state -1 represents that the host is dead (or its level of infection is unacceptable) and state M_0 amounts to a critical value that means the impossible recovery of the host if that level of infection M_0 is exceeded. Seasonal conditions in our model are reflected by means of state-dependent nonhomogeneous Poisson processes associated with the acquisition of parasites, the reproduction and death of parasites within the host, and the natural (no parasite-induced) mortality, and parasite-induced host mortality. Without any claim to an exhaustive enumeration, we can cite the work of Altizer et al. [6], Conlan and Grenfell [39], Dietz [45], Elton [49], Grassly and Fraser [55], Moneim [87], Parham and Michael [99], Peeters et al. [100], Stone et al. [118] and Turchin [127], who analyze seasonal

dynamics of infectious diseases in a variety of models by translating seasonality into time-dependent patterns. Keeling and Rohani [69, Chapter 5] present a good summary of models in a range of infectious diseases that show how seasonally varying parameters act as a forcing mechanism, and their dynamical consequences. In host-parasite models, the effect of parasite aggregation on coexistence is studied by Pugliese [103], who assumes that the number of parasites in one host may increase because of new infections at a time-dependent rate. In the model of Isham [68], the host is exposed over its lifetime to parasites at times that form a nonhomogeneous Poisson process, and the death rate of the host depends on its age. Similarly, Herbert and Isham [61] consider that the host is exposed to parasite larvae at time instants of a nonhomogeneous Poisson process and, during the adult stage, the parasite gives birth to clumps of offspring in a nonhomogeneous Poisson process. Reynolds et al. [106] model the interaction between plant defenses and herbivores by including seasonal forcing, a ubiquitous environmental influence in natural systems. Seasonality in [81] is connected to the periodic host absence, which is a central feature in plant epidemiology.

The general process described in terms of $\mathcal{X}$ is the basis in Chapter 4 to study grazing management strategies for the control of gastrointestinal nematodes in sheep under a seasonal environment. Gastrointestinal (GI) nematodes are arguably (see [121, 123]) the major cause of ill health and poor productivity in grazing sheep worldwide, especially in young stock. Allowing for inherent variability, this statement holds true regardless of farming system, climate, geographical region and host species; see, for example, the references [15, 31, 52, 116, 129], which are linked to studies on the epidemiology and seasonal dynamics of GI nematode infections in New South Wales, Denmark, Netherlands, Ethiopia and Spain, respectively. Productivity losses result from both parasite challenge and parasitism, while regular treatment of the infections is costly in terms of chemicals and labour. The relative cost of GI parasitism has become greater in recent decades as the availability of effective broad-spectrum anthelmintics (see [121, Chapter 5]) has enabled the intensification of pastoral agriculture. To an extent, it appears the success of the various anthelmintic

products developed since the 1960s has created a rod for our own backs, particularly as resistance has arisen to each active family in turn. We may point out that anthelmintic resistance in sheep has been demonstrated by Bjørn et al. [30], Entrocasso et al. [50], Maingi et al. [82], and Sutherland et al. [120], among others; as a related work, see [121, Chapter 6]. Furthermore, as consumers increasingly demand a reduction in chemical application to food and fibre producing animals, the pressure increases to control nematode parasites within intensive pastoral systems without recourse to regular drug treatment.

The options for control of GI nematode infections – which do not rely uniquely on the use of anthelmintics – include management procedures (involving intervention with anthelmintics, grazing management, level of nutrition and bioactive forages), biological control (with nematophagous fungi), selection for genetic resistance in sheep (within breed/use of selected breeds), and vaccination. The article by Stear et al. [117] gives an overview on alternatives to anthelmintics for the control of nematodes in livestock, and it complements and extends other review articles by Hein et al. [60], Knox [73], Sayers and Sweeney [112], and Waller and Thamsborg [133]; as a related work, see also [40].

1.5 Overview of the thesis

In this thesis, we focus on the use of stochastic models in order to describe the interactions presented in Sections 1.2-1.4. Specifically, our aim is to apply matrix-analytic methods [76, 91] in order to study different descriptors of the Ridler-Rowe process (Chapter 2), the Hitchcock process (Chapter 3), and the host-macroparasite interaction described in Section 1.4 (Chapter 4).

The contents of the thesis are structured as follows. In Chapter 2, the two-species competition process is the process under study. We consider the distribution of the extinction times, as well as the joint distribution of the identity of the species becoming extinct and the size of the surviving species. Our approach is mainly based on the replacement of the underlying absorbing Markov chain, which is a random walk in the quarter plane $\mathbb{N}_0 \times \mathbb{N}_0 - \{(0,0)\}$, by a suitably defined finite Markov chain. Based on the time to

reach the maximum number of individuals in the ecosystem, we derive iterative schemes for its mass function under the assumption of quasi-stationary regime. Our approximation method is also applied to the study of the number of births and deaths happening until extinction, and the survival of a certain individual. First, we derive the joint distribution of the extinction time, and the numbers of births and deaths occurring during an extinction cycle of the ecosystem. Then, the effects of the killing strategy on the survival of an individual are analyzed under various random and age-dependent assumptions. Our results are illustrated and the accuracy of our solution is tested with reference to simulated data. Numerical examples are presented to show the influence of the numbers of births and deaths on the dynamics of the two-species competition process and the survival of an individual.

In Chapter 3, our interest is in the Hitchcock process. First, we aim to study the maximum number of individuals alive during a fixed time interval $[0, t_0]$, which is an alternative descriptor to that in Chapter 2 related to an extinction cycle. Second, we are concerned with versions of the Hitchcock process that can exhibit correlation tendencies in the underlying processes generating events. We apply a block-structured state-dependent (BSDE) approach that provides a methodological tool to model state-dependent transitions operating in the presence of phases; for details on the BSDE approach, the reader is referred to the papers [12, 13]. The BSDE approach turns the Hitchcock model into a CTMC allowing correlated and non-exponentially generated events.

In Chapter 4 our interest is in host-macroparasite interactions, where the acquisition of parasites by a single host is studied. We examine nonlinear stochastic models for the parasite load of the host, where the age-dependent rates represent seasonal conditions. We present a basic model representing a host that, at a certain age τ_0, is isolated and treated with chemotherapeutic products. This means that the host is free living in a seasonal environment, and it is transferred to an uninfected area at age τ_0. In the uninfected area, the host does not acquire new parasites, undergoes an anthelmintic treatment to decrease the parasite load, and varies in its susceptibility to parasite-induced mortality and natural mortality. We present two criteria based in stochastic principles that

permit us to select an optimal intervention instant τ_0. An application of our model is shown to the development of GI nematode infection in sheep. In that case, grazing strategies combining the movement of the host to either an uninfected area or safe pasture, with the use of anthelmintic treatments are defined in terms of the intervention instant τ_0. We apply our criteria in order to select the value τ_0, where empirical data are obtained from [90, 128].

2

Stochastic Model of Competition Between Two Species

The two-species competition process of Ridler-Rowe [108] is a time-homogeneous CTMC $\mathcal{X} = \{X(t) = (M(t), N(t)) : t \geq 0\}$ on the state space $\mathcal{S} = \mathbb{N}_0 \times \mathbb{N}_0 - \{(0,0)\}$, where $M(t)$ and $N(t)$ denote the population sizes of two species, termed *species 1* and *species 2*. Individuals compete either directly or indirectly for common resources and, consequently, births and deaths depend on the population sizes of one or both of the species, as indicated in Figure 2.1. Specifically, for each initial state $(m,n) \in \mathcal{S}$ with $m > 0$ and $n > 0$, the non-null transition rates $q_{(m,n),(m',n')}$ of the Markov chain $\mathcal{X}$ are specified as

$$q_{(m,n),(m',n')} = \begin{cases} \alpha m, & \text{if } (m',n') = (m+1,n), \\ \beta n, & \text{if } (m',n') = (m,n+1), \\ \gamma mn, & \text{if } (m',n') = (m-1,n), \\ \delta mn, & \text{if } (m',n') = (m,n-1), \end{cases} \tag{2.1}$$

where α, β, γ and δ are strictly positive constants, and $q_{(m,n)} = -q_{(m,n),(m,n)} = (\alpha + \gamma n)m + (\beta + \delta m)n$. The positive axes $l(\cdot, 0) = \{(m,0) : m \geq 1\}$ and $l(0,\cdot) = \{(0,n) : n \geq 1\}$ constitute subsets of absorbing states; i.e., $q_{(m,0),(m',n')} = q_{(0,n),(m',n')} = 0$, for all $(m',n') \in \mathcal{S}$ and $m, n \geq 1$. This means that what happens to the population process $\mathcal{X}$ after the eventual extinction of one or other of the species is not of immediate interest. The state space $\mathcal{S}$ can be decomposed into a subset $\mathcal{C}_0 = l(\cdot,0) \cup l(0,\cdot)$ of absorbing states and an irreducible class $\mathcal{C} = \mathbb{N} \times \mathbb{N}$ of transient states. For later use, we express the class $\mathcal{C}$ in terms of levels as $\cup_{k=2}^{\infty} l(k)$, where the kth

level is given by $l(k) = \{(m,n) \in \mathbb{N}\times\mathbb{N} : m+n = k, m > 0, n > 0\}$, for $k \geq 2$.

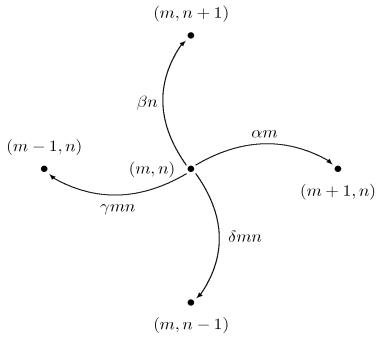

Fig. 2.1. Transitions among states at the two-species competition process $\mathcal{X}$

We may express the infinitesimal generator $\mathbf{Q}$ of $\mathcal{X}$ in the form

$$\mathbf{Q} = \begin{pmatrix} \mathbf{0} & \mathbf{0} \\ \mathbf{Q}_{\mathcal{C},\mathcal{C}_0} & \mathbf{Q}_{\mathcal{C},\mathcal{C}} \end{pmatrix},$$

by defining $\mathbf{Q}_{\mathcal{C},\mathcal{C}_0}$ and $\mathbf{Q}_{\mathcal{C},\mathcal{C}}$ suitably. The sub-matrix $\mathbf{Q}_{\mathcal{C},\mathcal{C}_0}$ has the form $\mathbf{Q}_{\mathcal{C},\mathcal{C}_0} = \mathrm{diag}\,(\mathbf{A}_{2,1}, \mathbf{A}_{3,2}, ...)$, where $\mathbf{A}_{k,k-1}$ contains the transition rates related to jumps from states of the kth level to absorbing states of the subset $\{(k-1,0),(0,k-1)\}$, for $k \geq 2$. Similarly, $\mathbf{Q}_{\mathcal{C},\mathcal{C}}$ is given by

$$\mathbf{Q}_{\mathcal{C},\mathcal{C}} = \begin{pmatrix} \mathbf{B}_{2,2} & \mathbf{B}_{2,3} & & & \\ \mathbf{B}_{3,2} & \mathbf{B}_{3,3} & \mathbf{B}_{3,4} & & \\ & \mathbf{B}_{4,3} & \mathbf{B}_{4,4} & \mathbf{B}_{4,5} & \\ & & \ddots & \ddots & \ddots \end{pmatrix},$$

where $\mathbf{B}_{k,k}$ is a diagonal matrix of dimension $k-1$ with ith entry $-q_{(k-i,i)}$, and the entries in $\mathbf{B}_{k,k'}$ are associated with jumps from states of the kth level to states of the k'th level, for $k' \in \{k-1, k+1\}$ and $k \geq 2$.

In order to specify expressions for sub-matrices $\mathbf{A}_{k,k-1}$, $\mathbf{B}_{k,k-1}$, $\mathbf{B}_{k,k}$ and $\mathbf{B}_{k,k+1}$, we define a natural ordering for absorbing states as

$$(1,0) \prec (0,1) \prec ... \prec (k,0) \prec (0,k) \prec ...$$

For states of the kth level, the ordering is defined as $(k-1,1) \prec (k-2,2) \prec ... \prec (2,k-2) \prec (1,k-1)$. Then, it can be readily verified that $\mathbf{A}_{2,1} = (\delta, \gamma)$,

$$\mathbf{A}_{k,k-1} = \begin{pmatrix} (k-1)\delta & 0 \\ 0 & 0 \\ \vdots & \vdots \\ 0 & 0 \\ 0 & (k-1)\gamma \end{pmatrix},$$

$$\mathbf{B}_{k,k-1} = \begin{pmatrix} (k-1)\gamma & & & & & \\ 2(k-2)\delta & 2(k-2)\gamma & & & & \\ & 3(k-3)\delta & 3(k-3)\gamma & & & \\ & & \ddots & \ddots & & \\ & & & 2(k-2)\delta & 2(k-2)\gamma & \\ & & & & (k-1)\delta \end{pmatrix},$$

for $k \geq 3$. For $k \geq 2$, $\mathbf{B}_{k,k}$ is a diagonal matrix of dimension $k-1$ with ith entry $-((k-i)(\alpha + i\gamma) + i(\beta + (k-i)\delta))$, and

$$\mathbf{B}_{k,k+1} = \begin{pmatrix} (k-1)\alpha & \beta & & & \\ & (k-2)\alpha & 2\beta & & \\ & & \ddots & \ddots & \\ & & & 2\alpha & (k-2)\beta \\ & & & & \alpha & (k-1)\beta \end{pmatrix}.$$

In a similar manner the standard transition function $\mathbf{P}(t) = (p_{(m,n),(m',n')}(t))$ over $\mathcal{S}$ has the structured form

$$\mathbf{P}(t) = \begin{pmatrix} \mathbf{I} & \mathbf{0} \\ \mathbf{P}_{\mathcal{C},\mathcal{C}_0}(t) & \mathbf{P}_{\mathcal{C},\mathcal{C}}(t) \end{pmatrix}.$$

2.1 Statement of the problem

It is stated in [105] that, with probability one, one or other of the species eventually becomes extinct, and that the expectation of the time at which this species first becomes extinct is finite. To be concrete, let the random variable T be the time till absorption in

$\mathcal{X}$, that is, $T = \inf\{t : X(t) \in \mathcal{C}_0\}$, and $\alpha_{(m,n)}$ be the absorption probabilityabsorption time defined as $P(T < \infty | X(0) = (m,n))$, for the initial state $(m,n) \in \mathcal{S}$. Then, it is derived in [105, Theorem 5] that $\alpha_{(m,n)} = 1$ and that the expected time $\tau_{(m,n)} = E[T|X(0) = (m,n)]$ to reach the set $\mathcal{C}_0$ of absorbing states is finite; we present below a corrected proof of [105, Theorem 5].

Theorem 2.1. *For the Ridler-Rowe process defined by (2.1), absorption is certain and the mean absorption times are finite regardless of the initial state* (m,n).

Proof. The proof in [105] is based on the following criterion: *Let* $\alpha_{(m,n)}$ *be the probability of reaching some state in* $\mathcal{C}_0$ *and* $\tau_{(m,n)}$ *be the expected time to reach the subset* $\mathcal{C}_0$ *from* $(m,n) \in \mathcal{C}$. *If there exist finite values* $u'_{(m,n)} \geq 0$ *such that*

$$\sum_{(m',n') \in \mathcal{S}} q_{(m,n),(m',n')} u'_{(m',n')} + 1 \leq 0, \tag{2.2}$$

then $\alpha_{(m,n)} = 1$ *and* $\tau_{(m,n)} \leq u'_{(m,n)} < \infty$, *for all* $(m,n) \in \mathcal{C}$.

The function $u'_{(m,n)}$ used in [105, Equation (35)] is given by

$$u'_{(m,n)} = m + n + \frac{A}{1-\rho}\left(2 - \rho^m - \rho^n\right), \quad (m,n) \in \mathcal{C}, \tag{2.3}$$

where the constants $\rho \leq 1$ and $A > 0$ are chosen according to [105, Equations (37)-(39)]. Although the choice in [105] for the constants ρ and A is not appropriate, we next show that the definition for $u'_{(m,n)}$ in (2.3) is valid if we first choose a value $\rho \in (0,1)$ such that

$$\rho < 2^{-1} \min\left\{\gamma\alpha^{-1}, \delta\beta^{-1}\right\}, \tag{2.4}$$

then choose an integer N so that

$$N \geq \rho^{-1} \max\left\{(1+\alpha)\gamma^{-1}, (1+\beta)\delta^{-1}\right\}, \tag{2.5}$$

and finally A verifying

$$A \geq 2(1+\alpha+\beta)\rho^{-(N-1)} \max\left\{\gamma^{-1}, \delta^{-1}\right\}. \tag{2.6}$$

Note that these constraints ensure that $u'_{(m,n)} \geq 0$ for every state (m,n).

For any state (m, n), we write down

$$\begin{aligned} v(m,n) &= -\sum_{(m',n')\in\mathcal{S}} q_{(m,n),(m',n')}u'_{(m',n')} \\ &= m\Big(\gamma n(1+A\rho^{m-1}) - \alpha\,(1+A\rho^{m})\Big) + n\Big(\delta m(1+A\rho^{n-1}) \\ &\quad -\beta\,(1+A\rho^{n})\Big). \end{aligned}$$

Now, we prove separately that the condition (2.2) holds in the four regions in the positive quadrant bounded by $m = N$ and $n = N$.

(i) $m \le N$, $n \le N$. We observe that

$$\begin{aligned} v(m,n) \ge m\Big(\gamma - \alpha + A\rho^{m-1}(\gamma - \rho\alpha)\Big) \\ +n\Big(\delta - \beta + A\rho^{n-1}(\delta - \rho\beta)\Big), \end{aligned}$$

where $\gamma - \alpha + A\rho^{m-1}(\gamma - \rho\alpha) \ge \gamma - \alpha + A\rho^{N-1}2^{-1}\gamma > 1$ and $\delta - \beta + A\rho^{n-1}(\delta - \rho\beta) \ge \delta - \beta + A\rho^{N-1}2^{-1}\delta > 1$, by (2.4) and (2.6). Hence, $v(m,n) > m + n > 1$ in this region.

(ii) $m > N$, $n > N$. We express $v(m,n)$ as

$$\begin{aligned} v(m,n) = m\Big(\gamma n - \alpha + A\rho^{m-1}(\gamma n - \rho\alpha)\Big) \\ +n\Big(\delta m - \beta + A\rho^{n-1}(\delta m - \rho\beta)\Big). \end{aligned}$$

Then, we note that $\gamma n - \alpha > \gamma N - \alpha > N\rho\gamma - \alpha \ge 1$ since $N\rho\gamma \ge 1 + \alpha$ by (2.5). Similarly, we have $\delta m - \beta > 1$. On the other hand, $\gamma n - \rho\alpha > \gamma 2^{-1}$ and $\delta m - \rho\beta > \delta 2^{-1}$ by (2.4). Thus, $v(m,n) > m + n > 1$ in this region.

(iii) $m \le N$, $n > N$. We first observe that

$$v(m,n) > n\Big(\gamma + \delta - (\alpha+\beta) + mA\rho^{m-1}\Big(\gamma - \frac{\rho\alpha}{n}\Big)\Big),$$

since $m < n$ and $nA\rho^{n-1}(\delta m - \rho\beta) > 0$ by (2.4). By (2.4) and $1 \le m \le N < n$, we also note that

$$mA\rho^{m-1}\Big(\gamma - \frac{\rho\alpha}{n}\Big) > A\rho^{N-1}2^{-1}\gamma.$$

Thus, we find that

$$v(m,n) > n\Big(\gamma + \delta - (\alpha+\beta) + A\rho^{N-1}2^{-1}\gamma\Big),$$

where $A\rho^{N-1}2^{-1}\gamma \geq 1+\alpha+\beta$ by (2.6). Hence, $v(m,n) > n > 1$ in this region.

(iv) $n \leq N$, $m > N$. In this region, it is seen that $v(m,n) > m > 1$. The analysis is similar to the case (iii).

So Reuter's criterion (2.2) is satisfied for all $(m,n) \in \mathcal{C}$ by taking $u'_{(m,n)}$ given by (2.3) and the constants ρ, and A satisfying (2.4)-(2.6). □

More generally, our interest in this section is in the joint distribution of the extinction time T and the *size* $X(T)$ of the surviving species when the other species becomes extinct. Our first step is then to define the probability of reaching the absorbing state $(m',n') \in \mathcal{C}_0$ having started in state $(m,n) \in \mathcal{S}$, that is,

$$a_{(m,n)}(m',n') = \lim_{t\to\infty} P\left(X(t) = (m',n') \middle| X(0) = (m,n)\right),$$

for $(m,n) \in \mathcal{S}$ and $(m',n') \in \mathcal{C}_0$.

For each absorbing state $(m',n') \in \mathcal{C}_0$, the absorption probabilities, having started in an absorbing state $(m,n) \in \mathcal{C}_0$, are given by

$$a_{(m,n)}(m',n') = \begin{cases} 1, & \text{if } (m,n) = (m',n'), \\ 0, & \text{if } (m,n) \in \mathcal{C}_0 - \{(m',n')\}, \end{cases}$$

and the column vector $\mathbf{a}_{\mathcal{C}}(m',n') = (a_{(m,n)}(m',n') : (m,n) \in \mathcal{C})$ is the minimal strictly positive solution to the system of linear equations

$$-\mathbf{Q}_{\mathcal{C},\mathcal{C}}\mathbf{a}_{\mathcal{C}}(m',n') = \mathbf{q}_{\mathcal{C}}(m',n'), \tag{2.7}$$

where $\mathbf{q}_{\mathcal{C}}(m',n')$ consists of the transition rates $q_{(m,n),(m',n')}$, for $(m,n) \in \mathcal{C}$, which correspond to jumps from states (m,n) of the transient class to the absorbing state (m',n'). Equation (2.7) is directly derived from [94, Theorem 3.3.1] in the set of nong-negative solutions. To prove that the entries of $\mathbf{a}_{\mathcal{C}}(m',n')$ are strictly positive, we fix the absorbing state $(m',n') \in \mathcal{C}_0$ and observe that

$p_{(m,n),(m',n')}(s) \leq p_{(m,n),(m',n')}(s+t)$, for $t, s \geq 0$ and all initial state $(m,n) \in \mathcal{C}$. If we assume $a_{(m,n)}(m',n') = 0$ for some $(m,n) \in \mathcal{C}$, then $p_{(m,n),(m',n')}(t) = 0$ for all $t > 0$ and, by the irreducibility of $\mathcal{C}$, for all $(m,n) \in \mathcal{C}$, contradicting the fact that all absorbing state $(m',n') \in \mathcal{C}_0$ is accessible from the class $\mathcal{C}$ of transient states. Hence, the entries of $\mathbf{a}_{\mathcal{C}}(m',n')$ verify $0 < a_{(m,n)}(m',n') < 1$ for all pair of states $(m,n) \in \mathcal{C}$ and $(m',n') \in \mathcal{C}_0$, since $\alpha_{(m,n)} = 1$ and

$$\alpha_{(m,n)} = \sum_{(m',n') \in \mathcal{C}_0} a_{(m,n)}(m',n').$$

We may also note that, for each absorbing state $(m',n') \in \mathcal{C}_0$, the column vector $\mathbf{a}_{\mathcal{C}}(m',n')$ is a strictly positive solution of the set of equations

$$\mathbf{a}_{\mathcal{C}}(m',n') = \mathbf{p}_{\mathcal{C}}(t;(m',n')) + \mathbf{P}_{\mathcal{C},\mathcal{C}}(t)\mathbf{a}_{\mathcal{C}}(m',n'), \quad t > 0,$$

where $\mathbf{p}_{\mathcal{C}}(t;(m',n'))$ is the column vector with entries $p_{(m,n),(m',n')}(t)$, for $(m,n) \in \mathcal{C}$; the proof of this property mostly repeats arguments of [132, Lemma 4], and it is thus omitted.

Based on the absorption probabilities, the expected absorption time $\tau_{(m,n)}$, for $(m,n) \in \mathcal{C}$, can be expressed as

$$\tau_{(m,n)} = \sum_{(m',n') \in \mathcal{C}_0} \tau^*_{(m,n)}(m',n') a_{(m,n)}(m',n'),$$

where $\tau^*_{(m,n)}(m',n') = E[T|X(0) = (m,n), X(T) = (m',n')]$, for $(m,n) \in \mathcal{C}$. Since $q_{(m,n)} > 0$ for all $(m,n) \in \mathcal{C}$, the vector $\boldsymbol{\tau}^*(m',n') = (\tau^*_{(m,n)}(m',n') : (m,n) \in \{(m',n')\} \cup \mathcal{C})$, for state $(m',n') \in \mathcal{C}_0$, is the minimal non-negative solution with $\tau^*_{(m',n')}(m',n') = 0$ to the system of linear equations

$$\sum_{(k,l) \in \{(m',n')\} \cup \mathcal{C}} q_{(m,n),(k,l)} a_{(k,l)}(m',n') u_{(k,l)}(m',n') = -a_{(m,n)}(m',n'), \quad (m,n) \in \mathcal{C}. \tag{2.8}$$

The proof of (2.8) follows the same lines as [94, Theorem 3.3.3]; alternatively, it can be derived as an extension of [132, Theorems 1 and 2] to the process $\mathcal{X}$ under consideration. It should be noted that Equation (2.8) can be thought of as the specialization of the

recurrence formulas for hitting times for semi-Markov processes derived by Silvestrov [115, Theorem 2]. For recurrence relations for moments of integer order for hitting times in Markov chains, the reader is referred to [36, 70, 75, 102], among others.

The solutions $\mathbf{a}_{\mathcal{C}}(m', n')$ and $\boldsymbol{\tau}^*(m', n')$, for each absorbing state $(m', n') \in \mathcal{C}_0$, may be specified uniquely by Equations (2.7) and (2.8), but these equations are not analytically tractable. It is worth noting that this analytical drawback is connected to the fact that the extinction time T amounts to a phase-type (PH) random variable defined on a countable class $\mathcal{C}$ of transient states, instead of a finite number [91, Chapter 2]. This is not the only problem since the Markov chain $\mathcal{X}$ defined by (2.1) does not satisfy the uniformly bounded condition $\sup_{(m,n)\in\mathcal{C}} q_{(m,n)} = c < \infty$. We refer the reader to [114] for a detailed discussion on the subclass of countable phase-type distributions with the additional condition $c < \infty$, for which uniform approximation results and error bounds are satisfactorily derived.

One way of analyzing (2.7) is to approximate the behavior of $\mathcal{X}$, when the initial population sizes are large, by an essentially deterministic motion with a random diffusion of smaller order superimposed upon it. This approach is used by Ridler-Rowe [108], who states the asymptotic distribution of the position $X(T)$ at which the process $\mathcal{X}$ first hits the subset $\mathcal{C}_0$ of absorbing states (i.e., the identity of the species that first becomes extinct and the size of the surviving species), and a limit result for the probability that a given species should survive the other; as a related work, see [19, Section 3]. To be concrete, it is derived by Ridler-Rowe [108] that, starting from the initial state $X(0)$, the random variable

$$\boldsymbol{\mu}(X(T) - X(0))N^{-1/2}$$

converges weakly, uniformly in $X(0)$, as $N \to \infty$ to a Normal random variable of zero mean and variance $\gamma\delta(\gamma+\delta)(\gamma^2+\delta^2)^{-3/2}$, where $\boldsymbol{\mu}$ is the unit vector in the direction of (γ, δ) and $N = r(X(0))$ is the signed distance from the initial population size $X(0)$ to the non-negative axes, measured in the $\boldsymbol{\mu}$-direction. An intuitive representation of this result is given in [108, Figure 2], presented here as Figure 2.2.

The Normal approximation in [108] alone may not answer all the questions which might reasonably be asked about the time T

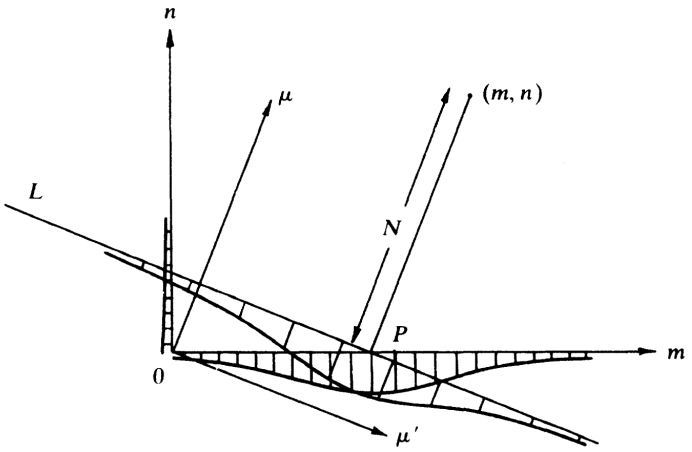

Fig. 2.2. Normal approximation of Ridler-Rowe [108, Figure 2]

at which one or other of the species first becomes extinct, and about the joint distribution of $(T, X(T))$, particularly under the assumption of small or moderate initial population sizes. In order to illustrate this assertion, we focus on the mean size of the surviving species obtained from the Normal approximation [108], which is denoted by μ_N, and carry out a set of numerical examples in twelve scenarios. These scenarios are defined in terms of the birth and death rates. Specifically, for species 1, we assume a birth rate $\alpha = 1.0$ and death rates $\gamma \in \{\alpha 2^{-1}, \alpha 4^{-1}\}$. The birth and death rates in species 2 are given by $\beta \in \{\alpha 2^{-1}, \alpha, 2\alpha\}$ and $\delta \in \{\beta 2^{-1}, \beta 4^{-1}\}$, respectively.

Values of μ_N are listed in Table 2.1 for the above scenarios with various initial population sizes $X(0)$, and compared with the corresponding mean sizes μ_S of the surviving species obtained from a simulation study of the process $\mathcal{X}$. In the simulation study, the identity of the surviving species and the expected number of individuals alive at time T are estimated from 10^5 simulations starting at the initial population size $X(0)$. For a fixed initial population size $X(0)$, each cell in Table 2.1 is related to a scenario $(\alpha, \gamma, \beta, \delta)$, and it lists, from top to bottom, the identity of the surviving species and the value of μ_N obtained from [108], and the identity of the surviving species and the value of μ_S as we develop simulations of $\mathcal{X}$. We use the digits 1 and 2 to identify species

Table 2.1. Mean sizes of the surviving species for 12 scenarios with $\alpha = 1.0$

$X(0)$	γ	(β, δ)	(0.5,0.25)	(0.5,0.125)	(1.0,0.5)	(1.0,0.25)	(2.0,1.0)	(2.0,0.5)
(24,24)	0.5	Surv. species	2	2	0	2	1	0
		μ_N	12.00000	18.00000	0.00000	12.00000	12.00000	0.00000
		Surv. species	2	2	2	2	1	2
		μ_S	14.39270	21.43380	0.01430	18.61660	14.23190	9.32360
	0.25	Surv. species	0	2	1	0	1	1
		μ_N	0.00000	12.00000	12.00000	0.00000	18.00000	12.00000
		Surv. species	1	2	1	1	1	1
		μ_S	9.24360	16.31350	18.70970	0.39100	21.40310	16.14890
(34,34)	0.5	Surv. species	2	2	0	2	1	0
		μ_N	17.00000	25.50000	0.00000	17.00000	17.00000	0.00000
		Surv. species	2	2	2	2	1	2
		μ_S	19.78675	29.23385	0.03875	24.31687	19.75218	9.63108
	0.25	Surv. species	0	2	1	0	1	1
		μ_N	0.00000	17.00000	17.00000	0.00000	25.50000	17.00000
		Surv. species	1	2	1	1	1	1
		μ_S	9.68797	22.74646	24.33355	0.12098	29.23894	22.71262
(54,54)	0.5	Surv. species	2	2	0	2	1	0
		μ_N	27.00000	40.50000	0.00000	27.00000	27.00000	0.00000
		Surv. species	2	2	1	2	1	2
		μ_S	30.30773	44.64161	0.00368	35.14275	30.28732	10.34857
	0.25	Surv. species	0	2	1	0	1	1
		μ_N	0.00000	27.00000	27.00000	0.00000	40.50000	27.00000
		Surv. species	1	2	1	2	1	1
		μ_S	10.35811	33.91493	35.13565	0.04100	44.63335	33.96864
(94,94)	0.5	Surv. species	2	2	0	2	1	0
		μ_N	47.00000	70.50000	0.00000	47.00000	47.00000	0.00000
		Surv. species	2	2	1	2	1	2
		μ_S	50.82155	75.13270	0.16130	56.11184	50.82980	10.97545
	0.25	Surv. species	0	2	1	0	1	1
		μ_N	0.00000	47.00000	47.00000	0.00000	70.50000	47.00000
		Surv. species	1	2	1	1	1	1
		μ_S	11.06055	54.87997	56.08494	0.06847	75.14674	54.97620
(174,174)	0.5	Surv. species	2	2	0	2	1	0
		μ_N	87.00000	130.50000	0.00000	87.00000	87.00000	0.00000
		Surv. species	2	2	1	2	1	2
		μ_S	91.46656	135.74034	0.08866	97.23700	91.38477	11.55587
	0.25	Surv. species	0	2	1	0	1	1
		μ_N	0.00000	87.00000	87.00000	0.00000	130.50000	87.00000
		Surv. species	1	2	1	2	1	1
		μ_S	11.65431	95.97211	97.31016	0.01220	135.70454	95.92758
(334,334)	0.5	Surv. species	2	2	0	2	1	0
		μ_N	167.00000	250.50000	0.00000	167.00000	167.00000	0.00000
		Surv. species	2	2	1	2	1	2
		μ_S	171.97778	256.35745	0.04989	178.46607	172.04491	12.35788
	0.25	Surv. species	0	2	1	0	1	1
		μ_N	0.00000	167.00000	167.00000	0.00000	250.50000	167.00000
		Surv. species	1	2	1	1	1	1
		μ_S	12.30379	177.14928	178.36785	0.05514	256.28266	177.13617

1 and 2 as surviving species; in the Normal approximation, the digit 0 amounts to the absorption in $(0, 0)$. An examination of Table 2.1 reveals an important drawback in the asymptotic result of [108] and its practical use: the Normal approximation leads to identical estimations in scenarios with common death rates γ and δ, regardless of concrete magnitudes of α and β. However, these preliminary numerical results also show that the birth rates α and

β influence noticeably on the dynamics of the process $\mathcal{X}$ if the initial population sizes $X(0)$ are assumed small or moderate.

Our major aim in this chapter is to present an alternative approach for analyzing $\mathcal{X}$, which incorporates the birth rates α and β into modelling aspects and is amenable to numerical calculation. This approach, based on the use of percentiles of the maximum number of individuals in the ecosystem, works specially under the assumption of small initial states $X(0)$, and it permits us to study some interesting descriptors like the time until the first extinction, the size of the surviving species, the number of births and deaths until the extinction, or the survival of a certain individual.

This chapter is organized as follows. In Section 2.2, we characterize the distribution of the maximum number of individuals in the ecosystem, which permits us to propose the PH approximation for the time until the first extinction and the size of the surviving species. We present a wide range of numerical results in order to discuss about the accuracy of our method, compare our approximation with the Normal approximation, and illustrate our results. The analysis of Section 2.2 is complemented in Sections 2.3 and 2.4 by applying similar truncation procedures in order to study the numbers of births and deaths happening during an extinction cycle, and the survival probability of a certain individual. Concluding remarks of this chapter are contained in Section 2.5.

2.2 Time until the first extinction and size of the surviving species

In Subsection 2.2.1, we deal with the distribution of the maximum number of individuals alive in the ecosystem, which measures the overpopulation on the ecosystem and allows us to present in Subsection 2.2.2 an approximating solution for the extinction times, and for the distribution of the identity and size of the surviving species. In Subsection 2.2.3, we present some numerical results to illustrate the effects of the birth and death rates on the expected extinction times and the extinction probabilities, depending on various quasi-stationary distributions for initial population sizes. We also develop a set of numerical experiments to compare our

approach with the asymptotic results of Ridler-Rowe [108], and results obtained by simulation.

2.2.1 Maximum number of individuals in the ecosystem

Define an extinction cycle as the period that starts from an initial population size $X(0) = (m, n) \in \mathcal{C}$, and it ends when one or the other species first becomes extinct. Our objective here is to derive the distribution of the maximum level visited by $\mathcal{X}$ (i.e., the maximum number of individuals alive at the same time in the ecosystem) during an extinction cycle, denoted by $X_{\max}$, since such a descriptor is an important measure in studying the effects of overpopulation on the ecosystem.

We may observe that, for $(m, n) \in \mathcal{C}$, the conditional probability $P(X_{\max} \leq x | X(0) = (m, n))$ is equal to the probability that, starting from (m, n), the process $\mathcal{X}$ enters the subset of absorbing states $\mathcal{C}_0$, but avoiding the states of $\cup_{k=x+1}^{\infty} l(k)$. Hence, for each fixed $x \in \{2, 3, ...\}$, we consider an absorbing process $\overline{\mathcal{X}}(x)$ defined on the state space

$$\overline{\mathcal{S}}(x) = \{0\} \cup \bigcup_{k=2}^{x} l(k) \cup \{x + 1\},$$

where the states 0 and $x+1$ are obtained by lumping the set $\mathcal{C}_0$ of absorbing states and the states of $\cup_{k=x+1}^{\infty} l(k)$ together to make two absorbing states. The infinitesimal generator of $\overline{\mathcal{X}}(x)$ is defined as

$$\overline{\mathbf{Q}}(x) = \begin{pmatrix} 0 & \mathbf{0}_{J(x)}^T & 0 \\ \mathbf{t}_0(x) & \mathbf{T}(x) & \mathbf{t}_{x+1}(x) \\ 0 & \mathbf{0}_{J(x)}^T & 0 \end{pmatrix},$$

where $J(x)$ is the cardinality of the set $\cup_{k=2}^{x} l(k)$ (i.e., $J(x) = x(x-1)2^{-1}$),

$$\mathbf{t}_0(x) = \begin{pmatrix} \mathbf{A}_{2,1}\mathbf{e}_2 \\ \mathbf{A}_{3,2}\mathbf{e}_2 \\ \vdots \\ \mathbf{A}_{x,x-1}\mathbf{e}_2 \end{pmatrix},$$

$$\mathbf{T}(x) = \begin{pmatrix} \mathbf{B}_{2,2} & \mathbf{B}_{2,3} & & & & \\ \mathbf{B}_{3,2} & \mathbf{B}_{3,3} & \mathbf{B}_{3,4} & & & \\ & \ddots & \ddots & \ddots & & \\ & & \mathbf{B}_{x-1,x-2} & \mathbf{B}_{x-1,x-1} & \mathbf{B}_{x-1,x} \\ & & & \mathbf{B}_{x,x-1} & \mathbf{B}_{x,x} \end{pmatrix}, \quad (2.9)$$

$$\mathbf{t}_{x+1}(x) = \begin{pmatrix} 0 \\ \vdots \\ 0 \\ \mathbf{B}_{x,x+1}\mathbf{e}_x \end{pmatrix}.$$

Since the class $\mathcal{C}$ is irreducible, the set $\cup_{k=2}^{x} l(k)$ consists of transient states and the sub-matrix $\mathbf{T}(x)$ is non-singular. The real part of each eigenvalue of $\mathbf{T}(x)$ is thus strictly negative and $\mathbf{T}(x)$ is stable. If one expands $\exp\{\mathbf{T}(x)t\}$ and $\mathbf{T}(x)$ is replaced by its Jordan form, then it is seen that $\lim_{t\to\infty} \exp\{\mathbf{T}(x)t\} = \mathbf{0}_{J(x)\times J(x)}$. Therefore, the column vector

$$\int_0^\infty \exp\{\mathbf{T}(x)u\}\mathbf{t}_0(x)du = \left(-\mathbf{T}^{-1}(x)\right)\mathbf{t}_0(x)$$

contains the conditional probabilities that the absorption into 0 occurs in a finite time; see [76, Section 2.4]. Note that the entries of the matrix exponential $\exp\{\mathbf{T}(x)u\}$ amount to the probabilities that up to time u the process $\mathcal{X}(x)$ does not leave the subset $\cup_{k=2}^{x} l(k)$ of transient states.

This has the following immediate consequence.

Theorem 2.2. *Let* $\mathbf{p}(x)$ *define a column vector of order* $J(x)$ *with entries* $P(X_{max} \leq x|X(0) = (m,n))$*, for* $(m,n) \in \cup_{k=2}^{x} l(k)$*. Then, we can express* $\mathbf{p}(x)$ *as follows:*

$$\mathbf{p}(x) = \left(-\mathbf{T}^{-1}(x)\right)\mathbf{t}_0(x), \quad x \in \{2,3,...\}.$$

Moreover, we have that $P(X_{max} \leq x|X(0) = (m,n)) = 1$ *if* $(m,n) \in \mathcal{C}_0$*, and* 0 *if* $(m,n) \in \bigcup_{k=x+1}^{\infty} l(k)$*.*

The probability distribution function $F_{max}(x) = P(X_{max} \leq x)$ is derived as

$$F_{max}(x) = \boldsymbol{\pi}(x)\mathbf{p}(x), \quad x \in \{2,3,...\},$$

where $\boldsymbol{\pi}(x)$ is a sub-vector that consists of initial probabilities over states of the subset $\cup_{k=2}^{x} l(k)$. We shall return briefly to the choice of $\boldsymbol{\pi}(x)$ at Remarks 2.1 and 2.2.

For a given probability $q \in (0,1)$, the $(100q)$th percentile K_q of X_{max} satisfies $F_{max}(K_q-1) \leq q < F_{max}(K_q)$. Assume that the support $\{2,3,...\}$ of X_{max} is replaced by the finite subset $\{2,3,...,K_q\}$. Then, the influence of the subset $\{K_q+1, K_q+2, ...\}$, which consists of those states removed from the support, becomes progressively negligible as q tends to one, since $P(X_{max} > K_q) < 1-q$. In Subsection 2.2.2, we use the parameter q and the resulting value K_q to replace the population process $\mathcal{X}$ defined on the quarter plane $\mathcal{S}$ by a process $\mathcal{X}(K_q)$ defined on a finite state space $\mathcal{S}(K_q)$, which yields a PH distribution for the time until extinction in the approximating process. The set $\mathcal{S}(K_q)$ essentially collects all state $(m,n) \in \mathcal{S}$ for which the total size $m+n$ of the ecosystem is not greater than the percentile K_q of the maximum number X_{max} of individuals alive during an extinction cycle.

The next algorithm provides an iterative procedure for computing the $(100q)$th percentile K_q of X_{max}, for $q \in (0,1)$. Its proof is based on a partition of $\mathbf{T}(x)$ by using sub-matrices associated with the previous value $x-1$, and it is inspired from block-Gaussian elimination; see e.g. [76].

Algorithm 2.1. Computation of K_q

Step 1 $x := 2$;
$-\mathbf{T}^{-1}(x) := (\alpha+\gamma+\beta+\delta)^{-1}$;
$\mathbf{t}_0(x) := \gamma+\delta$;
$\mathbf{p}(x) := (-\mathbf{T}^{-1}(x))\mathbf{t}_0(x)$;
$F_{max}(x) := \boldsymbol{\pi}(x)\mathbf{p}(x)$.

Step 2 $x := x+1$;
partition $\mathbf{T}(x)$ as $\begin{pmatrix} \mathbf{T}(x-1) & \mathbf{B}'_{x-1,x} \\ \mathbf{B}'_{x,x-1} & \mathbf{B}_{x,x} \end{pmatrix}$;
$\mathbf{C}_{2,2} := \left(-\mathbf{B}_{x,x} - \mathbf{B}'_{x,x-1}\left(-\mathbf{T}^{-1}(x-1)\right)\mathbf{B}'_{x-1,x}\right)^{-1}$;
$\mathbf{C}_{2,1} := \mathbf{C}_{2,2}\mathbf{B}'_{x,x-1}\left(-\mathbf{T}^{-1}(x-1)\right)$;
$\mathbf{C}_{1,2} := \left(-\mathbf{T}^{-1}(x-1)\right)\mathbf{B}'_{x-1,x}\mathbf{C}_{2,2}$;
$\mathbf{C}_{1,1} := \left(-\mathbf{T}^{-1}(x-1)\right) + \left(-\mathbf{T}^{-1}(x-1)\right)\mathbf{B}'_{x-1,x}\mathbf{C}_{2,1}$;
$-\mathbf{T}^{-1}(x) := \begin{pmatrix} \mathbf{C}_{1,1} & \mathbf{C}_{1,2} \\ \mathbf{C}_{2,1} & \mathbf{C}_{2,2} \end{pmatrix}$;

$$\mathbf{p}(x) := \begin{pmatrix} \mathbf{p}(x-1) + \mathbf{C}_{1,2}(\mathbf{B}'_{x,x-1}\mathbf{p}(x-1) + \mathbf{A}_{x,x-1}\mathbf{e}_2) \\ \mathbf{C}_{2,2}(\mathbf{B}'_{x,x-1}\mathbf{p}(x-1) + \mathbf{A}_{x,x-1}\mathbf{e}_2) \end{pmatrix};$$
$$F_{max}(x) := \boldsymbol{\pi}(x)\mathbf{p}(x).$$

Step 3 If $F_{max}(x-1) \leq q < F_{max}(x)$, then $K_q := x$; otherwise, store $-\mathbf{T}^{-1}(x)$, $\mathbf{p}(x)$ and $F_{max}(x)$, and repeat Step 2.

Remark 2.1. The convergence of Algorithm 2.1 is guaranteed since the absorption is certain. To avoid a low-order increase of $F_{max}(x)$, we advise to write a control statement allowing us to evaluate differences in magnitude between two values, say $x - x_0$ and x, as we handle large enough values of x. Therefore, Step 3 will progressively increase x until finding the percentile K_q (i.e., the value x satisfying $F_{max}(x-1) \leq q < F_{max}(x)$) or a value x such that $F_{max}(x) - F_{max}(x - x_0) < \varepsilon_0$, where $\varepsilon_0 > 0$ is an arbitrary small value and x_0 is a predetermined integer.

Remark 2.2. The sub-vector $\boldsymbol{\pi}(x)$ in Step 2 is a part of an appropriately defined probability vector $\boldsymbol{\pi}$ on the irreducible class $\mathcal{C}$ of transient states. More concretely, we partition the class $\mathcal{C}$ into two subsets, the first subset consisting of all states at $\cup_{k=2}^{x} l(k)$, and the second subset consisting of all states at $\cup_{k=x+1}^{\infty} l(k)$. This partitioning decomposes the vector $\boldsymbol{\pi}$ into two sub-vectors $(\boldsymbol{\pi}(x), \boldsymbol{\pi}'(x))$. An efficient way to approximate $\boldsymbol{\pi}$, when it cannot be obtained explicitly, is based on the use of augmented finite Markov chains; see Remark 2.3.

2.2.2 PH approximation

Once K_q is in hand, the next issue to deal with is the joint distribution of the random vector $(T, X(T))$, which records the time at which one or other of the species first becomes extinct, the identity of the species becoming extinct and the size of the surviving species.

To that end, the process $\mathcal{X}$ is replaced by an approximating process $\mathcal{X}(K_q)$ defined on the state space

$$\mathcal{S}(K_q) = \mathcal{C}_0(K_q) \cup \bigcup_{k=2}^{K_q} l(k),$$

where $\mathcal{C}_0(K_q) = \{(m,0) : 1 \le m \le K_q - 1\} \cup \{(0,n) : 1 \le n \le K_q - 1\}$. Its infinitesimal generator is given by

$$\mathbf{Q}(K_q) = \begin{pmatrix} \mathbf{0}_{2(K_q-1)\times 2(K_q-1)} & \mathbf{0}_{2(K_q-1)\times J(K_q)} \\ \mathbf{S}_0(K_q) & \mathbf{S}(K_q) \end{pmatrix},$$

where $\mathbf{S}_0(K_q) = \mathrm{diag}(\mathbf{A}_{2,1}, \mathbf{A}_{3,2}..., \mathbf{A}_{K_q,K_q-1})$ and $\mathbf{S}(K_q)$ is defined as the sub-matrix $\mathbf{T}(K_q)$ in (2.9) with $\mathbf{B}_{K_q,K_q}$ replaced by a diagonal matrix of order K_q-1 with ith entry given by $-i(K_q-i)(\gamma+\delta)$, for $1 \le i \le K_q - 1$.

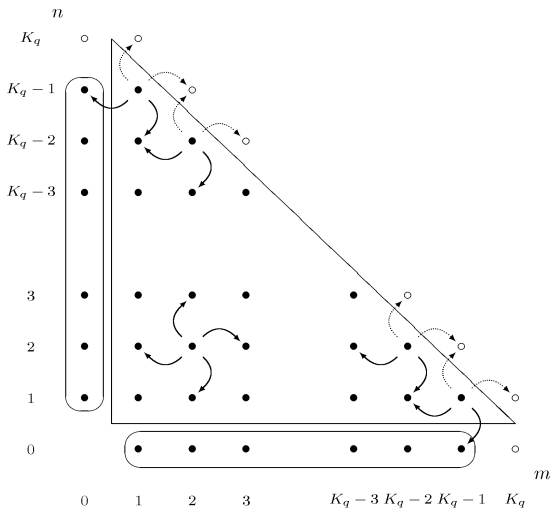

Fig. 2.3. State space $\mathcal{S}(K_q)$ and transitions in the approximating model $\mathcal{X}(K_q)$

To motivate the use of $\mathcal{X}(K_q)$, we remark that $\mathcal{X}(K_q)$ governs the dynamics of the original process $\mathcal{X}$ under the taboo that states of $\cup_{k=K_q+1}^{\infty} l(k)$ are not accessible. It can be observed that, under this constraint, the absorbing states $(K_q, 0)$ and $(0, K_q)$ are not accessible from $\mathcal{S}(K_q)$; see Figure 2.3. As q increases (and K_q thus increases), the likelihood in $\mathcal{X}$ of those transitions from states of the K_qth level to states of the $(K_q + 1)$st level progressively decreases, and therefore a majority of sample paths in $\mathcal{X}$ will not leave the set $\cup_{k=2}^{K_q} l(k)$ of *low* levels. To be concrete, assume that

the ecosystem has been going on for a long time, and that the extinction of one or other of the species has not occurred. The likelihood of the transitions from the K_qth level to the (K_q+1)st level can be thought of as a function of q and, in particular, it may be measured in terms of the probability p_q, starting from $\cup_{k=2}^{K_q} l(k)$, of leaving the states of $\cup_{k=2}^{K_q} l(k)$ in the next transition. We are expect the convergence of p_q towards zero to occur as q tends to one. This means that, for $q \in (0,1)$ large enough, we may find $p_q < \varepsilon$, for an arbitrary small value $\varepsilon > 0$.

This behavior becomes apparent in Table 2.2 where we list values of p_q for the twelve scenarios introduced in Section 2.1 and a variety of values of q, when the quasi-stationary distribution $\mathbf{v}(K_q)$ (see [44, Section 3]) defines the initial probability distribution over the set $\cup_{k=2}^{K_q} l(k)$ of transient states. The initial probability vector $\mathbf{v}(K_q)$ is given by the left eigenvector of $\mathbf{S}(K_q)$ corresponding to the characteristic value $\rho_1(K_q)$ with maximal real part. Note that $\rho_1(K_q)$ is real, simple and less than zero, and that $\mathbf{v}(K_q)$ is uniquely determined if it satisfies $\mathbf{v}(K_q)\mathbf{e}_{J(K_q)} = 1$ and $\mathbf{v}(K_q)\mathbf{w}(K_q) = 1$, where $\mathbf{w}(K_q)$ is its right eigenvector counterpart.

If $q \in (0,1)$ is close to one, the process $\mathcal{X}$ evolving before the absorption tends to move to low levels $\cup_{k=2}^{K_q} l(k)$, though even then it visits occasionally states of *high* levels $\cup_{k=K_q+1}^{\infty} l(k)$. In view of Table 2.2, the effect of the sample paths to states of the (K_q+1)st level, starting from $\cup_{k=2}^{K_q} l(k)$, becomes relatively negligible as q tends to one, which gives a satisfactory criterion to replace the original process $\mathcal{X}$ by the approximating process $\mathcal{X}(K_q)$ defined on the finite state space $\mathcal{S}(K_q)$. Then, the use of the $(100q)$th percentile K_q of X_{max} allows us to interpret the probability $1-q$ as a global error control.

Let $T(K_q)$ be the time at which one or other of the species first becomes extinct in the process $\mathcal{X}(K_q)$, and $\boldsymbol{\pi}(K_q)$ denote an initial distribution over the set $\cup_{k=2}^{K_q} l(k)$ of transient states.

Theorem 2.3. *Define the joint distribution of $T(K_q)$ and the size $X(T(K_q))$ of the surviving species in terms of the probabilities $F_q(t;(m,0)) = P(T(K_q) \le t, X(T(K_q)) = (m,0))$, for $1 \le m \le K_q - 1$, and $F_q(t;(0,n)) = P(T(K_q) \le t, X(T(K_q)) = (0,n))$, for*

Table 2.2. Values of K_q and p_q versus q for 12 scenarios with $\alpha = 1.0$

γ	β	δ	q	0.9	0.925	0.95	0.975	0.99	0.995	0.999
0.5	0.5	0.25	K_q	13	14	15	18	21	24	29
			p_q	0.01282	0.00908	0.00646	0.00235	0.00086	0.00032	0.00006
		0.125	K_q	20	22	24	29	34	39	48
			p_q	0.01276	0.00854	0.00574	0.00215	0.00081	0.00031	0.00005
0.5	1.0	0.5	K_q	11	11	12	14	16	17	21
			p_q	0.00994	0.00994	0.00586	0.00204	0.00071	0.00042	0.00005
		0.25	K_q	15	15	17	19	22	25	30
			p_q	0.01081	0.01081	0.00540	0.00273	0.00100	0.00037	0.00007
0.5	2.0	1.0	K_q	13	14	15	18	21	24	29
			p_q	0.01281	0.00908	0.00646	0.00235	0.00086	0.00032	0.00006
		0.5	K_q	17	19	21	24	28	31	37
			p_q	0.01480	0.00850	0.00491	0.00217	0.00073	0.00032	0.00006
0.25	0.5	0.25	K_q	17	19	21	24	28	31	37
			p_q	0.01480	0.00850	0.00491	0.00217	0.00073	0.00032	0.00006
		0.125	K_q	29	32	35	41	48	54	66
			p_q	0.01415	0.00904	0.00579	0.00238	0.00084	0.00035	0.00006
0.25	1.0	0.5	K_q	15	15	17	19	22	25	30
			p_q	0.01081	0.01081	0.00540	0.00273	0.00100	0.00037	0.00007
		0.25	K_q	22	24	25	29	33	36	43
			p_q	0.01276	0.00775	0.00604	0.00220	0.00079	0.00037	0.00006
0.25	2.0	1.0	K_q	20	22	24	29	34	39	48
			p_q	0.01276	0.00854	0.00574	0.00215	0.00081	0.00031	0.00005
		0.5	K_q	29	32	35	41	48	54	66
			p_q	0.01415	0.00904	0.00579	0.00238	0.00084	0.00035	0.00006

$1 \le n \le K_q - 1$. *Then,*

$$F_q(t;(m,0)) = \boldsymbol{\pi}(K_q)\left(\exp\{\mathbf{S}(K_q)t\} - \mathbf{I}_{J(K_q)}\right)\mathbf{S}^{-1}(K_q)\mathbf{S}_0(K_q) \times \mathbf{e}_{2(K_q-1)}(2m-1), \tag{2.10}$$

$$F_q(t;(0,n)) = \boldsymbol{\pi}(K_q)\left(\exp\{\mathbf{S}(K_q)t\} - \mathbf{I}_{J(K_q)}\right)\mathbf{S}^{-1}(K_q)\mathbf{S}_0(K_q) \times \mathbf{e}_{2(K_q-1)}(2n), \tag{2.11}$$

and the extinction time $T(K_q)$ follows a PH distribution with representation $(\boldsymbol{\pi}(K_q), \mathbf{S}(K_q))$ of order $J(K_q)$.

Proof. The standard transition function $\mathbf{P}(t;K_q)$ of the process $\mathcal{X}(K_q)$ is defined by the elements $P(X(t) = (m',n')|X(0) = (m,n))$, for $(m,n),(m',n') \in \mathcal{S}(K_q)$, and it is given by $\mathbf{P}(t;K_q) = \exp\{\mathbf{Q}(K_q)t\}$.

Straightforward algebra leads to the following expression for $\mathbf{P}(t; K_q)$:

$$\begin{pmatrix} \mathbf{I}_{2(K_q-1)\times 2(K_q-1)} & \mathbf{0}_{2(K_q-1)\times J(K_q)} \\ \left(\exp\{\mathbf{S}(K_q)t\} - \mathbf{I}_{J(K_q)}\right)\mathbf{S}^{-1}(K_q)\mathbf{S}_0(K_q) & \exp\{\mathbf{S}(K_q)t\} \end{pmatrix}. \tag{2.12}$$

Thus, the joint probabilities in (2.10) and (2.11) are directly derived from (2.12), and the marginal distribution of $T(K_q)$ follows from the structured form of $\mathbf{Q}(K_q)$ and the definition of a PH random variable [91]. □

A distinguishing property of the quasi-stationary distribution [44, Section 3] is that it provides a good approximation of the distribution of the numbers of individuals of each species alive at a certain time, conditional on non-extinction, after a suitable waiting time. Therefore, a natural choice for the initial distribution $\boldsymbol{\pi}(K_q)$ is the left eigenvector $\mathbf{v}(K_q)$ of $\mathbf{S}(K_q)$, whose characteristic value $\rho_1(K_q)$ has maximal real part. Two alternative choices for $\boldsymbol{\pi}(K_q)$ can be found in [44]. First, the *ratio of means* distribution [44, Section 2] is defined, for a given initial distribution $\boldsymbol{\chi}(K_q)$ over $\cup_{k=2}^{K_q} l(k)$, as the vector

$$\mathbf{v}'(K_q) = \left(\boldsymbol{\chi}(K_q)\left(-\mathbf{S}^{-1}(K_q)\right)\mathbf{e}_{J(K_q)}\right)^{-1}\boldsymbol{\chi}(K_q)\left(-\mathbf{S}^{-1}(K_q)\right).$$

It can be easily verified that, when $\boldsymbol{\chi}(K_q)$ is the left eigenvector $\mathbf{v}(K_q)$, the ratio of means distribution results in the quasi-stationary distribution, that is, $\mathbf{v}'(K_q) = \mathbf{v}(K_q)$. Second, based on a *doubly-limiting conditional* distribution [44, Section 4], the initial distribution $\boldsymbol{\pi}(K_q)$ can be defined as the vector $\mathbf{v}''(K_q)$ with ith entry $w_i(K_q)v_i(K_q)$, where $v_i(K_q)$ and $w_i(K_q)$ denote the ith entries of $\mathbf{v}(K_q)$ and $\mathbf{w}(K_q)$, respectively.

Remark 2.3. Note that, when $\boldsymbol{\pi}(K_q)$ is given by $\mathbf{v}(K_q)$, $\mathbf{v}'(K_q)$ or $\mathbf{v}''(K_q)$, we let the initial probability vector $\boldsymbol{\pi}$ be defined by

$$\boldsymbol{\pi} = \left(\boldsymbol{\pi}(K_q), \mathbf{0}_{K_q}^T, \mathbf{0}_{K_q+1}^T, ...\right).$$

Since K_q is unknown in advance, we shall adapt the evaluation of $\{F_{max}(x-k) : k \in \{1, ..., x-2\}\}$ at the xth iteration of Step 2

(in Algorithm 2.1) in order to generate a non-decreasing sequence of values $\{F_{max}(x) : x \in \{2,3,...\}\}$. To do that, we update at the xth iteration the previously-computed subsequence so that $F_{max}(2) \leq ... \leq F_{max}(x)$. This may be handled in the following manner: we first decompose the probability vector $\boldsymbol{\pi}(x)$ into two sub-vectors $\boldsymbol{\pi}(x) = (\boldsymbol{\pi}_{\leq x-1}(x), \boldsymbol{\pi}_x(x))$, where $\boldsymbol{\pi}_{\leq x-1}(x)$ and $\boldsymbol{\pi}_x(x)$ are associated with states of the subset $\cup_{k=2}^{x-1} l(k)$ and the xth level, respectively, and we replace the computed value $F_{max}(x-1)$ by

$$F_{max}(x-1) = \boldsymbol{\pi}_{\leq x-1}(x)\mathbf{p}(x-1),$$

so that $F_{max}(x-1) \leq F_{max}(x)$. For $k \in \{2,...,x-2\}$, a similar argument based on the decomposition $\boldsymbol{\pi}(x) = (\boldsymbol{\pi}_{\leq x-k}(x), \boldsymbol{\pi}_{x-k+1}(x), ..., \boldsymbol{\pi}_x(x))$ yields the updated values

$$F_{max}(x-k) = \boldsymbol{\pi}_{\leq x-k}(x)\mathbf{p}(x-k), \quad k \in \{2,...,x-2\},$$

verifying $F_{max}(2) \leq ... \leq F_{max}(x-1)$.

For $q \in (0,1)$ and $Re(s) \geq 0$, the Laplace-Stieltjes transforms

$$\varphi_q(s;(m,0)) = \int_{[0,\infty)} e^{-su} F_q(du;(m,0)), \quad 1 \leq m \leq K_q - 1,$$
$$\varphi_q(s;(0,n)) = \int_{[0,\infty)} e^{-su} F_q(du;(0,n)), \quad 1 \leq n \leq K_q - 1,$$

can be evaluated as

$$\varphi_q(s;(m,0)) = \boldsymbol{\pi}(K_q)\left(s\mathbf{I}_{J(K_q)} - \mathbf{S}(K_q)\right)^{-1}\mathbf{S}_0(K_q) \times \mathbf{e}_{2(K_q-1)}(2m-1),$$
$$\varphi_q(s;(0,n)) = \boldsymbol{\pi}(K_q)\left(s\mathbf{I}_{J(K_q)} - \mathbf{S}(K_q)\right)^{-1}\mathbf{S}_0(K_q)\mathbf{e}_{2(K_q-1)}(2n).$$

Since the eventual extinction of one or other of the species is certain, the extinction probabilities in the process $\mathcal{X}(K_q)$ can be defined as

$$p_{ext}(1;K_q) = \sum_{n=1}^{K_q-1} P(X(T(K_q)) = (0,n)),$$
$$p_{ext}(2;K_q) = 1 - p_{ext}(1;K_q),$$

where $P(X(T(K_q)) = (0,n)) = \varphi_q(0;(0,n))$, for $1 \leq n \leq K_q - 1$, that is,

$$p_{ext}(1;K_q) = \boldsymbol{\pi}(K_q)\left(-\mathbf{S}^{-1}(K_q)\right)\mathbf{S}_0(K_q)\mathbf{e}', \tag{2.13}$$

with $\mathbf{e}' = \sum_{n=1}^{K_q-1}\mathbf{e}_{2(K_q-1)}(2n)$. Similarly, it can be seen that

$$\begin{aligned} E[T^k(K_q);(m,0)] &= k!\boldsymbol{\pi}(K_q)\left(-\mathbf{S}^{-1}(K_q)\right)^{k+1}\mathbf{S}_0(K_q) \\ &\quad \times\mathbf{e}_{2(K_q-1)}(2m-1), \\ E[T^k(K_q);(0,n)] &= k!\boldsymbol{\pi}(K_q)\left(-\mathbf{S}^{-1}(K_q)\right)^{k+1}\mathbf{S}_0(K_q)\mathbf{e}_{2(K_q-1)}(2n), \end{aligned}$$

for $1 \le m,n \le K_q-1$, from which it follows that

$$E[T^k(K_q)] = k!\boldsymbol{\pi}(K_q)(-\mathbf{S}^{-1}(K_q))^k\mathbf{e}_{J(K_q)}, \quad k \ge 1.$$

In the case $\boldsymbol{\pi}(K_q) = \mathbf{v}(K_q)$, it can be routinely verified that

$$\begin{aligned} p_{ext}(1;K_q) &= \frac{1}{E[T(K_q)]}\sum_{n=1}^{K_q-1}E[T(K_q);(0,n)], \\ p_{ext}(2;K_q) &= \frac{1}{E[T(K_q)]}\sum_{m=1}^{K_q-1}E[T(K_q);(m,0)], \end{aligned}$$

which can be also derived from the theory of regenerative processes.

2.2.3 Numerical results

In this subsection we first propose a criterion for the selection of q. Then, we focus on the distribution of the size of the surviving species, illustrating our results with some numerical examples. Finally, we develop a comparative study between our solution and the Normal approximation by means of 10^5 simulations of the process $\mathcal{X}$, for the 12 scenarios defined in Table 2.1. We present our results in Tables 2.3-2.5 and Figures 2.11 and 2.12, where the initial state $X(0)$ is appropriately chosen according to a predetermined initial distribution, such as the quasi-stationary distribution and a degenerate distribution.

A criterion for the selection of q

We first discuss on the criterion for the selection of q. We suggest to focus on a criterion based on the probability $p_{ext}(1;K_q)$ that

Table 2.3. Values of K_q and relative errors for 12 scenarios with $\alpha = 1.0$

γ	β	δ	q	0.9	0.925	0.95	0.975	0.99	0.995
0.5	0.5	0.25	K_q	13	14	15	18	**21**	24
			$E(q)$	0.00946	0.00611	0.00393	0.00106	0.00028	0.00007
			$E'(q)$	0.00153	0.00076	0.00041	0.00015	0.00012	0.00012
			$E_{0.999}(q)$	0.00947	0.00612	0.00394	0.00107	0.00029	0.00008
			$E'_{0.999}(q)$	0.00140	0.00063	0.00028	0.00002	$< 10^{-5}$	$< 10^{-6}$
		0.125	K_q	20	22	24	29	**34**	39
			$E(q)$	0.01052	0.00599	0.00337	0.00066	0.00008	0.00030
			$E'(q)$	0.00135	0.00062	0.00034	0.00017	0.00016	0.00016
			$E_{0.999}(q)$	0.01090	0.00638	0.00376	0.00105	0.00030	0.00008
			$E'_{0.999}(q)$	0.00119	0.00046	0.00017	0.00001	$< 10^{-5}$	$< 10^{-6}$
	1.0	0.5	K_q	11	11	**12**	14	16	17
			$E(q)$	0.00081	0.00081	0.00081	0.00081	0.00081	0.00081
			$E'(q)$	0.00128	0.00128	0.00049	0.00012	0.00008	0.00007
			$E_{0.999}(q)$	0.00000	0.00000	0.00000	0.00000	0.00000	0.00000
			$E'_{0.999}(q)$	0.00120	0.00120	0.00041	0.00004	$< 10^{-5}$	$< 10^{-5}$
		0.25	K_q	15	15	17	**19**	22	25
			$E(q)$	0.00479	0.00479	0.00223	0.00111	0.00050	0.00033
			$E'(q)$	0.00068	0.00068	0.00164	0.00187	0.00194	0.00195
			$E_{0.999}(q)$	0.00453	0.00453	0.00196	0.00084	0.00024	0.00006
			$E'_{0.999}(q)$	0.00127	0.00127	0.00031	0.00007	$< 10^{-5}$	$< 10^{-5}$
	2.0	1.0	K_q	13	14	15	**18**	21	24
			$E(q)$	0.00701	0.00460	0.00304	0.00097	0.00041	0.00026
			$E'(q)$	0.00073	0.00002	0.00037	0.00063	0.00066	0.00066
			$E_{0.999}(q)$	0.00681	0.00440	0.00283	0.00076	0.00021	0.00005
			$E'_{0.999}(q)$	0.00140	0.00063	0.00028	0.00002	$< 10^{-5}$	$< 10^{-6}$
		0.5	K_q	17	19	**21**	24	28	31
			$E(q)$	0.00235	0.00127	0.00074	0.00040	0.00026	0.00022
			$E'(q)$	0.00012	0.00010	0.00009	0.00009	0.00009	0.00009
			$E_{0.999}(q)$	0.00214	0.00106	0.00053	0.00019	0.00005	0.00001
			$E'_{0.999}(q)$	0.00002	$< 10^{-5}$	$< 10^{-7}$	$< 10^{-7}$	$< 10^{-9}$	$< 10^{-10}$
0.25	0.5	0.25	K_q	17	19	21	**24**	28	31
			$E(q)$	0.00508	0.00246	0.00120	0.00038	0.00003	0.00004
			$E'(q)$	0.00094	0.00149	0.00149	0.00149	0.00149	0.00149
			$E_{0.999}(q)$	0.00514	0.00255	0.00128	0.00047	0.00012	0.00004
			$E'_{0.999}(q)$	0.00002	$< 10^{-5}$	$< 10^{-7}$	$< 10^{-7}$	$< 10^{-9}$	$< 10^{-10}$
		0.125	K_q	29	32	35	**41**	48	54
			$E(q)$	0.00491	0.00273	0.00153	0.00047	0.00009	0.00001
			$E'(q)$	0.00037	0.00037	0.00037	0.00037	0.00037	0.00037
			$E_{0.999}(q)$	0.00498	0.00280	0.00160	0.00054	0.00015	0.00005
			$E'_{0.999}(q)$	$< 10^{-5}$	$< 10^{-6}$	$< 10^{-7}$	$< 10^{-9}$	$< 10^{-11}$	$< 10^{-12}$
	1.0	0.5	K_q	15	15	17	19	**22**	25
			$E(q)$	0.00715	0.00715	0.00302	0.00122	0.00024	0.00003
			$E'(q)$	0.00001	0.00001	0.00097	0.00121	0.00127	0.00128
			$E_{0.999}(q)$	0.00729	0.00729	0.00316	0.00136	0.00038	0.00010
			$E'_{0.999}(q)$	0.00127	0.00127	0.00031	0.00007	$< 10^{-5}$	$< 10^{-5}$
		0.25	K_q	**22**	24	25	29	33	36
			$E(q)$	0.00002	0.00002	0.00002	0.00002	0.00002	0.00002
			$E'(q)$	0.00039	0.00038	0.00038	0.00038	0.00038	0.00038
			$E_{0.999}(q)$	0.00000	0.00000	0.00000	0.00000	0.00000	0.00000
			$E'_{0.999}(q)$	0.00001	$< 10^{-5}$	$< 10^{-6}$	$< 10^{-7}$	$< 10^{-9}$	$< 10^{-10}$
	2.0	1.0	K_q	20	22	24	29	**34**	39
			$E(q)$	0.01177	0.00695	0.00417	0.00128	0.00049	0.00026
			$E'(q)$	0.00074	0.00001	0.00027	0.00043	0.00044	0.00044
			$E_{0.999}(q)$	0.01160	0.00678	0.00400	0.00112	0.00032	0.00009
			$E'_{0.999}(q)$	0.00119	0.00046	0.00017	0.00001	$< 10^{-5}$	$< 10^{-6}$
		0.5	K_q	29	32	35	**41**	48	54
			$E(q)$	0.00292	0.00139	0.00055	0.00019	0.00046	0.00054
			$E'(q)$	0.00039	0.00039	0.00039	0.00039	0.00039	0.00039
			$E_{0.999}(q)$	0.00350	0.00197	0.00112	0.00038	0.00010	0.00003
			$E'_{0.999}(q)$	$< 10^{-5}$	$< 10^{-6}$	$< 10^{-7}$	$< 10^{-9}$	$< 10^{-11}$	$< 10^{-12}$

species 2 should survive species 1, and the expectation $E[T(K_q)]$ of the time at which a species first becomes extinct. Specifically, we start with an initial probability $q \in (0,1)$ and progressively increase the value of q until the changes in the corresponding relative errors are sufficiently small; that is, we choose the smallest value q with

$$E(q) = \left| 1 - \frac{p_{ext}(1; K_q)}{p_{ext}(1)} \right| < \varepsilon,$$
$$E'(q) = \left| 1 - \frac{E[T(K_q)]}{E[T]} \right| < \varepsilon,$$

for an arbitrary small $\varepsilon > 0$, where $p_{ext}(1)$ and $E[T]$ denote the *true* values of the probability that species 1 becomes extinct and the expectation of the extinction time in the original process $\mathcal{X}$, respectively. Since these values are unknown, we present two applications of this criterion. In the first case, we approximate $p_{ext}(1)$ and $E[T]$ by the values obtained from simulations of the process $\mathcal{X}$. In the second case, $p_{ext}(1)$ and $E[T]$ are replaced by the values $p_{ext}(1; K_{0.999})$ and $E[T(K_{0.999})]$, respectively, which are obtained from the approximating process $\mathcal{X}(K_{0.999})$; in this case, we let $E_{0.999}(q)$ and $E'_{0.999}(q)$ denote the corresponding relative errors.

Table 2.4. Values of $p_{ext}(1; K_q)$ for 12 scenarios with $\alpha = 1.0$

γ	β	δ	q 0.9	0.925	0.95	0.975	0.99	0.995	0.999	$p_{ext}(1)$
0.5	0.5	0.25	0.41430	0.41571	0.41662	0.41782	0.41814	0.41823	0.41827	0.41826
		0.125	0.50977	0.51210	0.51345	0.51485	0.51524	0.51535	0.51539	0.51519
	1.0	0.5	0.50000	0.50000	0.50000	0.50000	0.50000	0.50000	0.50000	0.49959
		0.25	0.61387	0.61387	0.61546	0.61615	0.61652	0.61663	0.61667	0.61683
	2.0	1.0	0.58569	0.58428	0.58337	0.58217	0.58185	0.58176	0.58172	0.58160
		0.5	0.70774	0.70698	0.70661	0.70637	0.70627	0.70625	0.70623	0.70608
0.25	0.5	0.25	0.29225	0.29301	0.29338	0.29362	0.29372	0.29374	0.29376	0.29373
		0.125	0.41102	0.41192	0.41242	0.41286	0.41302	0.41306	0.41308	0.41306
	1.0	0.5	0.38612	0.38612	0.38453	0.38384	0.38347	0.38336	0.38332	0.38337
		0.25	0.50000	0.50000	0.50000	0.50000	0.50000	0.50000	0.50000	0.49998
	2.0	1.0	0.49022	0.48789	0.48654	0.48514	0.48475	0.48464	0.48460	0.48451
		0.5	0.58897	0.58807	0.58757	0.58713	0.58697	0.58693	0.58691	0.58725

To support our selection criterion, we performed several preliminary results. We present in Tables 2.3 and 2.4 a few of our results when the quasi-stationary distribution $\mathbf{v}(K_q)$ defines the initial probability distribution $\boldsymbol{\pi}(K_q)$. For each fixed $q \in (0,1)$, we

recall that, according to the structured form of $\mathbf{Q}(K_q)$ in Subsection 2.2.2, the quasi-stationary vector $\mathbf{v}(K_q)$ on the set $\cup_{k=2}^{K_q} l(k)$ of transient states amounts to the left eigenvector of the sub-matrix $\mathbf{S}(K_q)$ that corresponds to the characteristic value $\rho_1(K_q)$ with maximal real part. Each cell in Table 2.3 is related to a scenario $(\alpha, \gamma, \beta, \delta)$, and it lists, from top to bottom, the percentile K_q (which was already given in Table 2.2), and the relative errors $E(q)$, $E'(q)$, $E_{0.999}(q)$ and $E'_{0.999}(q)$ for various values $q \in [0.9, 1.0)$. The numbers in bold indicate the lowest probabilities q verifying the criterion in terms of $E_{0.999}(q)$ and $E'_{0.999}(q)$ for $\varepsilon = 10^{-3}$. Our scenarios and numerical work not reported here mostly lead to values $q \leq 0.99$, so that the probability $q = 0.99$ could be a suitable selection for practical use. It should be remarked that, for the selection $q = 0.99$, the probability of leaving the states of $\cup_{k=2}^{K_{0.99}} l(k)$ satisfies $p_{0.99} \leq 10^{-3}$; see Table 2.2. In all cases, it can be observed that, as is to be expected, the $(100q)$th percentile K_q of the maximum number X_{max} of individuals alive behaves as a non-decreasing function of the probability q. We may notice that the relative errors $E_{0.999}(q)$ and $E'_{0.999}(q)$ are decreasing functions of q. Moreover, they satisfy $E_{0.999}(q) \leq E'_{0.999}(q)$, with the exception of those scenarios with $\alpha = \beta$ and $\gamma = \delta$. We may therefore conclude that, in terms of the relative errors $E_{0.999}(q)$ and $E'_{0.999}(q)$, this criterion seems to provide a better approximation for the mean extinction time. As intuition tells us, the choice $\alpha = \beta$ and $\gamma = \delta$ results in identical probabilities that a given species should survive the other (i.e., $p_{ext}(1; K_q) = p_{ext}(2; K_q) = 2^{-1}$), and identical mean extinction times

$$\sum_{n=1}^{K_q - 1} E[T(K_q); (0, n)] = \sum_{m=1}^{K_q - 1} E[T(K_q); (m, 0)],$$

in the approximating process $\mathcal{X}(K_q)$, for all $q \in (0, 1)$. It is clear that, in the case $\alpha = \beta$ and $\gamma = \delta$, the extinction probabilities $p_{ext}(1; K_q) = 2^{-1}$ and $p_{ext}(2; K_q) = 2^{-1}$ should be equal to the true values $p_{ext}(1)$ and $p_{ext}(2)$, respectively.

The monotone behavior of $E_{0.999}(q)$ and $E'_{0.999}(q)$ in Table 2.3 allows us to uniquely determine the smallest value q such that $E_{0.999}(q) < \varepsilon$ and $E'_{0.999}(q) < \varepsilon$. A similar remark for $E(q)$ and $E'(q)$ cannot be made because these relative errors do not neces-

sarily decrease with increasing values of q. Thus, in our numerical work in this section, we select the parameter q (and consequently the value of K_q) as the smallest value such that $E_{0.999}(q) < \varepsilon$ and $E'_{0.999}(q) < \varepsilon$.

In Table 2.4, it is observed that, when we fix the scenario, the extinction probability $p_{ext}(1; K_q)$ varies in a monotone manner as a function of q. The values of $p_{ext}(1)$ in Table 2.4 are obtained from a simulation study of the process $\mathcal{X}$. This justifies that, for a large enough $q \in (0, 1)$, the extinction probability $p_{ext}(1; K_q)$ in the approximating process $\mathcal{X}(K_q)$ does not necessarily correspond to a legitime upper or lower bound of the corresponding value of $p_{ext}(1)$ in Table 2.4.

Species becoming extinct and size of the surviving species

We next focus on the distribution of the random vector $X(T(K_q))$ that determines the identity of the species becoming extinct, and the size of the surviving species in the approximating process $\mathcal{X}(K_q)$.

Figures 2.4-2.6 illustrate the effect of q on the mass function of $X(T(K_q))$ for three scenarios $(\gamma, \beta, \delta) \in \{(0.5, 0.5, 0.25), (0.25, 0.5, 0.25), (0.25, 2.0, 1.0)\}$ with $\alpha = 1.0$, and the quasi-stationary distribution for initial population sizes. In these results, the support of $X(T(K_q))$ is expressed in terms of the subset $\{(m, 0) : 1 \leq m \leq K_q - 1\}$ of extinction of species 2, and the subset $\{(0, n) : 1 \leq n \leq K_q - 1\}$ of extinction of species 1. In each scenario, the influence of q is shown for (from top to bottom) four values $q = 0.9$, 0.95, 0.99 and 0.999. In the light of Tables 2.3 and 2.4, Figures 2.4-2.6 corroborate that $q = 0.99$ could be a good choice in approximating the original process $\mathcal{X}$ by $\mathcal{X}(K_q)$ since the essential characteristics (in particular, shape and magnitudes) of the mass function of the position $X(T)$ at which the process $\mathcal{X}$ first hits the set $\mathcal{C}_0$ of absorbing states appear to be appropriately captured by $X(T(K_q))$ when $q = 0.99$.

In Figures 2.4-2.6, we note that the mass function of $X(T(K_q))$ exhibits a two-modal behavior; that is, there exist a first absolute maximum over the subset of extinction of species 1, and a second absolute maximum over the subset of extinction of species 2. This two-modal behavior is closely related to the probabil-

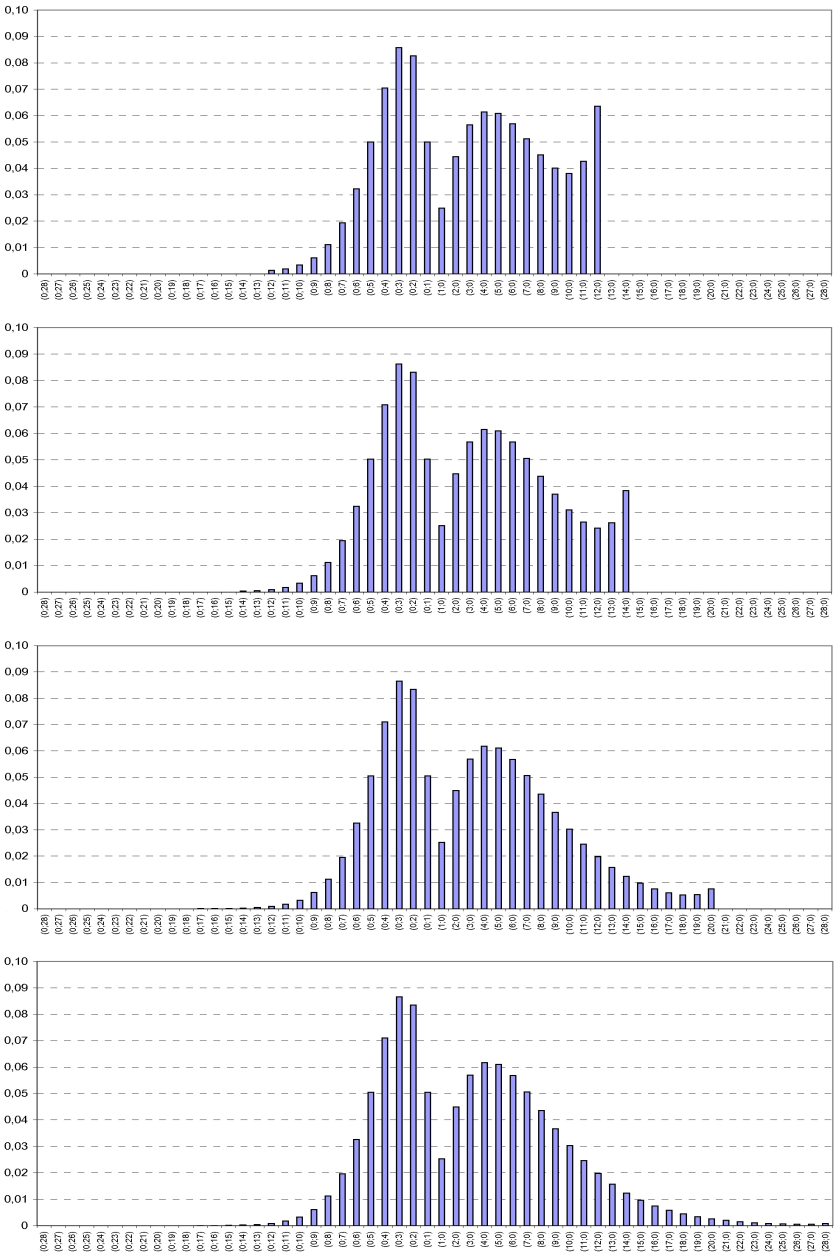

Fig. 2.4. The mass function of $X(T(K_q))$ for (from *top* to *bottom*) $q = 0.9$, 0.95, 0.99 and 0.999. Scenario $(\alpha, \gamma, \beta, \delta) = (1.0, 0.5, 0.5, 0.25)$

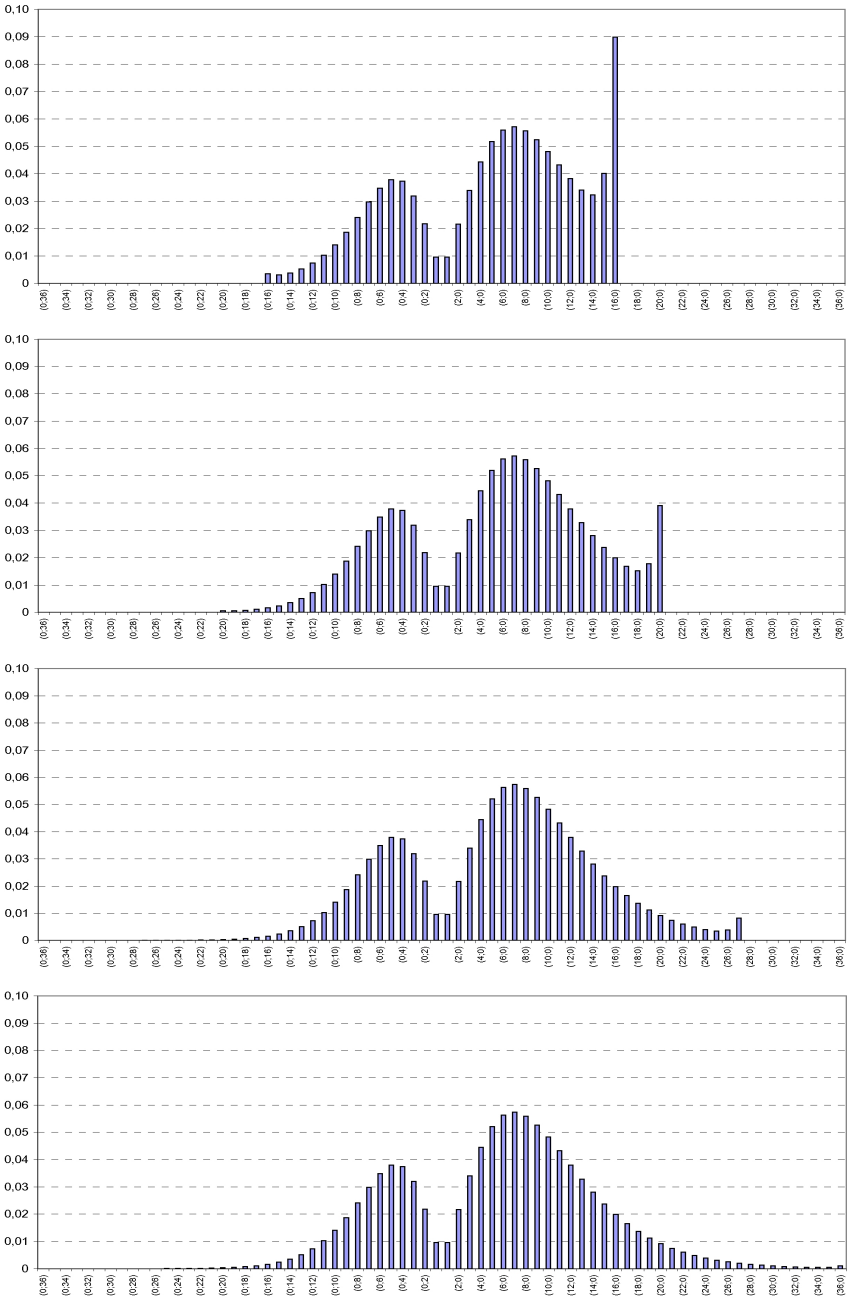

Fig. 2.5. The mass function of $X(T(K_q))$ for (from *top* to *bottom*) $q = 0.9$, 0.95, 0.99 and 0.999. Scenario $(\alpha, \gamma, \beta, \delta) = (1.0, 0.25, 0.5, 0.25)$

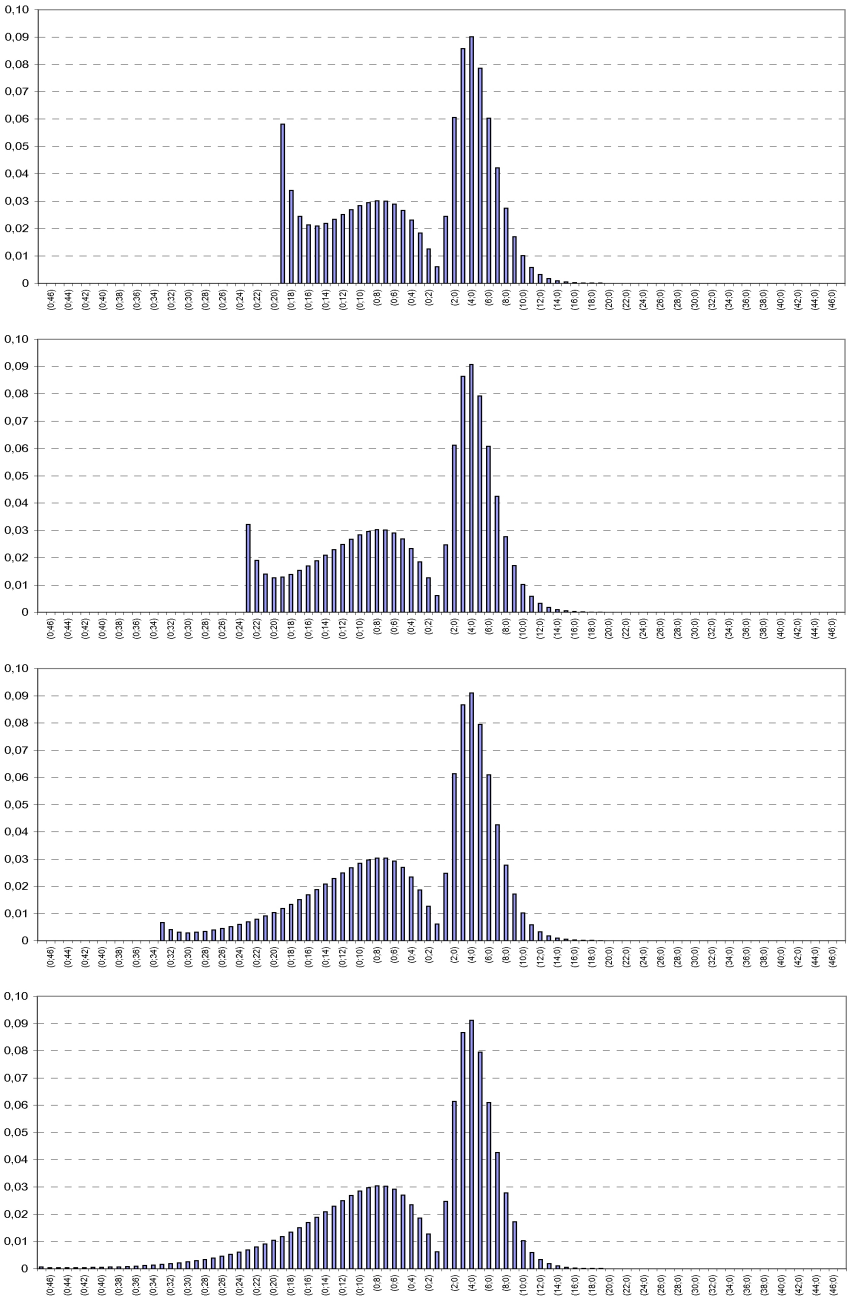

Fig. 2.6. The mass function of $X(T(K_q))$ for (from *top* to *bottom*) $q = 0.9$, 0.95, 0.99 and 0.999. Scenario $(\alpha, \gamma, \beta, \delta) = (1.0, 0.25, 2.0, 1.0)$

ity distribution used for the initial population sizes; see Figures 2.7 and 2.8 where we consider the uniform distribution over the state space $\mathcal{S}(K_q)$ of the approximating process $\mathcal{X}(K_q)$ and the doubly-limiting conditional distribution $\mathbf{v}''(K_q)$ [44, Section 4], and Figure 2.10 where we consider degenerate initial probability distributions. Needless to say, the quasi-stationary, uniform and doubly-limiting conditional distributions lead to strictly positive probabilities at all states of $\mathcal{S}(K_q)$, whereas our choices in Figure 2.10 concentrate probability 1 at a single point. We also note that the quasi-stationary and the doubly-limiting conditional distributions result in mass functions of $X(T(K_q))$ that are graphically undistinguished in our scenarios, whereas the mass function of $X(T(K_q))$ becomes more sparse under the assumption of uniformly distributed initial population sizes.

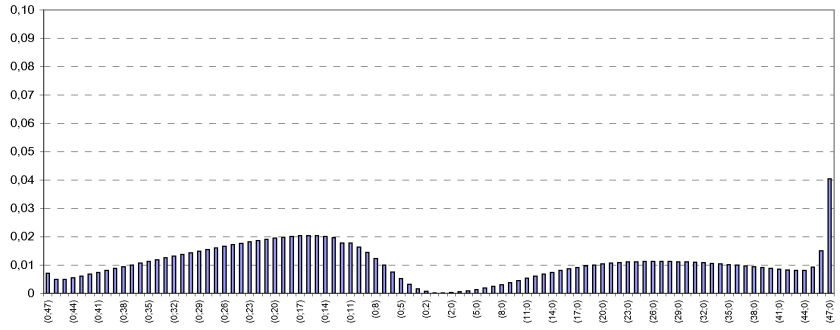

Fig. 2.7. The mass function of $X(T(K_{0.99}))$ for uniformly distributed initial population sizes. Scenario $(\alpha, \gamma, \beta, \delta) = (1.0, 0.25, 0.5, 0.125)$

A comparative analysis

A possible more interesting question concerns the comparative analysis between the solution based on $\mathcal{X}(K_q)$, and those results obtained from the Normal approximation in [108] and from simulations of the original process $\mathcal{X}$.

In Figures 2.9 and 2.10, we first focus on the scenario with parametres $(\alpha, \gamma, \beta, \delta) = (1.0, 0.25, 0.5, 0.125)$ and display the Normal approximation versus our solution. Specifically, we report in

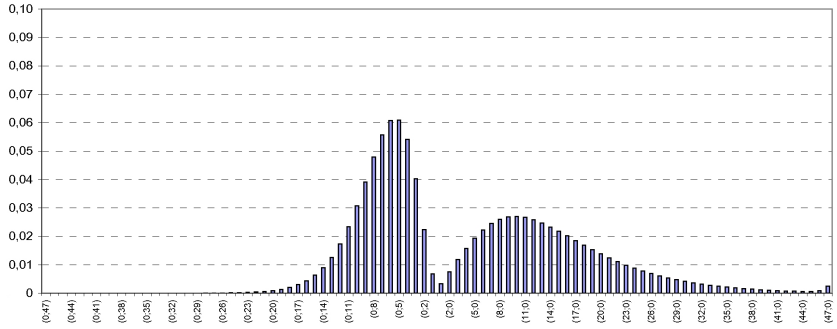

Fig. 2.8. The mass function of $X(T(K_{0.99}))$ for doubly-limiting conditional initial population sizes. Scenario $(\alpha, \gamma, \beta, \delta) = (1.0, 0.25, 0.5, 0.125)$

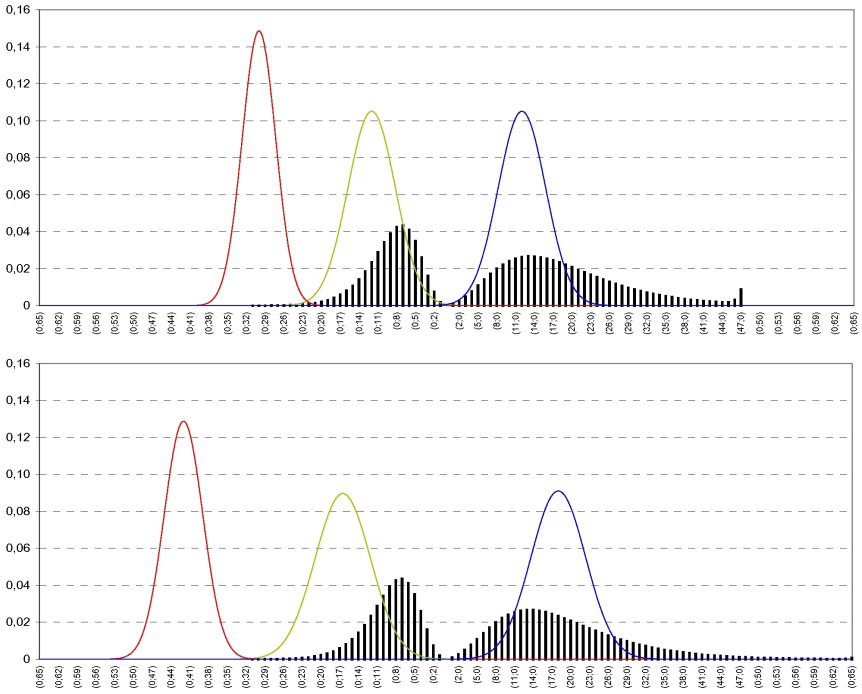

Fig. 2.9. The mass function of $X(T(K_q))$ for (from *top* to *bottom*) $q = 0.99$ and 0.999 versus the Normal approximation for (from *left* to *right*) initial population sizes $X(0) = (12, 36)$, $(24, 24)$ and $(36, 12)$ if $q = 0.99$, and $X(0) = (16, 50)$, $(33, 33)$ and $(50, 16)$ if $q = 0.999$. Scenario $(\alpha, \gamma, \beta, \delta) = (1.0, 0.25, 0.5, 0.125)$

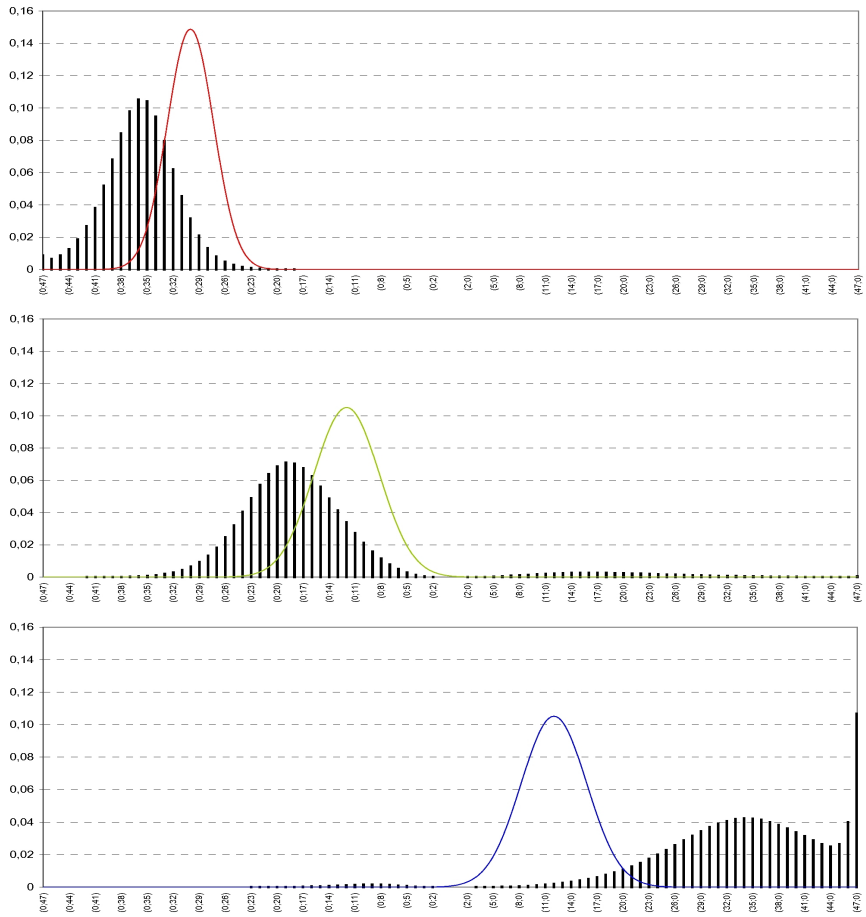

Fig. 2.10. The mass function of $X(T(K_{0.99}))$ and the Normal approximation for (from *top* to *bottom*) initial population sizes $X(0) = (12, 36)$, $(24, 24)$ and $(36, 12)$. Scenario $(\alpha, \gamma, \beta, \delta) = (1.0, 0.25, 0.5, 0.125)$

Figure 2.9 numerical results on the mass function of $X(T(K_q))$ for (from top to bottom) $q = 0.99$ and 0.999 when the quasi-stationary distribution defines the initial probability distribution, and the Normal density function for (from left to right) initial population sizes $X(0) = (12, 36)$, $(24, 24)$ and $(36, 12)$ in the case $q = 0.99$, and $X(0) = (16, 50)$, $(33, 33)$ and $(50, 16)$ in the case $q = 0.999$. In Figure 2.10, we plot the Normal density function for initial population sizes $X(0) = (12, 36)$, $(24, 24)$ and $(36, 12)$, and

the mass function of $X(T(K_q))$ when $q = 0.99$, for three degenerate initial probability distributions concentrating probability 1 at the respective points $(12, 36)$, $(24, 24)$ and $(36, 12)$. The existence of an anomalous mode at the point $(K_{0.99} - 1, 0) = (47, 0)$ in the case $X(0) = (36, 12)$ may be readily explained and softened by increasing the magnitude of $q \in (0.99, 1)$. Roughly speaking, the mass associated with $(K_{0.99} - 1, 0)$ partially accounts for the total probability accumulated by those points $\{(K_{0.99}, 0), (K_{0.99} + 1, 0), ...\}$ that are removed from the positive axis $l(\cdot, 0)$ of extinction of species 2 when the finite process $\mathcal{X}(K_{0.99})$ is defined. This means that, since the effect of the states $\{(K_{0.99}, 0), (K_{0.99} + 1, 0), ...\}$ on the ecosystem does not appear to be negligible, the finite subset $\{(m, 0) : 1 \leq m \leq K_{0.99} - 1)\}$ does not represent suitably the subset $l(\cdot, 0)$ of extinction of species 2. We thus use in Figure 2.12 the value $q = 0.999$, instead of $q = 0.99$, for the initial population sizes $X(0) = (36, 12)$.

Table 2.5. Mean size and standard deviation of the size of surviving species obtained from the process $\mathcal{X}(K_{0.99})$ and from a simulation of $\mathcal{X}$ for 12 scenarios with $\alpha = 1.0$

γ	(β, δ)	(0.5,0.25)	(0.5,0.125)	(1.0,0.5)	(1.0,0.25)	(2.0,1.0)	(2.0,0.5)
0.5	Surv. species	1	1	0	2	2	2
	$\mu_{0.99}$	2.55310	3.43484	0.00000	0.89103	2.55310	5.14032
	$\sigma_{0.99}$	6.42013	10.05517	5.72986	8.27594	6.42013	8.90772
	Surv. species	1	1	1	2	2	2
	μ_S	2.57964	3.48332	0.00624	0.87710	2.55456	5.14385
	σ_S	6.51781	10.23528	5.76100	8.35805	6.47556	8.97229
0.25	Surv. species	1	1	1	0	2	2
	$\mu_{0.99}$	5.14032	7.29157	0.89103	0.00000	3.43484	7.29157
	$\sigma_{0.99}$	8.90772	15.77390	8.27594	13.79382	10.05517	15.77390
	Surv. species	1	1	1	1	2	2
	μ_S	5.16416	7.33482	0.89626	0.00987	3.44114	7.31958
	σ_S	9.00627	15.98720	8.33451	13.87378	10.15926	15.92570

In Figures 2.11 and 2.12, we plot the mass function of $X(T(K_q))$ for those values of q, initial probability distributions and scenarios of Figures 2.9 and 2.10, versus the mass function of $X(T)$ (shown solid) obtained from simulations of $\mathcal{X}$. Both solutions are graphically undistinguished, thus showing that the solution based on $\mathcal{X}(K_q)$ performs better than the Normal solution of [108]. We il-

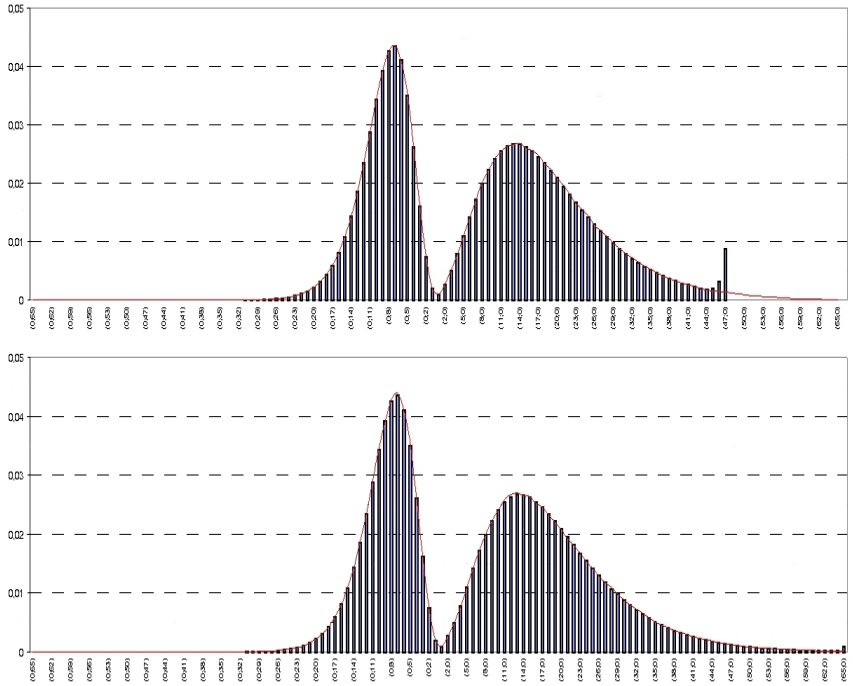

Fig. 2.11. The mass function of $X(T(K_q))$ for (from top to bottom) $q = 0.99$ and 0.999 versus a simulation study of the process $\mathcal{X}$. Scenario $(\alpha, \gamma, \beta, \delta) = (1.0, 0.25, 0.5, 0.125)$

lustrate in Table 2.5 the accuracy of our solution by comparing the identity of the surviving species, and the expectation μ_q and the standard deviation σ_q of the number of individuals alive at time $T(K_q)$, as the value $q = 0.99$ is selected, versus the corresponding characteristics obtained from a simulation study of the process $\mathcal{X}$; the resulting levels $K_{0.99}$ for each scenario were summarized in Tables 2.2 and 2.3. Similarly to Figures 2.11 and 2.12, entries in Table 2.5 allow us to corroborate that the use of the process $\mathcal{X}(K_q)$, instead of $\mathcal{X}$, yields more accurate estimations than those obtained from the Normal result in [108] if the initial population size $X(0)$ is not assumed to be large.

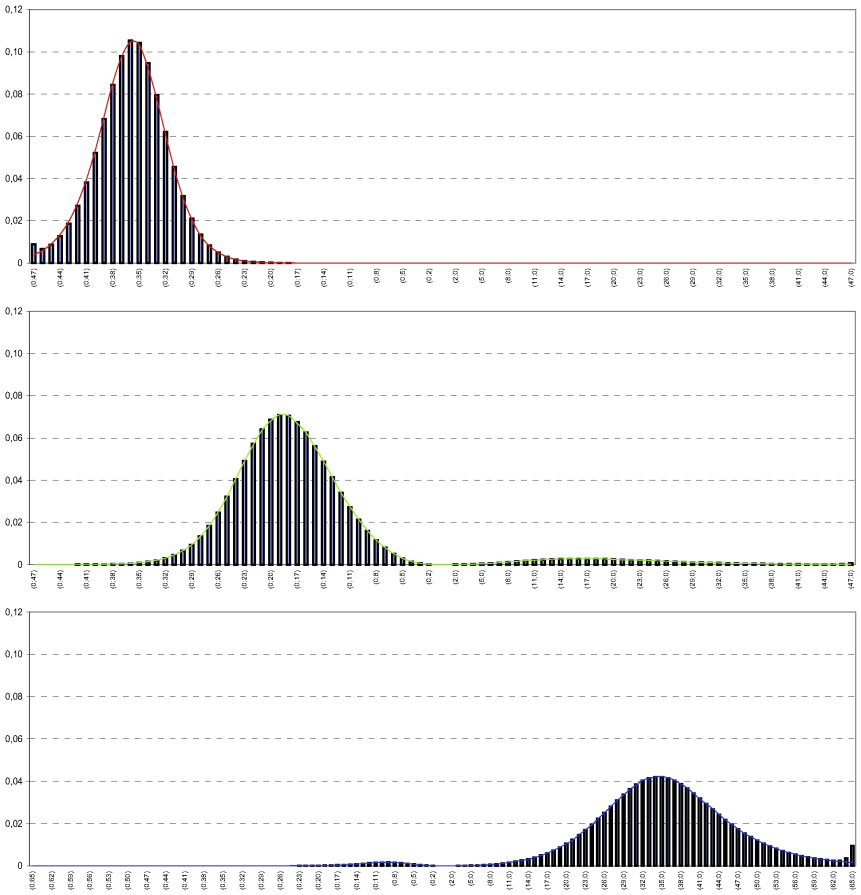

Fig. 2.12. The mass function of $X(T(K_q))$ versus a simulation study of the process $\mathcal{X}$ for (from top to bottom) initial population sizes $X(0) = (12, 36)$, $(24, 24)$ and $(36, 12)$. Scenario $(\alpha, \gamma, \beta, \delta) = (1.0, 0.25, 0.5, 0.125)$

2.3 Births and deaths

In the previous section, we defined an extinction cycle as the period that starts from an initial population size $X(0) = (m, n)$, and ends when one or the other species first becomes extinct. We exclude the trivial case $X(0) \in \mathcal{C}_0$, and from now on we assume that an extinction cycle starts at time $t = 0$ from a transient state $(m, n) \in \mathcal{C}$.

The main characteristics of an extinction cycle are its length, that we now denote by $T^{(m,n)}$ as the initial state is $(m,n) \in \mathcal{S}$, and the numbers $B_i^{(m,n)}$ of births and $D_i^{(m,n)}$ of deaths occurring within species i in the interval $[0, T^{(m,n)}]$, for $i \in \{1,2\}$. These measures should give an indication on the resistance of a certain species to the extinction, and how rapidly extinction occurs, in a similar manner to the maximum number $X_{\max}^{(m,n)}$ of individuals alive during the extinction cycle; see also [11].

The probability law of $(T^{(m,n)}, B_1^{(m,n)}, D_1^{(m,n)}, B_2^{(m,n)}, D_2^{(m,n)})$ can be specified in terms of

$$G(\mathbf{s}; m, n) = E\left[e^{-\theta T^{(m,n)}} y_1^{B_1^{(m,n)}} z_1^{D_1^{(m,n)}} y_2^{B_2^{(m,n)}} z_2^{D_2^{(m,n)}}\right],$$

where we denote $\mathbf{s} = (\theta, y_1, z_1, y_2, z_2)$, with $Re(\theta) \geq 0$, $|y_1| \leq 1$, $|z_1| \leq 1$, $|y_2| \leq 1$ and $|z_2| \leq 1$. If we define the densities $g_{(b_1,d_1,b_2,d_2)}(t; m, n)dt = P(t \leq T^{(m,n)} < t + dt, B_1^{(m,n)} = b_1, D_1^{(m,n)} = d_1, B_2^{(m,n)} = b_2, D_2^{(m,n)} = d_2)$, for $b_1, d_1, b_2, d_2 \in \mathbb{N}_0$, then we can write down

$$G(\mathbf{s}; m, n) = \int_0^\infty \sum_{b_1,d_1,b_2,d_2=0}^{\infty} g_{(b_1,d_1,b_2,d_2)}(t; m, n) e^{-\theta t} y_1^{b_1} z_1^{d_1} y_2^{b_2} z_2^{d_2} dt.$$

Thus, the Laplace transform $G(\theta, 1, 1, 1, 1; m, n)$ characterizes the marginal distribution of the continuous random variable $T^{(m,n)}$, and the marginal distributions of the discrete random variables $B_1^{(m,n)}$, $D_1^{(m,n)}$, $B_2^{(m,n)}$ and $D_2^{(m,n)}$ are uniquely specified by the generating functions $G(\mathbf{s}; m, n)$ at the respective points $\mathbf{s} = (0, y_1, 1, 1, 1)$, $(0, 1, z_1, 1, 1)$, $(0, 1, 1, y_2, 1)$ and $(0, 1, 1, 1, z_2)$.

It can be seen that the joint transforms $G(\mathbf{s}; m, n)$, for $(m,n) \in \mathcal{C}$, satisfy the following set of equations:

$$G(\mathbf{s}; 1, 1) = \frac{\alpha y_1 G(\mathbf{s}; 2, 1) + \beta y_2 G(\mathbf{s}; 1, 2) + \gamma z_1 + \delta z_2}{\theta + \alpha + \beta + \gamma + \delta}, \quad (2.14)$$

$$G(\mathbf{s}; m, 1) = \frac{\alpha m y_1 G(\mathbf{s}; m+1, 1) + \beta y_2 G(\mathbf{s}; m, 2)}{\theta + \alpha m + \beta + \gamma m + \delta m} + \frac{\gamma m z_1 G(\mathbf{s}; m-1, 1) + \delta m z_2}{\theta + \alpha m + \beta + \gamma m + \delta m}, \quad m \geq 2, \quad (2.15)$$

$$G(\mathbf{s};1,n) = \frac{\alpha y_1 G(\mathbf{s};2,n) + \beta n y_2 G(\mathbf{s};1,n+1) + \gamma n z_1}{\theta + \alpha + \beta n + \gamma n + \delta n} + \frac{\delta n z_2 G(\mathbf{s};1,n-1)}{\theta + \alpha + \beta n + \gamma n + \delta n}, \quad n \geq 2, \tag{2.16}$$

$$G(\mathbf{s};m,n) = \frac{\alpha m y_1 G(\mathbf{s};m+1,n) + \beta n y_2 G(\mathbf{s};m,n+1)}{\theta + \alpha m + \beta n + \gamma mn + \delta mn} + \frac{\gamma mn z_1 G(\mathbf{s};m-1,n) + \delta mn z_2 G(\mathbf{s};m,n-1)}{\theta + \alpha m + \beta n + \gamma mn + \delta mn}, \quad m,n \geq 2. \tag{2.17}$$

We may rewrite Equations (2.14)-(2.17) in matrix form as

$$\mathbf{g}(\mathbf{s}) = \mathbf{A}(\mathbf{s})\mathbf{g}(\mathbf{s}) + \mathbf{a}(\mathbf{s}), \tag{2.18}$$

where the column vector $\mathbf{g}(\mathbf{s})$ contains the transforms $G(\mathbf{s};m,n)$ with states $(m,n) \in \mathcal{C}$, and the matrix $\mathbf{A}(\mathbf{s})$ and the vector $\mathbf{a}(\mathbf{s})$ are constructed in the usual form. Besides, the matrix $\mathbf{A}(\mathbf{s})$ can be thought of as an operator which acts on the space l^∞ of all bounded sequences. Although it is readily shown that the operator $\mathbf{I} - \mathbf{A}(\mathbf{s})$ is invertible, the equality $\mathbf{g}(\mathbf{s}) = (\mathbf{I} - \mathbf{A}(\mathbf{s}))^{-1}\mathbf{a}(\mathbf{s})$ results only in a theoretical solution, which is not amenable to numerical implementation.

In what follows, we adopt a truncation procedure that, for a large enough value of K, examines the process $\mathcal{X}$ till absorption into the absorbing subset $\mathcal{C}_0$, but under the taboo that states of $\cup_{k=K+1}^{\infty} l(k)$ are avoided; in such a case, the absorption occurs in states of the finite set $\mathcal{C}_0(K) = \{(m,0) : 1 \leq m \leq K-1\} \cup \{(0,n) : 1 \leq n \leq K-1\}$. This procedure involves truncating the matrix $\mathbf{Q}$ (restricted to the class $\mathcal{C}$) to a finite matrix $\mathbf{Q}(K)$, and constructing a sequence $\{G_K(\mathbf{s};m,n) : K \geq m+n\}$ such that the Kth term $G_K(\mathbf{s};m,n)$ is given by the *restricted* transform of $(T^{(m,n)}, B_1^{(m,n)}, D_1^{(m,n)}, B_2^{(m,n)}, D_2^{(m,n)})$ on the sample paths of the process $\mathcal{X}$ verifying $X_{\max}^{(m,n)} \leq K$, that is, $G_K(\mathbf{s};m,n)$ is defined by

$$E\left[e^{-\theta T^{(m,n)}} y_1^{B_1^{(m,n)}} z_1^{D_1^{(m,n)}} y_2^{B_2^{(m,n)}} z_2^{D_2^{(m,n)}} ; X_{\max}^{(m,n)} \leq K\right].$$

This implies that, before absorption, only those sample paths of the process $\mathcal{X}$ evolving on the set $\cup_{k=2}^{K} l(k)$ of *accessible* states

are analyzed. However, since the subset of sample paths satisfying $X_{\max}^{(m,n)} \leq K$ converges to the set of all sample paths of the process $\mathcal{X}$ as K tends to infinite, one does expect that $G_K(\mathbf{s}; m, n)$ converges to $G(\mathbf{s}; m, n)$; we shall return to this question in Table 2.8 where the assertion is supported by simulated data.

For each initial state $(m, n) \in \mathcal{C}$, we suggest to estimate the joint transform $G(\mathbf{s}; m, n)$ by means of its restricted counterpart $G_K(\mathbf{s}; m, n)$ as we take successively larger truncations until the mass accumulated by the distribution of $(T^{(m,n)}, B_1^{(m,n)}, D_1^{(m,n)}, B_2^{(m,n)}, D_2^{(m,n)})$ on the set $\{X_{\max}^{(m,n)} \leq K\}$ is as close to 1 as desired; note that such a mass is given by the value $G_K(\mathbf{x}; m, n)$ with $\mathbf{x} = (0, 1, 1, 1, 1)$.

We next explain how to evaluate the above solution in an algorithmic manner. Let us denote by (M, N) the initial state $X(0)$ of the process $\mathcal{X}$, that is, our task is to determine $G_K(\mathbf{s}; M, N)$ for a large enough integer K satisfying $K \geq M + N$. For a concrete value K, the restricted transforms $\{G_K(\mathbf{s}; m, n) : (m, n) \in \mathcal{C}, m + n \leq K\}$ satisfy a set of $J(K) = K(K-1)2^{-1}$ equations that, for states of $\cup_{k=2}^{K-1} l(k)$, are defined from Equations (2.14)-(2.17) for the states $(1, 1)$, $(m, 1)$ with $2 \leq m \leq K-2$, $(1, n)$ with $2 \leq n \leq K-2$, and (m, n) with $2 \leq m, n \leq K-3$ and $m + n < K$, respectively. Starting from a state in level $l(K)$, only transitions due to the death rates γ and δ are registered in the restricted process; see Figure 2.3. This yields

$$G_K(\mathbf{s}; K-1, 1) = \frac{\gamma(K-1)z_1 G_K(\mathbf{s}; K-2, 1) + \delta(K-1)z_2}{\theta + \alpha(K-1) + \beta + \gamma(K-1) + \delta(K-1)},$$

$$G_K(\mathbf{s}; 1, K-1) = \frac{\gamma(K-1)z_1 + \delta(K-1)z_2 G_K(\mathbf{s}; 1, K-2)}{\theta + \alpha + \beta(K-1) + \gamma(K-1) + \delta(K-1)},$$

$$G_K(\mathbf{s}; m, n) = \frac{\gamma mn z_1 G_K(\mathbf{s}; m-1, n) + \delta mn z_2 G_K(\mathbf{s}; m, n-1)}{\theta + \alpha m + \beta n + \gamma mn + \delta mn},$$

for $2 \leq m, n \leq K-2$ and $m + n = K$.

This shows that, on each iteration, instead of (2.18) we solve

$$\mathbf{g}_K(\mathbf{s}) = \mathbf{A}_K(\mathbf{s})\mathbf{g}_K(\mathbf{s}) + \mathbf{a}_K(\mathbf{s}), \tag{2.19}$$

where $\mathbf{g}_K(\mathbf{s})$ is a column vector of dimension $J(K)$ with entries $G_K(\mathbf{s}; m, n)$, for $(m, n) \in \cup_{k=2}^{K} l(k)$; for later use, we decompose

$\mathbf{g}_K(\mathbf{s})$ by levels into sub-vectors $\mathbf{g}_K(\mathbf{s};k)$, for $2 \le k \le K$. In a similar manner to (2.9), we have for $\mathbf{A}_K(\mathbf{s})$ the expression

$$\begin{pmatrix} 0 & \mathbf{A}_{2,3}(\mathbf{s}_1) & & & & \\ \mathbf{A}_{3,2}(\mathbf{s}_2) & \mathbf{0}_{2\times 2} & \mathbf{A}_{3,4}(\mathbf{s}_1) & & & \\ & \ddots & \ddots & \ddots & & \\ & & \mathbf{A}_{K-1,K-2}(\mathbf{s}_2) & \mathbf{0}_{(K-2)\times(K-2)} & \mathbf{A}_{K-1,K}(\mathbf{s}_1) & \\ & & & \mathbf{A}_{K,K-1}(\mathbf{s}_2) & \mathbf{0}_{(K-1)\times(K-1)} \end{pmatrix},$$

and the vector $\mathbf{a}_K(\mathbf{s})$ has the form

$$\mathbf{a}_K(\mathbf{s}) = \begin{pmatrix} a(\mathbf{s}_2;2) \\ \mathbf{a}(\mathbf{s}_2;3) \\ \vdots \\ \mathbf{a}(\mathbf{s}_2;K) \end{pmatrix},$$

where $\mathbf{s}_1 = (\theta, y_1, y_2)$, $\mathbf{s}_2 = (\theta, z_1, z_2)$, and $\mathbf{A}_{k,k+1}(\mathbf{s}_1)$ and $\mathbf{A}_{k,k-1}(\mathbf{s}_2)$ are matrices of dimensions $(k-1)\times k$ and $(k-1)\times(k-2)$, respectively, with the following (i,j)th elements:

$$\left(\mathbf{A}_{k,k+1}(\mathbf{s}_1)\right)_{ij} = \begin{cases} \frac{\alpha(k-i)y_1}{\theta+\alpha(k-i)+\beta i+\gamma(k-i)i+\delta(k-i)i}, & \text{if } j=i, \\ \frac{\beta i y_2}{\theta+\alpha(k-i)+\beta i+\gamma(k-i)i+\delta(k-i)i}, & \text{if } j=i+1, \\ 0, & \text{otherwise,} \end{cases}$$

$$\left(\mathbf{A}_{k,k-1}(\mathbf{s}_2)\right)_{ij} = \begin{cases} \frac{\delta(k-i)iz_2}{\theta+\alpha(k-i)+\beta i+\gamma(k-i)i+\delta(k-i)i}, & \text{if } j=i-1, \\ \frac{\gamma(k-i)iz_1}{\theta+\alpha(k-i)+\beta i+\gamma(k-i)i+\delta(k-i)i}, & \text{if } j=i, \\ 0, & \text{otherwise.} \end{cases}$$

The entries of $\mathbf{a}_K(\mathbf{s})$ are given by $a(\mathbf{s}_2;2) = (\gamma z_1 + \delta z_2)(\theta+\alpha+\beta+\gamma+\delta)^{-1}$ and

$$\mathbf{a}(\mathbf{s}_2;k) = \begin{pmatrix} \frac{\delta(k-1)z_2}{\theta+\alpha(k-1)+\beta+\gamma(k-1)+\delta(k-1)} \\ \mathbf{0}_{k-3} \\ \frac{\gamma(k-1)z_1}{\theta+\alpha+\beta(k-1)+\gamma(k-1)+\delta(k-1)} \end{pmatrix}, \quad 3 \le k \le K.$$

The next algorithm shows how, in a specialized manner, one proceeds when solving $\mathbf{g}_K(\mathbf{s}) = (\mathbf{I}_{J(K)} - \mathbf{A}_K(\mathbf{s}))^{-1}\mathbf{a}_K(\mathbf{s})$ by block-Gaussian elimination, and it provides an efficient iterative procedure for computing the restricted transform $G_K(\mathbf{s};M,N)$ with a predetermined accuracy $\varepsilon > 0$; as a result, values of K depend

on the accuracy ε. Its proof is based on a partition of $\mathbf{A}_K(\mathbf{s})$ in terms of sub-matrices associated with the previous iteration $K-1$.

Algorithm 2.2. Estimation of $G(\mathbf{s}; M, N)$

Step 1 $\mathbf{x} := (0, 1, 1, 1, 1)$;
$\mathbf{y} := (0, 1, 1)$;
$K := 2$;
$\mathbf{H}_K := 1$;
$\mathbf{J}_K := a(\mathbf{y}; K)$;
$\mathbf{g}_K(\mathbf{x}; K) := \mathbf{H}_K \mathbf{J}_K$.

Step 2 While $K < M + N$ or $G_K(\mathbf{x}; M, N) \leq 1 - \varepsilon$, repeat
$K := K + 1$;
$\mathbf{H}_K := (\mathbf{I}_{K-1} - \mathbf{A}_{K,K-1}(\mathbf{y})\mathbf{H}_{K-1}\mathbf{A}_{K-1,K}(\mathbf{y}))^{-1}$;
$\mathbf{J}_K := \mathbf{A}_{K,K-1}(\mathbf{y})\mathbf{H}_{K-1}\mathbf{J}_{K-1} + \mathbf{a}(\mathbf{y}; K)$;
$\mathbf{g}_K(\mathbf{x}; K) := \mathbf{H}_K \mathbf{J}_K$;
for $j = K-1, K-2, ..., 2$, compute
$\mathbf{g}_K(\mathbf{x}; j) := \mathbf{H}_j \mathbf{A}_{j,j+1}(\mathbf{y}) \cdot ... \cdot \mathbf{H}_{K-1}\mathbf{A}_{K-1,K}(\mathbf{y})$;
$\mathbf{g}_K(\mathbf{x}; j) := \mathbf{g}_K(\mathbf{x}; j)\mathbf{g}_K(\mathbf{x}; K) + \mathbf{g}_{K-1}(\mathbf{x}; j)$;
and destroy $\mathbf{g}_{K-1}(\mathbf{x}; j)$;
read $G_K(\mathbf{x}; M, N)$ from $\mathbf{g}_K(\mathbf{x}; M + N)$.

Step 3 Estimate $G(\mathbf{s}; M, N)$ by means of $G_K(\mathbf{s}; M, N)$.

When we handle values of $K \geq M+N$ verifying $G_K(\mathbf{x}; M, N) \leq 1-\varepsilon$ in Step 2, we need to compute $\mathbf{g}_K(\mathbf{x}; j)$ only for $j = K-1, K-2, ..., M + N$. Algorithm 2.2 can yield a value of K such that the initial state (M, N) might be located near to the subset $\cup_{k=K+1}^{\infty} l(k)$ of non-accessible states. In this case, we suggest a selection of K at Step 2 verifying $K \geq M + N + k_0$, where k_0 is a predetermined non-negative integer.

It is observed that, for $j \geq 2$, the square matrix $\mathbf{H}_j$ of order $j-1$ records the expected times spent in states of the jth level, starting from an initial state in $l(j)$, before the first visit to either the state 0^* or to the state j^* in the discrete-time Markov chain (DTMC) defined on $\{0^*, j^*, l(j)\}$ with one-step transition probability matrix

$$\mathbf{P}(j) = \begin{pmatrix} 1 & 0 & \mathbf{0}_{j-1}^T \\ 0 & 1 & \mathbf{0}_{j-1}^T \\ \mathbf{J}_j & \mathbf{A}_{j,j+1}(\mathbf{y})\mathbf{e}_j & \mathbf{A}_{j,j-1}(\mathbf{y})\mathbf{H}_{j-1}\mathbf{A}_{j-1,j}(\mathbf{y}) \end{pmatrix}.$$

This property is stated here without proof as one merely needs to follow results of [71, page 134]. The underlying argument is repetitively applied to censored Markov chains on the state space $\mathcal{C}_0 \cup \{l(j), l(j+1), ...\}$. Owing to our interest in sojourn times for states in $l(j)$, we lump all the states of $\mathcal{C}_0$ and $\cup_{k=j+1}^{\infty} l(k)$ together to make two absorbing states 0^* and j^*.

We now turn our attention to evaluating moments of the random variables $T^{(m,n)}$, $B_i^{(m,n)}$ and $D_i^{(m,n)}$, for $i \in \{1,2\}$, by successive differentiation of (2.19). Let $\mathbf{t}(r)$, $\mathbf{b}_i(r)$ and $\mathbf{d}_i(r)$, for $i \in \{1,2\}$, be the column vectors defined by

$$\mathbf{t}(r) = (-1)^r \left. \frac{\partial^r \mathbf{g}_K(\mathbf{s})}{\partial \theta^r} \right|_{\mathbf{s}=\mathbf{x}},$$
$$\mathbf{b}_i(r) = \left. \frac{\partial^r \mathbf{g}_K(\mathbf{s})}{\partial y_i^r} \right|_{\mathbf{s}=\mathbf{x}},$$
$$\mathbf{d}_i(r) = \left. \frac{\partial^r \mathbf{g}_K(\mathbf{s})}{\partial z_i^r} \right|_{\mathbf{s}=\mathbf{x}},$$

for $r \geq 1$, and $\mathbf{t}(0) = \mathbf{b}_i(0) = \mathbf{d}_i(0) = \mathbf{g}_K(\mathbf{x})$. Note that, for $r \geq 1$, the entries of $\mathbf{t}(r)$ are given by the expected values $E[(T^{(m,n)})^r]$, and $\mathbf{b}_i(r)$ and $\mathbf{d}_i(r)$ have entries defined as the rth factorial moments of $B_i^{(m,n)}$ and $D_i^{(m,n)}$, respectively, for states $(m,n) \in \cup_{k=2}^{K} l(k)$ and $i \in \{1,2\}$. Straightforward algebra yields the equalities

$$\mathbf{t}(r) = \left(\mathbf{I}_{J(K)} - \mathbf{A}_K(\mathbf{x})\right)^{-1} \left((-1)^r \mathbf{a}_K^{r,\theta}(\mathbf{x}) + \sum_{j=1}^{r} \frac{r(r-1)\cdot ... \cdot (r-j+1)}{j!} (-1)^j \mathbf{A}_K^{j,\theta}(\mathbf{x}) \mathbf{t}(r-j) \right), \tag{2.20}$$

$$\mathbf{b}_i(r) = \left(\mathbf{I}_{J(K)} - \mathbf{A}_K(\mathbf{x})\right)^{-1} r \mathbf{A}_K^{1,y_i}(\mathbf{x}) \mathbf{b}_i(r-1), \tag{2.21}$$

$$\mathbf{d}_i(r) = \left(\mathbf{I}_{J(K)} - \mathbf{A}_K(\mathbf{x})\right)^{-1} \left(r \mathbf{A}_K^{1,z_i}(\mathbf{x}) \mathbf{d}_i(r-1) + \delta_{1,r} \mathbf{a}_K^{1,z_i}(\mathbf{x}) \right), \tag{2.22}$$

for $i \in \{1,2\}$ and $r \geq 1$, where $\mathbf{A}_K^{j,x}(\mathbf{x})$ and $\mathbf{a}_K^{j,x}(\mathbf{x})$ define the jth derivatives of $\mathbf{A}_K(\mathbf{s})$ and $\mathbf{a}_K(\mathbf{s})$ with respect to x at point $\mathbf{x}$.

The computation of the inverse $\left(\mathbf{I}_{J(K)} - \mathbf{A}_K(\mathbf{x})\right)^{-1}$ in (2.20)-(2.22) is an apparent requirement that can be simplified in a similar manner to the solution of (2.19) in Algorithm 2.2. To see this, we first decompose $\mathbf{t}(r)$, $\mathbf{b}_i(r)$ and $\mathbf{d}_i(r)$ by levels into sub-vectors $\mathbf{t}(r;k)$, $\mathbf{b}_i(r;k)$ and $\mathbf{d}_i(r;k)$, for $i \in \{1,2\}$ and $2 \le k \le K$. Then, solving (2.20)-(2.22) by levels, the sub-vectors $\mathbf{t}(r;k)$, $\mathbf{b}_i(r;k)$ and $\mathbf{d}_i(r;k)$ with $2 \le k \le K$ can be derived in terms of previously computed sub-vectors as follows:

Algorithm 2.2. (Continued)

Step 4 $r' := 0$;
$\mathbf{x} := (0,1,1,1,1)$;
$\mathbf{y} := (0,1,1)$;
for $j = 2,3,...,K$, compute
$\mathbf{t}(r';j) := \mathbf{g}_K(\mathbf{x};j)$;
$\mathbf{b}_i(r';j) := \mathbf{g}_K(\mathbf{x};j)$;
$\mathbf{d}_i(r';j) := \mathbf{g}_K(\mathbf{x};j)$.

Step 5 While $r' < r$, repeat
$r' := r' + 1$;
for $j = 2,3,...,K$, compute

$$\hat{\mathbf{J}}_j(r') := (1-\delta_{2,j})\mathbf{A}_{j,j-1}(\mathbf{y})\mathbf{H}_{j-1}\hat{\mathbf{J}}_{j-1}(r') + (-1)^{r'}\mathbf{a}^{r',\theta}(\mathbf{y};j) + \sum_{i=1}^{r'} \frac{r'(r'-1)...(r'-i+1)}{i!}(-1)^i \times \Big((1-\delta_{2,j})\mathbf{A}^{i,\theta}_{j,j-1}(\mathbf{y})\mathbf{t}(r'-i;j-1) + (1-\delta_{j,K})\mathbf{A}^{i,\theta}_{j,j+1}(\mathbf{y})\mathbf{t}(r'-i;j+1) \Big);$$

$$\tilde{\mathbf{J}}^i_j(r') := (1-\delta_{2,j})\mathbf{A}_{j,j-1}(\mathbf{y})\mathbf{H}_{j-1}\tilde{\mathbf{J}}^i_{j-1}(r') + (1-\delta_{j,K})r'\mathbf{A}^{1,y_i}_{j,j+1}(\mathbf{y})\mathbf{b}_i(r'-1;j+1);$$

$$\overline{\mathbf{J}}^i_j(r') := (1-\delta_{2,j})\Big(\mathbf{A}_{j,j-1}(\mathbf{y})\mathbf{H}_{j-1}\overline{\mathbf{J}}^i_{j-1}(r') + r'\mathbf{A}^{1,z_i}_{j,j-1}(\mathbf{y})\mathbf{d}_i(r'-1;j-1) \Big) + \delta_{1,r'}\mathbf{a}^{1,z_i}(\mathbf{y};j);$$

$\mathbf{t}(r';K) := \mathbf{H}_K\hat{\mathbf{J}}_K(r')$;
$\mathbf{b}_i(r';K) := \mathbf{H}_K\tilde{\mathbf{J}}^i_K(r')$;
$\mathbf{d}_i(r';K) := \mathbf{H}_K\overline{\mathbf{J}}^i_K(r')$;
for $j = K-1, K-2, ..., 2$, compute

$$\mathbf{t}(r';j) := \mathbf{H}_j\left(\mathbf{A}_{j,j+1}(\mathbf{y})\mathbf{t}(r';j+1) + \hat{\mathbf{J}}_j(r')\right);$$
$$\mathbf{b}_i(r';j) := \mathbf{H}_j\left(\mathbf{A}_{j,j+1}(\mathbf{y})\mathbf{b}_i(r';j+1) + \tilde{\mathbf{J}}^i_j(r')\right);$$
$$\mathbf{d}_i(r';j) := \mathbf{H}_j\left(\mathbf{A}_{j,j+1}(\mathbf{y})\mathbf{d}_i(r';j+1) + \overline{\mathbf{J}}^i_j(r')\right).$$

In this iterative solution, the sub-matrices $\mathbf{A}^{i,x}_{j,j+1}(\mathbf{y})$ and $\mathbf{A}^{i,x}_{j,j-1}(\mathbf{y})$, and the column vector $\mathbf{a}^{i,x}(\mathbf{y};j)$ denote the ith derivatives of $\mathbf{A}_{j,j+1}(\mathbf{s}_1)$, $\mathbf{A}_{j,j-1}(\mathbf{s}_2)$ and $\mathbf{a}(\mathbf{s}_2;j)$ with respect to x, at point $\mathbf{y} = (0,1,1)$, that is,

(i) The sub-matrices $\mathbf{A}^{i,\theta}_{j,j+1}(\mathbf{y})$ and $\mathbf{A}^{1,y_i}_{j,j+1}(\mathbf{y})$ have dimension $(j-1)\times j$. Their (k,k')th elements are given by

$$\left(\mathbf{A}^{i,\theta}_{j,j+1}(\mathbf{y})\right)_{k,k'} = \begin{cases} \frac{(-1)^i i!\alpha(j-k)}{(\alpha(j-k)+\beta k+\gamma(j-k)k+\delta(j-k)k)^{i+1}}, & \text{if } k'=k,\\ \frac{(-1)^i i!\beta k}{(\alpha(j-k)+\beta k+\gamma(j-k)k+\delta(j-k)k)^{i+1}}, & \text{if } k'=k+1,\\ 0, & \text{otherwise,}\end{cases}$$

$$\left(\mathbf{A}^{1,y_1}_{j,j+1}(\mathbf{y})\right)_{k,k'} = \begin{cases} \frac{\alpha(j-k)}{\alpha(j-k)+\beta k+\gamma(j-k)k+\delta(j-k)k}, & \text{if } k'=k,\\ 0, & \text{otherwise,}\end{cases}$$

$$\left(\mathbf{A}^{1,y_2}_{j,j+1}(\mathbf{y})\right)_{k,k'} = \begin{cases} \frac{\beta k}{\alpha(j-k)+\beta k+\gamma(j-k)k+\delta(j-k)k}, & \text{if } k'=k+1,\\ 0, & \text{otherwise.}\end{cases}$$

(ii) The sub-matrices $\mathbf{A}^{i,\theta}_{j,j-1}(\mathbf{y})$ and $\mathbf{A}^{1,z_i}_{j,j-1}(\mathbf{y})$ have dimension $(j-1)\times(j-2)$. Their (k,k')th elements are given by

$$\left(\mathbf{A}^{i,\theta}_{j,j-1}(\mathbf{y})\right)_{k,k'} = \begin{cases} \frac{(-1)^i i!\delta(j-k)k}{(\alpha(j-k)+\beta k+\gamma(j-k)k+\delta(j-k)k)^{i+1}}, & \text{if } k'=k-1,\\ \frac{(-1)^i i!\gamma(j-k)k}{(\alpha(j-k)+\beta k+\gamma(j-k)k+\delta(j-k)k)^{i+1}}, & \text{if } k'=k,\\ 0, & \text{otherwise,}\end{cases}$$

$$\left(\mathbf{A}^{1,z_1}_{j,j-1}(\mathbf{y})\right)_{k,k'} = \begin{cases} \frac{\gamma(j-k)k}{\alpha(j-k)+\beta k+\gamma(j-k)k+\delta(j-k)k}, & \text{if } k'=k,\\ 0, & \text{otherwise,}\end{cases}$$

$$\left(\mathbf{A}^{1,z_2}_{j,j-1}(\mathbf{y})\right)_{k,k'} = \begin{cases} \frac{\delta(j-k)k}{\alpha(j-k)+\beta k+\gamma(j-k)k+\delta(j-k)k}, & \text{if } k'=k-1,\\ 0, & \text{otherwise.}\end{cases}$$

(iii) In the case $j=2$, we have

$$a^{i,\theta}(\mathbf{y};2) = \frac{(-1)^i i!(\gamma+\delta)}{(\alpha+\beta+\gamma+\delta)^{i+1}},$$
$$a^{1,z_1}(\mathbf{y};2) = \frac{\gamma}{\alpha+\beta+\gamma+\delta},$$

$$a^{1,z_2}(\mathbf{y};2)=\frac{\delta}{\alpha+\beta+\gamma+\delta}.$$

If $j\geq 3$, then $\mathbf{a}^{i,\theta}(\mathbf{y};j)$ and $\mathbf{a}^{1,z_i}(\mathbf{y};j)$ are column vectors of order $j-1$ whose kth entries are given by

$$\left(\mathbf{a}^{i,\theta}(\mathbf{y};j)\right)_k=\begin{cases}\frac{\delta(j-1)}{(\alpha(j-1)+\beta+\gamma(j-1)+\delta(j-1))^{i+1}}, & \text{if } k=1,\\ \frac{\gamma(j-1)}{(\alpha+\beta(j-1)+\gamma(j-1)+\delta(j-1))^{i+1}}, & \text{if } k=j-1,\\ 0, & \text{otherwise,}\end{cases}$$

$$\left(\mathbf{a}^{1,z_1}(\mathbf{y};j)\right)_k=\begin{cases}\frac{\gamma(j-1)}{\alpha+\beta(j-1)+\gamma(j-1)+\delta(j-1)}, & \text{if } k=j-1,\\ 0, & \text{otherwise,}\end{cases}$$

$$\left(\mathbf{a}^{1,z_2}(\mathbf{y};j)\right)_k=\begin{cases}\frac{\delta(j-1)}{\alpha(j-1)+\beta+\gamma(j-1)+\delta(j-1)}, & \text{if } k=1,\\ 0, & \text{otherwise.}\end{cases}$$

Now, we focus on the behavior of K as a function of the accuracy ε; see Algorithm 2.2. We consider again the scenarios in Table 2.1; that is, the birth rate $\alpha=1.0$ and the death rate $\gamma\in\{\alpha 2^{-1},\alpha 4^{-1}\}$ in species 1, and $\beta\in\{\alpha 2^{-1},\alpha,2\alpha\}$ and $\delta\in\{\beta 2^{-1},\beta 4^{-1}\}$ in species 2. In Tables 2.6 and 2.7, the values of K are listed for these scenarios and choices of $\varepsilon\in\{10^{-2},10^{-3},10^{-4},10^{-5}\}$. We select three initial population sizes (M,N) that are equidistant on each level $l(M+N)$ with $M+N\in\{24,44,104,204\}$. Tables 2.6 and 2.7 show the nondecreasing behavior of K as a function of ε, though differences in magnitude are more apparent for initial sizes in lower levels. This means that the birth rates α and β influence noticeably on the dynamics of the process $\mathcal{X}$ if the initial population size (M,N) is assumed small or moderate. To carry out our numerical experiments, we will consider from now on the levels K derived with accuracy $\varepsilon=10^{-5}$ in Tables 2.6 and 2.7.

In order to validate the applicability of our approach, we list in Table 2.8 the relative errors associated with the expectations of $T^{(M,N)}$, $B_1^{(M,N)}$, $D_1^{(M,N)}$, $B_2^{(M,N)}$, and $D_2^{(M,N)}$, for initial sizes $(M,N)\in\{(26,78),(52,52),(78,26)\}$; specifically, for a random variable $Y^{(M,N)}$, the relative error is defined as

$$\textit{relative error}\left(Y^{(M,N)};K\right)=\left|1-\frac{E[Y^{(M,N)};X_{\max}^{(M,N)}\leq K]}{E[Y^{(M,N)}]}\right|,$$

Table 2.6. Values of K versus $X(0)$ and ε for 6 scenarios with $\alpha = 1.0$ and $\gamma = \alpha 2^{-1}$

$X(0)$	ε	(β, δ)	(0.5,0.25)	(0.5,0.125)	(1.0,0.5)	(1.0,0.25)	(2.0,1.0)	(2.0,0.5)
(6,18)	0.01		26	27	28	31	31	39
	0.001		28	30	32	36	38	48
	0.0001		31	33	36	41	45	56
	0.00001		34	36	40	46	52	65
(12,12)	0.01		26	26	26	27	26	30
	0.001		28	28	27	30	28	39
	0.0001		31	30	29	35	31	48
	0.00001		38	41	33	40	38	57
(18,6)	0.01		31	36	28	31	26	28
	0.001		38	49	32	38	28	32
	0.0001		45	61	36	45	31	37
	0.00001		52	73	40	52	34	43
(11,33)	0.01		46	46	46	46	46	52
	0.001		47	47	47	50	48	61
	0.0001		48	48	49	55	55	69
	0.00001		49	51	53	60	62	78
(22,22)	0.01		45	46	45	46	45	46
	0.001		46	47	46	47	46	47
	0.0001		47	48	47	48	47	52
	0.00001		48	49	48	49	48	61
(33,11)	0.01		46	46	46	46	46	46
	0.001		48	53	47	48	47	47
	0.0001		55	65	49	55	48	49
	0.00001		62	77	53	62	49	53
(26,78)	0.01		105	105	105	105	105	105
	0.001		106	106	106	106	106	106
	0.0001		106	107	107	107	107	108
	0.00001		107	107	107	108	108	114
(52,52)	0.01		105	105	105	105	105	105
	0.001		106	106	106	106	106	106
	0.0001		106	106	106	107	106	107
	0.00001		107	107	107	107	107	108
(78,26)	0.01		105	105	105	105	105	105
	0.001		106	106	106	106	106	106
	0.0001		107	107	107	107	106	107
	0.00001		108	108	107	108	107	108
(51,153)	0.01		205	205	205	205	205	205
	0.001		205	205	205	206	205	206
	0.0001		206	206	206	206	206	206
	0.00001		207	207	207	207	207	207
(102,102)	0.01		205	205	205	205	205	205
	0.001		205	205	205	205	205	205
	0.0001		206	206	206	206	206	206
	0.00001		206	207	206	207	206	207
(153,51)	0.01		205	205	205	205	205	205
	0.001		205	206	205	206	205	206
	0.0001		206	206	206	206	206	206
	0.00001		207	207	207	207	207	207

where $E[Y^{(M,N)}]$ denotes the *true* value of the expectation, and the restricted value $E[Y^{(M,N)}; X_{\max}^{(M,N)} \leq K]$ is obtained from Algorithm 2.2 for the level K. Since the expectations of $T^{(M,N)}$, $B_1^{(M,N)}$, $D_1^{(M,N)}$, $B_2^{(M,N)}$, and $D_2^{(M,N)}$ are unknown, they are estimated from 10^6 simulations of the process $\mathcal{X}$ starting at each initial population size (M, N). In Table 2.8, numbers in bold indicate the maximum

Table 2.7. Values of K versus $X(0)$ and ε for 6 scenarios with $\alpha = 1.0$ and $\gamma = \alpha 4^{-1}$

$X(0)$	ε	(β, δ)	(0.5,0.25)	(0.5,0.125)	(1.0,0.5)	(1.0,0.25)	(2.0,1.0)	(2.0,0.5)
(6,18)	0.01		28	31	31	40	36	55
	0.001		32	37	38	49	49	71
	0.0001		37	42	45	57	61	87
	0.00001		43	48	52	66	73	103
(12,12)	0.01		30	38	27	33	26	38
	0.001		39	54	30	42	28	54
	0.0001		48	70	35	51	30	70
	0.00001		57	86	40	60	41	86
(18,6)	0.01		39	55	31	40	27	31
	0.001		48	71	36	49	30	37
	0.0001		56	87	41	57	33	42
	0.00001		65	103	46	66	36	48
(11,33)	0.01		46	47	46	52	46	65
	0.001		47	51	48	61	53	81
	0.0001		49	56	55	70	65	97
	0.00001		53	61	62	79	77	113
(22,22)	0.01		46	46	46	46	46	46
	0.001		47	49	47	48	47	49
	0.0001		52	64	48	54	48	64
	0.00001		61	80	49	63	49	80
(33,11)	0.01		52	65	46	52	46	47
	0.001		61	81	50	61	47	51
	0.0001		69	97	55	70	48	56
	0.00001		78	113	60	79	51	61
(26,78)	0.01		105	105	105	106	105	106
	0.001		106	106	106	107	106	108
	0.0001		107	107	107	108	107	122
	0.00001		108	108	108	114	108	138
(52,52)	0.01		105	105	105	105	105	105
	0.001		106	106	106	106	106	106
	0.0001		107	107	107	107	106	107
	0.00001		108	108	107	108	107	108
(78,26)	0.01		105	106	105	106	105	105
	0.001		106	108	106	107	106	106
	0.0001		108	122	107	108	107	107
	0.00001		114	138	108	114	107	108
(51,153)	0.01		205	205	205	205	205	205
	0.001		206	206	206	206	206	206
	0.0001		206	206	206	207	206	207
	0.00001		207	207	207	207	207	208
(102,102)	0.01		205	205	205	205	205	205
	0.001		205	206	205	206	205	206
	0.0001		206	206	206	206	206	206
	0.00001		207	207	207	207	207	207
(153,51)	0.01		205	205	205	205	205	205
	0.001		206	206	206	206	205	206
	0.0001		206	207	206	207	206	206
	0.00001		207	208	207	207	207	207

relative errors for each scenario and initial size. Our scenarios and numerical work not reported here mostly lead to restricted expectations that fit the true values up to the second or third decimal digit. We may therefore conclude that, in terms of relative errors, the accuracy $\varepsilon = 10^{-5}$ in Algorithm 2.2 seems to provide

a good criterion to approximate the multidimensional transform $G(\mathbf{s}; M, N)$ by its restricted version $G_K(\mathbf{s}; M, N)$.

Table 2.8. Relative errors for 12 scenarios with $\alpha = 1.0$ and accuracy $\varepsilon = 10^{-5}$

$X(0)$	γ	(β, δ)	(0.5,0.25)	(0.5,0.125)	(1.0,0.5)	(1.0,0.25)	(2.0,1.0)	(2.0,0.5)
(26,78)	0.5	$T^{(26,78)}$	0.00012	0.00020	0.00043	0.00014	0.00034	0.00019
		$B_1^{(26,78)}$	0.00066	0.00070	**0.00147**	**0.00146**	**0.00082**	**0.00135**
		$D_1^{(26,78)}$	0.00001	0.00002	0.00003	0.00004	$< 10^{-5}$	0.00004
		$B_2^{(26,78)}$	**0.00070**	**0.00087**	0.00017	0.00044	0.00020	0.00019
		$D_2^{(26,78)}$	0.00018	0.00008	0.00018	0.00052	0.00045	0.00007
	0.25	$T^{(26,78)}$	0.00006	0.00006	**0.00209**	0.00019	0.00012	0.00108
		$B_1^{(26,78)}$	**0.00110**	**0.00090**	0.00124	**0.00139**	**0.00027**	**0.00179**
		$D_1^{(26,78)}$	0.00006	0.00004	0.00011	0.00007	$< 10^{-5}$	0.00004
		$B_2^{(26,78)}$	0.00026	0.00010	0.00123	0.00026	0.00012	0.00019
		$D_2^{(26,78)}$	0.00020	$< 10^{-5}$	0.00054	0.00044	$< 10^{-5}$	0.00063
(52,52)	0.5	$T^{(52,52)}$	0.00004	0.00035	0.00328	0.00036	0.00175	0.00179
		$B_1^{(52,52)}$	**0.00092**	**0.00037**	**0.00366**	0.00013	**0.00374**	**0.00260**
		$D_1^{(52,52)}$	0.00004	0.00002	0.00057	$< 10^{-6}$	0.00066	0.00064
		$B_2^{(52,52)}$	0.00012	0.00017	0.00124	**0.00043**	0.00031	0.00073
		$D_2^{(52,52)}$	0.00005	0.00007	0.00036	0.00024	0.00002	0.00022
	0.25	$T^{(52,52)}$	0.00227	0.00205	0.00260	**0.00373**	0.00003	**0.00247**
		$B_1^{(52,52)}$	**0.00260**	**0.00440**	**0.00287**	0.00194	**0.00155**	0.00236
		$D_1^{(52,52)}$	0.00087	0.00032	0.00004	0.00093	0.00011	0.00036
		$B_2^{(52,52)}$	0.00036	0.00027	0.00046	0.00069	0.00080	0.00011
		$D_2^{(52,52)}$	0.00091	0.00069	0.00001	0.00074	0.00025	0.00003
(78,26)	0.5	$T^{(78,26)}$	**0.00523**	0.00233	0.00166	**0.00575**	0.00257	0.00094
		$B_1^{(78,26)}$	0.00121	0.00045	**0.00222**	0.00128	**0.00498**	**0.00222**
		$D_1^{(78,26)}$	0.00019	0.00068	0.00021	0.00033	0.00054	0.00040
		$B_2^{(78,26)}$	0.00382	**0.00259**	0.00139	0.00423	0.00063	0.00134
		$D_2^{(78,26)}$	0.00007	0.00001	0.00003	0.00013	0.00002	0.00008
	0.25	$T^{(78,26)}$	**0.00428**	0.00602	0.00078	**0.00444**	**0.00517**	0.00085
		$B_1^{(78,26)}$	0.00207	0.00324	**0.00431**	0.00178	0.00088	**0.00313**
		$D_1^{(78,26)}$	0.00073	0.00110	0.00042	0.00046	0.00227	0.00026
		$B_2^{(78,26)}$	0.00016	**0.00660**	0.00110	0.00032	0.00294	0.00032
		$D_2^{(78,26)}$	$< 10^{-5}$	0.00032	0.00003	0.00001	0.00223	0.00001

The recursive scheme in Algorithm 2.2 is the key for the numerical inversion of the multidimensional transform $G_K(\mathbf{s}; M, N)$, as well as of its related marginal transforms. We illustrate in Figure 2.13 the graphs of the restricted distribution function of the length $T^{(M,N)}$ of an extinction cycle, which is defined as

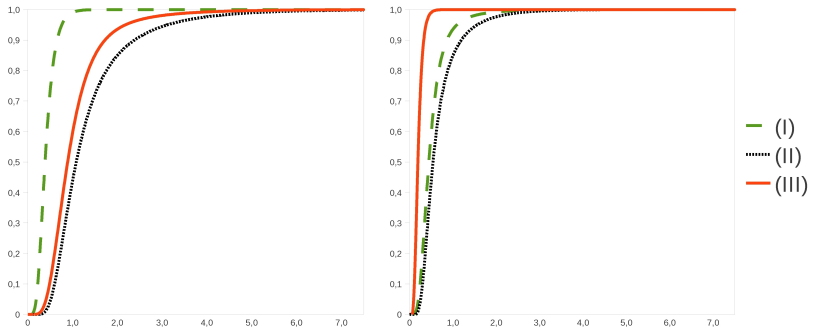

Fig. 2.13. $F(t; M, N)$ versus t for 2 scenarios defined by the choices $\beta = \alpha 2^{-1}$ (*left*) and $\beta = 2\alpha$ (*right*), with $(\alpha, \gamma, \delta) = (1.0, \alpha 4^{-1}, \beta 4^{-1})$. Initial sizes: (I) $(M, N) = (11, 33)$; (II) $(M, N) = (22, 22)$; (III) $(M, N) = (33, 11)$

$$F(t; M, N) = P\left(T^{(M,N)} \leq t, X_{\max}^{(M,N)} \leq K\right), \quad t \geq 0.$$

The choice of K with accuracy $\varepsilon = 10^{-5}$ guarantees limit values $F(\infty; M, N) \in (0.99999, 1.0]$. We display $F(t; M, N)$ for (from left to right) two scenarios specified by the choices $\beta \in \{\alpha 2^{-1}, 2\alpha\}$ in the case $\alpha = 1.0$, $\gamma = \alpha 4^{-1}$ and $\delta = \beta 4^{-1}$. In each figure, three curves associated with the initial population sizes $(M, N) \in \{(11, 33), (22, 22), (33, 11)\}$ are displayed. In both scenarios, the random variables $T^{(11,33)}$ and $T^{(33,11)}$ are shown to be stochastically smaller than the extinction time $T^{(22,22)}$. The stochastic monotonicity between $T^{(11,33)}$ and $T^{(33,11)}$ depends on the scenario under study. This behavior can be explained, from Figure 2.13 and Table 2.9, in terms of the death rate δ in species 2. To be concrete, we first notice that, with initial sizes $M = 11$ and $N = 33$, increasing values of δ imply a slight decrease of the extinction probability of species 1; see Table 2.4. At the same time, they yield a noticeable increment in the mean length of the extinction cycle, as the reader may graphically infer from Figure 2.13 and the equality

$$E[T^{(M,N)}; X_{\max}^{(M,N)} \leq K] = \int_0^\infty (1 - F(t; M, N))dt.$$

A similar observation can be made for the *dual* sizes $M = 33$ and $N = 11$ with the role of species 1 and the increasing behavior of $E[T^{(M,N)}; X_{\max}^{(M,N)} \leq K]$ replaced by species 2 and a decreasing behavior. For both initial sizes $(M, N) \in \{(11, 33), (33, 11)\}$,

the increment in δ is not sufficient to modify the identity of the species becoming extinct, that is, species 1 if $(M, N) = (11, 33)$, and species 2 if $(M, N) = (33, 11)$. This identity is strongly supported by high extinction probabilities, and it corresponds to that species with smaller size at time $t = 0$. On the contrary, as the initial sizes M and N are identical (in our examples, $M = N = 22$), the choices $\beta = \alpha 2^{-1}$ and $\beta = 2\alpha$ with $\delta = \beta 4^{-1}$ result in opposite identities for the species becoming extinct. These comments show the significance of the *drift* vector of the jump process, that is, $-(\gamma + \delta)^{-1}(\gamma, \delta)$, and they are closely related to the Ridler-Rowe approach [108] for the size of the surviving species as the initial sizes M and N tend suitably to infinity; see Section 2.1.

In Figure 2.13, we carry out the numerical inversion of the transform $G_K(\mathbf{s}; M, N)$ at points $\mathbf{s} = (\theta, 1, 1, 1, 1)$ with $Re(\theta) \geq 0$, using the algorithms EULER and POST-WIDDER described by Abate and Whitt [1]. Both methods are variants of the Fourier-series method but, as it is reported in [1], they might provide very different approaches to the inversion problem so they can be used in parallel to obtain the desired accuracy by checking on each other. For numerical inversion of multidimensional transforms of probability distributions of continuous random variables (Laplace-Stieltjes transforms) and/or discrete random variables (generating functions), see the paper by Choudhury et al. [35] and its references.

Table 2.9. Extinction probabilities of species 1 in scenarios with $\alpha = 1.0$ and $\gamma = \alpha 4^{-1}$

$X(0)$	$(\beta = \alpha 2^{-1}, \delta = \beta 4^{-1})$	$(\beta = 2\alpha, \delta = \beta 4^{-1})$
(11,33)	0.99999	0.98272
(22,22)	0.92887	0.07112
(33,11)	0.01727	$< 10^{-6}$

In Figures 2.14-2.17, we investigate how the birth rate β influences the numbers of births and deaths in four cases, which are defined by $(\gamma = \alpha 2^{-1}, \delta = \beta 2^{-1})$, $(\gamma = \alpha 4^{-1}, \delta = \beta 4^{-1})$, $(\gamma = \alpha 4^{-1}, \delta = \beta 2^{-1})$, and $(\gamma = \alpha 2^{-1}, \delta = \beta 4^{-1})$ with $\alpha = 1.0$ and initial population sizes $(M, N) = (52, 52)$. The domain of β

in these figures (i.e., $\beta \in [\alpha 2^{-1}, 2\alpha]$) is determined to deal with birth rates α and β comparable. Figures 2.14 and 2.15 focus on the expected numbers of births and deaths within species 1, and their corresponding coefficients of variation defined by the coefficients of variation of the random variables $B_1^{(M,N)} 1\{X_{\max}^{(M,N)} \leq K\}$ and $D_1^{(M,N)} 1\{X_{\max}^{(M,N)} \leq K\}$. Our interest in Figures 2.16 and 2.17 is in the correlation structure, which is analyzed in terms of the correlation coefficient between random variables of the form $Y^{(M,N)} 1\{X_{\max}^{(M,N)} \leq K\}$ and $Z^{(M,N)} 1\{X_{\max}^{(M,N)} \leq K\}$, for various choices of $Y^{(M,N)}$ and $Z^{(M,N)}$. Coefficients of variation and of correlation are denoted by $c.v.(\cdot)$ and $\rho(\cdot, \cdot)$, respectively.

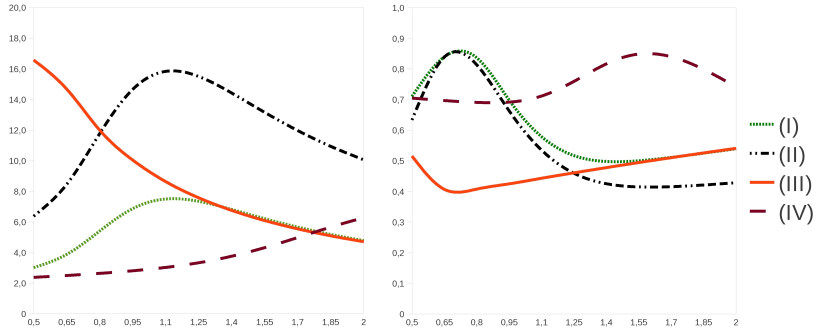

Fig. 2.14. $E[B_1^{(M,N)}; X_{\max}^{(M,N)} \leq K]$ (*left*) and $c.v.(B_1^{(M,N)}; X_{\max}^{(M,N)} \leq K)$ (*right*) versus β, for $(M, N) = (52, 52)$ and $\alpha = 1.0$. Cases: (I) $(\gamma, \delta) = (\alpha 2^{-1}, \beta 2^{-1})$; (II) $(\gamma, \delta) = (\alpha 4^{-1}, \beta 4^{-1})$; (III) $(\gamma, \delta) = (\alpha 4^{-1}, \beta 2^{-1})$; (IV) $(\gamma, \delta) = (\alpha 2^{-1}, \beta 4^{-1})$

An examination of Figures 2.14-2.17 reveals the following observations:

(i) As we expand the domain of β in Figures 2.14 and 2.15, we find that, irrespectively of the choice for the death rates γ and δ, the mean numbers of births and deaths within species 1 behave as non-monotone functions of the birth rate β. It is observed that the expected values $E[B_1^{(M,N)}; X_{\max}^{(M,N)} \leq K]$ and $E[D_1^{(M,N)}; X_{\max}^{(M,N)} \leq K]$ yield graphs with similar shapes in the cases $(\gamma = \alpha 2^{-1}, \delta = \beta 2^{-1})$ and $(\gamma = \alpha 4^{-1}, \delta = \beta 4^{-1})$, but the resulting magnitudes are notably different. In contrast, both shapes and magnitudes in the cases $(\gamma =$

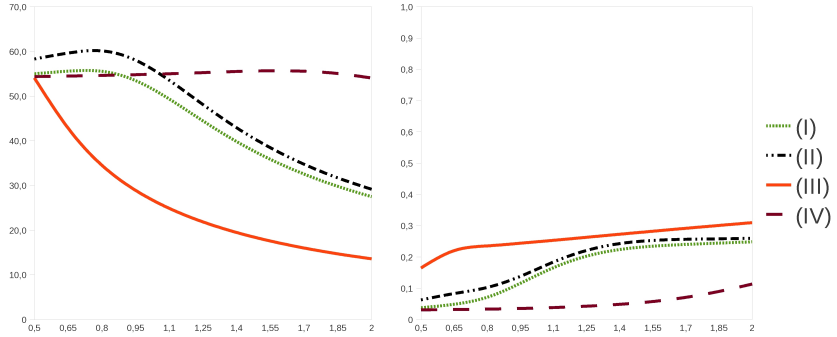

Fig. 2.15. $E[D_1^{(M,N)}; X_{\max}^{(M,N)} \leq K]$ (*left*) and $c.v.(D_1^{(M,N)}; X_{\max}^{(M,N)} \leq K)$ (*right*) versus β, for $(M, N) = (52, 52)$ and $\alpha = 1.0$. Cases: (I) $(\gamma, \delta) = (\alpha 2^{-1}, \beta 2^{-1})$; (II) $(\gamma, \delta) = (\alpha 4^{-1}, \beta 4^{-1})$; (III) $(\gamma, \delta) = (\alpha 4^{-1}, \beta 2^{-1})$; (IV) $(\gamma, \delta) = (\alpha 2^{-1}, \beta 4^{-1})$

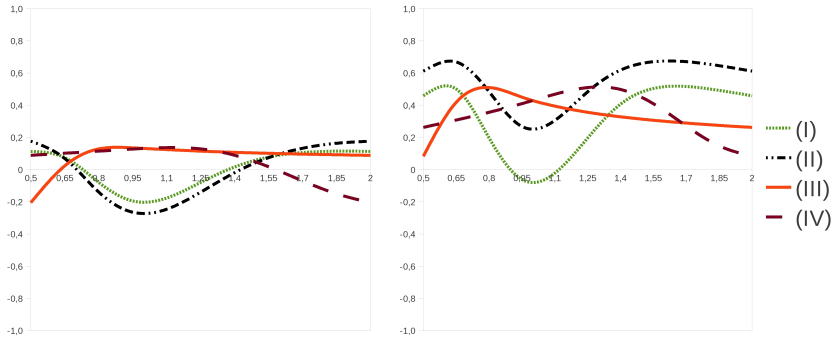

Fig. 2.16. $\rho(B_1^{(M,N)}, B_2^{(M,N)}; X_{\max}^{(M,N)} \leq K)$ (*left*) and $\rho(D_1^{(M,N)}, D_2^{(M,N)}; X_{\max}^{(M,N)} \leq K)$ (*right*) versus β, for $(M, N) = (52, 52)$ and $\alpha = 1.0$. Cases: (I) $(\gamma, \delta) = (\alpha 2^{-1}, \beta 2^{-1})$; (II) $(\gamma, \delta) = (\alpha 4^{-1}, \beta 4^{-1})$; (III) $(\gamma, \delta) = (\alpha 4^{-1}, \beta 2^{-1})$; (IV) $(\gamma, \delta) = (\alpha 2^{-1}, \beta 4^{-1})$

$\alpha 4^{-1}, \delta = \beta 2^{-1})$ and $(\gamma = \alpha 2^{-1}, \delta = \beta 4^{-1})$ are dramatically different.

(ii) An interesting feature in Figure 2.14 is that the values of $E[B_1^{(M,N)}; X_{\max}^{(M,N)} \leq K]$ in the cases $(\gamma = \alpha 2^{-1}, \delta = \beta 2^{-1})$ and $(\gamma = \alpha 4^{-1}, \delta = \beta 2^{-1})$ tend to be graphically undistinguished as β increases. This reveals that, unlike the mean value $E[D_1^{(M,N)}; X_{\max}^{(M,N)} \leq K]$, the incidence of the death rate γ on the number of births of species 1 is not relevant in

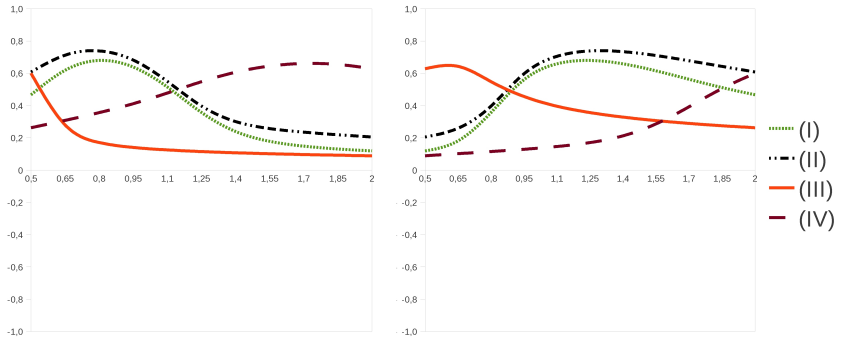

Fig. 2.17. $\rho(B_1^{(M,N)}, D_2^{(M,N)}; X_{\max}^{(M,N)} \leq K)$ (*left*) and $\rho(D_1^{(M,N)}, B_2^{(M,N)}; X_{\max}^{(M,N)} \leq K)$ (*right*) versus β, for $(M, N) = (52, 52)$ and $\alpha = 1.0$. Cases: (I) $(\gamma, \delta) = (\alpha 2^{-1}, \beta 2^{-1})$; (II) $(\gamma, \delta) = (\alpha 4^{-1}, \beta 4^{-1})$; (III) $(\gamma, \delta) = (\alpha 4^{-1}, \beta 2^{-1})$; (IV) $(\gamma, \delta) = (\alpha 2^{-1}, \beta 4^{-1})$

these cases, as the birth rate β (equivalently, the death rate δ) of species 2 becomes large.

(iii) The distributions of $B_1^{(M,N)}$ and $D_1^{(M,N)}$ on the set $\{X_{\max}^{(M,N)} \leq K\}$ can be considered *low-variance* by direct comparison with an exponential distribution. The coefficient of variation is a dimensionless number, so when comparing between $B_1^{(M,N)}$ and $D_1^{(M,N)}$, which have widely different expected values, it is observed that the restricted distribution of $D_1^{(M,N)}$ shows slower-variance.

(iv) Values of the correlation coefficient between the numbers $B_1^{(M,N)}$ and $B_2^{(M,N)}$ of births imply that, in the domain $\beta \in [\alpha 2^{-1}, 2\alpha]$, the linear dependence[1] between them is small or null. As a result, an increment in the number of births in a certain species should not be linearly inferred from the variability in the number of births in the other species. On the contrary, the linear dependence between the numbers $D_1^{(M,N)}$ and $D_2^{(M,N)}$ of deaths frequently becomes medium and large; in such a case, the correlation is positive. This means that, based on Figure 2.15, decreasing values of the number $D_1^{(M,N)}$

[1]The size of a correlation is here interpreted as *null* if $|\rho| < 0.1$, *small* if $0.1 \leq |\rho| < 0.3$, *medium* if $0.3 \leq |\rho| < 0.5$, and *large* if $0.5 \leq |\rho|$.

of deaths in species 1 imply decreasing values of the number $D_2^{(M,N)}$ of deaths in species 2, in the cases of large correlation.

(v) In a two-species competition interaction, the number of deaths in a certain species should increase as the number of births in the other species increases. This first principle is corroborated in Figure 2.17 in terms of the correlation coefficients associated with the pairs $(B_1^{(M,N)}, D_2^{(M,N)})$ and $(D_1^{(M,N)}, B_2^{(M,N)})$, even as the linear dependence is considered small or null. We may however observe that the maximum linear dependence between $B_1^{(M,N)}$ and $D_2^{(M,N)}$ does not necessarily correspond to the maximum value of $E[B_1^{(M,N)}; X_{\max}^{(M,N)} \leq K]$. A similar remark may be made for the linear dependence between $D_1^{(M,N)}$ and $B_2^{(M,N)}$.

2.4 Survival of a certain individual

In this section, we study the survival of a certain individual in an extinction cycle; without loss of generality, we focus on an individual who belongs to species 1. In practice, we can deliberately take interest in a certain individual because he possesses specific characteristics that differ from those of other individuals within species 1. Note that, if such an individual persists, his survival could noticeably influence on the dynamics of the remaining single population.

At this point, we remark the necessity of specifying the way individuals of species 1 are selected to die. Next, we deal with the following *killing* assumptions:

(i) *Random-order assignment (r-killing).* There exists identical chance for selecting the individual who dies, that is, a concrete individual should die with probability m^{-1} if species 1 consists of $m \geq 1$ individuals as a death within species 1 occurs.

(ii) *The-oldest-order assignment (o-killing).* In this age-dependent case, the oldest individual within species 1 is selected to die as a death in species 1 takes place.

(iii) *The-youngest-order assignment (y-killing).* This strategy is specified as the youngest individual in species 1 is selected to die.

2.4.1 Random-order assignment

Let us fix a time epoch, we say $t = 0$, and assume that species 1 and 2 consist of M and N individuals, respectively. To analyze the survival of an individual of species 1, we mark one of the M individuals in species 1, and study the random variable $T_r^{(M,N)}$ defined as the residual lifetime of the *marked* individual; in particular, the survival of the marked individual to the extinction cycle, starting at time $t = 0$ with population sizes $X(0) = (M, N)$, occurs if $T_r^{(M,N)} > T^{(M,N)}$.

Once the level K is in hand (Algorithm 2.2), we replace the original process $\mathcal{X}$ by its *restriction* to the set $\{X_{\max}^{(M,N)} \leq K\}$, if the extinction cycle starts with M and N individuals in species 1 and 2, respectively. Hence, instead of the true value $P(T_r^{(M,N)} > T^{(M,N)})$, we suggest to estimate the probability that the marked individual survives to the extinction cycle by means of $p_r(M, N) = P(X_{\max}^{(M,N)} \leq K, T_r^{(M,N)} > T^{(M,N)})$, which is equivalent to

$$p_r(M, N) = G_K(\mathbf{x}; M, N) - P(X_{\max}^{(M,N)} \leq K, T_r^{(M,N)} \leq T^{(M,N)}), \tag{2.23}$$

since $P(X_{\max}^{(M,N)} \leq K) = G_K(\mathbf{x}; M, N)$.

To derive the probability of the event $\{X_{\max}^{(M,N)} \leq K, T_r^{(M,N)} \leq T^{(M,N)}\}$, we proceed to evaluate in a more general setting the restricted transforms

$$H_r(\theta; m, n) = E\left[e^{-\theta T_r^{(m,n)}}; X_{\max}^{(m,n)} \leq K, T_r^{(m,n)} \leq T^{(m,n)}\right],$$

for $Re(\theta) \geq 0$, and states $(m, n) \in \cup_{k=2}^{K} l(k)$, with $K \geq M + N$, so that the term $P(X_{\max}^{(M,N)} \leq K, T_r^{(M,N)} \leq T^{(M,N)})$ in the right-hand side of (2.23) is routinely computed as the value of $H_r(\theta; M, N)$ at point $\theta = 0$. Based on a first-passage argument, it is found that the restricted transforms $\{H_r(\theta; m, n) : (m, n) \in \mathcal{C}, m + n \leq K\}$ satisfy a finite system of linear equations, which is specified as follows:

(i) For $(m, n) = (1, 1)$,

$$H_r(\theta; 1, 1) = \frac{\alpha H_r(\theta; 2, 1) + \beta H_r(\theta; 1, 2) + \gamma}{\theta + \alpha + \beta + \gamma + \delta}.$$

(ii) For $(m,n)=(m,1)$ with $2\le m\le K-2$,

$$H_r(\theta;m,1)=\frac{\alpha mH_r(\theta;m+1,1)+\beta H_r(\theta;m,2)}{\theta+\alpha m+\beta+\gamma m+\delta m}+\frac{\gamma\big((m-1)H_r(\theta;m-1,1)+G_K(\mathbf{x};m-1,1)\big)}{\theta+\alpha m+\beta+\gamma m+\delta m}.$$

(iii) For $(m,n)=(1,n)$ with $2\le n\le K-2$,

$$H_r(\theta;1,n)=\frac{\alpha H_r(\theta;2,n)+\beta nH_r(\theta;1,n+1)+\gamma n}{\theta+\alpha+\beta n+\gamma n+\delta n}+\frac{\delta nH_r(\theta;1,n-1)}{\theta+\alpha+\beta n+\gamma n+\delta n}.$$

(iv) For (m,n) with $m,n\ge 2$ and $m+n<K$,

$$H_r(\theta;m,n)=\frac{\alpha mH_r(\theta;m+1,n)+\beta nH_r(\theta;m,n+1)}{\theta+\alpha m+\beta n+\gamma mn+\delta mn}+\frac{\gamma n\big((m-1)H_r(\theta;m-1,n)+G_K(\mathbf{x};m-1,n)\big)}{\theta+\alpha m+\beta n+\gamma mn+\delta mn}+\frac{\delta mnH_r(\theta;m,n-1)}{\theta+\alpha m+\beta n+\gamma mn+\delta mn}.$$

(v) For (m,n) with $m,n\ge 1$ and $m+n=K$,

$$H_r(\theta;K-1,1)=\frac{\gamma(K-2)H_r(\theta;K-2,1)}{\theta+\alpha(K-1)+\beta+\gamma(K-1)+\delta(K-1)}+\frac{\gamma G_K(\mathbf{x};K-2,1)}{\theta+\alpha(K-1)+\beta+\gamma(K-1)+\delta(K-1)},$$

$$H_r(\theta;m,n)=\frac{\gamma n(m-1)H_r(\theta;m-1,n)}{\theta+\alpha m+\beta n+\gamma mn+\delta mn}+\frac{\gamma nG_K(\mathbf{x};m-1,n)}{\theta+\alpha m+\beta n+\gamma mn+\delta mn}+\frac{\delta mnH_r(\theta;m,n-1)}{\theta+\alpha m+\beta n+\gamma mn+\delta mn},\quad m,n\ge 2,$$

$$H_r(\theta;1,K-1)=\frac{\gamma(K-1)+\delta(K-1)H_r(\theta;1,K-2)}{\theta+\alpha+\beta(K-1)+\gamma(K-1)+\delta(K-1)}.$$

Equations in the above cases (i)-(v) can be arranged in matrix form as

$$\mathbf{h}_r(\theta) = \mathbf{C}_r(\theta)\mathbf{h}_r(\theta) + \mathbf{c}_r(\theta), \tag{2.24}$$

where the column vector $\mathbf{h}_r(\theta)$ of order $J(K)$ consists of the transforms $H_r(\theta; m, n)$ with states $(m, n) \in \cup_{k=2}^{K} l(k)$, and the square matrix $\mathbf{C}_r(\theta)$, and the column vector $\mathbf{c}_r(\theta)$ are constructed in the usual way. In particular, $\mathbf{C}_r(\theta)$ has the form

$$\begin{pmatrix} 0 & \mathbf{C}_{2,3}(\theta) & & & & \\ \mathbf{C}_{3,2}(\theta) & \mathbf{0}_{2\times 2} & \mathbf{C}_{3,4}(\theta) & & & \\ & \ddots & \ddots & \ddots & & \\ & & \mathbf{C}_{K-1,K-2}(\theta) & \mathbf{0}_{(K-2)\times(K-2)} & \mathbf{C}_{K-1,K}(\theta) & \\ & & & \mathbf{C}_{K,K-1}(\theta) & \mathbf{0}_{(K-1)\times(K-1)} \end{pmatrix},$$

and $\mathbf{c}_r(\theta)$ is given by

$$\mathbf{c}_r(\theta) = \begin{pmatrix} c(\theta; 2) \\ \mathbf{c}(\theta; 3) \\ \vdots \\ \mathbf{c}(\theta; K) \end{pmatrix},$$

where $\mathbf{C}_{k,k+1}(\theta) = \mathbf{A}_{k,k+1}(\theta, 1, 1)$, for $2 \le k \le K-1$, and the entries of the sub-matrices $\mathbf{C}_{k,k-1}(\theta)$, and the sub-vectors $\mathbf{c}_r(\theta; k)$ are specified as follows:

(i) For $2 \le j \le K-1$, we have $\mathbf{C}_{j,j+1}(\theta) = \mathbf{A}_{j,j+1}(\theta, 1, 1)$.

(ii) For $3 \le j \le K$, $\mathbf{C}_{j,j-1}(\theta)$ is a sub-matrix of dimension $(j-1) \times (j-2)$, whose (k, k')th entry is given by

$$(\mathbf{C}_{j,j-1}(\theta))_{k,k'} = \begin{cases} \frac{\delta(j-k)k}{\theta+\alpha(j-k)+\beta k+\gamma(j-k)k+\delta(j-k)k}, & \text{if } k' = k-1, \\ \frac{\gamma(j-k-1)k}{\theta+\alpha(j-k)+\beta k+\gamma(j-k)k+\delta(j-k)k}, & \text{if } k' = k, \\ 0, & \text{otherwise.} \end{cases}$$

(iii) In the case $j = 2$, we find that $c(\theta; 2) = \gamma(\theta+\alpha+\beta+\gamma+\delta)^{-1}$. For $3 \le j \le K$, the column vector $\mathbf{c}(\theta; j)$ has $j-1$ entries, which are given by

$$(\mathbf{c}(\theta; j))_k = \begin{cases} \frac{\gamma k G_K(\mathbf{x}; j-k-1, k)}{\theta+\alpha(j-k)+\beta k+\gamma(j-k)k+\delta(j-k)k}, & \text{if } 1 \le k \le j-2, \\ \frac{\gamma(j-1)}{\theta+\alpha+\beta(j-1)+\gamma(j-1)+\delta(j-1)}, & \text{if } k = j-1. \end{cases}$$

By using the structured form of $\mathbf{C}_r(\theta)$, the vector $\mathbf{h}_r(\theta)$ can be evaluated as $(\mathbf{I}_{J(K)} - \mathbf{C}_r(\theta))^{-1}\mathbf{c}_r(\theta)$ in a similar manner to the solution of (2.19). More concretely, for an extinction cycle starting with initial sizes $M > 0$ and $N > 0$ in species 1 and 2, Algorithm 2.3 computes the restricted transform $H_r(\theta; M, N)$ at each θ with $Re(\theta) \geq 0$. Sub-vectors $\mathbf{h}_r(\theta; k)$ in Algorithm 2.3 contain the transforms $H_r(\theta; m, n)$ for states (m, n) in the kth level, for $2 \leq k \leq K$.

Algorithm 2.3. Estimation of the restricted transform $E[\exp\{-\theta T_r^{(M,N)}\}; T_r^{(M,N)} \leq T^{(M,N)}]$

Step 1 $j := 2$;
$\mathbf{K}_j(\theta) := 1$;
$\mathbf{L}_j(\theta) := \gamma(\theta + \alpha + \beta + \gamma + \delta)^{-1}$.

Step 2 While $j < K$, repeat
$j := j + 1$;
$\mathbf{K}_j(\theta) := (\mathbf{I}_{j-1} - \mathbf{C}_{j,j-1}(\theta)\mathbf{K}_{j-1}(\theta)\mathbf{C}_{j-1,j}(\theta))^{-1}$;
$\mathbf{L}_j(\theta) := \mathbf{C}_{j,j-1}(\theta)\mathbf{K}_{j-1}(\theta)\mathbf{L}_{j-1}(\theta) + \mathbf{c}(\theta; j)$.

Step 3 $\mathbf{h}_r(\theta; K) := \mathbf{K}_K(\theta)\mathbf{L}_K(\theta)$;
for $j = K - 1, K - 2, ..., M + N$, compute
$\mathbf{h}_r(\theta; j) := \mathbf{K}_j(\theta)\left(\mathbf{C}_{j,j+1}(\theta)\mathbf{h}_r(\theta; j + 1) + \mathbf{L}_j(\theta)\right)$;
read $H_r(\theta; M, N)$ from $\mathbf{h}_r(\theta; M + N)$;
estimate $E[\exp\{-\theta T_r^{(M,N)}\}; T_r^{(M,N)} \leq T^{(M,N)}]$ by means of $H_r(\theta; M, N)$.

From (2.24), we can routinely compute, under the assumption that $X_{\max}^{(M,N)} \leq K$ and $T_r^{(M,N)} \leq T^{(M,N)}$, any arbitrary moment of the residual lifetime of the marked individual by using the recursion

$$\mathbf{t}_r(k) = \left(\mathbf{I}_{J(K)} - \mathbf{C}_r(0)\right)^{-1} \left((-1)^k \mathbf{c}_r^k(0) + \sum_{j=1}^{k} \frac{k(k-1)\cdot ... \cdot (k-j+1)}{j!} (-1)^j \mathbf{C}_r^j(0)\mathbf{t}_r(k-j) \right),$$

for values $k \geq 1$, with $\mathbf{t}_r(0) = \mathbf{h}_r(0)$, where the column vector $\mathbf{t}_r(k)$ of order $J(K)$ has entries $E[(T_r^{(m,n)})^k; X_{\max}^{(m,n)} \leq K, T_r^{(m,n)} \leq$

$T^{(m,n)}]$, for $(m,n) \in \cup_{k=2}^{K} l(k)$, and $\mathbf{C}_r^j(0)$ and $\mathbf{c}_r^j(0)$ denote the jth derivatives of $\mathbf{C}_r(\theta)$ and $\mathbf{c}_r(\theta)$ with respect to θ, at point $\theta = 0$. Specifically, we have

(i) For $2 \le j \le K-1$, $\mathbf{C}_{j,j+1}^i(0) = \mathbf{A}_{j,j+1}^{i,\theta}(\mathbf{y})$.

(ii) For $3 \le j \le K$, the ith derivative of $\mathbf{C}_{j,j-1}(\theta)$ at point $\theta = 0$ has elements

$$\left(\mathbf{C}_{j,j-1}^i(0)\right)_{k,k'} = \begin{cases} \frac{(-1)^i i!\delta(j-k)k}{(\alpha(j-k)+\beta k+\gamma(j-k)k+\delta(j-k)k)^{i+1}}, & \text{if } k' = k-1, \\ \frac{(-1)^i i!\gamma(j-k-1)k}{(\alpha(j-k)+\beta k+\gamma(j-k)k+\delta(j-k)k)^{i+1}}, & \text{if } k' = k, \\ 0, & \text{otherwise.} \end{cases}$$

(iii) In the case $j = 2$, the ith derivative of $c(\theta;2)$ at point $\theta = 0$ is given by $c^i(0;2) = (-1)^i i!\gamma(\alpha+\beta+\gamma+\delta)^{i+1}$. For $3 \le j \le K$, the entries of the sub-vector $\mathbf{c}^i(0;j)$, defined as the ith derivative of $\mathbf{c}(\theta;j)$ at point $\theta = 0$, are given by

$$\left(\mathbf{c}^i(0;j)\right)_k = \begin{cases} \frac{(-1)^i i!\gamma k G_K(\mathbf{x};j-k-1,k)}{(\alpha(j-k)+\beta k+\gamma(j-k)k+\delta(j-k)k)^{i+1}}, & \text{if } 1 \le k \le j-2, \\ \frac{(-1)^i i!\gamma(j-1)}{(\alpha+\beta(j-1)+\gamma(j-1)+\delta(j-1))^{i+1}}, & \text{if } k = j-1. \end{cases}$$

Needless to say, the inverse $(\mathbf{I}_{J(K)} - \mathbf{C}_r(0))^{-1}$ can be efficiently evaluated from a slight variant of Steps 4 and 5 in Algorithm 2.2.

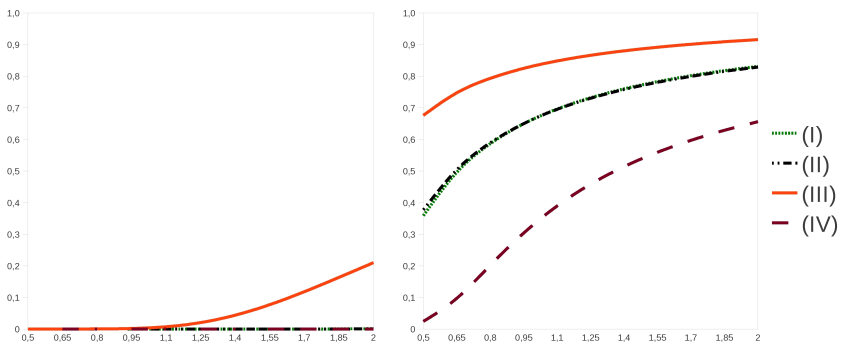

Fig. 2.18. Values of $p_r(M,N)$ versus β for initial sizes $M = 26$ and $N = 78$ (*left*), and $M = 78$ and $N = 26$ (*right*), and $\alpha = 1.0$. Cases: (I) $(\gamma,\delta) = (\alpha 2^{-1}, \beta 2^{-1})$; (II) $(\gamma,\delta) = (\alpha 4^{-1}, \beta 4^{-1})$; (III) $(\gamma,\delta) = (\alpha 4^{-1}, \beta 2^{-1})$; (IV) $(\gamma,\delta) = (\alpha 2^{-1}, \beta 4^{-1})$

In Figure 2.18, we plot the probability $p_r(M,N)$ that the marked individual survives to an extinction cycle, starting with

initial sizes $(M, N) \in \{(26, 78), (78, 26)\}$, as a function of the birth rate β in species 2. The graphs are reported for the cases $(\gamma = \alpha 2^{-1}, \delta = \beta 2^{-1})$, $(\gamma = \alpha 4^{-1}, \delta = \beta 4^{-1})$, $(\gamma = \alpha 4^{-1}, \delta = \beta 2^{-1})$, and $(\gamma = \alpha 2^{-1}, \delta = \beta 4^{-1})$. It should be noted that, with initial sizes $M = 26$ and $N = 78$, the surviving probability of species 1 is very small in the cases $(\gamma = \alpha 2^{-1}, \delta = \beta 2^{-1})$, $(\gamma = \alpha 4^{-1}, \delta = \beta 4^{-1})$, and $(\gamma = \alpha 2^{-1}, \delta = \beta 4^{-1})$, so that the marked individual will rarely survive to the time of the first extinction, regardless of the choice of β in the domain $[\alpha 2^{-1}, 2\alpha]$. In the case $(\gamma = \alpha 4^{-1}, \delta = \beta 2^{-1})$, the surviving probability of species 1 increases with increasing values of β (equivalently, of δ), thus implying a perceptible increment in $p_r(26, 78)$. With initial sizes $M = 78$ and $N = 26$, the survival of species 1 is supported by high probabilities in the four cases. Increasing values of β result in increasing values of the surviving probability of species 1. Hence, the probability $p_r(78, 26)$ behaves as an increasing function of β (equivalently, of δ). Smaller and higher values of $p_r(M, N)$ are associated with the cases $(\gamma = \alpha 2^{-1}, \delta = \beta 4^{-1})$ and $(\gamma = \alpha 4^{-1}, \delta = \beta 2^{-1})$, respectively. For fixed values of α, β and γ, the influence of the death rate δ in species 2 on the probability $p_r(78, 26)$ is relevant. Figure 2.18 reveals that, in contrast to the behavior of $E[B_1^{(78,26)}; X_{\max}^{(78,26)} \leq K]$ and $E[D_1^{(78,26)}; X_{\max}^{(78,26)} \leq K]$, the choices $(\gamma = \alpha 2^{-1}, \delta = \beta 2^{-1})$ and $(\gamma = \alpha 4^{-1}, \delta = \beta 4^{-1})$ do not lead to significant changes in the probability $p_r(78, 26)$ that the marked individual survives to the extinction cycle. We remark here that $E[B_1^{(78,26)}; X_{\max}^{(78,26)} \leq K]$ and $E[D_1^{(78,26)}; X_{\max}^{(78,26)} \leq K]$ behave similarly to the corresponding expectations shown in Figures 2.14 and 2.15 for $M = N = 52$.

Figure 2.19 shows the effects of the initial sizes M and N, and the birth and death rates on the restricted distribution of $T_r^{(M,N)}$ when $T_r^{(M,N)} \leq T^{(M,N)}$. We consider two scenarios defined by the choices $\beta \in \{\alpha 2^{-1}, 2\alpha\}$ with $\alpha = 1.0$, $\gamma = \alpha 4^{-1}$, $\delta = \beta 4^{-1}$, and initial population sizes $(M, N) \in \{(26, 78), (52, 52), (78, 26)\}$. By applying the algorithms EULER and POST-WIDDER [1] to Algorithm 2.3, we derive the restricted distribution function $F_r(t; M, N)$, which is defined as

$$P(T_r^{(M,N)} \leq t, X_{\max}^{(M,N)} \leq K, T_r^{(M,N)} \leq T^{(M,N)}), \quad t \geq 0.$$

Note that the limit value $F_r(\infty; M, N)$ corresponds to the value of the transform $H_r(\theta; M, N)$ at point $\theta = 0$, that is, the joint probability that the marked individual will not survive to the extinction cycle and the maximum population size will not exceed the value K, starting with initial sizes M and N. In both scenarios $\beta \in \{\alpha 2^{-1}, 2\alpha\}$, the function $F_r(t; 26, 78)$ is shown graphically to be stochastically smaller than $F_r(t; 52, 52)$, and $F_r(t; 52, 52)$ seems to be stochastically smaller than $F_r(t; 78, 26)$.

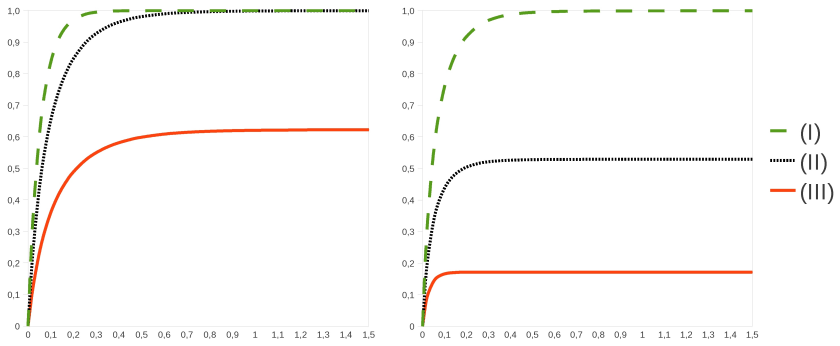

Fig. 2.19. $F_r(t; M, N)$ versus t for 2 scenarios defined by the choices $\beta = \alpha 2^{-1}$ (*left*) and $\beta = 2\alpha$ (*right*), with $(\alpha, \gamma, \delta) = (1.0, \alpha 4^{-1}, \beta 4^{-1})$. Initial sizes: (I) $(M, N) = (26, 78)$; (II) $(M, N) = (52, 52)$; (III) $(M, N) = (78, 26)$

2.4.2 Age-dependent assignments

In studying age-dependent strategies, we reformulate states (m, n) by adding a third component that amounts to the *age* of the marked individual within species 1. This results in states (m, n, a) with $0 \leq a \leq m$, where the values $a = 1$ and m indicate that the marked individual is the youngest and the oldest one within species 1, for an ecosystem with m and n individuals in species 1 and 2, respectively. In this formulation, the value $a = 0$ is related to the death of the marked individual, regardless of the concrete age-dependent strategy. This implies that, in the *augmented* version of the process $\mathcal{X}$, the state space $\mathcal{S}$ is replaced by $\mathcal{S}^* = \mathcal{C}_0^* \cup \mathcal{C}^*$, where the subset of absorbing states is expressed as

$$\mathcal{C}_0^* = \{(m, 0, a) : m \geq 1, 0 \leq a \leq m\} \cup \{(0, n, 0) : n \geq 1\},$$

and the class of transient states is specified by

$$\mathcal{C}^* = \bigcup_{m=1}^{\infty} L(m),$$

with the *level* $L(m) = \cup_{a=0}^{m} l(m,a)$, for $m \geq 1$, and the *sub-level* $l(m,a) = \{(m,n,a) : n \geq 1\}$, for $0 \leq a \leq m$. Figures 2.20 and 2.21 show transitions between augmented states in the o-killing and y-killing models, respectively.

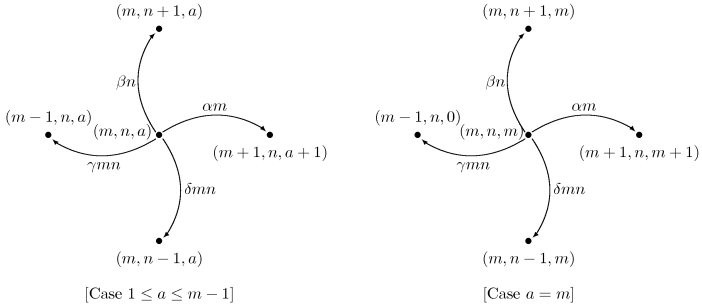

Fig. 2.20. Transitions between augmented states (m,n,a) in the o-killing model

Let us assume that, at time $t = 0$, an extinction cycle starts with $M > 0$ and $N > 0$ individuals of species 1 and 2, respectively. We mark one of the M individuals in species 1, and define $T_o^{(M,N,A)}$ and $T_y^{(M,N,A)}$ as the residual lifetimes of the marked individual in the o-killing and y-killing models, respectively, if the age of this individual at time $t = 0$ is given by $A \in \{1, 2, ..., M\}$.

Similarly to the random-order assignment, we proceed to estimate the survival probabilities $P(T_o^{(M,N,A)} > T^{(M,N,A)})$ and $P(T_y^{(M,N,A)} > T^{(M,N,A)})$ by their restricted counterparts

$$p_o(M,N,A) = P(X_{\max}^{(M,N)} \leq K, T_o^{(M,N,A)} > T^{(M,N,A)}),$$
$$p_y(M,N,A) = P(X_{\max}^{(M,N)} \leq K, T_y^{(M,N,A)} > T^{(M,N,A)}).$$

It should be noted that, in the o-killing model, $p_o(M,N,A)$ is given by

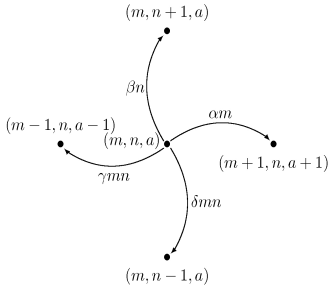

Fig. 2.21. Transitions between augmented states (m, n, a), for $1 \leq a \leq m$, in the y-killing model

$$p_o(M, N, A) = P\left(D_1^{(M,N)} \leq M - A, X_{\max}^{(M,N)} \leq K\right),$$

since the marked individual should survive to the extinction cycle as the number $D_1^{(M,N)}$ of deaths within species 1 is not greater than $M - A$. Note that this expression for $p_o(M, N, A)$ requires numerical inversion of the generating function $G_K(\mathbf{s}_o; M, N)$ defined at points $\mathbf{s}_o = (0, 1, z_1, 1, 1)$ with $|z_1| \leq 1$. Under the y-killing assumption, the marked individual should die as the process $\mathcal{X}$ first hits the line $m = M - A$ before absorption. One way of analyzing $p_y(M, N, A)$ implies the replacement of the state space $\mathcal{S}$ by the subset $\mathcal{S}(M, A) = \{(m, n) : m \geq M - A, n \geq 0\} - \{(M - A, 0)\}$. The probability that the marked individual survives to the extinction cycle, starting in a fixed state (M, N, A) with $M > 0$, $N > 0$ and $1 \leq A \leq M$, is equivalent to the absorption probability into the set $\{(m, 0) : m \geq M - A + 1\}$ of absorbing states in the resulting process defined from (2.1) for states in $\mathcal{S}(M, A)$.

Alternatively, we carry out a variant of our approach for the random-order assignment, and expressions for $p_o(M, N, A)$ and $p_y(M, N, A)$ are given respectively by

$$G_k(\mathbf{x}; M, N) - P\left(X_{\max}^{(M,N)} \leq K, T_o^{(M,N,A)} \leq T^{(M,N,A)}\right),$$
$$G_k(\mathbf{x}; M, N) - P\left(X_{\max}^{(M,N)} \leq K, T_y^{(M,N,A)} \leq T^{(M,N,A)}\right).$$

This means that, for each value of $K \geq M + N$, we examine the augmented version of $\mathcal{X}$ till absorption, but only on sample paths

evolving on states of the finite set $\cup_{m=1}^{K-1} L_K(m)$ of transient states, where $L_K(m) = \cup_{a=0}^{m} l_K(m,a)$ and $l_K(m,a) = \{(m,n,a) : 1 \le n \le K-m\}$, for $0 \le a \le m$ and $1 \le m \le K-1$. To do that, we introduce the notation

$$H_o(\theta; m, n, a) = E\left[e^{-\theta T_o^{(m,n,a)}}; X_{\max}^{(m,n)} \le K, T_o^{(m,n,a)} \le T^{(m,n,a)}\right],$$
$$H_y(\theta; m, n, a) = E\left[e^{-\theta T_y^{(m,n,a)}}; X_{\max}^{(m,n)} \le K, T_y^{(m,n,a)} \le T^{(m,n,a)}\right],$$

for $Re(\theta) \ge 0$, and states (m,n,a) such that $(m,n) \in \cup_{k=2}^{K} l(k)$, with $K \ge M+N$, and $1 \le a \le m$. It is then clear that $P(X_{\max}^{(M,N)} \le K, T_o^{(M,N,A)} \le T^{(M,N,A)})$ and $P(X_{\max}^{(M,N)} \le K, T_y^{(M,N,A)} \le T^{(M,N,A)})$ are given by the values of $H_o(\theta; M, N, A)$ and $H_y(\theta; M, N, A)$ at point $\theta = 0$.

From Figure 2.20, we readily find that the set $\{H_o(\theta; m, n, a) : (m,n) \in \cup_{k=2}^{K} l(k), 1 \le a \le m\}$ of restricted transforms verifies the following linear equations:

(i)' For $(m,n,a) = (1,1,1)$,

$$H_o(\theta; 1,1,1) = \frac{\alpha H_o(\theta; 2,1,2) + \beta H_o(\theta; 1,2,1) + \gamma}{\theta + \alpha + \beta + \gamma + \delta}.$$

(ii)' For $(m,n,a) = (m,1,a)$ with $2 \le m \le K-2$,

$$H_o(\theta; m,1,a) = \frac{\alpha m H_o(\theta; m+1,1,a+1) + \beta H_o(\theta; m,2,a)}{\theta + \alpha m + \beta + \gamma m + \delta m} + \frac{\gamma m H_o(\theta; m-1,1,a)}{\theta + \alpha m + \beta + \gamma m + \delta m}, \quad 1 \le a \le m-1,$$

$$H_o(\theta; m,1,m) = \frac{\alpha m H_o(\theta; m+1,1,m+1) + \beta H_o(\theta; m,2,m)}{\theta + \alpha m + \beta + \gamma m + \delta m} + \frac{\gamma m G_K(\mathbf{x}; m-1,1)}{\theta + \alpha m + \beta + \gamma m + \delta m}.$$

(iii)' For $(m,n,a) = (1,n,1)$ with $2 \le n \le K-2$,

$$H_o(\theta; 1,n,1) = \frac{\alpha H_o(\theta; 2,n,2) + \beta n H_o(\theta; 1,n+1,1) + \gamma n}{\theta + \alpha + \beta n + \gamma n + \delta n} + \frac{\delta n H_o(\theta; 1,n-1,1)}{\theta + \alpha + \beta n + \gamma n + \delta n}.$$

(iv)' For (m,n,a) with $m,n>1$ and $m+n<K$,

$$\begin{aligned}H_o(\theta;m,n,a)=&\frac{\alpha mH_o(\theta;m+1,n,a+1)}{\theta+\alpha m+\beta n+\gamma mn+\delta mn}\\&+\frac{\beta nH_o(\theta;m,n+1,a)}{\theta+\alpha m+\beta n+\gamma mn+\delta mn}\\&+\frac{\gamma mnH_o(\theta;m-1,n,a)}{\theta+\alpha m+\beta n+\gamma mn+\delta mn}\\&+\frac{\delta mnH_o(\theta;m,n-1,a)}{\theta+\alpha m+\beta n+\gamma mn+\delta mn},\\&\qquad 1\le a\le m-1,\\H_o(\theta;m,n,m)=&\frac{\alpha mH_o(\theta;m+1,n,m+1)}{\theta+\alpha m+\beta n+\gamma mn+\delta mn}\\&+\frac{\beta nH_o(\theta;m,n+1,m)}{\theta+\alpha m+\beta n+\gamma mn+\delta mn}\\&+\frac{\gamma mnG_K(\mathbf{x};m-1,n)}{\theta+\alpha m+\beta n+\gamma mn+\delta mn}\\&+\frac{\delta mnH_o(\theta;m,n-1,m)}{\theta+\alpha m+\beta n+\gamma mn+\delta mn}.\end{aligned}$$

(v)' For (m,n,a) with $m,n>1$ and $m+n=K$,

$$\begin{aligned}H_o(\theta;m,n,a)=&\frac{\gamma mnH_o(\theta;m-1,n,a)}{\theta+\alpha m+\beta n+\gamma mn+\delta mn}\\&+\frac{\delta mnH_o(\theta;m,n-1,a)}{\theta+\alpha m+\beta n+\gamma mn+\delta mn},\\&\qquad 1\le a\le m-1,\\H_o(\theta;m,n,m)=&\frac{\gamma mnG_K(\mathbf{x};m-1,n)}{\theta+\alpha m+\beta n+\gamma mn+\delta mn}\\&+\frac{\delta mnH_o(\theta;m,n-1,m)}{\theta+\alpha m+\beta n+\gamma mn+\delta mn}.\end{aligned}$$

(vi)' For $(m,n,a)=(K-1,1,a)$,

$$\begin{aligned}H_o(\theta;K-1,1,a)=&\frac{\gamma(K-1)H_o(\theta;K-2,1,a)}{\theta+\beta+(K-1)(\alpha+\gamma+\delta)},\\&\qquad 1\le a\le K-2,\\H_o(\theta;K-1,1,K-1)=&\frac{\gamma(K-1)G_K(\mathbf{x};K-2,1)}{\theta+\beta+(K-1)(\alpha+\gamma+\delta)}.\end{aligned}$$

(vii)' For $(m,n,a)=(1,K-1,1)$,

$$H_o(\theta;1,K-1,1)=\frac{\gamma(K-1)+\delta(K-1)H_o(\theta;1,K-2,1)}{\theta+\alpha+(K-1)(\beta+\gamma+\delta)}.$$

Equations in (i)'-(vii)' yield the equality $\mathbf{h}_o(\theta)=\mathbf{C}_o(\theta)\mathbf{h}_o(\theta)+\mathbf{c}_o(\theta)$, where the column vector $\mathbf{h}_o(\theta)$ contains the transforms $H_o(\theta;m,n,a)$ for all state (m,n,a) such as $(m,n)\in\cup_{k=2}^{K}l(k)$, with $K\geq M+N$, and $1\leq a\leq m$, and $\mathbf{C}_o(\theta)$ and $\mathbf{c}_o(\theta)$ have the structured form

$$\mathbf{C}_o(\theta)=\begin{pmatrix}\mathbf{C}^*_{1,1}(\theta)&\mathbf{C}^*_{1,2}(\theta)&&&&\\ \mathbf{C}^*_{2,1}(\theta)&\mathbf{C}^*_{2,2}(\theta)&\mathbf{C}^*_{2,3}(\theta)&&&\\ &\ddots&\ddots&\ddots&&\\ &&\mathbf{C}^*_{K-2,K-3}(\theta)&\mathbf{C}^*_{K-2,K-2}(\theta)&\mathbf{C}^*_{K-2,K-1}(\theta)\\ &&&\mathbf{C}^*_{K-1,K-2}(\theta)&\mathbf{C}^*_{K-1,K-1}(\theta)\end{pmatrix},$$

$$\mathbf{c}_o(\theta)=\begin{pmatrix}\mathbf{c}_o(\theta;1)\\ \mathbf{c}_o(\theta;2)\\ \vdots\\ \mathbf{c}_o(\theta;K-1)\end{pmatrix},$$

where

$$\mathbf{c}_o(\theta;m)=\begin{pmatrix}\mathbf{0}_{(m-1)(K-m)}\\ \mathbf{c}_o(\theta;m,m)\end{pmatrix},$$

and the kth entry of the column vector $\mathbf{c}_o(\theta;m,m)$ is given by

$$\left(\mathbf{c}_o(\theta;m,m)\right)_k=\frac{\gamma mkG_K(\mathbf{x};m-1,k)}{\theta+\alpha m+\beta k+\gamma mk+\delta mk},\quad 1\leq k\leq K-m.$$

Sub-matrices $\mathbf{C}^*_{m,m'}(\theta)$ are related to jumps from states in $L_K(m)$ to states in $L_K(m')$, for $m'\in\{m-1,m,m+1\}$. Specifically, we have $\mathbf{C}^*_{m,m}(\theta)=\mathrm{diag}(\mathbf{C}^{1,1}_{m,m}(\theta),\mathbf{C}^{2,2}_{m,m}(\theta),...,\mathbf{C}^{m,m}_{m,m}(\theta))$, the matrix $\mathbf{C}^*_{m,m-1}(\theta)$ has the form

$$\mathbf{C}^*_{m,m-1}(\theta)=\begin{pmatrix}\mathbf{C}^{1,1}_{m,m-1}(\theta)&&&\\ &\mathbf{C}^{2,2}_{m,m-1}(\theta)&&\\ &&\ddots&\\ &&&\mathbf{C}^{m-1,m-1}_{m,m-1}(\theta)\\ &&&\mathbf{0}_{(K-m)\times(K-m+1)}\end{pmatrix},$$

and $\mathbf{C}^{*}_{m,m+1}(\theta)$ is given by

$$\begin{pmatrix} \mathbf{0}_{(K-m)\times(K-m-1)}\ \mathbf{C}^{1,2}_{m,m+1}(\theta) & & & \\ & \mathbf{C}^{2,3}_{m,m+1}(\theta) & & \\ & & \ddots & \\ & & & \mathbf{C}^{m,m+1}_{m,m+1}(\theta) \end{pmatrix},$$

where $\mathbf{C}^{a,a}_{m,m-1}(\theta)$ is a sub-matrix of dimension $(K-m)\times(K-m+1)$ with elements

$$\left(\mathbf{C}^{a,a}_{m,m-1}(\theta)\right)_{k,k'} = \begin{cases} \frac{\gamma mk}{\theta+\alpha m+\beta k+\gamma mk+\delta mk}, & \text{if } k'=k, \\ 0, & \text{otherwise,} \end{cases}$$

the square matrix $\mathbf{C}^{a,a}_{m,m}(\theta)$ of dimension $K-m$ has elements

$$\left(\mathbf{C}^{a,a}_{m,m}(\theta)\right)_{k,k'} = \begin{cases} \frac{\delta mk}{\theta+\alpha m+\beta k+\gamma mk+\delta mk}, & \text{if } k'=k-1, \\ \frac{\beta k}{\theta+\alpha m+\beta k+\gamma mk+\delta mk}, & \text{if } k'=k+1, \\ 0, & \text{otherwise,} \end{cases}$$

and $\mathbf{C}^{a,a+1}_{m,m+1}(\theta)$ has dimension $(K-m)\times(K-m-1)$ and elements

$$\left(\mathbf{C}^{a,a+1}_{m,m+1}(\theta)\right)_{k,k'} = \begin{cases} \frac{\alpha m}{\theta+\alpha m+\beta k+\gamma mk+\delta mk}, & \text{if } k'=k, \\ 0, & \text{otherwise.} \end{cases}$$

It is worth noting that, for a given initial state (M,N,A), the solution $H_o(\theta;M,N,A)$ does not require the computation of the inverse $(\mathbf{I}_{J'(K)}-\mathbf{C}_o(\theta))^{-1}$, where $J'(K)$ denotes the cardinality of the set $\cup_{m=1}^{K-1}L_K(m)$; i.e., $J'(K)=(K-1)K(K+1)6^{-1}$. Specifically, if we decompose the column vector $\mathbf{h}_o(\theta)$ by levels into sub-vectors $\mathbf{h}_o(\theta;m)$, for $1\le m\le K-1$, and each sub-vector $\mathbf{h}_o(\theta;m)$ is partitioned by sub-levels into $\mathbf{h}_o(\theta;m,a)$, for $1\le a\le m$, then we have

$$\begin{aligned} \mathbf{h}_o(\theta;m,a) = \mathbf{M}_o(\theta;m,a)\Big(&\mathbf{N}_o(\theta;m,a) \\ &+(1-\delta_{m,K-1})\mathbf{C}^{a,a+1}_{m,m+1}(\theta)\mathbf{h}_o(\theta;m+1,a+1)\Big), \end{aligned} \tag{2.25}$$

for $1\le a\le m\le K-1$, where $\mathbf{M}_o(\theta;m,a)=(\mathbf{I}_{K-m}-(1-\delta_{m,K-1})\mathbf{C}^{a,a}_{m,m}(\theta))^{-1}$, for $1\le a\le m\le K-1$. The matrices $\mathbf{N}_o(\theta;m,a)$ are

defined by $\mathbf{N}_o(\theta; m, a) = \mathbf{C}^{a,a}_{m,m-1}(\theta)\mathbf{h}_o(\theta; m-1, a)$ if $1 \le a \le m-1$, and $\mathbf{N}_o(\theta; m, m) = \mathbf{c}_o(\theta; m, m)$ if $a = m$. Therefore, starting with $\mathbf{h}_o(\theta; K-1, K-1)$ (obtained from (vi)'), we may derive $H_o(\theta; M, N, A)$ by implementing (2.25) in the recursive manner shown in Figure 2.22.

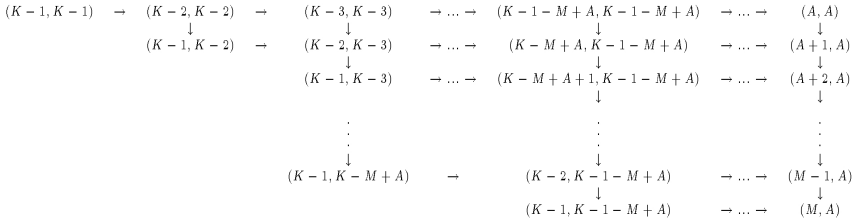

Fig. 2.22. Recursive computation of $H_o(\theta; M, N, A)$ as a component of $\mathbf{h}_o(\theta; M, A)$

$$(K-1, K-1-M+A) \;\to\; (K-2, K-2-M+A) \;\to \ldots \to\; (M+1, A+1) \;\to\; (M, A)$$

Fig. 2.23. Recursive computation of $H_y(\theta; M, N, A)$ as a component of $\mathbf{h}_y(\theta; M, A)$

In analyzing the y-killing model (see Figure 2.21), equations in (i)'-(vii)' should be replaced by

(i)" For $(m, n, a) = (1, 1, 1)$,

$$H_y(\theta; 1, 1, 1) = \frac{\alpha H_y(\theta; 2, 1, 2) + \beta H_y(\theta; 1, 2, 1) + \gamma}{\theta + \alpha + \beta + \gamma + \delta}.$$

(ii)" For $(m, n, a) = (m, 1, a)$ with $2 \le m \le K-2$,

$$H_y(\theta; m, 1, 1) = \frac{\alpha m H_y(\theta; m+1, 1, 2) + \beta H_y(\theta; m, 2, 1)}{\theta + \alpha m + \beta + \gamma m + \delta m} + \frac{\gamma m G_K(\mathbf{x}; m-1, 1)}{\theta + \alpha m + \beta + \gamma m + \delta m},$$

$$H_y(\theta; m, 1, a) = \frac{\alpha m H_y(\theta; m+1, 1, a+1) + \beta H_y(\theta; m, 2, a)}{\theta + \alpha m + \beta + \gamma m + \delta m} + \frac{\gamma m H_y(\theta; m-1, 1, a-1)}{\theta + \alpha m + \beta + \gamma m + \delta m}, \quad 2 \le a \le m.$$

(iii)" For $(m,n,a)=(1,n,1)$ with $2\le n\le K-2$,

$$H_y(\theta;1,n,1)=\frac{\alpha H_y(\theta;2,n,2)+\beta nH_y(\theta;1,n+1,1)+\gamma n}{\theta+\alpha+\beta n+\gamma n+\delta n}+\frac{\delta nH_y(\theta;1,n-1,1)}{\theta+\alpha+\beta n+\gamma n+\delta n}.$$

(iv)" For (m,n,a) with $m,n>1$ and $m+n<K$,

$$\begin{aligned}H_y(\theta;m,n,1)=&\frac{\alpha mH_y(\theta;m+1,n,2)}{\theta+\alpha m+\beta n+\gamma mn+\delta mn}\\&+\frac{\beta nH_y(\theta;m,n+1,1)}{\theta+\alpha m+\beta n+\gamma mn+\delta mn}\\&+\frac{\gamma mnG_K(\mathbf{x};m-1,n)}{\theta+\alpha m+\beta n+\gamma mn+\delta mn}\\&+\frac{\delta mnH_y(\theta;m,n-1,1)}{\theta+\alpha m+\beta n+\gamma mn+\delta mn},\end{aligned}$$

$$\begin{aligned}H_y(\theta;m,n,a)=&\frac{\alpha mH_y(\theta;m+1,n,a+1)}{\theta+\alpha m+\beta n+\gamma mn+\delta mn}\\&+\frac{\beta nH_y(\theta;m,n+1,a)}{\theta+\alpha m+\beta n+\gamma mn+\delta mn}\\&+\frac{\gamma mnH_y(\theta;m-1,n,a-1)}{\theta+\alpha m+\beta n+\gamma mn+\delta mn}\\&+\frac{\delta mnH_y(\theta;m,n-1,a)}{\theta+\alpha m+\beta n+\gamma mn+\delta mn},\ 2\le a\le m.\end{aligned}$$

(v)" For (m,n,a) with $m,n>1$ and $m+n=K$,

$$\begin{aligned}H_y(\theta;m,n,1)=&\frac{\gamma mnG_K(\mathbf{x};m-1,n)}{\theta+\alpha m+\beta n+\gamma mn+\delta mn}\\&+\frac{\delta mnH_y(\theta;m,n-1,1)}{\theta+\alpha m+\beta n+\gamma mn+\delta mn},\\H_y(\theta;m,n,a)=&\frac{\gamma mnH_y(\theta;m-1,n,a-1)}{\theta+\alpha m+\beta n+\gamma mn+\delta mn}\\&+\frac{\delta mnH_y(\theta;m,n-1,a)}{\theta+\alpha m+\beta n+\gamma mn+\delta mn},\ 2\le a\le m.\end{aligned}$$

(vi)" For $(m, n, a) = (K-1, 1, a)$,

$$H_y(\theta; K-1, 1, 1) = \frac{\gamma(K-1)G_K(\mathbf{x}; K-2, 1)}{\theta+\beta+(K-1)(\alpha+\gamma+\delta)},$$
$$H_y(\theta; K-1, 1, a) = \frac{\gamma(K-1)H_y(\theta; K-2, 1, a-1)}{\theta+\beta+(K-1)(\alpha+\gamma+\delta)}, \quad 2 \le a \le K-1.$$

(vii)" For $(m, n, a) = (1, K-1, 1)$,

$$H_y(\theta; 1, K-1, 1) = \frac{\gamma(K-1)+\delta(K-1)H_y(\theta; 1, K-2, 1)}{\theta+\alpha+(K-1)(\beta+\gamma+\delta)}.$$

After some algebra, it is readily verified that the column vector $\mathbf{h}_y(\theta; M, A)$ containing the transforms $H_y(\theta; M, n, A)$, for $1 \le n \le K-M$, can be evaluated by implementing the recursive procedure shown in Figure 2.23. Sub-vectors $\mathbf{h}_y(\theta; m, a)$ can be computed from (2.25) with $\mathbf{C}^{a,a'}_{m,m'}(\theta)$, $\mathbf{M}_o(\theta; m, a)$, and $\mathbf{N}_o(\theta; m, a)$ replaced by suitably defined matrices $\mathbf{D}^{a,a'}_{m,m'}(\theta)$, $\mathbf{M}_y(\theta; m, a)$, and $\mathbf{N}_y(\theta; m, a)$. More concretely, we have that $\mathbf{D}^{a,a+1}_{m,m+1}(\theta) = \mathbf{C}^{a,a+1}_{m,m+1}(\theta)$, for $1 \le a \le m \le K-2$, $\mathbf{D}^{a,a}_{m,m}(\theta) = \mathbf{C}^{a,a}_{m,m}(\theta)$, for $1 \le a \le m \le K-1$, and $\mathbf{D}^{a,a-1}_{m,m-1}(\theta) = \mathbf{C}^{a,a}_{m,m-1}(\theta)$, for $2 \le a \le m-1$ and $2 \le m \le K-1$. For $2 \le m \le K-1$, the sub-matrix $\mathbf{D}^{m,m-1}_{m,m-1}(\theta)$ has dimension $(K-m)\times(K-m+1)$ and its elements are specified by

$$\left(\mathbf{D}^{m,m-1}_{m,m-1}(\theta)\right)_{k,k'} = \begin{cases} \frac{\gamma mk}{\theta+\alpha m+\beta k+\gamma mk+\delta mk}, & \text{if } k' = k, \\ 0, & \text{otherwise.} \end{cases}$$

For $1 \le m \le K-1$, the matrix $\mathbf{M}_y(\theta; m, a)$ is recursively defined by

$$\mathbf{M}_y(\theta; m, a) = \Big(\mathbf{I}_{K-m} - (1-\delta_{1,a})\mathbf{D}^{a,a-1}_{m,m-1}(\theta)\mathbf{M}_y(\theta; m-1, a-1) \times \mathbf{D}^{a-1,a}_{m-1,m}(\theta) - (1-\delta_{m,K-1})\mathbf{D}^{a,a}_{m,m}(\theta)\Big)^{-1}, \quad (2.26)$$

for $1 \le a \le m$, and $\mathbf{N}_y(\theta; m, a)$ is evaluated as $\mathbf{N}_y(\theta; m, 1) = \mathbf{c}_y(\theta; m, 1)$ if $a = 1$, and $\mathbf{N}_y(\theta; m, a) = \mathbf{D}^{a,a-1}_{m,m-1}(\theta)\mathbf{M}_y(\theta; m-1, a-$

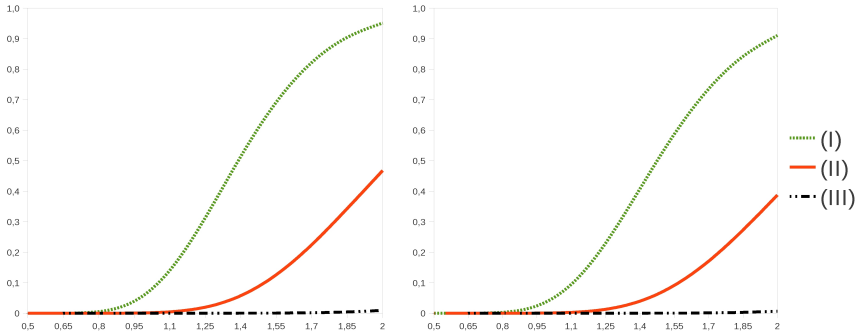

Fig. 2.24. $p_o(M, N, A)$ versus β for the choices $(\gamma = \alpha 2^{-1}, \delta = \beta 2^{-1})$ (*left*) and $(\gamma = \alpha 4^{-1}, \delta = \beta 4^{-1})$ (*right*), with $\alpha = 1.0$ and $(M, N) = (52, 52)$. Initial ages: (I) $A = 13$; (II) $A = 26$, (III) $A = 39$

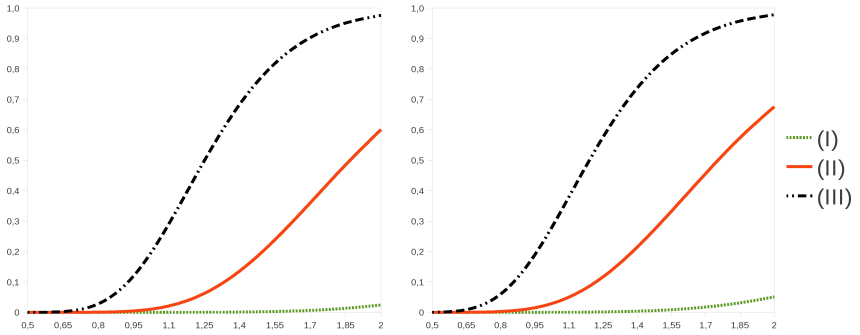

Fig. 2.25. $p_y(M, N, A)$ versus β for the choices $(\gamma = \alpha 2^{-1}, \delta = \beta 2^{-1})$ (*left*) and $(\gamma = \alpha 4^{-1}, \delta = \beta 4^{-1})$ (*right*), with $\alpha = 1.0$ and $(M, N) = (52, 52)$. Initial ages: (I) $A = 13$; (II) $A = 26$, (III) $A = 39$

$1)\mathbf{N}_y(\theta; m-1, a-1)$ if $2 \le a \le m$, with $\mathbf{c}_y(\theta; m, 1) = \mathbf{c}_o(\theta; m, m)$.

The survival of the marked individual, as a function of β, is analyzed in Figures 2.24 and 2.25 in terms of the probabilities $p_o(M, N, A)$ and $p_y(M, N, A)$ for the choices $(\gamma = \alpha 2^{-1}, \delta = \beta 2^{-1})$ and $(\gamma = \alpha 4^{-1}, \delta = \beta 4^{-1})$, and initial sizes $M = N = 52$. In each figure, we display three graphs that correspond to the choices $A \in \{13, 26, 39\}$ for the age of the marked individual at time $t = 0$. Under both killing assumptions, the probabilities $p_o(M, N, A)$ and $p_y(M, N, A)$ increase with increasing values

of β, since increasing values of β imply increasing values of δ in such a way that the surviving probability of species 1 increases; note that the surviving probabilities of each species do not depend on the killing strategy under consideration. As intuition tells us, the survival of the marked individual in the o-killing model will be more likely for younger individuals and, on the contrary, this will be more likely for older individuals under the y-killing assumption. In other words, $p_o(M, N, A)$ behaves as a decreasing function of the initial age A of the marked individual, and $p_y(M, N, A)$ increases as a function of A. For each initial state (M, N, A) with $M = N = 52$, values of $p_o(M, N, A)$ in the case $(\gamma = \alpha 4^{-1}, \delta = \beta 4^{-1})$ are shown graphically to be slightly smaller than those in the case $(\gamma = \alpha 2^{-1}, \delta = \beta 2^{-1})$. In the y-killing model, the case $(\gamma = \alpha 2^{-1}, \delta = \beta 2^{-1})$ yields smaller values of $p_y(M, N, A)$ than the case $(\gamma = \alpha 4^{-1}, \delta = \beta 4^{-1})$.

2.5 Conclusions

We may recall (Section 1.2) that, in analyzing the dynamics of the Ridler-Rowe process [108], the quadratic terms γmn and δmn in (2.1) due to the death of individuals make the solution intractable from an analytical point of view. One way of analyzing the process is to replace the absorbing Markov chain $\mathcal{X}$ defined on $\mathcal{S}$ by a finite Markov chain $\mathcal{X}(K)$, which is defined on those states $(m, n) \in \mathcal{S}$ such that the combined population of individuals $m + n$ is not greater than the value K. This means in Section 2.2 that, for a large enough value of K, we examine the process $\mathcal{X}$ till absorption under the taboo that states (m, n) verifying $m + n > K$ are not accessible; in Sections 2.3 and 2.4, it means that, for a large enough value of K, we study the process restricted to $\{X_{max}^{(M,N)} \leq K\}$. More concretely, we focus in Section 2.2 on the mean extinction time and the size of the surviving species. The truncating procedure permits us to approximate a countable PH distribution with a finite PH distribution. To be concrete, by replacing the space of states $\mathcal{S}$ by a finite set of states $\mathcal{S}(K_q)$, where K_q is selected from Algorithm 2.1 as a percentile of the maximum population size, we obtain the underlying joint distribution in Theorem 2.3. The probability q used in Algorithm 2.1 can be seen as a measure of

global error control. In Section 2.3 a similar truncating procedure has been presented, this time in terms of the joint transform of the random vector $(T^{(M,N)}, B_1^{(M,N)}, D_1^{(M,N)}, B_2^{(M,N)}, D_2^{(M,N)})$. The use of $\mathcal{X}(K)$, instead of the original process $\mathcal{X}$, allows us to reduce the problem to the solution of finite systems of linear equations. To be concrete, instead of the theoretical solution in (2.18) for the joint transform $G(\mathbf{s}; M, N)$ of the extinction time and the numbers of births and deaths until extinction, we suggest to solve (2.19). Our procedure in Algorithm 2.2 solves (2.19) by block-Gaussian elimination, and it computes the restricted transform $G_K(\mathbf{s}; M, N)$ with a predetermined accuracy $\varepsilon > 0$ in an efficient manner.

In Section 2.4 we specify the way individuals of a particular species are selected to die. We focus on three killing strategies that yield the r-killing, o-killing and y-killing models. Under these strategies, the survival probabilities $p_r(M, N)$, $p_o(M, N, A)$ and $p_y(M, N, A)$ are evaluated from finite systems of linear equations for the respective joint restricted transforms $H_r(\theta; M, N)$, $H_o(\theta; M, N, A)$ and $H_y(\theta; M, N, A)$ at point $\theta = 0$.

To illustrate our results, we develop a wide range of numerical experiments. From these numerical results in Sections 2.2, 2.3 and 2.4, we may remark that:

(i) With respect to Section 2.2, Figures 2.9-2.12 show that the Normal result in [108] and the approximating process $\mathcal{X}(K_q)$ lead to significantly different results. In view of Figures 2.11 and 2.12 and Table 2.5, we may conclude that we expect higher accuracy for moderate initial population sizes when, instead of the asymptotic solution [108], we use the approximating process $\mathcal{X}(K_q)$.

(ii) One of the main advantages of $\mathcal{X}(K_q)$ is related to the fact that it allows us to approximate the joint distribution of the extinction time T, the identity of the species becoming extinct and the number of individuals alive in the surviving species at time T, as well as to deal with non-degenerate probability distributions for initial population sizes.

(iii) From a computational point of view, the Normal solution yields a simple formula. The limit result in [108] is close enough to the true mass function of $X(T)$ when the initial population sizes become large, but it does not depend on the

birth rates α and β. On the other hand, the solution based on $\mathcal{X}(K_q)$ does depend on the birth rates α and β, but it is defined on a finite state space $\mathcal{S}(K_q)$. The incidence of the finiteness of $\mathcal{S}(K_q)$ on the resulting solution is attenuated by a suitable selection of the level K_q, which is based on a key descriptor X_{max} that appropriately describes the effects of overpopulation on the ecosystem.

(iv) Similar truncating procedures in Sections 2.3 and 2.4 allow us to analyze the descriptors $T^{(M,N)}$, $B_1^{(M,N)}$, $B_2^{(M,N)}$, $D_1^{(M,N)}$, $D_2^{(M,N)}$, $T_r^{(M,N)}$, $T_o^{(M,N,A)}$ and $T_y^{(M,N,A)}$. Figures 2.13-2.19, 2.24 and 2.25 are themselves explanatory and yield to interpretations that fit well with the dynamics that might be expected in a two-species competition process.

(v) In the numerical work, our interest is in 12 scenarios where the birth and death rates in each species are comparable in magnitude. These scenarios yield small and moderate levels of K_q in our solution, even if the value $q = 0.999$ is selected; see, for example, entries in Table 2.2. Algorithms 2.1-2.3 are seen to work well both regard to numerical accuracy and speed for moderate initial population sizes. However, if the *birth drift* of the process $\mathcal{X}$ (suitably defined from the birth rates α and β) is noticeably greater than its *death* counterpart (defined in terms of the death rates γ and δ), a larger cardinality of the set $\mathcal{S}(K)$ of states will imply more demanding memory requirements. The use of quasi-stationary vectors, as initial probability distribution over $\mathcal{S}(K_q)$, results in an increase of the execution times in Algorithm 2.1, since general-purpose numerical procedures to evaluate eigenvectors have to be implemented.

(vi) It is worth noting that, in the r-killing model, the vector $\mathbf{h}_r(\theta)$ consisting of the transforms $H_r(\theta; m, n)$ with initial states $(m, n) \in \mathcal{C}$ satisfying $m + n \leq K$ is numerically computed in a similar manner to the solution of (2.19). As a result, the algorithmic complexity in Algorithm 2.3 and the memory requirements are identical to those in Algorithm 2.2. In analyzing the survival probabilities in the age-dependent models, we must record the age of the marked individual, which implies more demanding memory requirements when equations

(i)'-(vii)' and (i)"-(vii)" in Subsection 2.4.2 are numerically solved by general-purpose algorithms. For instance, our numerical work indicates that LU-decomposition techniques applied to the inverse $(\mathbf{I}_{J'(K)} - \mathbf{C}_o(\theta))^{-1}$ fail to give satisfactory results as K increases. It is advisable then to write a driver routine by implementing the recursive procedures derived in (2.25) and (2.26) for the o-killing and y-killing models, respectively.

Other models of interacting biological populations may be appropriately studied by adapting our methodology. By way of example, consider the two-species competition process $\mathcal{X}$ defined on the state space $\mathcal{S} = \mathbb{N}_0 \times \mathbb{N}_0$ by the transition rates

$$q_{(m,n),(m',n')} = \begin{cases} \alpha_1 m, & \text{if } (m',n') = (m+1,n), \\ \beta_1 n, & \text{if } (m',n') = (m,n+1), \\ \gamma mn + \alpha_2 m, & \text{if } (m',n') = (m-1,n), \\ \delta mn + \beta_2 n, & \text{if } (m',n') = (m,n-1), \end{cases} \tag{2.27}$$

for all state $(m,n) \in \mathcal{S}$, where α_1, α_2, β_1, β_2, γ and δ are strictly positive. Given an initial population size $X(0) = (m,n)$ with $m > 0$ and $n > 0$, the process $\mathcal{X}$ evolving before hitting the class $\{(0,0)\} \cup \{(m,0) : m \geq 1\} \cup \{(0,n) : n \geq 1\}$ should be replaced by its approximating counterpart $\mathcal{X}(K_q)$ defined on the state space

$$\mathcal{S}(K_q) = \mathcal{C}_0(K_q) \cup \bigcup_{k=2}^{K_q} l(k),$$

where $\mathcal{C}_0(K_q) = \{(m,0) : 1 \leq m \leq K_q - 1\} \cup \{(0,n) : 1 \leq n \leq K_q - 1\}$. The infinitesimal generator of $\mathcal{X}(K_q)$ is defined as $\mathbf{Q}(K_q)$ in Subsection 2.2.2 with the rates αm, βn, γmn and δmn replaced by $\alpha_1 m$, $\beta_1 n$, $\gamma mn + \alpha_2 m$ and $\delta mn + \beta_2 n$, respectively. Then, for the approximating process $\mathcal{X}(K_q)$, Equations (2.10) and (2.11) determine the joint distribution of the hitting time $T(K_q)$ at which one or other of the species first becomes extinct, the identity of the species becoming extinct and the number of individuals on the surviving species alive at time $T(K_q)$. In particular, the hitting probabilities $\{P(X(T(K_q)) = (m,0)) : 1 \leq m \leq K_q - 1\} \cup \{P(X(T(K_q)) = (0,n)) : 1 \leq n \leq K_q - 1\}$ allow us to approximate the distribution $\{P(X(T) = (m,0)) : m \geq$

$1\} \cup \{P(X(T) = (0, n)) : n \geq 1\}$ of the original process $\mathcal{X}$ at time T at which the extinction of one or other of the species first occurs; similar remarks can be made in order to extend the approximating results in (2.19), (2.23) and (2.25) to the process defined by (2.27). The dynamics of the process $\mathcal{X}$ after the hitting time T can be readily studied from well-known results on birth and death processes. For instance, assume that species 1 becomes extinct and the size of species 2 equals $n_0 \geq 1$ at time T. Then, species 2 evolving after T behaves as a birth and death process on $\mathbb{N}_0$ with birth rates $\{\beta_1 n : n \geq 0\}$ and death rates $\{\beta_2 n : n \geq 1\}$; as a result, species 2 becomes extinct with probability one if $\beta_2 \geq \beta_1$, and with probability $(\beta_2/\beta_1)^{n_0}$ if $\beta_2 < \beta_1$. We refer the reader to [5, Theorems 6.2 and 6.3] for general results on extinction conditions of birth and death processes and explicit solutions for the expected time until extinction.

3

Stochastic Model for the Host-parasite Interaction

The host-parasitoid model in [62] describes the dynamics of a predator-prey process by means of a time-homogenous CTMC $\mathcal{X} = \{X(t) = (M(t), N(t)) : t \geq 0\}$ defined on the state space $\mathcal{S} = \mathbb{N}_0 \times \mathbb{N}_0 - \{(0,0), (1,0)\}$, where $M(t)$ and $N(t)$ represent the numbers of parasitoids (predators) and hosts (prey), respectively, alive at time t. The process $\mathcal{X}$ is uniquely specified in terms of its transition rates $q_{(m,n),(m',n')}$ as follows. For initial numbers of $m > 0$ parasitoids and $n > 0$ hosts, the non-null transition rates are given by

$$q_{(m,n),(m',n')} = \begin{cases} \alpha mn, & \text{if } (m',n') = (m+1, n-1), \\ \beta m, & \text{if } (m',n') = (m-1, n), \\ \lambda n, & \text{if } (m',n') = (m, n+1), \end{cases} \tag{3.1}$$

and $q_{(m,n)} = -q_{(m,n),(m,n)} = \alpha mn + \beta m + \lambda n$, where α and λ are strictly positive, and β is a non-negative constant. For initial population sizes $(m, 0)$ and $(0, n)$ with $m > 1$ and $n > 0$, the transition rates are specified as $q_{(m,0),(m',n')} = q_{(0,n),(m',n')} = 0$, for $(m', n') \in \mathcal{S}$. We may recall (Section 1.1) that, following to motivating comments in [62], parasitoids encounter hosts at random in such a way that, as an encounter occurs, one egg is laid in the host. The egg then develops into a new parasitoid and the host dies. Thus, the only possible events are birth of a host, death of a parasitoid and parasitism, and time delays are ignored. After one or other of the species becomes extinct, what happens to the surviving individuals is not of immediate interest; for instance, the remaining single population could follow a lin-

ear birth, linear death or linear birth-death process. If we denote $l(\cdot,0) = \{(m,0) : m \geq 2\}$ and $l(0,\cdot) = \{(0,n) : n \geq 1\}$, then $\mathcal{C}_0 = l(\cdot,0) \cup l(0,\cdot)$ constitutes the set of absorbing states, and the irreducible class $\mathcal{C} = \mathbb{N}\times\mathbb{N}$ consists of transient states. An eventual extinction of parasitoids and hosts will be associated with states in the subsets $l(0,\cdot)$ and $l(\cdot,0)$, respectively. For later use, we express the class $\mathcal{C}$ in terms of levels as $\cup_{k=2}^{\infty} l(k)$, where the kth level is given by $l(k) = \{(m,n) \in \mathcal{C} : m+n = k\}$, for $k \geq 2$. If states are labeled so that absorbing states precede transient states, then we may express the infinitesimal generator $\mathbf{Q}$ of $\mathcal{X}$ in the structured form

$$\mathbf{Q} = \begin{pmatrix} \mathbf{0} & \mathbf{0} \\ \mathbf{Q}_{\mathcal{C},\mathcal{C}_0} & \mathbf{Q}_{\mathcal{C},\mathcal{C}} \end{pmatrix}, \tag{3.2}$$

by defining $\mathbf{Q}_{\mathcal{C},\mathcal{C}_0}$ and $\mathbf{Q}_{\mathcal{C},\mathcal{C}}$ suitably. The sub-matrix $\mathbf{Q}_{\mathcal{C},\mathcal{C}_0}$ takes the form

$$\mathbf{Q}_{\mathcal{C},\mathcal{C}_0} = \begin{pmatrix} \mathbf{A}_{2,1} & \mathbf{A}_{2,2} & & \\ & \mathbf{A}_{3,2} & \mathbf{A}_{3,3} & \\ & & \ddots & \ddots \end{pmatrix}, \tag{3.3}$$

where $\mathbf{A}_{k,k-1}$ and $\mathbf{A}_{k,k}$ contain transition rates related to jumps of $\mathcal{X}$ from states of the kth level to absorbing states of the subsets $\{(k-1,0),(0,k-1)\}$ and $\{(k,0),(0,k)\}$, respectively, for $k \geq 2$. Similarly, the sub-matrix $\mathbf{Q}_{\mathcal{C},\mathcal{C}}$ has the block tri-diagonal form

$$\mathbf{Q}_{\mathcal{C},\mathcal{C}} = \begin{pmatrix} \mathbf{B}_{2,2} & \mathbf{B}_{2,3} & & \\ \mathbf{B}_{3,2} & \mathbf{B}_{3,3} & \mathbf{B}_{3,4} & \\ & \mathbf{B}_{4,3} & \mathbf{B}_{4,4} & \mathbf{B}_{4,5} \\ & & \ddots & \ddots \end{pmatrix}, \tag{3.4}$$

where $\mathbf{B}_{k,k'}$ records transition rates related to jumps of $\mathcal{X}$ from states of the kth level to states of the k'th level, for $k' \in \{k-1,k,k+1\}$, and diagonal elements of $\mathbf{B}_{k,k}$ are given by $-q_{(k-i,i)}$, for $1 \leq i \leq k-1$. The following specifications for $\mathbf{A}_{k,k'}$ and $\mathbf{B}_{k,k'}$ are readily derived from (3.1), under the assumption that states are ordered in a similar manner to Chapter 2:

$$\mathbf{A}_{2,1} = \beta,$$
$$\mathbf{A}_{k,k-1} = \begin{pmatrix} \mathbf{0}_{k-2} & \mathbf{0}_{k-2} \\ 0 & \beta \end{pmatrix}, \quad k \geq 3,$$

$$\mathbf{A}_{k,k} = \begin{pmatrix} (k-1)\alpha & 0 \\ \mathbf{0}_{k-2} & \mathbf{0}_{k-2} \end{pmatrix}, \quad k \geq 2,$$

$$\mathbf{B}_{k,k-1} = \begin{pmatrix} (k-1)\beta & 0 & \cdots & 0 \\ 0 & (k-2)\beta & \cdots & 0 \\ \vdots & \vdots & \ddots & \vdots \\ 0 & 0 & \cdots & 2\beta \\ 0 & 0 & \cdots & 0 \end{pmatrix}, \quad k \geq 3,$$

$$\mathbf{B}_{k,k} = \begin{pmatrix} -q_{(k-1,1)} & 0 & 0 & \cdots & 0 \\ 2(k-2)\alpha & -q_{(k-2,2)} & 0 & \cdots & 0 \\ 0 & 3(k-3)\alpha & -q_{(k-3,3)} & \cdots & 0 \\ \vdots & \vdots & \ddots & \ddots & \vdots \\ 0 & 0 & \cdots & (k-1)\alpha & -q_{(1,k-1)} \end{pmatrix}, \quad k \geq 2,$$

$$\mathbf{B}_{k,k+1} = \begin{pmatrix} 0 & \lambda & 0 & \cdots & 0 & 0 \\ 0 & 0 & 2\lambda & \cdots & 0 & 0 \\ \vdots & \vdots & \vdots & \ddots & \vdots & \vdots \\ 0 & 0 & 0 & \cdots & (k-2)\lambda & 0 \\ 0 & 0 & 0 & \cdots & 0 & (k-1)\lambda \end{pmatrix}, \quad k \geq 2.$$

As was remarked in Chapter 1, the assumptions made on the transition rates $q_{(m,n),(m',n')}$ as functions of m and n guarantee that the process $\mathcal{X}$ is specified uniquely by its transition rates, that the ultimate extinction of either parasitoids or hosts is certain, and that the expected time $\tau_{(m,n)}$ to the first extinction is always finite, regardless of the initial numbers m of parasitoids and n of hosts; see [62]. Specifically, let T be the time till absorption in $\mathcal{X}$, that is, $T = \inf\{t : X(t) \in \mathcal{C}_0\}$, and $\alpha_{(m,n)}$ be the absorption probability defined as $P(T < \infty | X(0) = (m,n))$, for $(m,n) \in \mathcal{C}$. Then, it is derived in [62, 109] that $\alpha_{(m,n)} = 1$ and that the expected time $\tau_{(m,n)} = E[T|X(0) = (m,n)]$ to reach the set $\mathcal{C}_0$ of absorbing states is finite. Moreover, Ridler-Rowe [109] proved that the mean extinction time $\tau_{(m,n)}$ tends to zero as the combined initial population of parasitoids and hosts $m+n$ becomes large.

This chapter essentially consists of two parts, each of them addressing one question associated with the Hitchcock model defined by (3.1):

(i) The distribution of the maximum number of individuals alive during a fixed time interval $[0, t_0]$.
(ii) The possibility of including correlation tendencies in the underlying processes generating events, by the consideration of more realistic distributional assumptions.

More concretely, in Section 3.1, we characterize the distribution of the maximum number of individuals alive during a certain time interval $[0, t_0]$ in matrix exponential form. In Section 3.2, we present an algorithmic procedure for the computation of the matrix exponential solution. This approximation for the general case $\beta > 0$, that works under very general conditions on the rates α and λ, is inspired from the exact solution in the special case $\beta = 0$. Our approximation method is based on splitting methods and the Trotter product formula [126]. The accuracy of our solution is measured in terms of the l_∞ vector norm, which permits a probabilistic interpretation of the error control, and is tested in Section 3.3. In Section 3.4, we discuss on the use of the maximum number of individuals alive in an attempt to describe how a community of parasitoids and hosts is affected by extreme values. In Section 3.5, we construct BSDE versions which generalize the basic model given by (3.1) allowing correlated and non-exponentially generated events. We focus on a concrete specification of matrices for the BSDE model in Section 3.6, such that relevant properties in the basic process $\mathcal{X}$ are appropriately satisfied by the resulting BSDE version. These properties are related to the ultimate extinction of either parasitoids or hosts, and the extinction times when events in the host-parasitoid association are generated from a Markovian arrival process (MAP). In Section 3.7, numerical examples are presented to illustrate the effects of the correlation structure on the extinction times and the extinction probabilities. Finally, Section 3.8 contains some concluding remarks.

3.1 Maximum number of individuals alive

Let $Z(t_0)$ be the maximum number of individuals (parasitoids and hosts) alive during the interval $[0, t_0]$, for a fixed epoch $t_0 > 0$. It is clear that $Z(t_0) = m + n$ for every initial size $(m, n) \in \mathcal{C}_0$. Thus, we assume from now on that $X(0) = (m, n) \in \mathcal{C}$, and we

evaluate $P(Z(t_0) \leq x|X(0) = (m,n))$ for values $x \geq m+n$, since $P(Z(t_0) \leq x|X(0) = (m,n)) = 0$ if $x < m+n$.

For each value $x \geq m+n$, we consider an absorbing process $\overline{\mathcal{X}}(x) = \{\overline{X}(t) : t \geq 0\}$ defined on the state space $\overline{\mathcal{S}}(x) = \{0\} \cup \bigcup_{k=2}^{x} l(k) \cup \{x+1\}$. The states 0 and $x+1$ are obtained by lumping the set $\mathcal{C}_0$ of absorbing states and the states of $\cup_{k=x+1}^{\infty} l(k)$ together to make two absorbing states. The infinitesimal generator of $\overline{\mathcal{X}}(x)$ has the form

$$\overline{\mathbf{Q}}(x) = \begin{pmatrix} 0 & \mathbf{0}_{J(x)}^T & 0 \\ \mathbf{t}_0(x) & \mathbf{T}(x) & \mathbf{t}_{x+1}(x) \\ 0 & \mathbf{0}_{J(x)}^T & 0 \end{pmatrix},$$

where $J(x) = 2^{-1}x(x-1)$ is the cardinality of the subset $\cup_{k=2}^{x} l(k)$. The column vectors $\mathbf{t}_0(x)$ and $\mathbf{t}_{x+1}(x)$, and the matrix $\mathbf{T}(x)$ are specified (similarly to (2.9)) by

$$\mathbf{t}_0(x) = \begin{pmatrix} \mathbf{A}_{2,1} + \mathbf{A}_{2,2}\mathbf{e}_2 \\ (\mathbf{A}_{3,2} + \mathbf{A}_{3,3})\mathbf{e}_2 \\ \vdots \\ (\mathbf{A}_{x,x-1} + \mathbf{A}_{x,x})\mathbf{e}_2 \end{pmatrix},$$

$$\mathbf{T}(x) = \begin{pmatrix} \mathbf{B}_{2,2} & \mathbf{B}_{2,3} & & & \\ \mathbf{B}_{3,2} & \mathbf{B}_{3,3} & \mathbf{B}_{3,4} & & \\ \ddots & \ddots & \ddots & & \\ & \mathbf{B}_{x-1,x-2} & \mathbf{B}_{x-1,x-1} & \mathbf{B}_{x-1,x} \\ & & \mathbf{B}_{x,x-1} & \mathbf{B}_{x,x} \end{pmatrix},$$

$$\mathbf{t}_{x+1}(x) = \begin{pmatrix} \mathbf{0}_{J(x-1)} \\ \mathbf{B}_{x,x+1}\mathbf{e}_x \end{pmatrix}.$$

We observe that, for $x \geq m+n$ and $(m,n) \in \mathcal{C}$, the conditional probability $P(Z(t_0) > x|X(0) = (m,n))$ is equivalent to the probability that, starting from the initial state $\overline{X}(0) = (m,n)$, the process $\overline{\mathcal{X}}(x)$ visits the absorbing state $x+1$ at time t_0. In structured form, the standard transition function $\overline{\mathbf{P}}(t_0;x)$ (with elements $P(\overline{X}(t_0) = (m',n')|\overline{X}(0) = (m,n))$, for $(m,n),(m',n') \in \overline{\mathcal{S}}(x)$) of the process $\overline{\mathcal{X}}(x)$ can be expressed as

$$\overline{\mathbf{P}}(t_0;x) = \begin{pmatrix} 1 & \mathbf{0}_{J(x)}^T & 0 \\ \overline{\mathbf{p}}_0(t_0;x) & \overline{\mathbf{P}}^*(t_0;x) & \overline{\mathbf{p}}_{x+1}(t_0;x) \\ 0 & \mathbf{0}_{J(x)}^T & 1 \end{pmatrix}.$$

Therefore, we have that

$$P(Z(t_0) > x | X(0) = (m,n)) = \overline{\mathbf{e}}_{J(x)}(m,n)\overline{\mathbf{p}}_{x+1}(t_0;x),$$

where $\overline{\mathbf{e}}_k(m,n)$ is a row vector of order k such that all its entries are equal to 0, except for the entry associated with the state (m,n) which is equal to 1. It is well known that $\overline{\mathbf{P}}(t_0;x) = \exp\{\overline{\mathbf{Q}}(x)t_0\}$. Then, straightforward algebra yields

$$\overline{\mathbf{p}}_{x+1}(t_0;x) = \left(\mathbf{I}_{J(x)} - \exp\left\{\mathbf{T}(x)t_0\right\}\right)\left(-\mathbf{T}^{-1}(x)\right)\mathbf{t}_{x+1}(x), \quad (3.5)$$

We may observe that the matrix $-\mathbf{T}^{-1}(x)$ in (3.5) is non-negative, since it contains the expected total times spent in each state (m',n') during the time until absorption, starting from initial numbers of $m > 0$ parasitoids and $n > 0$ hosts, for each pair of states $(m,n),(m',n') \in \cup_{k=2}^{x} l(k)$.

This has the following immediate consequence.

Theorem 3.1. *For initial numbers $m > 0$ of parasitoids and $n > 0$ of hosts, the distribution of the maximum number of individuals alive during the interval $[0,t_0]$ is characterized by $P\left(Z(t_0) \leq x | X(0) = (m,n)\right) = 0$ if $x < m+n$, and $1 - \overline{\mathbf{e}}_{J(x)}(m,n)$ $\overline{\mathbf{p}}_{x+1}(t_0;x)$ if $m+n \leq x$, where $\overline{\mathbf{p}}_{x+1}(t_0;x)$ was given in (3.5).*

A slight modification of our arguments in Subsection 2.2.1 leads us to observe that the column vector

$$\int_0^\infty \exp\{\mathbf{T}(x)u\}\mathbf{t}_{x+1}(x)du = (-\mathbf{T}^{-1}(x))\mathbf{t}_{x+1}(x)$$

consists of the conditional probabilities that the absorption into $x+1$ occurs in a finite time. Then, by using sub-matrices of the previous value $x-1$, we can apply block-Gaussian elimination to compute the column vector $(-\mathbf{T}^{-1}(x))\mathbf{t}_{x+1}(x)$ in an iterative manner as in the next algorithm:

Algorithm 3.1. Computation of $(-\mathbf{T}^{-1}(x))\mathbf{t}_{x+1}(x)$

Step 1 $y := 2$;
$\mathbf{M}_{y,y}(y) := -\mathbf{B}_{y,y}^{-1}$.

Step 2 While $y < x$, repeat

$y := y + 1$;

$\mathbf{M}_{y,y}(y) := (-\mathbf{B}_{y,y} - \mathbf{B}_{y,y-1}\mathbf{M}_{y-1,y-1}(y-1)\mathbf{B}_{y-1,y})^{-1}$;

for $i = 2, 3, ..., y-1$, compute

$\mathbf{M}_{i,y}(y) := \mathbf{M}_{i,y-1}(y-1)\mathbf{B}_{y-1,y}\mathbf{M}_{y,y}(y)$.

Step 3 Compute $(-\mathbf{T}^{-1}(x))\mathbf{t}_{x+1}(x) := \begin{pmatrix} \mathbf{M}_{2,x}(x)\mathbf{B}_{x,x+1}\mathbf{e}_x \\ \mathbf{M}_{3,x}(x)\mathbf{B}_{x,x+1}\mathbf{e}_x \\ \vdots \\ \mathbf{M}_{x,x}(x)\mathbf{B}_{x,x+1}\mathbf{e}_x \end{pmatrix}$.

3.2 Computation of the matrix exponential solution

In principle, the matrix exponential $\exp\{\mathbf{T}(x)t_0\}$ in (3.5) could be computed in many ways; see e.g. [14, 86]. In practice, consideration of computational stability and efficiency indicates that some of the methods are preferable to others, but that none are completely satisfactory when they are implemented as general-purpose algorithms. Under a simple assumption on the constants α, β and λ, we present here an explicit expression for the matrix exponential solution in the special case $\beta = 0$, and we use splitting methods to derive two algorithmic approximations in the case $\beta > 0$.

To provide motivation for our assumption on the per capita rates α, β and λ of change of population sizes, we first express conditions for diagonalization of the sub-matrices $\mathbf{B}_{y,y}$ with $y \geq 2$ in terms of eigenvalues.

Lemma 3.1. *(i) For each value $y \geq 2$, a sufficient condition for the sub-matrix $\mathbf{B}_{y,y}$ to be diagonalizable is*

$$\lambda \neq (y - p - p')\,\alpha + \beta, \tag{3.6}$$

for every pair (p, p') of integers with $p' < p$ and $p, p' \in \{1, 2, ..., y-1\}$.

(ii) Under the assumption that Equation (3.6) is verified for every pair (p, p') with $p' < p$ and $p, p' \in \{1, 2, ..., y-1\}$, the $y-1$ eigenvalues $r(y; l) = -(\alpha(y-l)l + \beta(y-l) + \lambda l)$, for $1 \leq l \leq y-1$, of the sub-matrix $\mathbf{B}_{y,y}$ are distinct. Moreover, we can specify left and right eigenvectors, respectively denoted by $\mathbf{w}(y; l) = (w_i(y; l))$

and $\mathbf{v}(y;l) = (v_i(y;l))$*, belonging to the eigenvalue* $r(y;l)$ *from their ith entries*

$$w_i(y;l) = \begin{cases} 1, & if\ i = 1, \\ \frac{1}{l}\binom{l}{i} \prod_{k=2}^{i} \left(\frac{(l-1)\alpha - \lambda + \beta}{(y-k)\alpha} - 1 \right), & if\ 2 \le i \le l, \\ 0, & if\ l+1 \le i \le y-1, \end{cases} \tag{3.7}$$

$$v_i(y;l) = \begin{cases} 0, & if\ 1 \le i \le l-1, \\ \binom{y-l-1}{i-l} \prod_{k=1}^{y-i-1} \left(\frac{(y-l)\alpha + \lambda - \beta}{(y-k)\alpha} - 1 \right), & if\ l \le i \le y-2, \\ 1, & if\ i = y-1. \end{cases} \tag{3.8}$$

Proof. The eigenvalues of the sub-matrix $\mathbf{B}_{y,y}$ are given by its diagonal elements since $\mathbf{B}_{y,y}$ is bi-diagonal, that is, $r(y;l) = -q_{(y-l,l)}$, for $1 \le l \le y-1$. Then, the eigenvalues $r(y;1), r(y;2), ..., r(y;y-1)$ are distinct if and only if (3.6) holds for every pair (p,p') with $p' < p$ and $p, p' \in \{1, 2, ..., y-1\}$, as the reader may readily verify.

To derive (3.7), we rewrite the matrix equation $\mathbf{w}(y;l)\mathbf{B}_{y,y} = r(y;l)\mathbf{w}(y;l)$ as

$$\begin{aligned} (i+1)(y-(i+1))\alpha w_{i+1}(y;l) &= (r(y;l) - r(y,i))w_i(y;l), \\ & \qquad 1 \le i \le y-2, \\ (r(y;l) - r(y;y-1))w_{y-1}(y;l) &= 0. \end{aligned}$$

If (3.6) is verified for the pairs (p,p') of integers with $p' < p$ and $p, p' \in \{1, 2, ..., y-1\}$, then $r(y;l) \neq r(y,l')$ for every integer $l' \in \{l+1, ..., y-1\}$, from which it follows that $w_{y-1}(y;l) = w_{y-2}(y;l) = ... = w_{l+1}(y;l) = 0$. Then, the above equations result in

$$w_i(y;l) = \prod_{k=2}^{i} \frac{r(y;l) - r(y;k-1)}{k(y-k)\alpha} w_1(y;l), \quad 2 \le i \le l.$$

This completes the proof of (3.7) if we select the value $w_1(y;l) = 1$. Expressions for the entries of $\mathbf{v}(y;l)$ in (3.8) are similarly derived from the matrix equality $\mathbf{B}_{y,y}\mathbf{v}(y;l) = r(y;l)\mathbf{v}(y;l)$. □

Assume that (3.6) holds for every pair (p,p') with $p' < p$ and $p, p' \in \{1, 2, ..., y-1\}$. Then, the right (respectively, left) eigenvectors $\mathbf{v}(y;1), \mathbf{v}(y;2), ..., \mathbf{v}(y;y-1)$ (respectively, $\mathbf{w}(y;1), \mathbf{w}(y;2), ...,$

$\mathbf{w}(y;y-1))$ belonging to the respective eigenvalues $r(y;1), r(y;2)$, $..., r(y;y-1)$ are linearly independent, and the sub-matrix $\mathbf{B}_{y,y}$ can be diagonalized, that is, it can be expressed as

$$\mathbf{B}_{y,y} = \mathbf{P}_y \mathbf{D}_y \mathbf{P}_y^{-1},$$

where the lth column of $\mathbf{P}_y$ is the right eigenvector $\mathbf{v}(y;l)$, for $1 \leq l \leq y-1$, of $\mathbf{B}_{y,y}$ and $\mathbf{D}_y = \text{diag}(r(y;1), r(y;2), ..., r(y;y-1))$. By [66, Theorem 4.4.8], the matrix $\mathbf{P}_y$ is non-singular, and the lth row of $\mathbf{P}_y^{-1}$ is specified by the *normalized* left eigenvector $c^{-1}(y;l)\mathbf{w}(y;l)$, for $1 \leq l \leq y-1$, where the constant $c(y;l)$ is specified by $c(y;l) = \sum_{i=1}^{y-1} w_i(y;l)v_i(y;l)$; note that $c(y;l) = w_l(y;l)v_l(y;l)$ by (3.7) and (3.8). Using this fact, it is seen that

$$\exp\{\mathbf{B}_{y,y}t_0\} = \mathbf{P}_y \mathbf{D}_y(t_0) \mathbf{P}_y^{-1}, \quad y \geq 2, \tag{3.9}$$

where $\mathbf{D}_y(t_0) = \text{diag}(e^{r(y;1)t_0}, e^{r(y;2)t_0}, ..., e^{r(y;y-1)t_0})$, and $r(y;l) = -(\alpha(y-l)l + \beta(y-l) + \lambda l)$, for $1 \leq l \leq y-1$.

Our solution in Subsections 3.2.1 and 3.2.2 is strongly based on the decomposition formula (3.9). Hence, the preceding discussion motivates the following condition on the values of α, β and λ:

Condition (A) For a community of $m > 0$ parasitoids and $n > 0$ hosts and each value $x \geq m + n$, the rates α, β and λ satisfy the properties

(A.1) $\lambda \neq (y - p - p')\,\alpha + \beta$ for every $2 \leq y \leq x$ and every pair (p, p') of integers with $p' < p$ and $p, p' \in \{1, 2, ..., y-1\}$.

(A.2) $p'\lambda + (y' - p')(p'\alpha + \beta) \neq p\lambda + (y - p)(p\alpha + \beta)$ for every pair (y, y') of integers with $2 \leq y' < y \leq x$, and integers $p \in \{1, 2, ..., y-1\}$ and $p' \in \{1, 2, ..., y'-1\}$.

As the reader may easily verify, part (A.1) means by Lemma 3.1(ii) that the eigenvalues $r(y;1), r(y;2), ..., r(y;y-1)$ of the sub-matrix $\mathbf{B}_{y,y}$ are distinct; similarly, part (A.2) implies that eigenvalues $r(y;l)$ and $r(y';l')$ of sub-matrices $\mathbf{B}_{y,y}$ and $\mathbf{B}_{y',y'}$ with $y' < y$, respectively, are also distinct.

3.2.1 The special case $\beta = 0$

In this subsection we show that, under Condition (A), the matrix exponential $\exp\{\mathbf{T}(x)t_0\}$ in (3.5) can be evaluated in an explicit

manner in the special case $\beta = 0$. Our notation and results here will be used as part of the analysis in Subsection 3.2.2. For example, our approximating solutions (see Theorem 3.2) in the case $\beta > 0$ use the decomposition formula (3.11) and the diagonalized form (3.12); of course, Equations (3.11) and (3.12) should be appropriately evaluated in Subsection 3.2.2 with $\beta > 0$, instead of $\beta = 0$.

To begin with, we notice that the fact that $\beta = 0$ turns $\mathbf{T}(x)$ into a block bi-diagonal matrix, whence its eigenvalues are given by the eigenvalues of the sub-matrices $\mathbf{B}_{y,y}$, for $2 \leq y \leq x$. As a result, for a fixed value $x \geq m+n$, Condition (A) implies that the eigenvalues $\{r(y;l) = -(\alpha(y-l)l + \lambda l) : 1 \leq l \leq y-1, 2 \leq y \leq x\}$ of the matrix $\mathbf{T}(x)$ are distinct, and that $\mathbf{T}(x)$ can be diagonalized since it possesses $J(x)$ linearly independent eigenvectors. To be concrete, we write down

$$\mathbf{T}(x) = \mathbf{R}_x \mathbf{E}_x \mathbf{R}_x^{-1},$$

where $\mathbf{E}_x$ is a diagonal matrix whose diagonal entries are given by the eigenvalues $\{r(y;l) = -(\alpha(y-l)l + \lambda l) : 1 \leq l \leq y-1, 2 \leq y \leq x\}$ of $\mathbf{T}(x)$, and the columns of $\mathbf{R}_x$ correspond to right eigenvectors of $\mathbf{T}(x)$ associated with these eigenvalues. From Lemma 3.1, it is seen that $\mathbf{R}_x$ can be expressed as

$$\mathbf{R}_x = \begin{pmatrix} \mathbf{P}_2 & \mathbf{L}(3;2) & \mathbf{L}(4;2) & \cdots & \mathbf{L}(x-1;2) & \mathbf{L}(x;2) \\ & \mathbf{P}_3 & \mathbf{L}(4;3) & \cdots & \mathbf{L}(x-1;3) & \mathbf{L}(x;3) \\ & & \mathbf{P}_4 & \cdots & \mathbf{L}(x-1;4) & \mathbf{L}(x;4) \\ & & & \ddots & \vdots & \vdots \\ & & & & \mathbf{P}_{x-1} & \mathbf{L}(x;x-1) \\ & & & & & \mathbf{P}_x \end{pmatrix},$$

where we recall that the lth column of $\mathbf{P}_y$ is defined from (3.8), with $\beta = 0$, as the right eigenvector $\mathbf{v}(y;l)$, for $1 \leq l \leq y-1$. The columns of the sub-matrix

$$\mathbf{L}(y;l) = (\mathbf{l}(y;l,1), \mathbf{l}(y;l,2), ..., \mathbf{l}(y;l,y-1))$$

are specified as

$$\mathbf{l}(y;l,l') = \prod_{y'=l}^{y-1} \left(r(y;l')\mathbf{I}_{y'-1} - \mathbf{B}_{y',y'}\right)^{-1} \mathbf{B}_{y',y'+1} \mathbf{v}(y;l'),$$

for $1 \leq l' \leq y-1$. Note that, by [66, page 150], the matrices $(r(y;l')\mathbf{I}_{y'-1} - \mathbf{B}_{y',y'})^{-1}$ are given by

$$(r(y;l')\mathbf{I}_{y'-1} - \mathbf{B}_{y',y'})^{-1} = \sum_{k=1}^{y'-1} \frac{\mathbf{v}(y';k)\mathbf{w}(y';k)}{r(y;l') - r(y';k)}, \quad (3.10)$$

where the left and right eigenvectors $\mathbf{w}(y';k)$ and $\mathbf{v}(y';k)$ are evaluated from (3.7) and (3.8) with $\beta = 0$.

The equality $\mathbf{T}(x) = \mathbf{R}_x\mathbf{E}_x\mathbf{R}_x^{-1}$ implies

$$\exp\{\mathbf{T}(x)t_0\} = \mathbf{R}_x\mathbf{E}_x(t_0)\mathbf{R}_x^{-1}, \quad (3.11)$$

where we have that $\mathbf{E}_x(t_0) = \text{diag}(e^{r(2;1)t_0}, e^{r(3;1)t_0}, e^{r(3;2)t_0}, \ldots, e^{r(x;1)t_0}, \ldots, e^{r(x;x-1)t_0})$ and $r(y;l) = -(\alpha(y-l)l + \lambda l)$, for $1 \leq l \leq y-1$ and $2 \leq y \leq x$. If we express the matrices $\mathbf{R}_x$ and $\mathbf{E}_x(t_0)$ in structured form as

$$\mathbf{R}_x = \begin{pmatrix} \mathbf{R}_{x-1} & \mathbf{N}_x \\ \mathbf{0}_{(x-1)\times J(x-1)} & \mathbf{P}_x \end{pmatrix},$$

$$\mathbf{E}_x(t_0) = \begin{pmatrix} \mathbf{E}_{x-1}(t_0) & \mathbf{0}_{J(x-1)\times(x-1)} \\ \mathbf{0}_{(x-1)\times J(x-1)} & \mathbf{D}_x(t_0) \end{pmatrix},$$

then we can reduce the computation in (3.11) to previously computed sub-matrices. Starting with $\exp\{\mathbf{T}(2)t_0\} = e^{-(\alpha+\lambda)t_0}$, the end result is the expression

$$\exp\{\mathbf{T}(x)t_0\} = \begin{pmatrix} \exp\{\mathbf{T}(x-1)t_0\} & \mathbf{N}_x(t_0) \\ \mathbf{0}_{(x-1)\times J(x-1)} & \exp\{\mathbf{B}_{x,x}t_0\} \end{pmatrix}, \quad (3.12)$$

for $x \geq 3$, where $\mathbf{N}_x(t_0) = \mathbf{N}_x\mathbf{P}_x^{-1}\exp\{\mathbf{B}_{x,x}t_0\} - \exp\{\mathbf{T}(x-1)t_0\}\mathbf{N}_x\mathbf{P}_x^{-1}$. We recall here that $\exp\{\mathbf{B}_{x,x}t_0\} = \mathbf{P}_x\mathbf{D}_x(t_0)\mathbf{P}_x^{-1}$ by (3.9), and that the sub-matrices $\mathbf{N}_x$, $\mathbf{P}_x$ and $\mathbf{P}_x^{-1}$ are appropriately specified from the left and right eigenvectors defined in (3.7) and (3.8) with $\beta = 0$.

Under Condition (A), the solution in the case $\beta = 0$ can be iteratively evaluated from (3.12) as $P(Z(t_0) \leq x | X(0) = (m,n)) = 1 - \overline{\mathbf{e}}_{J(x)}(m,n)(\mathbf{I}_{J(x)} - \exp\{\mathbf{T}(x)t_0\})(-\mathbf{T}^{-1}(x))\mathbf{t}_{x+1}(x)$, for each value $x \geq m+n$, by starting with $\exp\{\mathbf{T}(2)t_0\} = e^{-(\alpha+\lambda)t_0}$.

3.2.2 The general case $\beta > 0$

Next we focus on computational issues in the case $\beta > 0$. Based on splitting methods, we present two approximations to $P(Z(t_0) \leq$

$x|X(0) = (m, n)$) (equivalently, to $\exp\{\mathbf{T}(x)t_0\}$ by Theorem 3.1) for each value $x \geq m+n$. The main idea in our approach is closely related to the additive law, which fails unless we have commutativity. Specifically, for a certain splitting $\mathbf{T}(x) = \mathbf{U}(x)+\mathbf{V}(x)$, it is known that $\exp\{\mathbf{T}(x)t_0\} = \exp\{\mathbf{U}(x)t_0\}\exp\{\mathbf{V}(x)t_0\}$ if and only if $[\mathbf{U}(x), \mathbf{V}(x)] = \mathbf{0}_{J(x)\times J(x)}$, where the commutator of two matrices is defined by $[\mathbf{U}(x), \mathbf{V}(x)] = \mathbf{U}(x)\mathbf{V}(x) - \mathbf{V}(x)\mathbf{U}(x)$. However, as $\mathbf{U}(x)$ and $\mathbf{V}(x)$ do not commute, the exponentials of the matrices $\mathbf{U}(x)$ and $\mathbf{V}(x)$ are directly related to that of $\mathbf{T}(x)$ by the Trotter product formula [126]

$$\exp\{\mathbf{T}(x)t_0\} = \lim_{p\to\infty}\left(\exp\left\{\mathbf{U}(x)\frac{t_0}{p}\right\}\exp\left\{\mathbf{V}(x)\frac{t_0}{p}\right\}\right)^p.$$

Thus, it is suggested in [86, Section 7] that the Trotter result be used to approximate $\exp\{\mathbf{T}(x)t_0\}$ by splitting $\mathbf{T}(x)$ into $\mathbf{U}(x) + \mathbf{V}(x)$, and then using the approximation

$$\exp\{\mathbf{T}(x)t_0\} \backsimeq (\exp\{\mathbf{U}(x)t\}\exp\{\mathbf{V}(x)t\})^{p_0}, \qquad (3.13)$$

where $t = p_0^{-1}t_0$, for an appropriately selected integer p_0. This approach to computing $\exp\{\mathbf{T}(x)t_0\}$ is of particular interest when the exponentials of the matrices $\mathbf{U}(x)t$ and $\mathbf{V}(x)t$ can be accurately and efficiently computed, which is our case here. This allows us to indicate that our splitting proposals in Approximations 1 and 2, and the resulting expressions (3.14)-(3.17) are preferable to other methods in the literature [86].

It should be noted that, in principle, the *uniformization* method might be used to compute the cumulative distribution function of $Z(t_0)$; see e.g. [76, Section 2.8]. More concretely, we may first uniformize the absorbing CTMC $\overline{\mathcal{X}}(x)$ with infinitesimal generator $\overline{\mathbf{Q}}(x)$ by choosing

$$c(x) = \max\{q_{(m',n')} : \ (m', n') \in \overline{\mathcal{S}}(x)\},$$

and then derive a simple algorithm to compute $P(Z(t_0) \leq x|X(0) = (m, n))$ for values $x \geq m + n$. Unfortunately, it is not a very satisfactory result for our problem since there is no clear relationship between the underlying matrices associated with an application of [76, Figure 2.4] to successive values x and $x + 1$. This drawback is closely related to the fact that $c(x)$ increases with increasing

values of x, and it converges to infinity as x tends to infinity. Even for values $x \geq m + n$, the uniformization method might require some care if $t_0 c(x)$ should happen to be large.

For the host-parasitoid model defined by (3.1) with $\beta > 0$, we suggest the use of the following choices for $\mathbf{U}(x)$ and $\mathbf{V}(x)$:

Approximation 1. We consider the splitting $\mathbf{T}(x) = \mathbf{U}_1(x) + \mathbf{V}_1(x)$ with

$$\mathbf{U}_1(x) = \begin{pmatrix} \mathbf{B}_{2,2} & \mathbf{B}_{2,3} & & & & \\ & \mathbf{B}_{3,3} & \mathbf{B}_{3,4} & & & \\ & & \ddots & \ddots & & \\ & & & \mathbf{B}_{x-1,x-1} & \mathbf{B}_{x-1,x} & \\ & & & & \mathbf{B}_{x,x} \end{pmatrix},$$

$$\mathbf{V}_1(x) = \begin{pmatrix} 0 & & & & \\ \mathbf{B}_{3,2} & & & & \\ & \mathbf{B}_{4,3} & & & \\ & & \ddots & & \\ & & & \mathbf{B}_{x,x-1} & \mathbf{0}_{(x-1)\times(x-1)} \end{pmatrix}.$$

Approximation 2. In this case, we express $\mathbf{T}(x) = \mathbf{U}_2(x) + \mathbf{V}_2(x)$ with

$$\mathbf{U}_2(x) = \begin{pmatrix} \mathbf{B}_{2,2} & & & & \\ \mathbf{B}_{3,2} & \mathbf{B}_{3,3} & & & \\ \ddots & \ddots & & & \\ & \mathbf{B}_{x-1,x-2} & \mathbf{B}_{x-1,x-1} & & \\ & & \mathbf{B}_{x,x-1} & \mathbf{B}_{x,x} \end{pmatrix},$$

$$\mathbf{V}_2(x) = \begin{pmatrix} 0 & \mathbf{B}_{2,3} & & & \\ & \mathbf{B}_{3,4} & & & \\ & & \ddots & & \\ & & & \mathbf{B}_{x-1,x} & \\ & & & \mathbf{0}_{(x-1)\times(x-1)} \end{pmatrix}.$$

The first term $\mathbf{U}_i(x)$, for $i \in \{1, 2\}$, in Approximations 1 and 2 is a block bi-diagonal matrix. Under Condition (A), we can therefore evaluate the exponential of the matrix $\mathbf{U}_i(x)t$ by adapting our

arguments in Subsection 3.2.1 to the case $\beta > 0$. To be concrete, Condition (A) leads to

$$\exp\{\mathbf{U}_i(x)t\} = \mathbf{R}_x(i)\mathbf{E}_x(t)\mathbf{R}_x^{-1}(i),$$

for $i \in \{1, 2\}$, where the matrices $\mathbf{E}_x(t)$ and $\mathbf{R}_x(1)$ are defined similarly to the matrices $\mathbf{E}_x(t)$ and $\mathbf{R}_x$, respectively, in Subsection 3.2.2 with $\beta > 0$, instead of $\beta = 0$. The matrix $\mathbf{R}_x(2)$ has the structured form

$$\begin{pmatrix} \mathbf{P}_2 & & & & \\ \mathbf{K}(2;3) & \mathbf{P}_3 & & & \\ \mathbf{K}(2;4) & \mathbf{K}(3;4) & \mathbf{P}_4 & & \\ \vdots & \vdots & \vdots & \ddots & \\ \mathbf{K}(2;x-1) & \mathbf{K}(3;x-1) & \mathbf{K}(4;x-1) & \cdots & \mathbf{P}_{x-1} \\ \mathbf{K}(2;x) & \mathbf{K}(3;x) & \mathbf{K}(4;x) & \cdots & \mathbf{K}(x-1;x)\ \mathbf{P}_x \end{pmatrix},$$

where the l'th column of the matrix $\mathbf{K}(y;l) = (\mathbf{k}(y;l,1), \mathbf{k}(y;l,2), ..., \mathbf{k}(y;l,y-1))$ is given by

$$\mathbf{k}(y;l,l') = \prod_{y'=l}^{y+1} \left(r(y;l')\mathbf{I}_{y'-1} - \mathbf{B}_{y',y'}\right)^{-1} \mathbf{B}_{y',y'-1}\mathbf{v}(y;l'),$$

for $1 \le l' \le y-1$. Similarly to Subsection 3.2.1, we may evaluate $(r(y;l')\mathbf{I}_{y'-1} - \mathbf{B}_{y',y'})^{-1}$ from (3.10), where the entries of $\mathbf{w}(y';k)$ and $\mathbf{v}(y';k)$ are now computed from (3.7) and (3.8) with $\beta > 0$.

Since the structured matrices

$$\mathbf{R}_x(1) = \begin{pmatrix} \mathbf{R}_{x-1}(1) & \mathbf{N}_x(1) \\ \mathbf{0}_{(x-1)\times J(x-1)} & \mathbf{P}_x \end{pmatrix},$$

$$\mathbf{R}_x(2) = \begin{pmatrix} \mathbf{R}_{x-1}(2)\ \mathbf{0}_{J(x-1)\times(x-1)} \\ \mathbf{N}_x(2) \qquad \mathbf{P}_x \end{pmatrix},$$

it is readily shown that, under Condition (A), $\exp\{\mathbf{U}_1(x)t\}$ and $\exp\{\mathbf{U}_2(x)t\}$ can be iteratively computed starting with the value $\exp\{\mathbf{U}_1(2)t\} = \exp\{\mathbf{U}_2(2)t\} = e^{-(\alpha+\beta+\lambda)t}$. The proof of Theorem 3.2 is a slight modification of our arguments in Subsection 3.2.1, and it is thus omitted.

Theorem 3.2. *Let us assume that the rates α, β and λ of change of population sizes satisfy Condition (A).*

(i) Starting from $\exp\{\mathbf{U}_1(2)t\} = e^{-(\alpha+\beta+\lambda)t}$*, the matrix exponential* $\exp\{\mathbf{U}_1(x)t\}$ *can be computed as*

$$\exp\{\mathbf{U}_1(x)t\} = \begin{pmatrix} \exp\{\mathbf{U}_1(x-1)t\} & \mathbf{N}_x(t;1) \\ \mathbf{0}_{(x-1)\times J(x-1)} & \exp\{\mathbf{B}_{x,x}t\} \end{pmatrix}, \quad x \geq 3, \tag{3.14}$$

with $\mathbf{N}_x(t;1) = \mathbf{N}_x(1)\mathbf{D}_x(t)\mathbf{P}_x^{-1} - \exp\{\mathbf{U}_1(x-1)t\}\mathbf{N}_x(1)\mathbf{P}_x^{-1}$.

(ii) Starting from $\exp\{\mathbf{U}_2(2)t\} = e^{-(\alpha+\beta+\lambda)t}$*, the matrix exponential* $\exp\{\mathbf{U}_2(x)t\}$ *can be computed as*

$$\exp\{\mathbf{U}_2(x)t\} = \begin{pmatrix} \exp\{\mathbf{U}_2(x-1)t\} & \mathbf{0}_{J(x-1)\times(x-1)} \\ \mathbf{N}_x(t;2) & \exp\{\mathbf{B}_{x,x}t\} \end{pmatrix}, \quad x \geq 3, \tag{3.15}$$

with $\mathbf{N}_x(t;2) = \mathbf{N}_x(2)\mathbf{E}_{x-1}(t)\mathbf{R}_{x-1}^{-1}(2) - \exp\{\mathbf{B}_{x,x}t\}\mathbf{N}_x(2)\mathbf{R}_{x-1}^{-1}(2)$.

Based on the sparse form of the matrix $\mathbf{V}_i(x)$, for $i \in \{1,2\}$, in Approximations 1 and 2, we derive an explicit expression for its exponential. For the sake of brevity, we only remark here that, since $\mathbf{V}_i(x)$ is nilpotent, it is easily seen that $\exp\{\mathbf{V}_1(x)t\} = \sum_{x'=0}^{x-2}(\mathbf{V}_1(x)t)^{x'}/x'!$, from which it follows that

$$\exp\{\mathbf{V}_1(x)t\} = \begin{pmatrix} 1 & & & & \\ \mathbf{M}(1;2) & \mathbf{I}_2 & & & \\ \mathbf{M}(2;2) & \mathbf{M}(1;3) & \mathbf{I}_3 & & \\ \vdots & \vdots & \vdots & \ddots & \\ \mathbf{M}(x-2;2) & \mathbf{M}(x-3;3) & \mathbf{M}(x-4;4) & \cdots & \mathbf{I}_{x-1} \end{pmatrix}, \tag{3.16}$$

where $\mathbf{M}(y;l) = (m_{k,k'}(y;l))$ is a matrix of dimension $(y+l-1)\times(l-1)$ whose (k,k')th entry is given by

$$m_{k,k'}(y;l) = \begin{cases} \binom{y+l-k}{l-k} t^y \beta^y, & \text{if } k' = k, \\ 0, & \text{otherwise.} \end{cases}$$

This expression for the entries $m_{k,k'}(y;l)$ is routinely derived from the identity $\mathbf{M}(y;l) = \mathbf{B}_{y+l,y+l-1}\mathbf{B}_{y+l-1,y+l-2}\cdot\ldots\cdot\mathbf{B}_{l+1,l}t^y/y!$, for $1 \leq y \leq x-2$ and $2 \leq l \leq x-y$. In a similar manner, it is shown that

$$\exp\{\mathbf{V}_2(x)t\} = \begin{pmatrix} 1 & \mathbf{M}'(1;2) & \mathbf{M}'(2;2) & \cdots & \mathbf{M}'(x-2;2) \\ & \mathbf{I}_2 & \mathbf{M}'(1;3) & \cdots & \mathbf{M}'(x-3;3) \\ & & \mathbf{I}_3 & \cdots & \mathbf{M}'(x-4;4) \\ & & & \ddots & \vdots \\ & & & & \mathbf{I}_{x-1} \end{pmatrix}, \tag{3.17}$$

where the matrix $\mathbf{M}'(y;l) = (m'_{k,k'}(y;l))$ of dimension $(l-1) \times (y+l-1)$ is defined by its entries

$$m'_{k,k'}(y;l) = \begin{cases} \binom{y+k-1}{k-1} t^y \lambda^y, \text{ if } k' = y+k, \\ 0, \qquad\qquad \text{otherwise.} \end{cases}$$

Unlike the expressions (3.14) and (3.15), our expressions in (3.16) and (3.17) do not involve any condition associated with the eigenvectors and/or eigenvalues of the sub-matrices $\mathbf{B}_{y,y}$, for $2 \leq y \leq x$. Hence, (3.16) and (3.17) are valid in full generality, that is, even if the rates α, β and λ do not satisfy Condition (A).

For a fixed epoch $t_0 > 0$ and each value of $x \geq m+n$, expressions (3.14)-(3.17) allow us to approximate the exponential of the matrix $\mathbf{T}(x)t_0$ from (3.13), with the matrices $\mathbf{U}(x)$ and $\mathbf{V}(x)$ replaced by $\mathbf{U}_i(x)$ and $\mathbf{V}_i(x)$, respectively, for $i \in \{1,2\}$. We next select the value of p_0 in (3.13) by using bounds based on the spectral norm and the norm induced by the l_∞ vector norm.

Criterion I. For the splitting $\mathbf{T}(x) = \mathbf{U}_i(x) + \mathbf{V}_i(x)$ with $i \in \{1,2\}$, the value of p_0 in (3.13) is commonly determined (see [86, Appendix B]) from the inequality

$$||\exp\{\mathbf{T}(x)t_0\} - (\exp\{\mathbf{U}_i(x)t\} \exp\{\mathbf{V}_i(x)t\})^{p_0}||_S \leq \frac{g_i(x;t_0)}{2p_0}, \tag{3.18}$$

where the function $g_i(x;t_0)$ is defined by

$$g_i(x;t_0) = |||[\mathbf{U}_i(x), \mathbf{V}_i(x)]|||_S t_0^2 e^{(||\mathbf{U}_i(x)||_S + ||\mathbf{V}_i(x)||_S)t_0}, \tag{3.19}$$

and $||\cdot||_S$ denotes the spectral norm of a matrix, that is, it is given by $||\mathbf{W}||_S = \sup_{||\mathbf{w}||_2=1} ||\mathbf{W}\mathbf{w}||_2$ for any square matrix $\mathbf{W}$, where $||\cdot||_2$ is the Euclidean norm of a vector.

By (3.18), we may choose for any $\varepsilon > 0$ the value of p_0 as the first positive integer such that $(2\varepsilon)^{-1} g_i(x; t_0) < p_0$, for $i \in \{1, 2\}$. As a result, we have

$$||\exp\{\mathbf{T}(x)t_0\} - (\exp\{\mathbf{U}_i(x)t\} \exp\{\mathbf{V}_i(x)t\})^{p_0}||_S < \varepsilon. \quad (3.20)$$

Note that, for $i \in \{1, 2\}$ and a predetermined $\varepsilon > 0$, the integer p_0 satisfying $(2\varepsilon)^{-1} g_i(x; t_0) < p_0$ depends on t_0 and $x \geq m + n$.

In evaluating the function $g_i(x; t_0)$ for $i \in \{1, 2\}$, the singular values of the matrix $[\mathbf{U}_i(x), \mathbf{V}_i(x)]^T [\mathbf{U}_i(x), \mathbf{V}_i(x)]$ play a pivotal role. In Approximation 1, it is readily seen that $|||[\mathbf{U}_1(2), \mathbf{V}_1(2)]||_S = 0$ and $||\mathbf{V}_1(x)||_S = (x-1)\beta$, for $x \geq 3$, from which it follows that

$$g_1(x; t_0) = \begin{cases} 0, & \text{if } x = 2, \\ |||[\mathbf{U}_1(x), \mathbf{V}_1(x)]||_S t_0^2 e^{((x-1)\beta + ||\mathbf{U}_1(x)||_S)t_0}, & \text{if } x \geq 3. \end{cases}$$

To compute $|||[\mathbf{U}_1(x), \mathbf{V}_1(x)]||_S$ for $x \geq 3$, we first evaluate the largest singular value θ of the matrix $[\mathbf{U}_1(x), \mathbf{V}_1(x)]^T [\mathbf{U}_1(x), \mathbf{V}_1(x)]$, and we then derive the spectral norm of the commutator as

$$|||[\mathbf{U}_1(x), \mathbf{V}_1(x)]||_S = \sqrt{\theta},$$

see e.g. [63, Chapter 5]. To evaluate θ, we may observe that the matrix $[\mathbf{U}_1(x), \mathbf{V}_1(x)]^T [\mathbf{U}_1(x), \mathbf{V}_1(x)]$ has the structured form

$$\begin{pmatrix} \mathbf{Y}_3^T \mathbf{Y}_3 & & & & & \\ & \mathbf{Y}_4^T \mathbf{Y}_4 & & & & \\ & & \ddots & & & \\ & & & \mathbf{Y}_{x-1}^T \mathbf{Y}_{x-1} & & \\ & & & & \mathbf{Y}_x^T \mathbf{Y}_x \; \mathbf{Y}_x^T \mathbf{X}_x \\ & & & & \mathbf{X}_x^T \mathbf{Y}_x \; \mathbf{X}_x^T \mathbf{X}_x \end{pmatrix}, \quad (3.21)$$

where $\mathbf{Y}_k$ and $\mathbf{X}_x$ are given by $\mathbf{Y}_k = \mathbf{B}_{k,k}\mathbf{B}_{k,k-1} - \mathbf{B}_{k,k-1}\mathbf{B}_{k-1,k-1}$, for $3 \leq k \leq x$, and $\mathbf{X}_x = -\mathbf{B}_{x,x-1}\mathbf{B}_{x-1,x}$. This means that the set of singular values of $[\mathbf{U}_1(x), \mathbf{V}_1(x)]^T [\mathbf{U}_1(x), \mathbf{V}_1(x)]$ consists of the eigenvalues of the sub-matrices $\mathbf{Y}_k^T \mathbf{Y}_k$, for $3 \leq k \leq x$, and the eigenvalues of

$$\begin{pmatrix} \mathbf{Y}_x^T \mathbf{Y}_x \; \mathbf{Y}_x^T \mathbf{X}_x \\ \mathbf{X}_x^T \mathbf{Y}_x \; \mathbf{X}_x^T \mathbf{X}_x \end{pmatrix}.$$

Thus, the value θ can be accurately and efficiently computed from the spectral radii of these sub-matrices, since they are symmetric

matrices. In a similar manner, the function $g_2(x;t_0)$ in Approximation 2 is expressed as

$$g_2(x;t_0) = \begin{cases} 0, & \text{if } x = 2, \\ |||[\mathbf{U}_2(x), \mathbf{V}_2(x)]|||_S t_0^2 e^{((x-2)\lambda + ||\mathbf{U}_2(x)||_S)t_0}, & \text{if } x \geq 3. \end{cases}$$

In this case, the matrix $[\mathbf{U}_2(x), \mathbf{V}_2(x)]^T[\mathbf{U}_2(x), \mathbf{V}_2(x)]$ has the structured form

$$\begin{pmatrix} 0 & & & & \\ & (\mathbf{Y}'_2)^T\mathbf{Y}'_2 & & & \\ & & \ddots & & \\ & & & (\mathbf{Y}'_{x-2})^T\mathbf{Y}'_{x-2} & \\ & & & & (\mathbf{Y}'_{x-1})^T\mathbf{Y}'_{x-1} + \mathbf{X}_x^T\mathbf{X}_x \end{pmatrix}, \tag{3.22}$$

with $\mathbf{Y}'_k = \mathbf{B}_{k,k}\mathbf{B}_{k,k+1} - \mathbf{B}_{k,k+1}\mathbf{B}_{k+1,k+1}$, for $2 \leq k \leq x-1$. For $x \geq 3$, the spectral norm of the commutator $[\mathbf{U}_2(x), \mathbf{V}_2(x)]$ can be then evaluated as the value

$$|||[\mathbf{U}_2(x), \mathbf{V}_2(x)]|||_S = \max\{0, \sqrt{\theta}\},$$

where θ denotes the largest spectral radius of the sub-matrices $(\mathbf{Y}'_k)^T\mathbf{Y}'_k$, for $2 \leq k \leq x-2$, and $(\mathbf{Y}'_{x-1})^T\mathbf{Y}'_{x-1} + \mathbf{X}_x^T\mathbf{X}_x$.

Equations (3.21) and (3.22) reduce the computation of $|||[\mathbf{U}_i(x), \mathbf{V}_i(x)]|||_S$, for $i \in \{1, 2\}$, to the numerical evaluation of spectral radii of smaller sub-matrices; we refer the reader to [63] for first principles on the *power method* for finding the largest eigenvalue of a matrix.

Criterion II. In this case, our interest is in the *maximum row sum matrix* norm $||\cdot||_\infty$, instead of the spectral norm $||\cdot||_S$. The $||\cdot||_\infty$-norm of a square matrix $\mathbf{W} = (w_{ij})$ of order k is defined by $||\mathbf{W}||_\infty = \max_{1 \leq i \leq k} \sum_{j=1}^{k} |w_{ij}|$, and it can be thought of as the norm induced by the l_∞ vector norm; see e.g. [63, page 295]. We can then derive Theorem 5 of [86] by adapting arguments followed by Moler and Van Loan in [86, Appendix B] for the $||\cdot||_S$-norm to the $||\cdot||_\infty$-norm. Specifically, for the splitting $\mathbf{T}(x) = \mathbf{U}_i(x) + \mathbf{V}_i(x)$ with $i \in \{1, 2\}$, it is shown that inequality (3.18) holds with the spectral norm $||\cdot||_S$ and the function $g_i(x;t_0)$ replaced by the $||\cdot||_\infty$-norm and the function

$$h_i(x;t_0) = |||[\mathbf{U}_i(x), \mathbf{V}_i(x)]|||_\infty t_0^2 e^{(\mu_\infty(\mathbf{U}_i(x))+\mu_\infty(\mathbf{V}_i(x)))t_0}, \quad (3.23)$$

where $\mu_\infty(\cdot)$ denotes the logarithmic norm of a matrix, that is, it is specified by $\mu_\infty(\mathbf{W}) = \lim_{h\to 0+} h^{-1}(||\mathbf{I}_k - h\mathbf{W}||_\infty - 1)$, and it can be evaluated as $\mu_\infty(\mathbf{W}) = \max_{1\le i\le k}(w_{ii} + \sum_{j\neq i}|w_{ij}|)$; see e.g. [119].

Straightforward algebra yields explicit expressions for the values $\mu_\infty(\mathbf{U}_i(x))$, $\mu_\infty(\mathbf{V}_i(x))$ and $|||[\mathbf{U}_i(x), \mathbf{V}_i(x)]|||_\infty$ in (3.23), for $i \in \{1,2\}$. As a result, the functions $h_1(x;t_0)$ and $h_2(x;t_0)$ are expressed as

$$h_1(x;t_0) = \begin{cases} 0, & \text{if } x = 2, \\ 2\beta \max\{2\alpha, \alpha+\beta+\lambda\} t_0^2 e^{(\beta - \min\{\alpha, 2\lambda\})t_0}, & \text{if } x = 3, \\ \beta \max\{(x-1)(\alpha+\beta+\lambda), \eta_1(x)\} t_0^2 e^{(x-2)\beta t_0}, & \text{if } x \ge 4, \end{cases}$$

$$h_2(x;t_0) = \begin{cases} 0, & \text{if } x = 2, \\ \lambda \max\{3\alpha+\lambda, 2\beta\} t_0^2 e^{-\min\{\alpha+\beta, 2\alpha, \beta+\lambda\}t_0}, & \text{if } x = 3, \\ \lambda \max\{\eta_2(x), \eta_3(x)\} t_0^2 e^{((x-3)\lambda - \min\{\alpha+\beta, 2\alpha, \lambda\})t_0}, & \text{if } x \ge 4, \end{cases}$$

where $\eta_1(x) = \max_{2\le j\le x-2} G_1(x,j)$ with $G_1(x,j) = (x-j)(3j\alpha + \beta + j\lambda)$, and $\eta_k(x) = \max_{1\le j\le x-2} G_k(x,j)$, for $k \in \{2,3\}$, with $G_2(x,j) = j(x-j)\beta$ and $G_3(x,j) = j(3(x-1-j)\alpha + \lambda)$; for values $x \ge 4$, they are specified as

$$\eta_1(x) = \begin{cases} (x-2)(6\alpha+\beta+2\lambda), & \text{if } x \le 4 + (3\alpha+\lambda)^{-1}\beta, \\ \max\{G_1(x,j_x), G_1(x,j_x+1)\}, & \text{if } x > 4 + (3\alpha+\lambda)^{-1}\beta, \end{cases}$$

$$\eta_2(x) = \max\{G_2(x,j'_x), G_2(x,j'_x+1)\},$$

$$\eta_3(x) = \begin{cases} (x-2)(3\alpha+\lambda), & \text{if } x \le 3 + (3\alpha)^{-1}\lambda, \\ \max\{G_3(x,j''_x), G_3(x,j''_x+1)\}, & \text{if } x > 3 + (3\alpha)^{-1}\lambda, \end{cases}$$

where $j_x = [2^{-1}(x - (3\alpha+\lambda)^{-1}\beta)]$, $j'_x = [2^{-1}x]$, $j''_x = [2^{-1}(x - 1 + (3\alpha)^{-1}\lambda)]$, and $[\cdot]$ denotes the integer part of a number.

Under Criterion II we suggest to select the first integer p_0 such that $(2\varepsilon)^{-1}h_i(x;t_0) < p_0$ for a predetermined $\varepsilon > 0$, and to approximate the matrix exponential $\exp\{\mathbf{T}(x)t_0\}$ by means of $(\exp\{\mathbf{U}_i(x)t\}\exp\{\mathbf{V}_i(x)t\})^{p_0}$, where the exponentials of the matrices $\mathbf{U}_i(x)t$ and $\mathbf{V}_i(x)t$ are given by (3.14)-(3.17), for $i \in \{1,2\}$. This means that, similarly to (3.20), it is verified

$$||\exp\{\mathbf{T}(x)t_0\} - (\exp\{\mathbf{U}_i(x)t\}\exp\{\mathbf{V}_i(x)t\})^{p_0}||_\infty < \varepsilon, \quad (3.24)$$

for $i \in \{1, 2\}$.

It is important to notice that, for each value $x \geq m+n$, our expression for $P(Z(t_0) \leq x|X(0) = (m, n))$ in Theorem 3.1 requires the accurate estimation of a single row of the matrix exponential $\exp\{\mathbf{T}(x)t_0\}$; in particular, the row is related to initial numbers of $m > 0$ parasitoids and $n > 0$ hosts. In this sense, we point out that the elegance of (3.20) is somewhat marred by the lack of clear probabilistic significance of the $||\cdot||_S$-norm. If, on the contrary, we use the $||\cdot||_\infty$-norm and approximate $P(Z(t_0) \leq x|X(0) = (m, n))$ by the value

$$\begin{aligned} p(x; t_0) = 1 - \tau_{(m,n)}(x) &\left(\mathbf{I}_{J(x)} - (\exp\{\mathbf{U}_i(x)t\}\exp\{\mathbf{V}_i(x)t\})^{p_0}\right) \\ &\times(-\mathbf{T}^{-1}(x))\mathbf{t}_{x+1}(x), \end{aligned}$$

then it is seen for any $\varepsilon > 0$ that

$$|P(Z(t_0) \leq x|X(0) = (m, n)) - p(x; t_0)| < \varepsilon. \quad (3.25)$$

Note that (3.25) is readily derived from the equality

$$(-\mathbf{T}^{-1}(x))\mathbf{t}_{x+1}(x) = \mathbf{e}_{J(x)} - (-\mathbf{T}^{-1}(x))\mathbf{t}_0(x)$$

and (3.24), since Criterion II prescribes an integer p_0 satisfying $(2\varepsilon)^{-1}h_i(x; t_0) < p_0$ and

$$\begin{aligned} \tau_{(m,n)}(x)|\exp\{\mathbf{T}(x)t_0\} - (\exp\{\mathbf{U}_i(x)t\}\exp\{\mathbf{V}_i(x)t\})^{p_0}|\mathbf{e}_{J(x)} \\ \leq\ ||\exp\{\mathbf{T}(x)t_0\} - (\exp\{\mathbf{U}_i(x)t\}\exp\{\mathbf{V}_i(x)t\})^{p_0}||_\infty. \end{aligned}$$

3.3 The accuracy of the solution

We first discuss on the criterion for a suitable choice of p_0. In the case $\beta > 0$, the numerical value of p_0 is rarely, if ever, of interest by itself. Its major use is in providing an approximation of $\exp\{\mathbf{T}(x)t_0\}$ in (3.5), as accurately as possible, by using the Trotter product $(\exp\{\mathbf{U}_i(x)t\}\exp\{\mathbf{V}_i(x)t\})^{p_0}$. For a fixed epoch $t_0 > 0$ and each value $x \geq m+n$, we have derived in Subsection 3.2.2 the lower bounds $(2\varepsilon)^{-1}g_i(x; t_0)$ and $(2\varepsilon)^{-1}h_i(x; t_0)$ for the integer p_0, which are related to the $||\cdot||_S$- and $||\cdot||_\infty$-norms, respectively, and

the splitting $\mathbf{T}(x) = \mathbf{U}_i(x) + \mathbf{V}_i(x)$ with $i \in \{1, 2\}$. Therefore, it is natural to select p_0 for any $\varepsilon > 0$ as the first integer such that

$$\min_{i\in\{1,2\}} \{(2\varepsilon)^{-2} g_i(x; t_0), (2\varepsilon)^{-2} h_i(x; t_0)\} < p_0. \tag{3.26}$$

This leads us to the inequalities (3.20) and (3.24) when the above minimum is equal to $(2\varepsilon)^{-2} g_i(x; t_0)$ and $(2\varepsilon)^{-2} h_i(x; t_0)$, respectively.

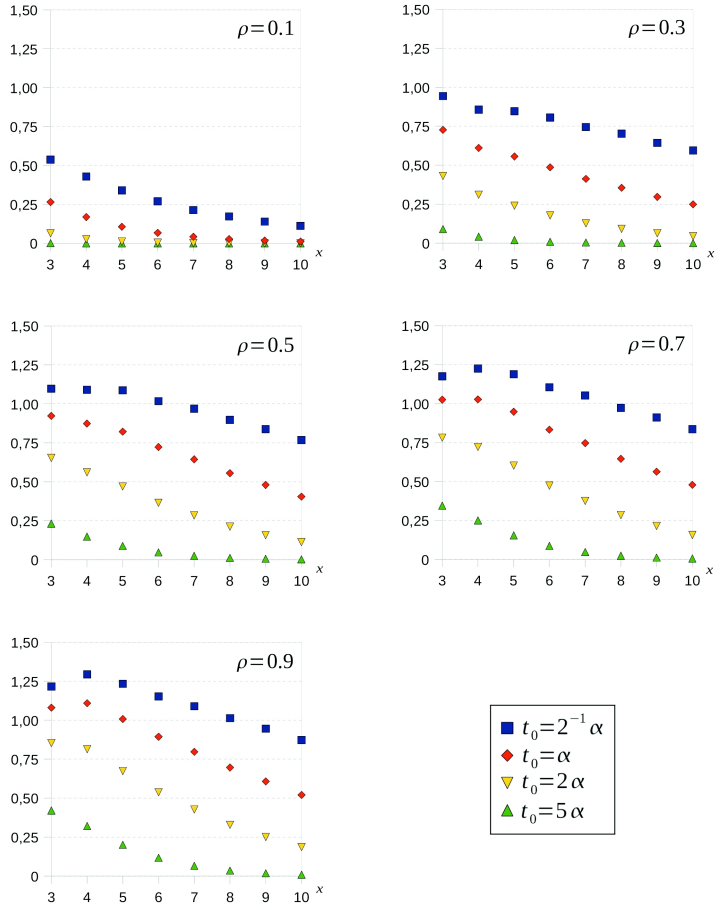

Fig. 3.1. The ratio $h_1(x; t_0)/g_1(x; t_0)$ as a function of x for various choices of t_0

We may compare the lower bounds $(2\varepsilon)^{-1} g_i(x; t_0)$ and $(2\varepsilon)^{-1}$ $h_i(x; t_0)$, with $i \in \{1, 2\}$, in terms of the resulting ratios $g_i^{-1}(x; t_0)$

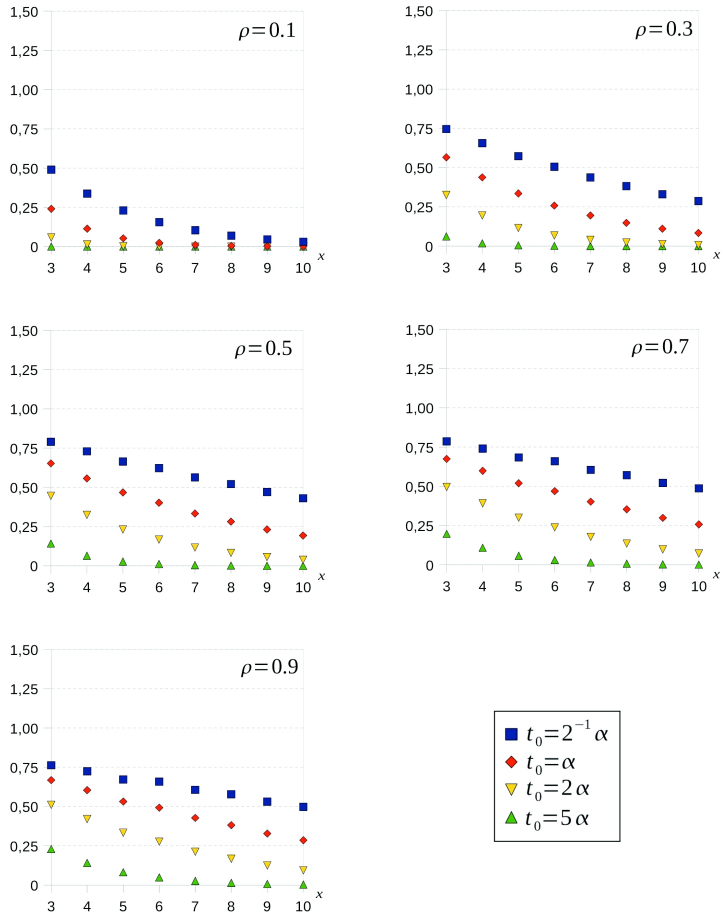

Fig. 3.2. The ratio $h_2(x;t_0)/g_2(x;t_0)$ as a function of x for various choices of t_0

$h_i(x;t_0)$, for $i \in \{1,2\}$, $h_1^{-1}(x;t_0)h_2(x,t_0)$ and $g_1^{-1}(x;t_0)h_2(x,t_0)$. Note that values $f^{-1}(x;t_0)\, g_i(x;t_0) < 1$ and $f^{-1}(x;t_0)h_i(x;t_0) < 1$ give support for any $\varepsilon > 0$ to the use of the splitting $\mathbf{T}(x) = \mathbf{U}_i(x) + \mathbf{V}_i(x)$ and the selection of p_0 from the lower bounds based on the $||\cdot||_S$-norm and the $||\cdot||_\infty$-norm, respectively, versus the use of the splitting and the norm associated with another function $f(x;t_0)$.

To support the selection criterion based on (3.26), we performed several preliminary results. A few of these preliminary results are presented in Figures 3.1-3.4, where we plot the val-

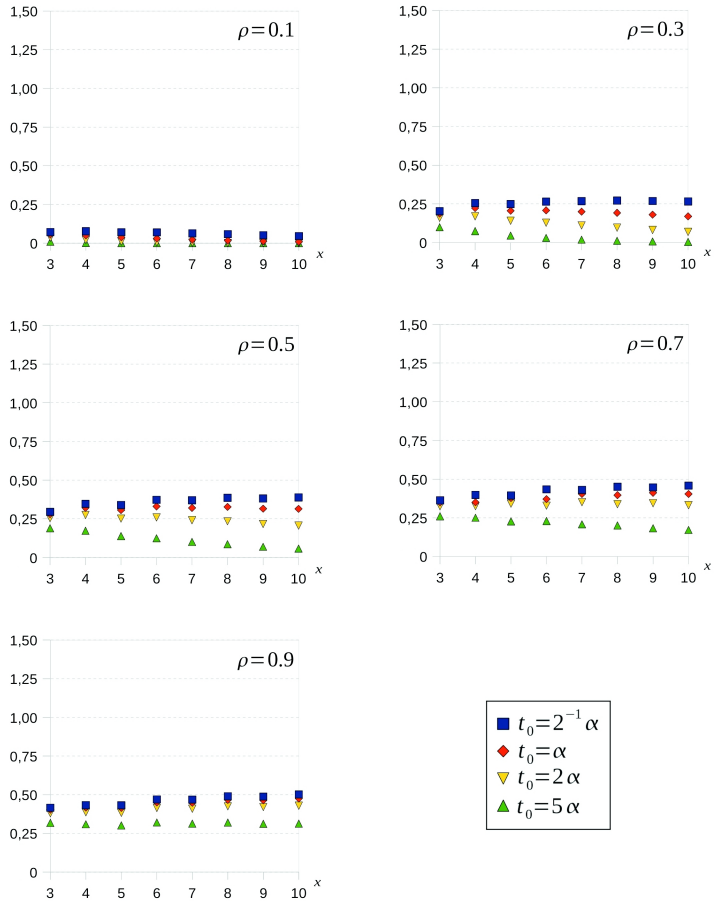

Fig. 3.3. The ratio $h_2(x;t_0)/h_1(x;t_0)$ as a function of x for various choices of t_0

ues of $g_1^{-1}(x;t_0)h_1(x;t_0)$, $g_2^{-1}(x;t_0)h_2(x;t_0)$, $h_1^{-1}(x;t_0)h_2(x,t_0)$ and $g_1^{-1}(x;t_0)h_2(x,t_0)$, as a function of the pair (t_0,x) in scenarios with $\alpha = 0.1$, $\beta = \rho^{-1}\lambda$ and $\lambda = 0.2\sqrt{5}$. With these rates α, β and λ of change of population sizes, we let ρ be the proportion M^*/N^*, where $M^* = \alpha^{-1}\lambda$ and $N^* = \alpha^{-1}\beta$ are the numbers of parasitoids and hosts, respectively, at the deterministic equilibrium position. We select values $\rho \in \{0.1, 0.3, 0.5, 0.7, 0.9\}$, whence we restrict ourselves to the typical case $\rho < 1$, which is connected to practical ecological situations where there are more hosts than parasitoids.

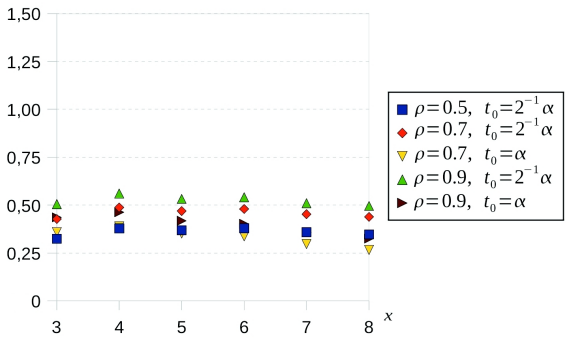

Fig. 3.4. The ratio $h_2(x;t_0)/g_1(x;t_0)$ as a function of x for those choices of (ρ, t_0) in Figure 3.1 with $h_1(x;t_0)/g_1(x;t_0) > 1$

Our numerical experiments in Figures 3.1-3.4 establish the superiority of the selection criterion combining the splitting $\mathbf{T}(x) = \mathbf{U}_2(x) + \mathbf{V}_2(x)$ and the use of the $||\cdot||_\infty$-norm for epochs $t_0 \in \{2^{-1}\alpha, \alpha, 2\alpha, 5\alpha\}$ and values $x \in \{3, 4, ..., 10\}$. Specifically, Figures 3.2 and 3.3 reveal that the selection of p_0 from the splitting $\mathbf{T}(x) = \mathbf{U}_2(x)+\mathbf{V}_2(x)$ and the $||\cdot||_\infty$-norm is preferred to the use of $\mathbf{T}(x) = \mathbf{U}_2(x)+\mathbf{V}_2(x)$ combined with the $||\cdot||_S$-norm, and the use of $\mathbf{T}(x) = \mathbf{U}_1(x) + \mathbf{V}_1(x)$ combined with the $||\cdot||_\infty$-norm, respectively. For the splitting $\mathbf{T}(x) = \mathbf{U}_1(x) + \mathbf{V}_1(x)$, Figure 3.1 shows that the selection criterion based on the $||\cdot||_\infty$-norm yields better results than that based on the $||\cdot||_S$-norm, with the exception of a few cases. With respect to these cases, we may conclude by Figures 3.3 and 3.4 that the splitting $\mathbf{T}(x) = \mathbf{U}_2(x)+\mathbf{V}_2(x)$ combined with the $||\cdot||_\infty$-norm provides the smallest value of p_0 and an approximation for the matrix exponential $\exp\{\mathbf{T}(x)t_0\}$, as accurate as possible, regardless of the pair (t_0, x) in our scenarios. We also remark that, for $i \in \{1, 2\}$ and each value x, a value of $g_i^{-1}(x;t_0)h_i(x;t_0) < 1$ implies the inequality $g_i^{-1}(x;t_0')h_i(x;t_0') < 1$ for every $t_0' \geq t_0$, since it is readily seen that $||\mathbf{V}_i(x)||_S = \mu_\infty(\mathbf{V}_i(x))$. Therefore, our conclusion can be even extended to larger values of t_0.

3.4 Numerical results

In this section, we discuss on the distribution of the maximum number $Z(t_0)$ of individuals alive during $[0, t_0]$ in the Hitch-

cock model defined by (3.1). First, the focus is on $Z(t_0)$ and its extinction-time counterpart $Z(T)$, which is the analogue of the descriptor X_{max} studied in Chapter 2. Then, we show how to use the descriptor $Z(t_0)$ in analyzing the dynamics of the host-parasitoid model. Based on Section 3.3, numerical results in this section are derived by using the selection criterion that combines the splitting $\mathbf{T}(x) = \mathbf{U}_2(x) + \mathbf{V}_2(x)$ and the $||\cdot||_\infty$-norm.

In order to specify conditions under which the random variable $Z(t_0)$ is preferred to its extinction-cycle version $Z(T)$, we point out that these conditions mainly concern with the selection of the epoch t_0 and the initial numbers $m > 0$ of parasitoids and $n > 0$ of hosts. To be concrete, the interval $[0, t_0]$ under consideration is suggested to be comparatively smaller, on average, than the random-length interval $[0, T]$ describing an extinction cycle; otherwise, it is reasonable that the asymptotic distribution of $Z(t_0)$ converges weakly to that of $Z(T)$ as t_0 tends to the expected value $\tau_{(m,n)}$. To illustrate this assertion, we focus on the $(100q)$th percentiles $K_q(t_0)$ and K_q of the respective random variables $Z(t_0)$ and $Z(T)$, and we list in Tables 3.1 and 3.2 values of $K_q(t_0)$ and K_q for scenarios with $\alpha = 1.0$, $\lambda = 0.2\sqrt{5}$ and $\beta = \rho^{-1}\lambda$, initial population sizes $(m, n) \in \{(2, 6), (4, 6)\}$, various choices of $\rho < 1$ and a variety of probabilities $q \in (0, 1)$. For each pair (ρ, q), we display the values of $K_q(t_0)$ for choices of $t_0 = a\tau_{(m,n)}$, with $a \in \{0.1, 0.3, 0.5, 0.7, 0.9\}$, and the value of K_q as ordered set values; for example, in Table 3.2, the cell associated with the pair $(\rho, q) = (3^{-1}2\sqrt{2}, 0.99)$ lists, from top to bottom, the entries 11, 12, 12, 12, 13 and 13, which means that $K_{0.99}(0.1\tau_{(4,6)}) = 11$, $K_{0.99}(0.3\tau_{(4,6)}) = 12$, $K_{0.99}(0.5\tau_{(4,6)}) = 12$, $K_{0.99}(0.7\tau_{(4,6)}) = 12$, $K_{0.99}(0.9\tau_{(4,6)}) = 13$ and $K_{0.99} = 13$. The values of K_q in Tables 3.1 and 3.2 are computed from a slight variant of Algorithm 2.1. As intuition tells us, the values of K_q are fitted by the corresponding percentiles $K_q(t_0)$ of $Z(t_0)$, if t_0 is close enough to the expected length $\tau_{(m,n)}$ of an extinction cycle, that is, if the constant $a \in (0, 1)$ is large enough. We also recall that the mean extinction time $\tau_{(m,n)}$ tends to zero as the combined initial number $m + n$ of parasitoids and hosts becomes large; see [109]. More concretely, we stress that, as $m + n$ increases, the parasitism dominance over a host birth and a parasitoid death implies shorter

Table 3.1. Values of $K_q(t_0)$ versus q and t_0 for scenarios with $\alpha = 1.0$, $\lambda = 0.2\sqrt{5}$ and $\beta = \rho^{-1}\lambda$, and initial population size $(m, n) = (2, 6)$

ρ	t_0	q	0.5	0.7	0.9	0.925	0.95	0.975	0.99
$6^{-1}\sqrt{2}$	$0.1\tau_{(2,6)}$		8	8	9	9	9	9	10
	$0.3\tau_{(2,6)}$		8	8	9	9	10	10	10
	$0.5\tau_{(2,6)}$		8	9	9	9	10	10	11
	$0.7\tau_{(2,6)}$		8	9	9	10	10	10	11
	$0.9\tau_{(2,6)}$		8	9	9	10	10	10	11
	Extinction cycle		8	9	9	10	10	10	11
$3^{-1}\sqrt{2}$	$0.1\tau_{(2,6)}$		8	8	9	9	9	9	10
	$0.3\tau_{(2,6)}$		8	8	9	9	10	10	11
	$0.5\tau_{(2,6)}$		8	9	9	10	10	10	11
	$0.7\tau_{(2,6)}$		8	9	10	10	10	11	11
	$0.9\tau_{(2,6)}$		8	9	10	10	10	11	11
	Extinction cycle		8	9	10	10	10	11	11

Table 3.2. Values of $K_q(t_0)$ versus q and t_0 for scenarios with $\alpha = 1.0$, $\lambda = 0.2\sqrt{5}$ and $\beta = \rho^{-1}\lambda$, and initial population size $(m, n) = (4, 6)$

ρ	t_0	q	0.5	0.7	0.9	0.925	0.95	0.975	0.99
$3^{-1}\sqrt{2}$	$0.1\tau_{(4,6)}$		10	10	10	11	11	11	11
	$0.3\tau_{(4,6)}$		10	10	11	11	11	12	12
	$0.5\tau_{(4,6)}$		10	10	11	11	11	12	12
	$0.7\tau_{(4,6)}$		10	10	11	11	11	12	12
	$0.9\tau_{(4,6)}$		10	10	11	11	11	12	12
	Extinction cycle		10	10	11	11	11	12	12
$3^{-1}2\sqrt{2}$	$0.1\tau_{(4,6)}$		10	10	10	10	11	11	11
	$0.3\tau_{(4,6)}$		10	10	11	11	11	12	12
	$0.5\tau_{(4,6)}$		10	10	11	11	11	12	12
	$0.7\tau_{(4,6)}$		10	10	11	11	12	12	12
	$0.9\tau_{(4,6)}$		10	10	11	11	12	12	13
	Extinction cycle		10	10	11	11	12	12	13

(on average) extinction cycles, and higher values for the probability that the parasitoids should survive the hosts. Thus, we prefer the use of $Z(t_0)$ to its extinction-cycle version $Z(T)$ as the number $m+n$ of individuals in the initial community is small, and the predetermined epoch t_0 is comparatively smaller than the expected extinction time $\tau_{(m,n)}$.

As was shown in Chapter 2, one way of analyzing the dynamics of the host-parasitoid process is to replace the absorbing Markov

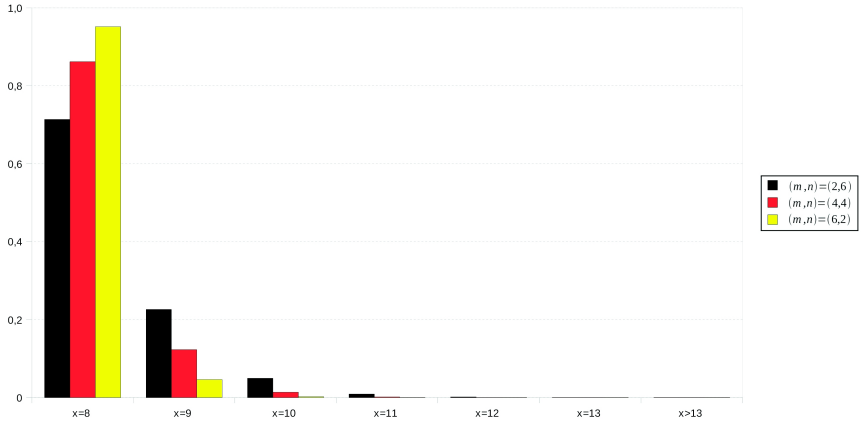

Fig. 3.5. The mass function $P(Z(t_0) = x|X(0) = (m, n))$ for scenarios with $\alpha = 1.0$, $\lambda = 0.2\sqrt{5}$, $\beta = \rho^{-1}\lambda$ and $\rho = 3^{-1}\sqrt{2}$, and initial population sizes $(m, n) \in \{(2, 6), (4, 4), (6, 2)\}$

chain $\mathcal{X}$ defined on $\mathcal{S} = \mathcal{C}_0 \cup \mathcal{C}$ by a suitably defined Markov chain $\mathcal{X}(x)$, which is defined on a finite set $\mathcal{S}(x)$. In a similar manner to Section 2.2, the level x can be chosen as the $(100q)$th percentile $K_q(t_0)$ of $Z(t_0)$ if $q \in (0, 1)$ is large enough. It is important to observe that, as q increases (and therefore K_q increases), the likelihood in $\mathcal{X}$ of those transitions from states of the level $l(K_q)$ to states in $l(K_q + 1)$ (i.e., due to a host birth) progressively decreases and, as a result, a majority of sample paths in $\mathcal{X}$ will not leave the set $\cup_{k=2}^{K_q} l(k)$ of low levels. This behavior is closely related to the unimodal distribution of $Z(t_0)$, which is illustrated in Figures 3.5 and 3.6 for scenarios with $\alpha = 1.0$, $\lambda = 0.2\sqrt{5}$, $\beta = \rho^{-1}\lambda$ and $\rho \in \{3^{-1}\sqrt{2}, 6^{-1}\sqrt{2}\}$, and initial sizes $(m, n) \in \{(2, 6), (4, 4), (6, 2)\}$. Starting from $\cup_{k=2}^{K_q} l(k)$, the effect of the sample paths to states of the level $l(K_q + 1)$ should become negligible if $q \in (0, 1)$ is large enough, which gives a satisfactory criterion to replace the original host-parasitoid process $\mathcal{X}$ by its approximating version $\mathcal{X}(K_q)$ defined on the finite state space $\mathcal{S}(K_q)$; see Chapter 2. In this case, the extinction time T in $\mathcal{X}(K_q)$ can be also derived as a PH random variable, and extinction probabilities can be recursively computed.

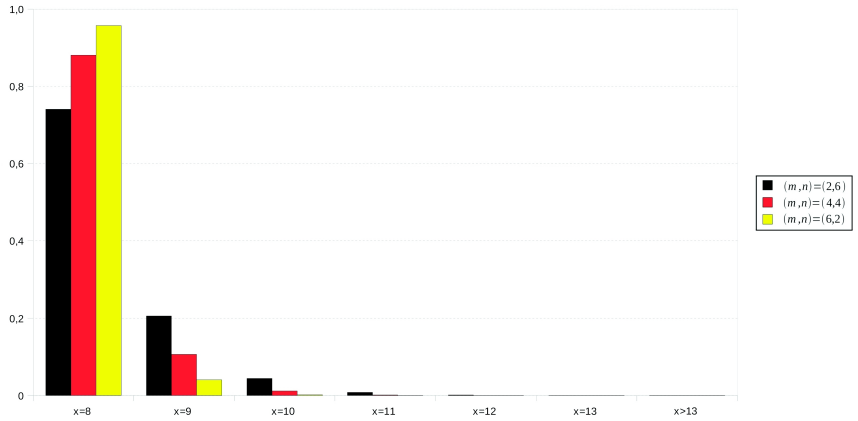

Fig. 3.6. The mass function $P(Z(t_0) = x|X(0) = (m, n))$ for scenarios with $\alpha = 1.0$, $\lambda = 0.2\sqrt{5}$, $\beta = \rho^{-1}\lambda$ and $\rho = 6^{-1}\sqrt{2}$, and initial population sizes $(m, n) \in \{(2, 6), (4, 4), (6, 2)\}$

3.5 Construction of BSDE models

In the BSDE version of $\mathcal{X}$, we are concerned with an *augmented* CTMC $(\mathcal{X}, \mathcal{Y}) = \{(X(t), Y(t)) : t \geq 0\}$ defined on the state space $\mathcal{S}_{(\mathcal{X},\mathcal{Y})} = \mathcal{C}_0 \cup \mathcal{C}^*$, where $\mathcal{C}^* = \cup_{k=2}^{\infty} l^*(k)$ and $l^*(k) = \{(m, n, y) : m+n = k, m > 0, n > 0, 1 \leq y \leq L\}$. The random variable $Y(t)$ is called *phase*, and the augmented process $(\mathcal{X}, \mathcal{Y})$ is regular, time-homogeneous, and irreducible in a similar manner to the basic process $\mathcal{X}$; see [12, 13].

The basic state (m, n) is updated in the light of the observed value of a random vector $(Z_1, Z_2)|_{(m,n)}$, which records the events taking place when the sojourn time that $\mathcal{X}$ spends in (m, n) expires. The resulting basic state (m', n') is of the form

$$(m', n') = f\left((m, n), (Z_1, Z_2)|_{(m,n)}\right),$$

where the basic state function is defined as $f((m, n), (z_1, z_2)) = (m + z_1, n + z_2)$ for pairs $(m, n) \in \mathcal{C}$ and $(z_1, z_2) \in \{(0, 0), (1, -1), (-1, 0), (0, 1)\}$. The pairs $(z_1, z_2) = (1, -1)$, $(-1, 0)$ and $(0, 1)$ amount to parasitism, a parasitoid death and a host birth, respectively, in the basic host-parasitoid model and their occurrence may imply a jump in the phase variable; on the contrary, the pair

$(z_1, z_2) = (0, 0)$ means a transition between phases, but it does not correspond to any event in the process $\mathcal{X}$.

For the derivation of the infinitesimal generator $\mathbf{Q}^*$ of the augmented process $(\mathcal{X}, \mathcal{Y})$, we introduce a family

$$\mathcal{F} = \bigcup_{(m,n)\in\mathcal{C}} \big\{\mathbf{C}_{(m,n)}(z_1, z_2) : (z_1, z_2) = (0, 0), (1, -1), (-1, 0), (0, 1)\big\}$$

of (possibly infinitely many) square matrices of order L, where $\mathbf{C}_{(m,n)}(z_1, z_2)$ with $(z_1, z_2) \in \{(1, -1), (-1, 0), (0, 1)\}$ are nonnegative, $\mathbf{C}_{(m,n)}(0, 0)$ has nonnegative off-diagonal elements and strictly negative diagonal elements, and $\mathbf{C}_{(m,n)} \equiv \mathbf{C}_{(m,n)}(0, 0) + \mathbf{C}_{(m,n)}(1, -1) + \mathbf{C}_{(m,n)}(-1, 0) + \mathbf{C}_{(m,n)}(0, 1)$ defines an irreducible infinitesimal generator. Then, $\mathbf{Q}^*$ has the structured form of $\mathbf{Q}$ in (3.2) with $\mathbf{A}_{k,k'}$ and $\mathbf{B}_{k,k'}$ in (3.3) and (3.4) replaced by sub-matrices $\mathbf{A}^*_{k,k'}$ and $\mathbf{B}^*_{k,k'}$. Specifically, sub-matrices $\mathbf{A}^*_{k,k-1}$ and $\mathbf{A}^*_{k,k}$ are given by the respective expressions

$$\mathbf{A}^*_{k,k-1} = \begin{pmatrix} \mathbf{0}_{(k-2)L} & \mathbf{0}_{(k-2)L} \\ \mathbf{0}_L & \mathbf{C}_{(1,k-1)}(-1, 0)\mathbf{e}_L \end{pmatrix},$$
$$\mathbf{A}^*_{k,k} = \begin{pmatrix} \mathbf{C}_{(k-1,1)}(1, -1)\mathbf{e}_L & \mathbf{0}_L \\ \mathbf{0}_{(k-2)L} & \mathbf{0}_{(k-2)L} \end{pmatrix}.$$

Sub-matrices $\mathbf{B}^*_{k,k-1}$, $\mathbf{B}^*_{k,k}$ and $\mathbf{B}^*_{k,k+1}$ are given, respectively, by

$$\begin{pmatrix} \mathbf{C}_{(k-1,1)}(-1, 0) & & & \\ & \mathbf{C}_{(k-2,2)}(-1, 0) & & \\ & & \ddots & \\ & & & \mathbf{C}_{(2,k-2)}(-1, 0) \\ & & & \mathbf{0}_{L\times L} \end{pmatrix},$$

$$\begin{pmatrix} \mathbf{C}_{(k-1,1)}(0, 0) & & & \\ \mathbf{C}_{(k-2,2)}(1, -1) & \mathbf{C}_{(k-2,2)}(0, 0) & & \\ & \ddots & \ddots & \\ & & \mathbf{C}_{(1,k-1)}(1, -1) & \mathbf{C}_{(1,k-1)}(0, 0) \end{pmatrix},$$

$$\begin{pmatrix} \mathbf{0}_{L\times L} & \mathbf{C}_{(k-1,1)}(0, 1) & & \\ & \mathbf{C}_{(k-2,2)}(0, 1) & & \\ & & \ddots & \\ & & & \mathbf{C}_{(1,k-1)}(0, 1) \end{pmatrix}.$$

Roughly speaking, each basic state $(m,n) \in \mathcal{C}$ in $\mathcal{X}$ translates into a set $\{(m,n,y) : 1 \leq y \leq L\}$ of augmented states in $(\mathcal{X},\mathcal{Y})$, and the transition rates αmn, βm and λn in (3.1) are replaced by matrices $\mathbf{C}_{(m,n)}(1,-1)$, $\mathbf{C}_{(m,n)}(-1,0)$ and $\mathbf{C}_{(m,n)}(0,1)$ of infinitesimal rates, respectively.

The augmented process $(\mathcal{X},\mathcal{Y})$ can be thought of as the *state-dependent* version of a marked Markovian arrival process (MMAP); see [59]. Specifically, for initial numbers of $m > 0$ parasitoids and $n > 0$ hosts, the matrices $\mathbf{C}_{(m,n)}(z_1,z_2)$ with $(z_1,z_2) \in \{(0,0),(1,-1),(-1,0),(0,1)\}$ result in a single MMAP with set of marks $\{(1,-1),(-1,0),(0,1)\}$, and fundamental arrival rate of type-(z_1,z_2) marks

$$\lambda_{(m,n)}(z_1,z_2) = \boldsymbol{\theta}_{(m,n)}\mathbf{C}_{(m,n)}(z_1,z_2)\mathbf{e}_L,$$

where $\boldsymbol{\theta}_{(m,n)}$ is the stationary vector of $\mathbf{C}_{(m,n)}$. We may then notice that, in the stationary version of the MMAP, the fundamental rates $\lambda_{(m,n)}(1,-1)$, $\lambda_{(m,n)}(-1,0)$ and $\lambda_{(m,n)}(0,1)$ correspond to the asymptotic values of the instantaneous rates of parasitism, a parasitoid death and a host birth, respectively, in the augmented process $(\mathcal{X},\mathcal{Y})$; in the scalar case $L = 1$, such fundamental rates are given by αmn, βm and λn, respectively.

3.6 Modeling correlated events with state-dependent Markovian arrivals

In this section, we focus on a concrete family $\mathcal{F}$ such that the resulting BSDE model remains sufficiently tractable, yet enough versatile for computational purposes. To begin with, we consider three independent MAPs. Let $(\mathbf{D}_0,\mathbf{D}_1)$, $(\mathbf{E}_0,\mathbf{E}_1)$ and $(\mathbf{F}_0,\mathbf{F}_1)$ be the characteristic matrices of these auxiliary MAPs of orders L_d, L_e and L_f, respectively, and fundamental arrival rates λ_d, λ_e and λ_f. In a similar manner to (3.1), the family $\mathcal{F}$ is specified by the matrices

$$\mathbf{C}_{(m,n)}(z_1,z_2) = \begin{cases} \lambda_f^{-1}\alpha mn\mathbf{I}_{L_dL_e} \otimes \mathbf{F}_1, & \text{if } (z_1,z_2) = (1,-1), \\ \lambda_e^{-1}\beta m\mathbf{I}_{L_d} \otimes \mathbf{E}_1 \otimes \mathbf{I}_{L_f}, & \text{if } (z_1,z_2) = (-1,0), \\ \lambda_d^{-1}\lambda n\mathbf{D}_1 \otimes \mathbf{I}_{L_eL_f}, & \text{if } (z_1,z_2) = (0,1), \end{cases} \tag{3.27}$$

and $\mathbf{C}_{(m,n)}(0,0) = (\lambda_d^{-1}\lambda n\mathbf{D}_0) \oplus (\lambda_e^{-1}\beta m\mathbf{E}_0) \oplus (\lambda_f^{-1}\alpha mn\mathbf{F}_0)$, for states $(m,n) \in \mathcal{C}$.

To motivate the above specification of $\mathcal{F}$, we first describe the dynamics of the basic model defined by (3.1) in terms of *scheduled events*. This means that, when the process $\mathcal{X}$ enters state $(m,n) \in \mathcal{C}$ at time t, the next transition is triggered by events $E_{(m,n)}(1,-1)$, $E_{(m,n)}(-1,0)$ and $E_{(m,n)}(0,1)$, in such a way that these events are scheduled to occur at times $t+\tau_{(m,n)}(1,-1)$, $t+\tau_{(m,n)}(-1,0)$ and $t+\tau_{(m,n)}(0,1)$, respectively. The random lengths $\tau_{(m,n)}(1,-1)$, $\tau_{(m,n)}(-1,0)$ and $\tau_{(m,n)}(0,1)$ are independent and exponentially distributed with parameters αmn, βm and λn, respectively, and they are also independent of the history of the process $\mathcal{X}$ up to time t. If it is found that

$$\tau_{(m,n)}(z_1,z_2) = \min\{\tau_{(m,n)}(1,-1), \tau_{(m,n)}(-1,0), \tau_{(m,n)}(0,1)\},$$

then $E_{(m,n)}(z_1,z_2)$ is the next event that takes place after the process $\mathcal{X}$ moves into state (m,n). Thus, the basic model spends in state (m,n) until $t+\tau_{(m,n)}(z_1,z_2)$ and then moves to state $(m',n') = (m+z_1, n+z_2)$. All other scheduled events are then canceled, a new set of events denoted by $E_{(m',n')}(1,-1)$, $E_{(m',n')}(-1,0)$ and $E_{(m',n')}(0,1)$ are scheduled at times $t+\tau_{(m',n')}(1,-1)$, $t+\tau_{(m',n')}(-1,0)$ and $t+\tau_{(m',n')}(0,1)$, and the process continues.

In this visualization of a simple path of the basic model that is being modeled by the process $\mathcal{X}$, the next event $E_{(m,n)}(z_1,z_2)$ is related to a superposition of three independent Poisson processes with arrival rates αmn, βm and λn, for every state $(m,n) \in \mathcal{C}$. In the BSDE model with augmented process $(\mathcal{X},\mathcal{Y})$, we construct the superposition from independent *scaled* MAPs[1] instead of Poisson streams; since $\mathbf{D}_1\mathbf{e}_{L_d} \neq \mathbf{0}_{L_d}$, $\mathbf{E}_1\mathbf{e}_{L_e} \neq \mathbf{0}_{L_e}$ and $\mathbf{F}_1\mathbf{e}_{L_f} \neq \mathbf{0}_{L_f}$, we have the certain knowledge that the birth of a host, the death of a parasitoid and parasitism will always occur, irrespective of the sizes $m > 0$ and $n > 0$. If we express the phase variable $Y(t)$ as $(Y_d(t), Y_e(t), Y_f(t))$ in the BSDE version, then expressions in (3.27) are readily derived when the *joint* phases $y = (y_d, y_e, y_f)$ are arranged in the lexicographical order. The number L of joint

[1]The respective *scaled* MAPs are defined by the characteristic matrices $(\lambda_f^{-1}\alpha mn\mathbf{F}_0, \lambda_f^{-1}\alpha mn\mathbf{F}_1)$, $(\lambda_e^{-1}\beta m\mathbf{E}_0, \lambda_e^{-1}\beta m\mathbf{E}_1)$ and $(\lambda_d^{-1}\lambda n\mathbf{D}_0, \lambda_d^{-1}\lambda n\mathbf{D}_1)$, for numbers of $m > 0$ parasitoids and $n > 0$ hosts.

phases is given by $L_d L_e L_f$. Moreover, it is readily seen that, in a similar manner to $\mathcal{X}$, the fundamental arrival rates of these scaled MAPs are given by

$$\lambda_{(m,n)}(z_1, z_2) = \begin{cases} \alpha mn, \text{ if } (z_1, z_2) = (1, -1), \\ \beta m, \quad \text{if } (z_1, z_2) = (-1, 0), \\ \lambda n, \quad \text{if } (z_1, z_2) = (0, 1), \end{cases}$$

regardless of the number L of phases. It is also observed the *correlation-invariance* property[2] for the auxiliary MAPs and their scaled counterparts.

The specification of $\mathcal{F}$ in (3.27) leads us to some interesting properties in the augmented process $(\mathcal{X}, \mathcal{Y})$ which are shown in the following result:

Theorem 3.3. *Let us consider the augmented process $(\mathcal{X}, \mathcal{Y})$ defined by the family $\mathcal{F}$ in (3.27). Let $T_{(\mathcal{X},\mathcal{Y})}$ be the time till absorption in $(\mathcal{X}, \mathcal{Y})$, and $\alpha_{(m,n,y)}$ be the absorption probability defined as $\alpha_{(m,n,y)} = P(T_{(\mathcal{X},\mathcal{Y})} < \infty | X(0) = (m, n), Y(0) = y)$, for $(m, n, y) \in \mathcal{C}^*$.*

(i) The augmented process $(\mathcal{X}, \mathcal{Y})$ is a regular time-homogeneous CTMC.

(ii) If the rate

$$f_{min} = \min\{(-\mathbf{F}_0 \mathbf{e}_{L_f})_y : 1 \leq y \leq L_f\}$$

is strictly positive, then $\alpha_{(m,n,y)} = 1$ and the expected time

$$\tau_{(m,n,y)} = E[T_{(\mathcal{X},\mathcal{Y})} | X(0) = (m, n), Y(0) = y]$$

to reach the set $\mathcal{C}_0$ of absorbing states is finite, for every initial state $(m, n, y) \in \mathcal{C}^*$. Furthermore, the expected time $\tau_{(m,n,y)}$ tends to zero as $m + n \to \infty$ uniformly in $y \in \{1, ..., L\}$.

[2] Let X_l be the lth inter-arrival time in the MAP with matrices $(\mathbf{F}_0, \mathbf{F}_1)$. The random variables X_l and X_{l+k} (with $k \geq 1$) are identically distributed, but they are not necessarily independent; see [12, Section 2.3.2]. Let $\rho_f(k)$ denote the coefficient of correlation between X_l and X_{l+k}, that is, $\rho_f(k) = \rho_f(X_l, X_{l+k})$. The *correlation-invariance* property states that $\rho_f(k) = \rho_f(k; m, n)$, where $\rho_f(k; m, n)$ denotes the coefficient of correlation between X_l and X_{l+k} in the MAP with matrices $(\lambda_f^{-1} \alpha mn \mathbf{F}_0, \lambda_f^{-1} \alpha mn \mathbf{F}_1)$, for every $(m, n) \in \mathcal{C}$. It is similarly seen that $\rho_d(k) = \rho_d(k; m, n)$ and $\rho_e(k) = \rho_e(k; m, n)$.

Proof. For statement (i) we use the following regularity criterion (see [10, page 80]): *a CTMC with infinitesimal generator* $\mathbf{Q}^*$ *is regular if the inequality* $\mathbf{Q}^*\mathbf{z} \geq \gamma\mathbf{z}$ *with* $\mathbf{0} \leq \mathbf{z} \leq \mathbf{e}$ *has no nontrivial solution, for some (and therefore for all)* $\gamma > 0$.

Let us denote the entries of $\mathbf{z}$ by $z_{(m,n)}$ if $(m,n) \in \mathcal{C}_0$, and $z_{(m,n,y)}$ if $(m,n,y) \in \mathcal{C}^*$. Then, the inequality $\mathbf{Q}^*\mathbf{z} \geq \gamma\mathbf{z}$ for states $(m,n) \in \mathcal{C}_0$ becomes $\gamma z_{(m,n)} \leq 0$. Thus, $z_{(m,n)} = 0$ for every absorbing state $(m,n) \in \mathcal{C}_0$ since $\gamma > 0$ and $0 \leq z_{(m,n)} \leq 1$. We next proof that $z_{(m,n,y)} = 0$ for states $(m,n,y) \in \mathcal{C}^*$ by showing that the maximal values $\chi_k = \max\{z_{(m,n,y)} : m+n = k, m > 0, n > 0, 1 \leq y \leq L\}$ with $k \geq 2$ are all equal to zero. To do this, we express $\mathbf{Q}^*\mathbf{z} \geq \gamma\mathbf{z}$ for levels $l^*(k)$ with $k \geq 2$ as

$$\left(\gamma\mathbf{I}_{(k-1)L} - \mathbf{B}^*_{k,k}\right)\mathbf{z}(k) \leq \mathbf{B}^*_{k,k-1}\mathbf{z}(k-1) + \mathbf{B}^*_{k,k+1}\mathbf{z}(k+1), \tag{3.28}$$

where $\mathbf{z}(k)$ is a column vector that consists of sub-vectors $\mathbf{z}(k-1,1)$, $\mathbf{z}(k-2,2)$, ..., $\mathbf{z}(1,k-1)$ with entries $(\mathbf{z}(m,n))_y = z_{(m,n,y)}$ for $m+n = k$, $m > 0$, $n > 0$ and $1 \leq y \leq L$. If the maximum χ_k is attained at state (m_k, n_k, y_k) with $m_k + n_k = k$ and $1 \leq y_k \leq L$, then it is readily seen from (3.28) that

$$\begin{aligned}\lambda_d^{-1}\lambda n_k \left((-\mathbf{D}_0\mathbf{e}_{L_d}) \otimes \mathbf{e}_{L_eL_f}\right)_{y_k} (\chi_{k+1} - \chi_k) &\geq \gamma\chi_k \\ + \lambda_e^{-1}\beta m_k \left(\mathbf{e}_{L_d} \otimes (-\mathbf{E}_0\mathbf{e}_{L_e}) \otimes \mathbf{e}_{L_f}\right)_{y_k} (\chi_k - \chi_{k-1}), &\quad k \geq 2,\end{aligned} \tag{3.29}$$

with $\chi_1 \equiv 0$. For the values $\mu_k = \max\{\lambda_d^{-1}\lambda n((-\mathbf{D}_0\mathbf{e}_{L_d}) \otimes \mathbf{e}_{L_eL_f})_y : 1 \leq n \leq k-1, 1 \leq y \leq L\}$ and $\xi_k = \min\{\lambda_e^{-1}\beta m(\mathbf{e}_{L_d} \otimes (-\mathbf{E}_0\mathbf{e}_{L_e}) \otimes \mathbf{e}_{L_f})_y : 1 \leq m \leq k-1, 1 \leq y \leq L\}$, it is observed that $\mu_k = (k-1)\mu$ and $\xi_k = \xi$ where $\mu = \lambda_d^{-1}\lambda d_{max} > 0$ and $\xi = \lambda_e^{-1}\beta e_{min} \geq 0$, with

$$\begin{aligned} d_{max} &= \max\{(-\mathbf{D}_0\mathbf{e}_{L_d})_y : 1 \leq y \leq L_d\}, \\ e_{min} &= \min\{(-\mathbf{E}_0\mathbf{e}_{L_e})_y : 1 \leq y \leq L_e\}. \end{aligned}$$

Thus, (3.29) yields

$$\mu_k(\chi_{k+1} - \chi_k) \geq \gamma\chi_k + \xi(\chi_k - \chi_{k-1}), \quad k \geq 2, \tag{3.30}$$

which implies that $\chi_{k+1} \geq \chi_k$ since $\chi_k \geq 0$. If $z_{(m,n,y)}$ is not identically zero, then there exists a first integer $k_0 \geq 2$ such

that $\chi_{k_0} > 0$. In such a case, (3.30) leads to $\chi_{k+1} - \chi_k \geq \mu_k^{-1}\gamma\chi_{k_0} + \mu_k^{-1}\xi(\chi_k - \chi_{k-1}) \geq \mu_k^{-1}\gamma\chi_{k_0}$ for every $k \geq k_0$. This inequality can be written as $\chi_{k+1} \geq \chi_k + (k-1)^{-1}K$ for $k \geq k_0$, where $K = \mu^{-1}\gamma\chi_{k_0} > 0$ is independent of k. Thus, it is seen that $\chi_k = 0$ if $k < k_0$, and $\chi_{k+1} \geq \chi_{k_0} + K\sum_{l=k_0-1}^{k-1} l^{-1}$ if $k \geq k_0$. Since $\chi_{k_0} > 0$, $K > 0$ and $\sum_{l=k_0-1}^{\infty} l^{-1}$ diverges, we find that χ_k tends to ∞ as $k \to \infty$, contrary to the fact that $0 \leq z_{(m,n,y)} \leq 1$ for states $(m,n,y) \in \mathcal{C}^*$. Therefore, $z_{(m,n,y)} = 0$ for states $(m,n,y) \in \mathcal{C}^*$. Needless to say, the CTMC $(\mathcal{X},\mathcal{Y})$ is clearly time-homogeneous by (3.27).

The proof of statement (ii) is based on the criterion used in Theorem 2.1 (see [105, Theorem 5]); for easy of presentation, this criterion is rewritten in terms of our notation here as follows: *for an absorbing CTMC with states $x \in \mathcal{S}^*$ and infinitesimal generator $\mathbf{Q}^*$, let α_x be the probability of reaching some state in the set of absorbing states, and τ_x be the expected time to reach the set of absorbing states from the transient state x. If there exist finite constants $u_x \geq 0$ such that*

$$\Delta u_x = q_x^* u_x - \sum_{x' \neq x} q_{xx'}^* u_{x'} \geq 1, \tag{3.31}$$

then $\alpha_x = 1$ and $\tau_x \leq u_x < \infty$ for every transient state x.

For the augmented process $(\mathcal{X},\mathcal{Y})$, the inequality (3.31) may be conveniently rephrased in matrix form as $\Delta\mathbf{u}(k) \geq \mathbf{e}_{(k-1)L}$ if $k \geq 2$, by defining column vectors $\mathbf{u}(k)$ that consist of sub-vectors $\mathbf{u}(k-1,1)$, $\mathbf{u}(k-2,2)$, ..., $\mathbf{u}(1,k-1)$ with entries $(\mathbf{u}(m,n))_y = u_{(m,n,y)}$ for $m+n=k$, $m>0$, $n>0$ and $1 \leq y \leq L$. It is also seen that

$$\Delta\mathbf{u}(2) = -\mathbf{B}_{2,2}^*\mathbf{u}(2) - \mathbf{B}_{2,3}^*\mathbf{u}(3) - \mathbf{A}_{2,1}^*\mathbf{u}(0,1) - \mathbf{A}_{2,2}^*\begin{pmatrix}\mathbf{u}(2,0)\\ \mathbf{u}(0,2)\end{pmatrix}, \tag{3.32}$$

$$\begin{aligned}\Delta\mathbf{u}(k) = {} & -\mathbf{B}_{k,k-1}^*\mathbf{u}(k-1) - \mathbf{B}_{k,k}^*\mathbf{u}(k) - \mathbf{B}_{k,k+1}^*\mathbf{u}(k+1) \\ & -\mathbf{A}_{k,k-1}^*\begin{pmatrix}\mathbf{u}(k-1,0)\\ \mathbf{u}(0,k-1)\end{pmatrix} - \mathbf{A}_{k,k}^*\begin{pmatrix}\mathbf{u}(k,0)\\ \mathbf{u}(0,k)\end{pmatrix}, \quad k \geq 3,\end{aligned} \tag{3.33}$$

with $\mathbf{u}(m,n) = u_{(m,n)}$ for states $(m,n) \in \mathcal{C}_0$.

The sub-vectors of constants that we try first are of the form $\mathbf{v}(m,n) = Av_0(m,n)\mathbf{e}_L$ if $(m,n) \in \mathcal{C}$, and $Av_0(m,n)$ if $(m,n) \in \mathcal{C}_0$, where $A > 0$ is a constant to be chosen later and, in a similar manner to [109],

$$v_0(m,n) = \frac{1}{m+n} \log \frac{(m+n+1)(n+1)}{m+1}.$$

From (3.32) and (3.33), straightforward algebra yields the following expression for $\Delta\mathbf{v}(m,n)$:

$$\begin{aligned}
&\lambda_d^{-1} A\lambda n(-\mathbf{D}_0\mathbf{e}_{L_d}) \otimes \mathbf{e}_{L_eL_f} \left(v_0(m,n) - v_0(m,n+1)\right) \\
&+ \lambda_e^{-1} A\beta m \mathbf{e}_{L_d} \otimes (-\mathbf{E}_0\mathbf{e}_{L_e}) \otimes \mathbf{e}_{L_f} \left(v_0(m,n) - v_0(m-1,n)\right) \\
&+ \lambda_f^{-1} A\alpha mn \mathbf{e}_{L_dL_e} \otimes (-\mathbf{F}_0\mathbf{e}_{L_f}) \left(v_0(m,n) - v_0(m+1,n-1)\right),
\end{aligned}$$

for states $(m,n) \in \mathcal{C}$, and an appeal to the mean value theorem leads us to the inequalities

$$\begin{aligned}
v_0(m,n) - v_0(m+1,n-1) &> \frac{m+n+2}{(m+n)(m+2)(n+1)}, \\
v_0(m,n) - v_0(m-1,n) &> -\frac{1}{m+n-1}\left(\frac{n}{(m+n)m}\right. \\
&\qquad \left. + \frac{1}{m+n-1} \log \frac{(m+n+1)(n+1)}{m}\right), \\
v_0(m,n) - v_0(m,n+1) &> -\frac{1}{m+n}\left(\frac{1}{m+n+1} + \frac{1}{n+1}\right).
\end{aligned}$$

Thus, we write down

$$\begin{aligned}
\Delta\mathbf{v}(m,n) > A\Bigg(&\frac{\alpha' mn(m+n+2)}{(m+n)(m+2)(n+1)} - \frac{\beta' m}{m+n-1} \\
&\times \left(\frac{n}{(m+n)m} + \frac{1}{m+n-1} \log \frac{(m+n+1)(n+1)}{m}\right) \\
&- \frac{\lambda' n}{m+n}\left(\frac{1}{m+n+1} + \frac{1}{n+1}\right)\Bigg) \mathbf{e}_L, \qquad (3.34)
\end{aligned}$$

where $\alpha' = \lambda_f^{-1}\alpha f_{min}$, $\beta' = \lambda_e^{-1}\beta e_{max}$ and $\lambda' = \lambda_d^{-1}\lambda d_{max}$ with

$$e_{max} = \max\{(-\mathbf{E}_0\mathbf{e}_{L_e})_y : 1 \le y \le L_e\}.$$

Values α', β' and λ' in (3.34) are strictly positive since $-\mathbf{D}_0\mathbf{e}_{L_d} \neq \mathbf{0}_{L_d}$, $-\mathbf{E}_0\mathbf{e}_{L_e} \neq \mathbf{0}_{L_e}$ and, by assumption, $f_{min} > 0$. Based on (3.34), we notice that there exist constants $A > 0$ and $K \geq 1$, which depend on the parameters α', β' and λ', such that $\Delta\mathbf{v}(m,n) \geq \mathbf{e}_L$ for states $(m,n) \in \mathcal{C}$ with $m+n > K$.

To construct sub-vectors $\mathbf{u}(m,n)$ of constants verifying the inequality $\Delta\mathbf{u}(m,n) \geq \mathbf{e}_L$ for every state $(m,n) \in \mathcal{C}$, we introduce a correction term $\mathbf{w}(m,n)$ and try sub-vectors of the form $\mathbf{u}(m,n) = \mathbf{v}(m,n)+\mathbf{w}(m,n)$. Specifically, we define $\mathbf{w}(m,n) = Bw_0(m,n)\mathbf{e}_L$ if $(m,n) \in \mathcal{C}$, and $Bw_0(m,n)$ if $(m,n) \in \mathcal{C}_0$, where

$$w_0(m,n) = \frac{1-\rho^{m+2n}}{1-\rho}$$

and $\rho \in (0,1)$ and $B > 0$ are constants to be chosen later. For $(m,n) \in \mathcal{C}$, it is readily seen that

$$\begin{aligned}\Delta\mathbf{w}(m,n) = B\rho^{m+2n-1} \big(&\lambda_f^{-1}\alpha mn\mathbf{e}_{L_dL_e} \otimes (-\mathbf{F}_0\mathbf{e}_{L_f}) \\ &+\lambda_e^{-1}\beta m\mathbf{e}_{L_d} \otimes (-\mathbf{E}_0\mathbf{e}_{L_e}) \otimes \mathbf{e}_{L_f} \\ &-\lambda_d^{-1}\rho(1+\rho)\lambda n(-\mathbf{D}_0\mathbf{e}_{L_d}) \otimes \mathbf{e}_{L_eL_f}\big)\,,\end{aligned}$$

from which it follows that

$$\Delta\mathbf{w}(m,n) \geq B\rho^{m+2n-1}\left(\alpha' mn + \beta'' m - \rho(1+\rho)\lambda' n\right)\mathbf{e}_L,$$

for states $(m,n) \in \mathcal{C}$, where $\beta'' = \lambda_e^{-1}\beta e_{min}$. Since $\alpha' > 0$, $\beta'' \geq 0$ and $\lambda' > 0$, we may derive $\Delta\mathbf{w}(m,n) > \mathbf{0}_L$ for $(m,n) \in \mathcal{C}$, provided ρ is chosen sufficiently small, that is, $\rho \in (0, \min\{\rho', 1\})$ with $\rho' = -2^{-1} + \sqrt{1+(\lambda')^{-1}4\alpha'}$.

Thus, for all constant $B > 0$, it is seen that $\Delta\mathbf{u}(m,n) \geq \mathbf{e}_L$ if $(m,n) \in \mathcal{C}$ and $m+n > K$. On the finite set of states $(m,n) \in \mathcal{C}$ with $m+n \leq K$, we may then choose $B > 0$ such that $\Delta\mathbf{w}(m,n) \geq \mathbf{e}_L - \Delta\mathbf{v}(m,n)$. Hence, by defining $\mathbf{u}(m,n) = \mathbf{v}(m,n)+\mathbf{w}(m,n)$, we have $\Delta\mathbf{u}(k) \geq \mathbf{e}_{(k-1)L}$ as required. It is also noticed that the entries of $\mathbf{w}(m,n)$ are bounded, and $\mathbf{v}(m,n)$ tends to zero as $m+n \to \infty$, uniformly in $(m,n) \in \mathcal{C}$. This means that the expected absorption times $\tau_{(m,n,y)}$ are bounded since [105, Theorem 5] implies $\alpha_{(m,n,y)} = 1$ and $0 \leq \tau_{(m,n,y)} \leq u_{(m,n,y)}$ for every $(m,n,y) \in \mathcal{C}^*$, and the entries of $u_{(m,n,y)}$ are bounded.

To proof that $\tau_{(m,n,y)} \to 0$ as $m+n \to \infty$, we construct *refined* constants $u_{(m,n,y)}$ for which $\Delta\mathbf{u}(m,n) \geq \mathbf{e}_L$ for $(m,n) \in \mathcal{C}$, and

$u_{(m,n,y)} \to 0$ as $m+n \to \infty$. To do this, we first replace the constant B by B' in the definition of $\mathbf{w}(m,n)$, and then choose $B' > 0$ satisfying $\mathbf{w}(m,n) < \mathbf{v}(m,n)$ on the finite set of states $(m,n) \in \mathcal{C}$ with $m+n \leq K$. It can be easily verified that the set of states $(m,n) \in \mathcal{C}$ such that $\mathbf{w}(m,n) < \mathbf{v}(m,n)$ is also finite, and it trivially contains states $(m,n) \in \mathcal{C}$ with $m+n \leq K$ satisfying $\mathbf{w}(m,n) < \mathbf{v}(m,n)$. We can then choose a constant $C > 1$ such that

$$C\Delta\mathbf{w}(m,n) \geq \mathbf{e}_L,$$

for every state $(m,n) \in \mathcal{C}$ verifying $\mathbf{w}(m,n) < \mathbf{v}(m,n)$.

This means that the sub-vectors

$$\mathbf{u}(m,n) = C\min\{\mathbf{v}(m,n), \mathbf{w}(m,n)\}$$

satisfy $\Delta\mathbf{u}(m,n) \geq \mathbf{e}_L$ for $(m,n) \in \mathcal{C}$, and $\mathbf{u}(m,n) \to \mathbf{0}_L$ as $m+n \to \infty$, since $A > 0$, $C > 1$ and $v_0(m,n) \to 0$ as $m+n \to \infty$. This completes the proof. □

The basic process $\mathcal{X}$ and the process $(\mathcal{X}, \mathcal{Y})$ defined by (3.27) possess identical structural properties by Theorem 3.3 provided that $f_{min} > 0$, but only $(\mathcal{X}, \mathcal{Y})$ allows us to have correlated events, and non-exponential distributional assumptions on parasitism, a parasitoid death and a host birth. The inequality $f_{min} > 0$ in Theorem 3.3(ii) is a technical condition that guarantees the occurrence of parasitism in the BSDE version from every phase $y \in \{1, ..., L\}$ in the MAP with characteristic matrices $(\lambda_f^{-1}\alpha mn\mathbf{F}_0, \lambda_f^{-1}\alpha mn\mathbf{F}_1)$, irrespective of state $(m,n) \in \mathcal{C}$. It should be noted that the case $f_{min} = 0$ might lead us to inadvisable BSDE versions where the dominance of parasitism – over the death of a parasitoid and the birth of a host – is not eventually preserved as $m+n \to \infty$.

3.7 Comparative analysis among BSDE models

An interesting question concerns the comparative analysis between the basic model and its BSDE version defined by (3.27). We illustrate in this section the preceding theoretical work by carrying out numerical results for various BSDE scenarios, which are defined in terms of the following two choices of Markovian arrival streams with positive and negative correlation:

(i) *MAP with positive correlation (MAP$^+$)*

$$\mathbf{G}_0^+ = \begin{pmatrix} -0.87478 & 0.5 & 0.0 \\ 0.0 & -0.87478 & 0.0 \\ 0.0 & 0.0 & -94.76811 \end{pmatrix},$$

$$\mathbf{G}_1^+ = \begin{pmatrix} 0.08748 & 0.0 & 0.28730 \\ 0.78730 & 0.0 & 0.08748 \\ 7.28985 & 0.0 & 87.47826 \end{pmatrix}.$$

(ii) *MAP with negative correlation (MAP$^-$)*

$$\mathbf{G}_0^- = \begin{pmatrix} -0.87478 & 0.68353 & 0.0 \\ 0.0 & -0.87478 & 0.0 \\ 0.0 & 0.0 & -94.76811 \end{pmatrix},$$

$$\mathbf{G}_1^- = \begin{pmatrix} 0.10377 & 0.0 & 0.08748 \\ 0.08748 & 0.0 & 0.78730 \\ 87.47826 & 0.0 & 7.28985 \end{pmatrix}.$$

These Markovian processes generate correlated arrivals and have respective coefficients of correlation $\rho_{MAP^+}(1) = 0.35016$ and $\rho_{MAP^-}(1) = -0.35016$. Six scenarios, termed *Scenarios I.a*, *I.b*, *II.a*, *II.b*, *III.a* and *III.b*, are defined by replacing a single Poisson stream governing events in the basic process $\mathcal{X}$ (i.e., parasitism, a parasitoid death or a host birth) by a MAP with positive or negative correlation. Table 3.3 summarizes the choices in (3.27) leading us to these six BSDE scenarios; for example, events in Scenario I.a are generated by the superposition of two Poisson processes of rates βm and λn, and a MAP of order $L_f = 3$ with fundamental arrival rate $\lambda_{(m,n)}(1,-1) = \alpha mn$ and characteristic matrices $(\lambda_{MAP^+}^{-1}\alpha mn\mathbf{G}_0^+, \lambda_{MAP^+}^{-1}\alpha mn\mathbf{G}_1^+)$, for every state $(m,n) \in \mathcal{C}$.

In Figures 3.7-3.11, we illustrate the effects of the correlation structure in the underlying Markovian stream on the extinction probabilities, that is, on the mass function of the random variable $X(T)$. Note that, in the basic process, the mass function of $X(T)$ is given by the conditional probabilities $P(X(T) = (m',n')|X(0) = (m,n))$ for states $(m',n') \in \mathcal{C}_0$ and a fixed state $(m,n) \in \mathcal{C}$; for a BSDE version, we first consider a state-independent vector $\boldsymbol{\pi} = (\pi_1, ..., \pi_L)$ of initial phase probabilities, and then evaluate the mass function of $X(T)$ as

Table 3.3. Six BSDE scenarios defined in terms of the matrices $\mathbf{C}_{(m,n)}(z_1, z_2)$ with $(z_1, z_2) \in \{(1,-1),(-1,0),(0,1)\}$

Scenario	$(1,-1)$ – Parasitism	$(-1,0)$ – A parasitoid death	$(0,1)$ – A host birth
I.a	$\lambda_{MAP^+}^{-1}\alpha mn\mathbf{G}_1^+$	$\beta m\mathbf{I}_3$	$\lambda n\mathbf{I}_3$
I.b	$\lambda_{MAP^-}^{-1}\alpha mn\mathbf{G}_1^-$	$\beta m\mathbf{I}_3$	$\lambda n\mathbf{I}_3$
II.a	$\alpha mn\mathbf{I}_3$	$\lambda_{MAP^+}^{-1}\beta m\mathbf{G}_1^+$	$\lambda n\mathbf{I}_3$
II.b	$\alpha mn\mathbf{I}_3$	$\lambda_{MAP^-}^{-1}\beta m\mathbf{G}_1^-$	$\lambda n\mathbf{I}_3$
III.a	$\alpha mn\mathbf{I}_3$	$\beta m\mathbf{I}_3$	$\lambda_{MAP^+}^{-1}\lambda n\mathbf{G}_1^+$
III.b	$\alpha mn\mathbf{I}_3$	$\beta m\mathbf{I}_3$	$\lambda_{MAP^-}^{-1}\lambda n\mathbf{G}_1^-$

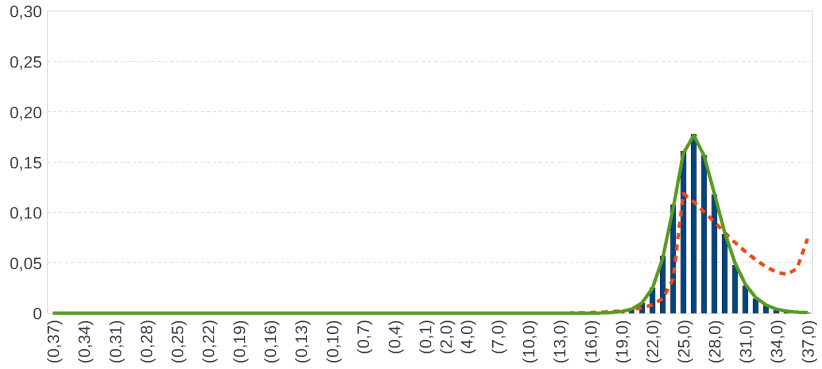

Fig. 3.7. Mass functions of $X(T(K_{0.999}))$ in the basic process (*histogram*) and Scenarios I.a (*broken* line) and I.b (*solid* line). Parameters $(\alpha, \beta, \lambda) = (1.0, 0.5, 3.0)$; initial numbers $(m, n) = (10, 15)$

$$\sum_{y'=1}^{L}\sum_{y=1}^{L} P(X(T) = (m', n'), Y(T) = y' | X(0) = (m, n), Y(0) = y)\pi_y. \tag{3.35}$$

Similarly to Section 3.4 we remark that, in analyzing the extinction time T and the size $X(T)$ of the surviving species, the quadratic term αmn in (3.1) due to parasitism makes the solution intractable from an analytical point of view. Thus, we suggest once again to replace the absorbing Markov chain $\mathcal{X}$ defined on $\mathcal{S} = \mathcal{C}_0 \cup \mathcal{C}$ by an approximating Markov chain $\mathcal{X}(x)$, which is now defined on

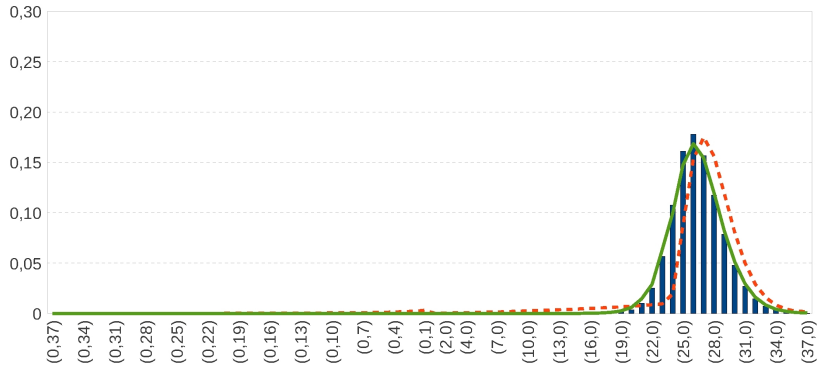

Fig. 3.8. Mass functions of $X(T(K_{0.999}))$ in the basic process (*histogram*) and Scenarios II.a (*broken* line) and II.b (*solid* line). Parameters $(\alpha, \beta, \lambda) = (1.0, 0.5, 3.0)$; initial numbers $(m, n) = (10, 15)$

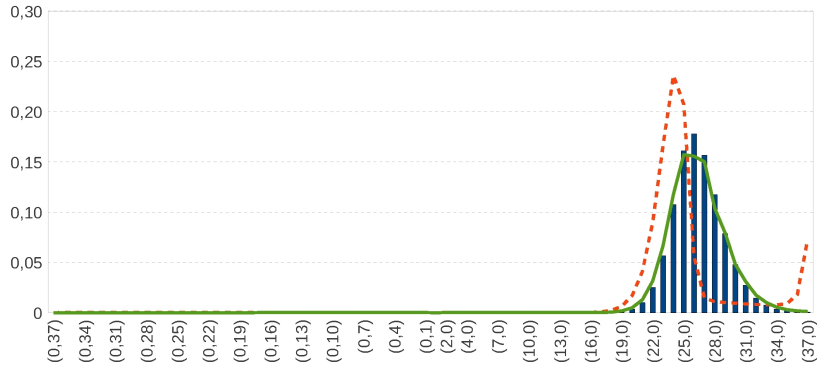

Fig. 3.9. Mass functions of $X(T(K_{0.999}))$ in the basic process (*histogram*) and Scenarios III.a (*broken* line) and III.b (*solid* line). Parameters $(\alpha, \beta, \lambda) = (1.0, 0.5, 3.0)$; initial numbers $(m, n) = (10, 15)$

a finite set $\mathcal{S}(x)$ of states; more concretely, $\mathcal{S}(x)$ consists of the subset $\cup_{k=2}^{x} l(k)$ of transient states and those states in the set $\mathcal{C}_0$ of absorbing states that are accessible from states in $\cup_{k=2}^{x} l(k)$. We choose the level x as the $(100q)$th percentile K_q of the maximum number of individuals (parasitoids or hosts) alive during an extinction cycle. This allows us to observe that the resulting process $\mathcal{X}(K_q)$ governs the dynamics of the basic process $\mathcal{X}$ under the restriction that states of higher levels $\cup_{k=K_q+1}^{\infty} l(k)$ are not accessible.

For a BSDE version, the augmented process is readily replaced by the finite process $(\mathcal{X}(K_q), \mathcal{Y})$.

In Figures 3.7-3.9, we display the mass function of $X(T(K_q))$ in the basic process versus the corresponding mass functions in Scenarios I.a and I.b (Figure 3.7), Scenarios II.a and II.b (Figure 3.8), and Scenarios III.a and III.b (Figure 3.9). Specifically, we consider initial numbers of $m = 10$ parasitoids and $n = 15$ hosts, and per capita rates $\alpha = 1.0$, $\beta = 0.5$ and $\lambda = 3.0$. The value $q = 0.999$ yields the percentile $K_{0.999} = 37$ in the approximating process $\mathcal{X}(K_q)$, and the vector $\boldsymbol{\pi}$ in (3.35) of initial phase probabilities corresponds to the stationary probability vector of the phase process $\mathcal{Y}$. In Figures 3.7-3.9, histograms are related to the basic process $\mathcal{X}$, and broken and solid lines are associated with BSDE versions defined from Markovian streams with positive and negative values, respectively, for the coefficient of correlation. It is observed that the essential characteristics (in particular, shape and magnitudes) of the mass function of the position $X(T(K_q))$ at which the approximating process $\mathcal{X}(K_q)$ first hits the set $\mathcal{C}_0$ of absorbing states appear to be appropriately captured by BSDE versions with negative correlation (i.e., Scenarios I.b, II.b and III.b with $\rho_f(1) = \rho_e(1) = \rho_d(1) = -0.35016$) and, on the contrary, they are notably modified in BSDE versions with positive correlation (i.e., Scenarios I.a, II.a and III.a with $\rho_f(1) = \rho_e(1) = \rho_d(1) = 0.35016$). This dramatically different behavior is closely related to how transitions between phases are generated in the augmented process. To illustrate this assertion we display, in Figures 3.10 and 3.11, the mass functions of $X(T(K_q))$ in the basic model and BSDE versions for Scenarios I.a and I.b; in each figure, broken, solid and dashed lines refer to the BSDE versions with initial phases $y = 1$ (i.e., $\boldsymbol{\pi} = (1, 0, 0)$ in (3.35)), 2 (i.e., $\boldsymbol{\pi} = (0, 1, 0)$), and 3 (i.e., $\boldsymbol{\pi} = (0, 0, 1)$), respectively. To be concrete, the initial phase y in the BSDE versions with negative correlation appears to have a very minor effect on the number of surviving parasitoids, while such a number is strongly influenced by the initial phase in the case of BSDE versions with positive correlation. Figure 3.10 can be seen as an example of how *atypical* mass functions of $X(T(K_q))$ associated with certain initial phases (for example, Scenario I.a with $y = 3$) are appropriately softened by the use of stationary

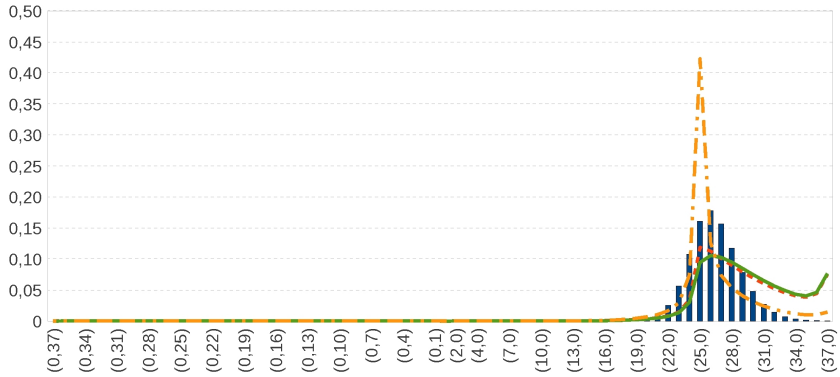

Fig. 3.10. Mass functions of $X(T(K_{0.999}))$ in the basic process (*histogram*) and BSDE versions in Scenario I.a. Parameters $(\alpha, \beta, \lambda) = (1.0, 0.5, 3.0)$; initial numbers $(m, n) = (10, 15)$; initial phases $y = 1$ (*broken* line), 2 (*solid* line), 3 (*dashed* line)

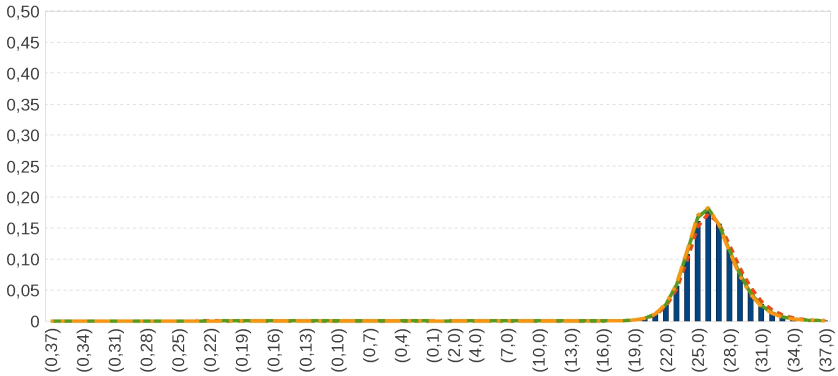

Fig. 3.11. Mass functions of $X(T(K_{0.999}))$ in the basic process (*histogram*) and BSDE versions in Scenario I.b. Parameters $(\alpha, \beta, \lambda) = (1.0, 0.5, 3.0)$; initial numbers $(m, n) = (10, 15)$; initial phases $y = 1$ (*broken* line), 2 (*solid* line), 3 (*dashed* line)

probabilities of the phase process; see Figure 3.7. It is important to observe from Figures 3.7 and 3.9 that, in the BSDE versions, the effect of the removed states $\{(K_{0.999} + 1, 0), (K_{0.999} + 2, 0), ...\}$ on the ecosystem does not appear to be negligible, and thus the finite set $\{(m, 0) : 2 \leq m \leq K_{0.999}\}$ does not represent suitably the subset $l(\cdot, 0)$ of extinction of hosts.

Tables 3.4 and 3.5 list the relative values

$$\left|1 - \frac{\tau_{(m,n)}^{(BSDE)}}{\tau_{(m,n)}}\right| \qquad \text{and} \qquad \left|1 - \frac{M_{(m,n)}^{(BSDE)}}{M_{(m,n)}}\right|,$$

where the expected extinction time $\tau_{(m,n)}$ and the mean number $M_{(m,n)} = E[M(T)|X(0) = (m,n)]$ of remaining parasitoids are related to the basic process. For a BSDE version with vector $\boldsymbol{\pi}$ of initial phase probabilities, $\tau_{(m,n)}^{(BSDE)}$ is given by

$$\tau_{(m,n)}^{(BSDE)} = \sum_{y=1}^{L} \tau_{(m,n,y)} \pi_y, \tag{3.36}$$

and $M_{(m,n)}^{(BSDE)}$ is evaluated as

$$\sum_{y'=1}^{L} \sum_{y=1}^{L} E[M(T); Y(T) = y' | X(0) = (m,n), Y(0) = y] \pi_y. \tag{3.37}$$

Tables 3.4 and 3.5 contain four entries for each scenario: the first entry, denoted by $\boldsymbol{\pi}$, corresponds to the values in (3.36) and (3.37) computed with the stationary probability distribution of the phase process; in the second, third and fourth entries, denoted by $y = 1$, 2 and 3, we select a single initial phase y. We may observe that BSDE versions with negative correlation (i.e., Scenarios I.b, II.b and III.b) essentially yield expected extinction times and expected numbers of remaining parasitoids that are not significantly different from the corresponding mean values in the basic model. Differences in magnitude are more relevant in the case of BSDE versions defined by Markovian arrivals with positive correlation. More particularly, Scenario I.a results in the more significative differences, regardless of distributional assumption on the initial phase.

It is clear that Equation (3.27) is a concrete specification of the family $\mathcal{F}$ of matrices in the construction of BSDE host-parasitoid models. More concretely, the matrices $\mathbf{C}_{(m,n)}(z_1, z_2)$ with $(z_1, z_2) \in \{(1,-1), (-1,0), (0,1)\}$ in (3.27) preserve structural properties of the basic process $\mathcal{X}$ by Theorem 3.3, and contribute to consider non-exponential inter-event times and the existence of correlation between successive events. In our numerical

Table 3.4. Relative values $|1 - \tau^{-1}_{(m,n)}\tau^{(BSDE)}_{(m,n)}|$ for six scenarios and various initial phase conditions

Scenario		*I*	*II*	*III*
a	$\boldsymbol{\pi}$	0.18955	0.03346	0.02108
	$y = 1$	0.18543	0.02332	0.01930
	$y = 2$	0.22767	0.00485	0.01671
	$y = 3$	0.19217	0.72611	0.11330
b	$\boldsymbol{\pi}$	0.00686	0.00111	0.00549
	$y = 1$	0.00620	0.01191	0.00036
	$y = 2$	0.02336	0.01733	0.01191
	$y = 3$	0.02868	0.04623	0.02128

experiments, only exponential distributional assumptions of a single type of marks (z_1, z_2) are effectively generalized by a state-dependent non-Poisson stream; more concretely, $(z_1, z_2) = (1, -1)$ in Scenarios I.a and I.,b; $(-1, 0)$ in Scenarios II.a and II.b; and $(0, 1)$ in Scenarios III.a and III.b. This particular way of generalization may be seen as elementary, but it shows –under simple circumstances– a significant influence of the underlying Markovian stream on the number of remaining parasitoids, and the expected extinction times. The initial numbers $m = 10$ and $n = 15$ are selected meaningfully to emphasize that certain BSDE versions yield noticeably different results from the basic model, even in the case of initial dominance of parasitism on the death of a parasitoid and the birth of a host.

Table 3.5. Relative values $|1 - M^{-1}_{(m,n)}M^{(BSDE)}_{(m,n)}|$ for six scenarios and various initial phase conditions

Scenario		*I*	*II*	*III*
a	$\boldsymbol{\pi}$	0.10949	0.00562	0.03616
	$y = 1$	0.10951	0.00859	0.03752
	$y = 2$	0.11873	0.02765	0.05613
	$y = 3$	0.00505	0.33072	0.23988
b	$\boldsymbol{\pi}$	0.00222	0.00014	0.00111
	$y = 1$	0.00684	0.01314	0.01749
	$y = 2$	0.00360	0.01629	0.01955
	$y = 3$	0.00598	0.01784	0.02670

3.8 Conclusions

Overpopulation in host-parasitoid models has implications for species and habitat conservation. In an attempt to measure the effects of extreme values on a community of parasitoids and hosts, we present in Sections 3.1-3.4 a new probabilistic descriptor, namely the maximum number $Z(t_0)$ of individuals alive during a time interval $[0, t_0]$ with a fixed length $t_0 > 0$. We investigate its application to the host-parasitoid model defined by (3.1), which was first analyzed by Hitchcock [62, Model 1] as a fully stochastic model where the only possible events are birth of a host, death of a parasitoid, and parasitism.

For practical use, a fixed value of t_0 might amount to the epoch of a planned inspection. In a closed community, inspections are frequently scheduled in a periodic manner, and they may mean immigration from outside and slaughtering of a certain subset of remaining individuals, among other possible decisions to guarantee the survival of parasitoids and hosts, and the habitat conservation. Then, the random variable $Z(t_0)$ allows us somehow to estimate in advance those maximum resources that the community of parasitoids and hosts needs from the habitat to have the certain knowledge that it will survive during an inter-inspection interval $[0, t_0]$.

For the host-parasitoid model analyzed by Hitchcock [62, Model 1], we derive in Section 3.1 a matrix exponential form for the probability distribution function of $Z(t_0)$ in a community starting from strictly positive numbers m of parasitoids and n of hosts. The solution in Theorem 3.1 is an exact solution, but it needs to be complemented with algorithmic tools allowing us to compute the exponential of the matrix $\mathbf{T}(x)t_0$ in an accurate and efficient manner. We present in Section 3.2 an approach which is strongly based on splitting methods and the use of eigenvalues and eigenvectors. In terms of Condition (A), we assume simple conditions on the per capita rates α, β and δ of change of population sizes for the resulting matrix exponential to be explicit or amenable to numerical calculation. It is clear that Condition (A) is a technical requirement to guarantee that the eigenvalues in the set $\{r(y; l) : 1 \leq l \leq y - 1 \leq x - 1\}$ are distinct for every $x \geq m + n$, but it can be thought of as sufficiently general to be applied in

actual biological situations. Under Condition (A), the solution is explicitly specified in the special case $\beta = 0$, that is, if the process governing the death of parasitoids is not relevant. A particularly appealing feature of Equation (3.12) is that it allows us to evaluate $\exp\{\mathbf{T}(x)t_0\}$ and, consequently, $P(Z(t_0) \leq x|X(0) = (m, n))$ for each value $x \geq m + n$, in an iterative manner by starting with $\exp\{\mathbf{T}(2)t_0\} = e^{-(\alpha+\lambda)t_0}$.

In the general setting $\beta > 0$, we suggest to approximate the matrix exponential solution, as accurately as possible, by using the Trotter product; see Equation (3.13). Specifically, we first analyze two splitting proposals (i.e., Approximations 1 and 2 with $\mathbf{U}_i(x) + \mathbf{V}_i(x)$, for $i \in \{1, 2\}$) for the underlying matrix $\mathbf{T}(x)$, and we then study practical qualities as each concrete splitting is combined with the spectral norm $||\cdot||_S$ (Criterion I) and the matrix norm $||\cdot||_\infty$ induced by the l_∞ vector norm (Criterion II). The significance of the results reported in Sections 3.3 and 3.4 can be summarized as follows:

(i) The first term $\mathbf{U}_i(x)$, for $i \in \{1, 2\}$, in Approximations 1 and 2 is a block bi-diagonal matrix. Similarly to the case $\beta = 0$, this means that, under Condition (A), the matrix exponential $\exp\{\mathbf{U}_i(x)t\}$ can be iteratively computed by (3.14) and (3.15) starting with $\exp\{\mathbf{U}_i(2)t\} = e^{-(\alpha+\beta+\lambda)t}$.

(ii) The second term $\mathbf{V}_i(x)$, for $i \in \{1, 2\}$, in Approximations 1 and 2 has a single non-null block diagonal, and it is thus nilpotent. As a result, the exponential of the matrix $\mathbf{V}_i(x)t$, for $i \in \{1, 2\}$, has the explicit form (3.16) and (3.17), and it can be readily expressed in terms of the matrix exponential $\exp\{\mathbf{V}_i(x - 1)t\}$. Thus, (3.16) and (3.17) result in iterative schemes for computing $\exp\{\mathbf{V}_i(x)t\}$, regardless of Condition (A).

(iii) Equations (3.14)-(3.17) lead us to the approximation (3.13) for an appropriately selected integer p_0. For a suitable choice of p_0, we suggest the use of the splitting $\mathbf{T}(x) = \mathbf{U}_2(x) + \mathbf{V}_2(x)$ combined with the $||\cdot||_\infty$-norm. More particularly, we derive bounds for the accuracy of our solution when a concrete splitting $\mathbf{T}(x) = \mathbf{U}_i(x) + \mathbf{V}_i(x)$ is combined with the $||\cdot||_S$-norm and the $||\cdot||_\infty$-norm, for $i \in \{1, 2\}$. For both splitting proposals, it is seen that the $||\cdot||_\infty$-norm allows us

to obtain global error control in terms of an arbitrary small value $\varepsilon > 0$; see Equation (3.25).

We specify in Section 3.4 conditions under which the descriptor $Z(t_0)$ is preferred to its extinction-cycle version $Z(T)$. These conditions concern with the length t_0 of the interval and the expected length $\tau_{(m,n)}$ of an extinction cycle, and the number $m+n$ of individuals in the initial community. Our conclusions in Section 3.4 cannot be extrapolated to other host-parasitoid models since they are essentially explained by noting three facts, which are closely related to the model defined by (3.1): (i) the ultimate extinction of either parasitoids or hosts is certain, given initial numbers of m parasitoids and n hosts; (ii) the expected time $\tau_{(m,n)}$ to the first extinction is always finite; and (iii) the mean extinction time $\tau_{(m,n)}$ tends to zero as the combined initial number $m+n$ becomes large. In analyzing the descriptors $Z(t_0)$ and $Z(T)$ in other host-parasitoid models, we stress here that, unlike the random variable $Z(t_0)$ whose distribution is always nondefective, the distribution of $Z(T)$ might be defective (i.e., $P(Z(T) < \infty | X(0) = (m,n)) < 1$) if the ultimate extinction is not certain.

An area of further investigation concerns the use of the descriptor $Z(t_0)$ in other models of host-parasitoid interaction. By the way of example, we comment on the Hitchcock model with immigration and emigration of individuals, that is, a time-homogeneous CTMC $\mathcal{X}$ defined on the state space $\mathbb{N}_0 \times \mathbb{N}_0$ by the following non-null transition rates:

(i) For $(m,n) = (0,0)$,

$$q_{(0,0),(m',n')} = \begin{cases} \lambda', \text{ if } (m',n') = (1,0), \\ \lambda'', \text{ if } (m',n') = (0,1), \end{cases} \tag{3.38}$$

and $q_{(0,0)} = -q_{(0,0),(0,0)} = \lambda' + \lambda''$, where λ' and λ'' are strictly positive constants.

(ii) For $(m,n) = (m,0)$ with $m > 0$,

$$q_{(m,0),(m',n')} = \begin{cases} \beta m + \delta'_{(m,0)}, & \text{if } (m',n') = (m-1,0), \\ \lambda', & \text{if } (m',n') = (m+1,0), \\ \lambda'', & \text{if } (m',n') = (m,1), \end{cases} \tag{3.39}$$

and $q_{(m,0)} = -q_{(m,0),(m,0)} = \beta m + \delta'_{(m,0)} + \lambda' + \lambda''$, where β and $\delta'_{(m,0)}$ are strictly positive for $m > 0$.

(iii) For $(m, n) = (0, n)$ with $n > 0$,

$$q_{(0,n),(m',n')} = \begin{cases} \delta''_{(0,n)}, & \text{if } (m', n') = (0, n-1), \\ \lambda', & \text{if } (m', n') = (1, n), \\ \lambda n + \lambda'', & \text{if } (m', n') = (0, n+1), \end{cases} \tag{3.40}$$

and $q_{(0,n)} = -q_{(0,n),(0,n)} = \delta''_{(0,n)} + \lambda' + \lambda n + \lambda''$, where λ and $\delta''_{(0,n)}$ are strictly positive for $n > 0$.

(iv) For $(m, n) \in \mathbb{N} \times \mathbb{N}$,

$$q_{(m,n),(m',n')} = \begin{cases} \alpha mn, & \text{if } (m', n') = (m+1, n-1), \\ \beta m + \delta'_{(m,n)}, & \text{if } (m', n') = (m-1, n), \\ \delta''_{(m,n)}, & \text{if } (m', n') = (m, n-1), \\ \lambda', & \text{if } (m', n') = (m+1, n), \\ \lambda n + \lambda'', & \text{if } (m', n') = (m, n+1), \end{cases} \tag{3.41}$$

and $q_{(m,n)} = -q_{(m,n),(m,n)} = \alpha mn + \beta m + \delta'_{(m,n)} + \delta''_{(m,n)} + \lambda' + \lambda n + \lambda''$, where α, $\delta'_{(m,n)}$ and $\delta''_{(m,n)}$ are strictly positive for $(m, n) \in \mathbb{N} \times \mathbb{N}$.

Note that, in the terminology of [105], the CTMC $\mathcal{X}$ defined by (3.38)-(3.41) is a competition process of Type II with irreducible infinitesimal generator, and the Hitchcock model defined in (3.1) is a competition process of Type I since all states $(m, 0)$ and $(0, n)$ are absorbing. The random variable $Z(t_0)$ in the host-parasitoid model defined by (3.38)-(3.41) may be appropriately investigated by adapting our methodology. More concretely, since Equations (3.38)-(3.41) define an irreducible quasi-birth-death process (QBD), a slight variant of our arguments in Section 3.1 yields a matrix exponential solution for $P(Z(t_0) \leq x | X(0) = (m, n))$ if $m + n \leq x$, where the resulting matrix $\mathbf{T}(x)$ is a block tri-diagonal matrix. Therefore, we may use splitting methods and eigenvalues/eigenvectors to approximate the matrix exponential solution under certain conditions on the rates of change of population sizes, which should be established for concrete specifications of the emigration rates $\delta'_{(m,n)}$ and $\delta''_{(m,n)}$.

A multivariate version of the competition process (see e.g. [10, Chapter 9] and [67]) is necessary to incorporate other features of the biology of host-parasitoid systems, such as parasite-induced acquired immunity, and mature and larval stages of the parasite. Inspired from the aim of incorporating more realistic assumptions in this kind of models, we analyzed a BSDE approach in Sections 3.5-3.7. In a general setting, its goal in stochastic modeling is the possibility of dealing with events generated by non-exponential correlated flows, but keeping the dimensionality of the underlying Markov chain model tractable. This means that the dimensionality L in the BSDE host-parasitoid model remains constant, while it increases with increasing values of the combined number $m+n$ of parasitoids and hosts in the case of Markov-modulated models based on the replacement of the exponential lifetimes of the individuals by, for example, PH random variables. Recent work on the BSDE approach includes applications to the quasi-stationary distribution [12] and the time to extinction [13] of SIS epidemic models, and the propagation of virus in computer networks [7] by using SIS and SIR epidemic models. An area for further investigation concerns the use of BSDE versions in practice and, more particularly, the development of good fitting methods. Our work in this thesis and references [7, 12, 13] can be thus extended in aspects of inference and identifiability of BSDE processes into the matrix-analytic methods.

Other models of host-parasitoid association may be appropriately investigated by adapting our methodology. We illustrate this comment with the Hitchcock model with immigration and emigration of individuals defined by (3.38)-(3.41). In the BSDE version of this process $\mathcal{X}$, the augmented CTMC $(\mathcal{X}, \mathcal{Y})$ is defined on the state space $\mathcal{S}_{(\mathcal{X},\mathcal{Y})} = \mathcal{S} \times \{1, ..., L\}$, and the basic state (m, n) is updated by using the basic state function $f((m, n), (z_1, z_2)) = (m + z_1, n + z_2)$, where the event pairs (z_1, z_2) depend on the numbers of m parasitoids and n of hosts. Specifically, we have that $(z_1, z_2) \in \{(0, 0), (1, 0), (0, 1)\}$ if $(m, n) = (0, 0)$, $(z_1, z_2) \in \{(0, 0), (-1, 0), (1, 0), (0, 1)\}$ if $(m, n) = (m, 0)$ with $m > 0$, $(z_1, z_2) \in \{(0, 0), (0, -1), (1, 0), (0, 1)\}$ if $(m, n) = (0, n)$ with $n > 0$, and $(z_1, z_2) \in \{(0, 0), (1, -1), (-1, 0), (0, -1), (1, 0), (0, 1)\}$ if $(m, n) \in \mathbb{N} \times \mathbb{N}$. Similarly to the BSDE version of the Hitch-

cock model in Section 3.5, the pairs $(z_1, z_2) = (0, 0)$ and $(1, -1)$ are related to a transition between phases, and parasitism, respectively. On the contrary, $(z_1, z_2) = (-1, 0)$ and $(0, -1)$ amount to emigration or death of a parasitoid, and a host emigration, respectively, and $(z_1, z_2) = (1, 0)$ and $(0, 1)$ are respectively associated with immigration of a parasitoid and of a host.

The infinitesimal generator $\mathbf{Q}^*$ of the augmented CTMC $(\mathcal{X}, \mathcal{Y})$ is readily derived from a family $\mathcal{F}$ of square matrices $\mathbf{C}_{(m,n)}(z_1, z_2)$ for states $(m, n) \in \mathcal{S}$ and the above-mentioned pairs (z_1, z_2). In a similar manner to (3.27), a concrete family $\mathcal{F}$ may be specified by considering five independent MAPs with characteristic matrices $(\mathbf{D}_0, \mathbf{D}_1)$, $(\mathbf{E}_0, \mathbf{E}_1)$, $(\mathbf{F}_0, \mathbf{F}_1)$, $(\mathbf{G}_0, \mathbf{G}_1)$ and $(\mathbf{H}_0, \mathbf{H}_1)$ of respective orders L_d, L_e, L_f, L_g and L_h, and fundamental arrivals rates λ_d, λ_e, λ_f, λ_g and λ_h; for example, as joint phases $y = (y_d, y_e, y_f, y_g, y_h)$ are arranged in lexicographical order, the matrices $\mathbf{C}_{(m,n)}(z_1, z_2)$ for states $(m, n) \in \mathbb{N} \times \mathbb{N}$ may be defined as

$$\mathbf{C}_{(m,n)}(z_1, z_2) = \begin{cases} \lambda_d^{-1}(\lambda n + \lambda'')\mathbf{D}_1 \otimes \mathbf{I}_{L_e L_f L_g L_h}, \\ \qquad\qquad\qquad\qquad \text{if } (z_1, z_2) = (0, 1), \\ \lambda_e^{-1}(\beta m + \delta'_{(m,n)})\mathbf{I}_{L_d} \otimes \mathbf{E}_1 \otimes \mathbf{I}_{L_f L_g L_h}, \\ \qquad\qquad\qquad\qquad \text{if } (z_1, z_2) = (-1, 0), \\ \lambda_f^{-1}\alpha mn\mathbf{I}_{L_d L_e} \otimes \mathbf{F}_1 \otimes \mathbf{I}_{L_g L_h}, \text{ if } (z_1, z_2) = (1, -1), \\ \lambda_g^{-1}\lambda'\mathbf{I}_{L_d L_e L_f} \otimes \mathbf{G}_1 \otimes \mathbf{I}_{L_h}, \quad \text{if } (z_1, z_2) = (1, 0), \\ \lambda_h^{-1}\delta''_{(m,n)}\mathbf{I}_{L_d L_e L_f L_g} \otimes \mathbf{H}_1, \quad \text{if } (z_1, z_2) = (0, -1), \end{cases}$$

and $\mathbf{C}_{(m,n)}(0, 0) = (\lambda_d^{-1}(\lambda n + \lambda'')\mathbf{D}_0) \oplus (\lambda_e^{-1}(\beta m + \delta'_{(m,n)})\mathbf{E}_0) \oplus (\lambda_f^{-1}\alpha mn\mathbf{F}_0) \oplus (\lambda_g^{-1}\lambda'\mathbf{G}_0) \oplus (\lambda_h^{-1}\delta''_{(m,n)})\mathbf{H}_0)$. A slight modification of our description in Section 3.6 leads us to observe that, regardless of the number $L = L_d L_e L_f L_g L_h$ of phases, the fundamental arrival rates of the underlying scaled MAPs are given by

$$\lambda_{(m,n)}(z_1, z_2) = \begin{cases} \alpha mn, & \text{if } (z_1, z_2) = (1, -1), \\ \beta m + \delta'_{(m,n)}, & \text{if } (z_1, z_2) = (-1, 0), \\ \delta''_{(m,n)}, & \text{if } (z_1, z_2) = (0, -1), \\ \lambda', & \text{if } (z_1, z_2) = (1, 0), \\ \lambda n + \lambda'', & \text{if } (z_1, z_2) = (0, 1), \end{cases}$$

for every state $(m, n) \in \mathbb{N} \times \mathbb{N}$. Straightforward algebra allows us to verify the correlation-invariance principle for the five auxiliary

MAPs and their scaled variants. However, other structural properties of $\mathcal{X}$ and $(\mathcal{X}, \mathcal{Y})$, such as regularity, classification of states, and extinction times, should be studied for concrete specifications of the emigration rates $\delta'_{(m,n)}$ and $\delta''_{(m,n)}$.

4

Individual-based Model of Host-parasite Interaction

In the present chapter, our interest is in a stochastic model that incorporates host-macroparasite interactions, for a single host infected by parasites in a seasonal environment. Seasonal conditions in our model are reflected by means of state-dependent nonhomogeneous Poisson processes associated with the acquisition of parasites, the reproduction and death of parasites within the host, and the natural and parasite-induced host mortality.

The chapter is organized as follows. The formal definition of the model is given in Section 4.1, where exact analytical results are derived for the number of parasites acquired by the host up to a certain time instant τ, given a dose-and-move intervention at a certain age τ_0. The key problem in Section 4.2 is to investigate how the host will develop immunity to the parasite population as a result of isolation and vaccination at instant τ_0. We suggest two criteria allowing us to find the time instant τ_0 that appropriately balances efficiency and cost of vaccination. In the spirit of control systems discussed by Barger [21], our approach in Section 4.2 concerns with the role of grazing management in reducing anthelmintic use and improving helminth control. Specifically, we focus on methodological aspects in Section 4.2, and we examine seasonal changes of gastrointestinal (GI) nematode burden in growing lambs in Section 4.3. Moreover, we extend the mathematical model by using splitting methods (Appendix) in order to study other control strategies involving movement to safe pasture (with a low infestation level) or set-stocking, instead of isolation. Finally, concluding remarks are given in Section 4.4.

4.1 Basic mathematical model

We consider a single host that is born, parasite-free, at time $t = 0$ and over its lifetime is exposed to parasites at times that form a nonhomogeneous Poisson process of rate $\lambda(t)$. At an exposure instant, the host acquires a single parasite, independently from one exposure to another. The number of parasites within the host may increase due to parasite reproduction. Let $\lambda_m^*(t)$ be the rate of the underlying nonhomogeneous Poisson process governing parasite reproduction when the number of parasites in the host equals m. Let $\delta(t)$ be the death rate of the host at age t in the absence of any parasite burden, and assume that this rate is increased by an amount $\gamma_m^*(t)$, which is related to the parasite-induced host mortality as there are m parasites within the host. For later use, we introduce the *combined* rates $\lambda_m(t) = \lambda(t) + \lambda_m^*(t)$ and $\delta_m(t) = \delta(t) + \gamma_m(t)$.

At age τ, our interest is in the number $M(\tau)$ of parasites acquired by the host up to time instant τ. For convenience, we first consider (in Sections 4.1 and 4.2) the case in which the host is moved to an *uninfected area* at a certain age $\tau_0 < \tau$, staying there until the end of the time interval $(0, \tau)$. In the uninfected area, the host lives under noninfectious conditions. This means that the host does not acquire new parasites, the reproduction of parasites within the host is stopped, the host undergoes a concrete treatment (vaccination) to decrease the number of parasites acquired up to the *intervention instant* τ_0, and varies in its susceptibility to natural and parasite-induced mortality. As a result, the death rate of the host becomes in $\delta_m(t) = \delta(t) + \gamma_m(t)$ if $t \in [0, \tau_0)$, and $\delta'(t) + \gamma'_m(t)$ if $t \in [\tau_0, \tau]$, and the arrival rate of parasites becomes in $\lambda_m(t) = \lambda(t) + \lambda_m^*(t)$ if $t \in [0, \tau_0)$, and $\lambda'(t) + \lambda_m^{**}(t)$ if $t \in [\tau_0, \tau]$. Let $\eta_m(t)$ be the death rate of parasites when there are m parasites within the host; then, $\eta_m(t) = 0$ if $t \in [0, \tau_0)$, and $\eta'_m(t)$ if $t \in [\tau_0, \tau]$.

The host develops immunity to the parasite infection if it is alive and parasite-free at age τ; in such a case, the host is returned to its original ecosystem. Often biologists and ecologists assume that there is a critical number M_0 of parasites that do not permit the host to develop immunity to the parasite infection, that is, isolation and vaccination are ineffective when the number of parasites

picked up by the host up to age τ_0 is strictly greater than M_0. We make no attempt to incorporate parasite death during the interval $(0, \tau_0)$ in the basic model because we implicitly assume that the age τ is comparatively smaller that the expected lifetime of a parasite within the host. However, we point out that this feature could be easily incorporated to the model by using similar techniques to those in Subsection 4.3.4 and Appendix. We remark that, for practical use, the random variable $M(\tau)$ may be interpreted in a more general manner, such as the *level of infection* at time τ used in our application to GI nematode burden in Section 4.3.

The problem of selecting the age τ_0 became established in the applied veterinary parasitology jargon with the epithet of *evasive* strategy; see the references [22, 51, 52], among others. Evasive strategies can be seen as variations of the dose-and-move procedure devised by Michel [85] for the control of GI nematodes in calves, which relies on removal of a moderate existing infection by chemotherapeutic (anthelmintic) treatment, allied with a movement of the treated host to a safe pasture, just before the population of infective larvae on the original pasture rose to dangerously high concentrations. We refer the reader to [21, Section 2.2] for concrete specifications of evasive strategies under various epidemiological circumstances. In [21, Sections 2.1 and 2.3], the reader may also find complementary information on *preventive* and *diluting* management strategies for control of helminth parasites.

To begin with, we define $\mathcal{Z}$ as the general process $\{M(t) : 0 \leq t < \tau\}$. In this section, we deal with the case of a *free-living* interval $[0, \tau_0)$, in which the host is acquiring parasites, and the *isolated-living* interval $[\tau_0, \tau]$ in which the host has been isolated and vaccinated. We let $\mathcal{X}$ and $\mathcal{Y}$ be the processes $\{M(t) : 0 \leq t < \tau_0\}$ and $\{M(t) : \tau_0 \leq t \leq \tau\}$, respectively, which are both defined on the state space $\{-1\} \cup \mathcal{S}$ with $\mathcal{S} = \{0, 1, ..., M_0\}$; the state $M(t) = -1$ amounts to the host death or a number of parasites acquired up to age t greater than M_0.

For a host that has survived to age t with $t < \tau_0$ and $M(t) = m \in \mathcal{S}$, the possible transitions in the free-living interval are as follows (Figure 4.1):

(i) $m \to m + 1$ at rate $\lambda_m(t)$, for values $m \in \{0, 1, ..., M_0 - 1\}$;
(ii) $m \to -1$ at rate $\delta_m(t)$, for values $m \in \{0, 1, ..., M_0 - 1\}$;

(iii) $M_0 \to -1$ at rate $\delta_{M_0}(t) + \lambda_{M_0}(t)$.

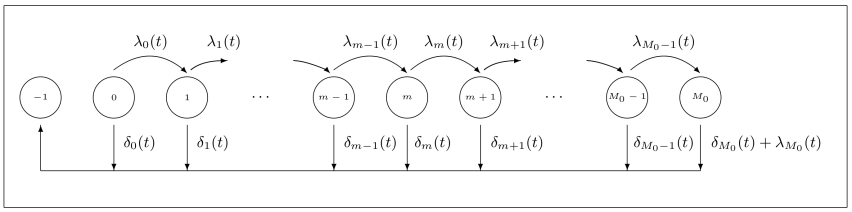

Fig. 4.1. State space and transitions of the process $\mathcal{X}$

In terms of $\pi_m(t) = P(M(t) = m|M(0) = 0)$ for $m \in \{-1\} \cup \mathcal{S}$, the dynamics of the process $\mathcal{X}$ become

$$\frac{d\pi_{-1}(t)}{dt} = \sum_{m=0}^{M_0-1} \delta_m(t)\pi_m(t) + (\delta_{M_0}(t) + \lambda_{M_0}(t))\,\pi_{M_0}(t), \tag{4.1}$$

$$\frac{d\pi_m(t)}{dt} = -\,(\lambda_m(t) + \delta_m(t))\,\pi_m(t) + (1 - \delta_{0,m})\lambda_{m-1}(t)\pi_{m-1}(t), \quad m \in \mathcal{S}, \tag{4.2}$$

for time instants $t < \tau_0$.

Since $\pi_0(0) = 1$ and $\pi_{-1}(t) + \sum_{m=0}^{M_0} \pi_m(t) = 1$, it is readily seen that the solution to (4.1) and (4.2) can be expressed as

$$\pi_{-1}(t) = 1 - \sum_{m=0}^{M_0} R_m(t)e^{-(\Lambda_m(t)+\Delta_m(t))}, \tag{4.3}$$

$$\pi_m(t) = R_m(t)e^{-(\Lambda_m(t)+\Delta_m(t))}, \quad m \in \mathcal{S}, \tag{4.4}$$

where $\Lambda_m(t) = \int_0^t \lambda_m(u)du$ and $\Delta_m(t) = \int_0^t \delta_m(u)du$. The functions $R_m(t)$ are iteratively computed, starting with $R_0(t) = 1$, as

$$R_m(t) = \int_0^t \lambda_{m-1}(u)R_{m-1}(u)e^{\tilde{\Lambda}_m(u)+\tilde{\Delta}_m(u)}du, \quad 1 \le m \le M_0,$$

with $\tilde{\Lambda}_m(t) = \Lambda_m(t) - \Lambda_{m-1}(t)$ and $\tilde{\Delta}_m(t) = \Delta_m(t) - \Delta_{m-1}(t)$.

At age τ_0, the host can be *dead* (i.e., $M(\tau_0) = -1$), *alive and parasite-free* (i.e., $M(\tau_0) = 0$), or *alive and infected* (i.e., $M(\tau_0) = m$ with $m \in \{1, 2, ..., M_0\}$); we recall that the state $M(\tau_0) = -1$

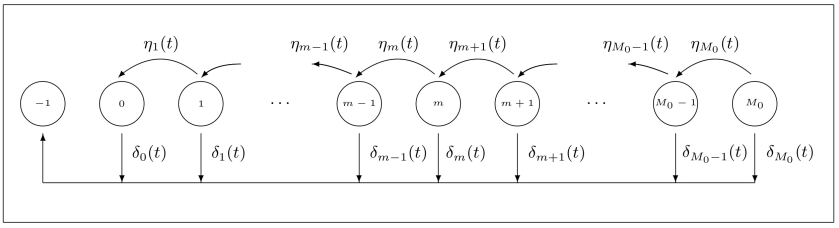

Fig. 4.2. State space and transitions of the process $\mathcal{Y}$

amounts to the physical death of the host or a number of parasites acquired by the host up to the time instant τ_0 that is greater than the number M_0. We assume that the host is alive and infected at age τ_0, and we let $\bar{\boldsymbol{\pi}} = (\bar{\pi}_m : m \in \{1, 2, ..., M_0\})$ be a probability distribution defining the vaccination strategy; for example, in our illustrative examples in Section 4.2, we select $\bar{\boldsymbol{\pi}}$ with entries

$$\bar{\pi}_m = \begin{cases} 0, & \text{if } 1 \le m \le m' - 1, \\ P^{-1}_{\ge m'}(\tau_0)\pi_m(\tau_0), & \text{if } m' \le m \le M_0, \end{cases} \tag{4.5}$$

where $P_{\ge m'}(t) = \sum_{m=m'}^{M_0} \pi_m(t)$ and $m' \in \{1, 2, ..., M_0\}$ is a predetermined threshold. An eventual *intervention* (i.e., isolation and vaccination of the host) is therefore prescribed by a minimum number m' of parasites infecting the host.

For a host that has survived to age t with $\tau_0 < t < \tau$ and $M(t) = m \in \mathcal{S}$, the possible transitions are given by (Figure 4.2)

(i) $m \to m - 1$ at rate $\eta_m(t)$, for values $m = 1, ..., M_0$;
(ii) $m \to -1$ at rate $\delta_m(t)$, for values $m \in \mathcal{S}$.

For a selected strategy $\bar{\boldsymbol{\pi}}$, the dynamics of $\mathcal{Y}$ are described in terms of the probabilities $\pi_m(\tau_0; t) = P_{\bar{\boldsymbol{\pi}}}(M(t) = m)$, for $m \in \{-1\} \cup \mathcal{S}$ and $t \in (\tau_0, \tau]$, and the initial conditions $\pi_{-1}(\tau_0; \tau_0) = \pi_0(\tau_0; \tau_0) = 0$, and $\pi_m(\tau_0; \tau_0) = \bar{\pi}_m$ for $m \in \{1, 2, ..., M_0\}$. It is readily seen that

$$\begin{aligned} \frac{d\pi_{-1}(\tau_0; t)}{dt} &= \sum_{m=0}^{M_0} \delta_m(t)\pi_m(\tau_0; t), \\ \frac{d\pi_m(\tau_0; t)}{dt} &= -\left(\delta_m(t) + (1 - \delta_{0,m})\eta_m(t)\right)\pi_m(\tau_0; t) \\ &\quad + (1 - \delta_{m,M_0})\eta_{m+1}(t)\pi_{m+1}(\tau_0; t), \quad m \in \mathcal{S}. \end{aligned}$$

It is straightforward to derive the following expressions for $\pi_m(\tau_0;t)$ with $m \in \{-1\} \cup \mathcal{S}$ and $t \in (\tau_0, \tau]$:

$$\pi_{-1}(\tau_0;t) = 1 - \sum_{m=0}^{M_0} \pi_m(\tau_0;t), \tag{4.6}$$

$$\pi_m(\tau_0;t) = \Bigg((1-\delta_{m,M_0}) \sum_{j=0}^{M_0-1-m} \pi_{m+1+j}(\tau_0;\tau_0) \tilde{R}^j_{m+1}(\tau_0;t) + (1-\delta_{0,m})\pi_m(\tau_0;\tau_0) \Bigg) e^{-(\Delta_m(\tau_0;t)+H_m(\tau_0;t))}, \quad m \in \mathcal{S}, \tag{4.7}$$

where $\Delta_m(\tau_0;t) = \int_{\tau_0}^t \delta_m(u)du$, $H_m(\tau_0;t) = \int_{\tau_0}^t \eta_m(u)du$ (with $H_0(\tau_0;t) \equiv 0$), $\tilde{\Delta}_m(\tau_0;t) = \Delta_m(\tau_0;t) - \Delta_{m-1}(\tau_0;t)$ and $\tilde{H}_m(\tau_0;t) = H_m(\tau_0;t) - H_{m-1}(\tau_0;t)$. The functions $\tilde{R}^0_m(\tau_0;t)$ are evaluated from

$$\tilde{R}^0_m(\tau_0;t) = \int_{\tau_0}^t \eta_m(u) e^{-(\tilde{\Delta}_m(\tau_0;u)+\tilde{H}_m(\tau_0;u))}du, \quad 1 \le m \le M_0. \tag{4.8}$$

For $1 \le j \le M_0 - m$ and $1 \le m \le M_0 - 1$, the functions $\tilde{R}^j_m(\tau_0;t)$ are specified by

$$\tilde{R}^j_m(\tau_0;t) = \int_{\tau_0}^t \eta_m(u) e^{-(\tilde{\Delta}_m(\tau_0;u)+\tilde{H}_m(\tau_0;u))} \tilde{R}^{j-1}_{m+1}(\tau_0;u)du. \tag{4.9}$$

4.2 Parasite-induced host mortality and disease control

With no control strategy, the impact of the parasite load on the host will often result in significantly high values of the probability $\pi_{-1}(\tau)$ that the host does not survive to age τ, and small values of the probability $\pi_0(\tau)$ that the host is alive and parasite-free. Figure 4.3 illustrates a typical situation for the host-parasite model with critical parasite load $M_0 = 10$, and combined rates $\lambda_m(t) = 20.0\sin^2(4\pi t)$ and $\delta_m(t) = 0.2 + 0.1\cos(2\pi t)$. We may observe in Figure 4.3 that the probability $\pi_0(\tau)$ that the host is alive and parasite-free at age $\tau = 1$ year is negligible, and the probability $\pi_{-1}(\tau)$ that the host does not survive is very significant,

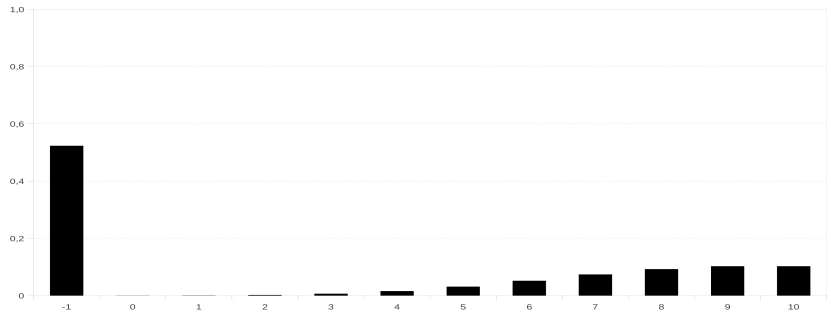

Fig. 4.3. The mass function of $M(\tau)$ for $\tau = 1$ year under the assumption that the host is free living in the interval $[0, \tau]$. Critical parasite load $M_0 = 10$; combined rates $\lambda_m(t) = 20.0 \sin^2(4\pi t)$ and $\delta_m(t) = 0.2 + 0.1 \cos(2\pi t)$

even greater than the host survival probability $\sum_{m=0}^{M_0} \pi_m(\tau)$. This simple model used in Figure 4.3 provides in Subsections 4.2.1 and 4.2.2 a basis for comparisons with results when a control strategy applies and, as a result, the host lives under noninfectious conditions in the interval (τ_0, τ).

In this section, our interest is mainly in methodological aspects, and therefore the age-dependent rates are not linked to empirical patterns; on the contrary, concrete specifications illustrating monthly fluctuations of worm burden of GI nematodes in growing lambs are used in Section 4.3.

In our numerical experiments in Subsections 4.2.1 and 4.2.2, the function of acquisition and reproduction of parasites produces four periods per year of high transmission, whereas there are two peaks per year in mortality coinciding with the beginning and end of an annual cycle. We are particularly inspired by the well-documented article [6], which gives a survey on the mechanisms by which seasonality operates on host-parasite interactions, and how and when parasite control measures should be applied. More concretely, Altizer et al. [6] review how seasonality can be described mathematically and several important dynamical consequences; in [6, Table 1] the reader may find a summary of parasites and pathogens from humans and vertebrate animals for which seasonal drivers generate annual peaks or longer-term variation in incidence, as well as a well-aimed list of related references.

4.2.1 Control strategies

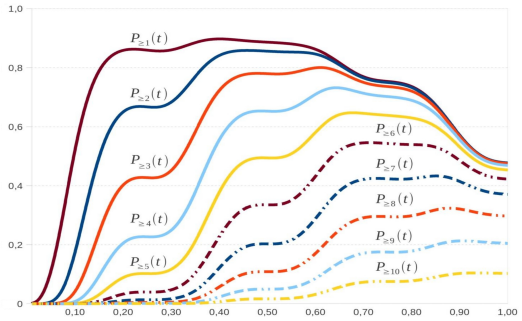

Fig. 4.4. The age-dependent probability $P_{\geq m'}(t)$ as a function of $t \in (0, \tau)$ with $\tau = 1$ year, for numbers $m' \in \{1, 2, ..., M_0\}$. Critical parasite load $M_0 = 10$; combined rates $\lambda_m(t) = 20.0 \sin^2(4\pi t)$ and $\delta_m(t) = 0.2 + 0.1 \cos(2\pi t)$

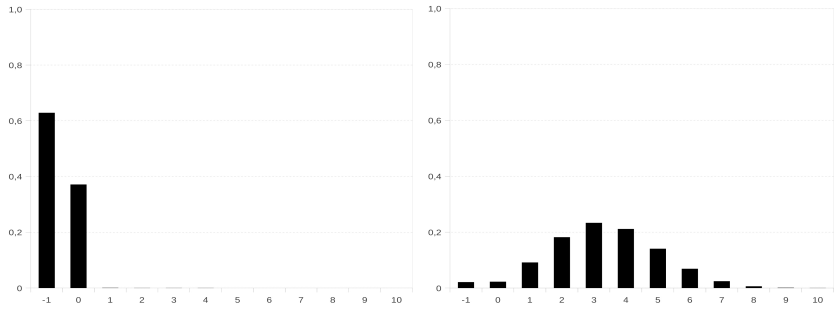

Fig. 4.5. The mass functions of $M(\tau)$ for $\tau = 1$ year under the assumption that the host is transferred to the uninfected area at ages $\tau_0 = \inf\{t : t \in I_{\geq m'}\}$ (*left*) and $\tau_0 = \sup\{t : t \in I_{\geq m'}\}$ (*right*) with $m' = 1$. Critical parasite load $M_0 = 10$; combined rates $\lambda_m(t) = 20.0 \sin^2(4\pi t)$ and $\delta_m(t) = 0.2 + 0.1 \cos(2\pi t)$ during the free-living interval; combined rates $\eta_m(t) = 8.0m$ and $\delta_m(t) = 0.2\tau_0^{-1}t$ during the isolated-living interval

A control strategy is specified by an age τ_0 and a probability vector $\bar{\boldsymbol{\pi}}$ defining the vaccination strategy, which is related to a concrete number $m' \in \{1, 2, ..., M_0\}$ by (4.5). For a suitable selection of τ_0, it is advisable to consider the age-dependent probability $P_{\geq m'}(t)$ and determine the set $I_{\geq m'}$ of *potential* intervention (vac-

cination, in this section) instants $t \in (0, \tau)$ verifying

$$P_{\geq m'}(t) \geq p,$$

for a predetermined probability $p \in (0, 1)$, provided that $I_{\geq m'}$ is nonempty for the number m'. This means that the resulting set $I_{\geq m'}$ depends on p and m', and that, for a fixed pair (m', p), time instants $t \notin I_{\geq m'}$ can be termed *low-risk* vaccination instants and, consequently, they are not considered in subsequent arguments. In Figure 4.4, we display the age-dependent probability $P_{\geq m'}(t)$ versus $m' \in \{1, 2, ..., M_0\}$ for the host-parasite model used in Figure 4.3. As the reader may see, moderate values of p may lead us to various nonempty sets $I_{\geq m'}$; for example, $p = 0.7$ results in nonempty sets for $m' = 1$, 2, 3 and 4. On the contrary, increasing values of p will lead us to empty sets $I_{\geq m'}$ for every number m'; in particular, the selection $p > 0.9$ yields empty sets $I_{\geq m'}$ for every value $m' \in \{1, 2, ..., M_0\}$.

Assume that a fixed pair (m', p) results in the nonempty set $I_{\geq m'}$ of potential vaccination instants. Then, the problem is to find the time instant $\tau_0 \in I_{\geq m'}$ that adequately balances the effectiveness and cost of vaccination. In our approach, effectiveness may be measured in terms of the probability $\pi_0(\tau_0; \tau)$ that the host is alive and parasite-free and, in contrast, we may make the cost of vaccination depend on the probability $\pi_{-1}(\tau_0; \tau)$ that it does not survive at age τ. In Section 4.3 we show how these measures could be effectively generalized by measuring effectiveness and cost of vaccination in terms of the expected proportions of time that, during the interval $(0, \tau)$, the process $\mathcal{Z}$ remains in states 0 and -1, respectively. To motivate ideas for choosing τ_0, we first focus on two crude criteria:

(i) Choose τ_0 as the smallest time instant in $I_{\geq m'}$;
(ii) Choose τ_0 as the highest time instant in $I_{\geq m'}$.

Figure 4.5 compares the choices of τ_0 based on (i) and (ii) for the host-parasite model of Figure 4.3 when the host is moved to the uninfected area at appropriately selected ages τ_0. In Figure 4.5, the vaccination rule is specified by $m' = 1$, and the death rate of parasites and the death rate of the host at time $t \in (\tau_0, \tau)$ are given by $\eta_m(t) = m\eta$ and $\delta_m(t) = \delta\tau_0^{-1}t$, respectively, with $\eta = 8.0$ and

$\delta = 0.2$. As a result, the functions in (4.8) and (4.9) are specified by

$$\tilde{R}^{j}_{m-j}(\tau_0;t) = \binom{m}{j+1}\left(1-e^{-(t-\tau_0)\eta}\right)^{j+1}, \quad 0 \le j \le m-1,$$

since $\tilde{\Delta}_m(\tau_0;t) = 0$ and $\tilde{H}_m(\tau_0;t) = (t-\tau_0)\eta$, for $1 \le m \le M_0$. It is thus assumed that, during the isolated-living interval, each parasite evolves independently of all others, and each present parasite dies at rate η. The rate $\delta_m(t) = \delta\tau_0^{-1}t$ if $t \in [\tau_0, \tau]$ reflects that the parasite load does not affect host death during the isolated-living interval, and the host's natural death rate increases with increasing values of t.

In the choice of τ_0 suggested in (i), there is an emphasis on an early vaccination, which leads us to relevant values for the probability $\pi_0(\tau_0;\tau)$ that the host is alive and parasite-free at age τ at the expense of a significantly high value for the probability $\pi_{-1}(\tau_0;\tau)$ that the host does not survive. Moreover, the probability $1-\pi_{-1}(\tau_0;\tau)-\pi_0(\tau_0;\tau)$ that the host is alive and infected at age τ is negligible. In the choice of τ_0 suggested in (ii), there is an emphasis on a late vaccination, which means that the parasite load at time τ does not essentially differ from the parasite load at time τ_0. It is then observed that smaller values of $\pi_{-1}(\tau_0;\tau)$ are derived at the expense of obtaining small values of $\pi_0(\tau_0;\tau)$, that is, at the expense of maximizing the probability that the host is alive and infected at age τ.

4.2.2 Control criteria and discussion

There are two lines of reasoning that can be taken to provide a balance between the effectiveness and cost of vaccination. They are specified as follows:

Criterion 1. The objective is to minimize the cost of vaccination and to maintain a minimum level of effectiveness. We thus translate the minimum level of effectiveness into a certain probability $p_1 \in (0,1)$, and determine the subset $J^1_{\ge m'}$ of potential vaccination instants $t \in I_{\ge m'}$ satisfying

$$\pi_0(t;\tau) \ge p_1.$$

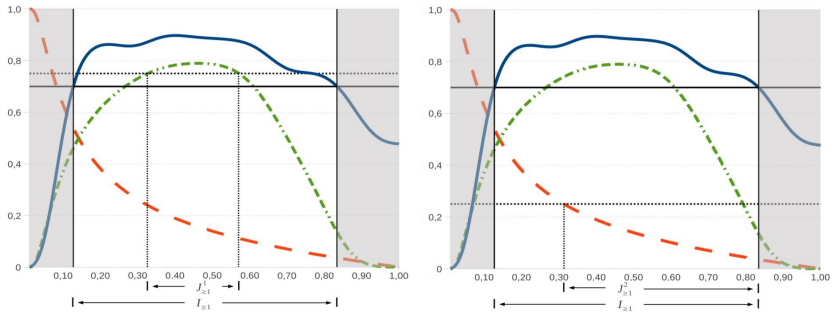

Fig. 4.6. Applying Criterion 1 (*left*) with $p_1 = 0.75$ and Criterion 2 (*right*) with $p_2 = 0.25$ to a host-parasite model with critical parasite load $M_0 = 10$ and vaccination rule specified by $m' = 1$ and $p = 0.7$. *Solid*, *broken* and *dashed* lines correspond to the age-dependent probabilities $P_{\geq m'}(t)$, $\pi_{-1}(t;\tau)$ and $\pi_0(t;\tau)$, respectively, with $\tau = 1$ year

Then, we suggest to choose the vaccination age τ_0 verifying $\pi_{-1}(\tau_0;\tau) = \inf\{\pi_{-1}(t;\tau) : t \in J^1_{\geq m'}\}$.

Criterion 2. The objective is to maximize the effectiveness and to set an upper bound to the cost of vaccination. For a suitably chosen probability $p_2 \in (0,1)$, we first determine the subset $J^2_{\geq m'}$ of time instants $t \in I_{\geq m'}$ verifying

$$\pi_{-1}(t;\tau) \leq p_2,$$

and then select the vaccination age τ_0 such that $\pi_0(\tau_0;\tau) = \sup\{\pi_0(t;\tau) : t \in J^2_{\geq m'}\}$.

One difficulty with both lines of reasoning is that the age τ_0 is chosen according to $\pi_{-1}(t;\tau)$ and $\pi_0(t;\tau)$, which requires inverting (4.6) and (4.7). An analytical formula for τ_0 is not simple, but the solution of this problem is straightforward as concrete specifications for the age-dependent rates $\lambda_m(t)$, $\delta_m(t)$, and $\eta_m(t)$ in $t \in [0,\tau]$ are assumed. We illustrate in Figure 4.6 how Criteria 1 and 2 are applied to the host-parasite model used in Figure 4.5. Solid lines are related to the age-dependent probability $P_{\geq m'}(t)$ with $m' = 1$, and they lead us to a single set $I_{\geq m'}$ of potential vaccination instants in the case $p = 0.7$. Broken and dashed lines correspond to the probabilities $\pi_{-1}(t;\tau)$ and $\pi_0(t;\tau)$, respectively. Such broken and dashed lines lead us to the respective subsets $J^2_{\geq m'}$ and $J^1_{\geq m'}$ by application of Criteria 2 and 1. More concretely,

Criterion 1 (left) yields a concrete subset $J^1_{\geq m'} \subset I_{\geq m'}$ containing every time instant t satisfying $\pi_0(t;\tau) \geq 0.75$. Similarly, Criterion 2 (right) prescribes the subset $J^2_{\geq m'} \subset I_{\geq m'}$ consisting of every time t such that $\pi_{-1}(t;\tau) \leq 0.25$.

Tables 4.1 and 4.2 summarize the set $I_{\geq m'}$ of potential vaccination instants, the subsets $J^1_{\geq m'}$ and $J^2_{\geq m'}$, and the optimal vaccination ages τ_0 derived by applying Criteria 1 and 2 to the host-parasite model used in Figure 4.5 with $p = 0.7$ and $m' \in \{1, 2, 3, 4\}$. Figures 4.7 and 4.8 complement these tables by showing the effects of the resulting ages τ_0 on the parasite load at age $\tau = 1$ year in the cases $m' = 1$ and 4. In Figure 4.7, for every state $m \in \{-1\} \cup \mathcal{S}$ we display six histograms that, from left to right, correspond to the probabilities $\pi_m(\tau)$ (that is, probabilities at time τ whithout any intervention) and $\pi_m(\tau_0;\tau)$ for ages $\tau_0 = 0.46$, 0.48, 0.57, 0.61 and 0.63. Specifically, the values $\tau_0 = 0.57$, 0.61 and 0.63 are derived by applying Criterion 1 with $p_1 \in \{0.75, 0.70, 0.65\}$, and $\tau_0 = 0.46$ and 0.48 are associated with Criterion 2 and $p_2 \in \{0, 25, 0.20, 0.15\}$. In Figure 4.8, for every state $m \in \{-1\} \cup \mathcal{S}$ we plot three histograms that, from left to right, are related to the probabilities $\pi_m(\tau)$ and $\pi_m(\tau_0;\tau)$ for ages $\tau_0 = 0.60$ and 0.62, which are obtained by applying Criteria 2 and 1 with $p_2 \in \{0.25, 0.20, 0.15\}$ and $p_1 = 0.65$, respectively. An examination of Figures 4.7 and 4.8 reveals that, regardless of the number $m' \in \{1, 4\}$, the use of Criteria 1 and 2 is clearly supported by high values of the probability $\pi_0(\tau_0;\tau)$ that the host is alive and parasite-free at age τ, and a noticeable decrease of the probability $\pi_{-1}(\tau_0;\tau)$ that the host does not survive. It is also observed that magnitudes of $\pi_m(\tau_0;\tau)$ become negligible for moderate and large values of the parasite load m.

In any host-parasite model like this, because of the seasonal conditions, a preliminary analysis of the probabilities $\pi_{-1}(\tau_0;\tau)$ and $\pi_0(\tau_0;\tau)$ is frequently required in order to determine concrete values p_1 and p_2 so that Criteria 1 and 2 result in nonempty subsets $J^1_{\geq m'}$ and $J^2_{\geq m'}$, respectively. A graphical representation of $\pi_{-1}(\tau_0;\tau)$ and $\pi_0(\tau_0;\tau)$ can help in measuring allowable values for the minimum level of effectiveness and the maximum cost of vaccination in terms of p_1 and p_2, respectively. For the host-parasite model under consideration, Figure 4.9 shows how $\pi_{-1}(\tau_0;\tau)$ and

Table 4.1. Vaccination instants τ_0 versus m' and p_1 for $p = 0.7$. Criterion 1

m'	p_1	$I_{\geq m'}$	$J^1_{\geq m'}$	τ_0
1	0.75	[0.13,0.83]	[0.33,0.57]	0.57
	0.70	[0.13,0.83]	[0.27,0.61]	0.61
	0.65	[0.13,0.83]	[0.23,0.63]	0.63
2	0.75	[0.32,0.83]	[0.33,0.56]	0.56
	0.70	[0.32,0.83]	[0.32,0.60]	0.60
	0.65	[0.32,0.83]	[0.32,0.63]	0.63
3	0.75	[0.39,0.82]	[0.39,0.56]	0.56
	0.70	[0.39,0.82]	[0.39,0.60]	0.60
	0.65	[0.39,0.82]	[0.39,0.63]	0.63
4	0.75	[0.60,0.76]	—	—
	0.70	[0.60,0.76]	—	—
	0.65	[0.60,0.76]	[0.60,0.62]	0.62

Table 4.2. Vaccination instants τ_0 versus m' and p_2 for $p = 0.7$. Criterion 2

m'	p_2	$I_{\geq m'}$	$J^2_{\geq m'}$	τ_0
1	0.25	[0.13,0.83]	[0.32,0.83]	0.46
	0.20	[0.13,0.83]	[0.39,0.83]	0.46
	0.15	[0.13,0.83]	[0.48,0.83]	0.48
2	0.25	[0.32,0.83]	[0.32,0.83]	0.46
	0.20	[0.32,0.83]	[0.39,0.83]	0.46
	0.15	[0.32,0.83]	[0.48,0.83]	0.48
3	0.25	[0.39,0.82]	[0.39,0.82]	0.45
	0.20	[0.39,0.82]	[0.39,0.82]	0.45
	0.15	[0.39,0.82]	[0.48,0.82]	0.48
4	0.25	[0.60,0.76]	[0.60,0.76]	0.60
	0.20	[0.60,0.76]	[0.60,0.76]	0.60
	0.15	[0.60,0.76]	[0.60,0.76]	0.60

$\pi_0(\tau_0;\tau)$ behave in terms of τ_0 for various choices of the parameters η and δ. Note that it is seen that the probability $\pi_{-1}(\tau_0;\tau)$ that the host does not survive at age τ decreases as the vaccination instant τ_0 increases for every choice of the pair (η,δ) and, for fixed values of δ, such a probability does not depend on the per capita rate η. Our choices of (η,δ) in Figure 4.9 yield graphs for $\pi_0(\tau_0;\tau)$ with similar shapes, but the resulting magnitudes are notably different.

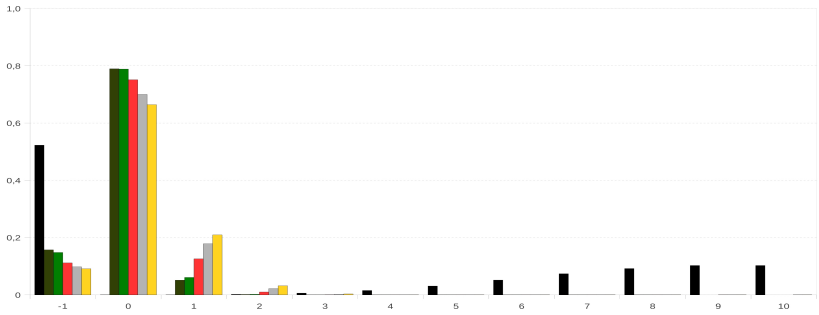

Fig. 4.7. The mass functions of $M(\tau)$ for $\tau = 1$ year when, from left to right, the host is free living up to age τ or, on the contrary, it is transferred to the uninfected area at ages $\tau_0 = 0.46$, 0.48, 0.57, 0.61 and 0.63. Critical parasite load $M_0 = 10$; combined rates $\lambda_m(t) = 20.0\sin^2(4\pi t)$ and $\delta_m(t) = 0.2 + 0.1\cos(2\pi t)$ during the free-living interval; combined rates $\eta_m(t) = 8.0m$ and $\delta_m(t) = 0.2\tau_0^{-1}t$ during the isolated-living interval

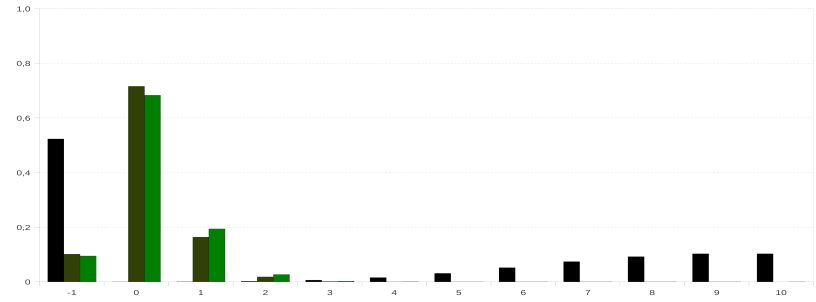

Fig. 4.8. The mass functions of $M(\tau)$ for $\tau = 1$ year when, from left to right, the host is free living up to age τ or, on the contrary, it is transferred to the uninfected area at ages $\tau_0 = 0.60$ and 0.62. Critical parasite load $M_0 = 10$; combined rates $\lambda_m(t) = 20.0\sin^2(4\pi t)$ and $\delta_m(t) = 0.2 + 0.1\cos(2\pi t)$ during the free-living interval; combined rates $\eta_m(t) = 8.0m$ and $\delta_m(t) = 0.2\tau_0^{-1}t$ during the isolated-living interval

4.3 GI nematode burden in growing lambs

In this section, we apply Criteria 1 and 2 to the development of GI parasitism in growing lambs. We consider various grazing management strategies, which are specified in terms of an intervention instant τ_0 that, under certain specifications, implies a movement of animals to uninfected/safe pasture and/or anthelmintic treatment. Our interest is in the parasite *Nematodirus* spp. with *Nematodirus battus*, *Nematodirus filicollis* and *Nematodirus spathiger* as

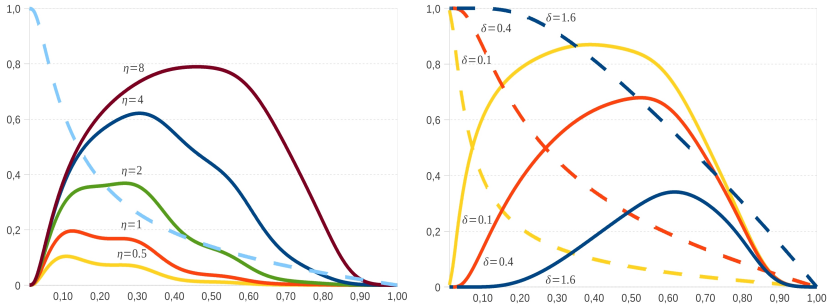

Fig. 4.9. The probabilities $\pi_{-1}(\tau_0;\tau)$ (*broken* lines) and $\pi_0(\tau_0;\tau)$ (*solid* lines) versus η (*left*) with $\delta = 0.2$ and δ (*right*) with $\eta = 8.0$. Critical parasite load $M_0 = 10$; combined rates $\lambda_m(t) = 20.0\sin^2(4\pi t)$ and $\delta_m(t) = 0.2 + 0.1\cos(2\pi t)$ during the free-living interval; combined rates $\eta_m(t) = m\eta$ and $\delta_m(t) = \delta\tau_0^{-1}t$ during the isolated-living interval

main species. Results herein are related to the study conducted by Uriarte et al. [128], which was designed to describe the monthly fluctuations of nematode burden in sheep raised under irrigated conditions in Ebro Valley (Spain) by using worm-free tracer lambs and monitoring the faecal excretion of eggs by ewes. Empirical data in [128] are appropriately combined with those derived in [90] on the clinical efficacy assessment of anthelmintics in lambs parasited with nematode infective larvae.

To begin with, we comment on the life cycle of *Nematodirus* spp., the presence of infective larvae on the small intestine, and aids to diagnosis of GI nematode infection in sheep. Our comments in Subsection 4.3.1 are first used in Subsection 4.3.2 to define the mathematical model, and then to identify age-dependent patterns from empirical data in [90, 128]. In Subsection 4.3.3, we apply Criteria 1 and 2 to the grazing strategy termed TI, which is related to the treatment with anthelmintics and isolation of the host. In Subsection 4.3.4, the mathematical model is extended in such a way that it can be applied for a wide range of strategies, such as UM (the host is left untreated but moved to a paddock with safe pasture), TS (the host is treated with anthelmintics and set-stocked) and TM (the host is treated with anthelmintics and moved to a paddock with safe pasture), as well as other grazing strategies of interest.

4.3.1 Preliminary comments

The nematodes are biologically quite distinct from other helminths, such as the platyhelminthes and acanthocephala. Nematodes are morphologically very similar, sharing a relatively simple body plan with an essentially cylindrical, unsegmented tube. In nematodes, the sexes are separate, and the males are generally smaller that the females, which lay eggs or larvae. During its development, a nematode moults at intervals, shedding its cuticle. More particularly, in the complete life cycle of *Nematodirus* spp. there are four moults, the successive larval stages being designated L_1, L_2, L_3, L_4 and finally L_5, which is the immature adult. Larvae develop to the ensheathed L_3 stage within the egg. The parasitic phase of its life cycle can only commence when the L_3 encounters the host. This is a largely passive process with the grazing animal inadvertently ingesting larvae with herbage as it feeds. The L_3 exhibit a negative geotaxis since they migrate vertically on grass and make themselves more available for passive ingestion of animals. Once in the host, the first step in the transition to the parasitic phase is the completion (ecdysis) of the second moult, which means loss of the retained sheath – exsheathment. Exsheathment is triggered by chemical conditions present in the proximal GI tract of the host. As a result, infection occurs by ingestion of the free-living L_3, with establishment proportions of L_3 in susceptible lambs ranging between 45% and 60%; see e.g. [20, 23, 46]. Moisture levels, temperature and the availability of oxigen are key drivers, affecting not only how quickly eggs hatch and larvae develop, but also how long larvae and eggs survive on pasture. Thus, the occurrence of nematode infections in sheep is inherently connected to diversities of physiographic and climatic conditions; see the references [15, 31, 52, 116, 128, 129], among others. For further details on nematode taxonomy and morphology, and the treatment and control of parasitic gastroenteritis in sheep, we refer the reader to the monographs [121, 123]; the article by Waller and Thamsborg [133] gives a brief overview on non-chemotherapeutic options for parasite control and how they might play a role either in organic farming or in other low-input farming systems.

The adverse effects of GI nematode parasites on productivity are diverse. Parasitism affects both feed intake and feed utilization,

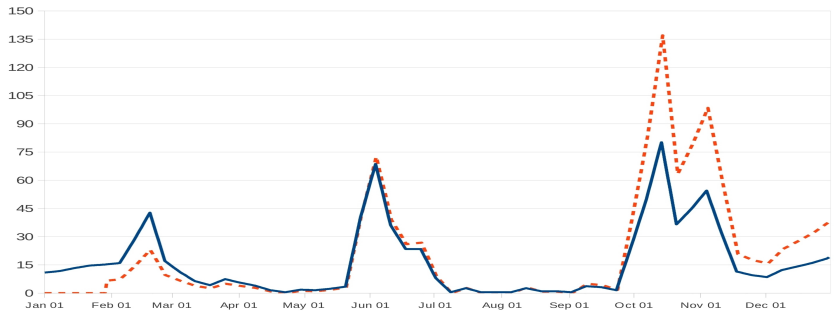

Fig. 4.10. Numbers of L_3 infective larvae on pasture (*solid* line), and increments in the number of L_3 infective larvae on the small intestine (*broken* line). Establishment proportion: 55%. Parasite: *Nematodirus* spp.

and its major impact is therefore on growing rates. Reductions of liveweight gain in growing stock have been recorded as being as high as $60\% - 100\%$. The impact of nematode parasitism can extend beyond interference in musculoskeletal growth since the production of wool and milk and reproductive performance may also be affected. Anthelmintics are drugs which are effective in removing existing burdens or which prevent establishment of ingested L_3. Despite the impact of helminths in veterinary medicine, there have been very few successful, broad-spectrum anthelmintic families discovered and commercialized for use in grazing livestock in the last five decades. The primary reason behind this lack of success in developing novel active families appears to be economic. The success of *ivermectin* and related compounds also appeared to make the development of any other compounds unnecessary.

Our starting point is the set of data in [128, Figure 2] recording the number of L_3 infective larvae on herbage samples at weekly intervals from a fixed paddock of the farm. Results are expressed as infective larvae per kilogram of dry matter (L_3 kg^{-1} DM) after drying the herbage overnight at 60^o C. The numbers of L_3 infective larvae on herbage samples in [128, Figure 2] correspond to *Chabertia ovina* and *Haemonchus* spp. (9.6%), *Nematodirus* spp. (4.0%), *Ostertagia* spp. (71.4%), and *Trichostrongylus* spp. (15.0%). The variation of L_3 infective larvae on herbage over time (Figure 4.10, solid line) shows three periods of maximum pasture contamination, with 42.0 L_3 kg^{-1} DM (by mid-February), 68.0 L_3

kg^{-1} DM (by June 2) and 80.0 L_3 kg^{-1} DM (between October and November) as maximum values. Then, the increments in the number of L_3 infective larvae on the small intestine (Figure 4.10, broken line) are estimated by fixing the establishment proportion and incorporating specifications for the lamb growth pre-weaning and post-weaning. In our examples, the establishment proportion equals 55%, and we consider a lamb that is born on January 1 (i.e., day 0 in our tables); otherwise, we should handle the set of data in [128] starting from the day on which the lamb were born. It is assumed that the lamb birth weight equals 5 kg, the pre-weaning period consists of four weeks, and the lamb growth rate from birth to weaning is given by 0.3 kg per day. The lamb growth rate on pasture post-weaning is assumed to be equal to 0.15 kg per day, and the daily DM intake amounts to the 6% of body weight (BW). Details on lamb growth rates on pasture may be found, for example, in [56].

It should be pointed out that the efficacy of anthelmintics against GI nematodes of sheep is commonly measured in terms of the reduction in faecal eggs per gram (EPG) percentages pre-treatment and post-treatment; see e.g. [123, Chapter 15]. The presence of nematode eggs in faeces is a useful aid to laboratory diagnosis of worm infections as they can be identified and counted in faecal samples. In the faecal egg count (FEC) reduction test, animals are allocated to groups of ten based on pre-treatment FEC, with one group of ten for each anthelmintic treatment tested and a further untreated control group. This requires, for instance, the use of forty animals in [90], where efficacy of three anthelmintics (*ivermectin*, *fenbendazole* and *albendazole*) against GI nematodes is investigated. Each animal is periodically sampled for FEC, and bulk samples of faeces are cultured for larval differentiation. A full FEC reduction test is understandably expensive and takes a significant length of time before farmers are presented with the results, and accurate larval differentiation also demands a high degree of skill. A *points system* (see [2]) serves as a crude guide to interpreting worm counts, which is based on the fact that *1 point* is equivalent to the presence of 4000 worms, a total of *2 points* in a young sheep is likely to be causing measurable losses of productivity, and clinical signs and deaths are unlikely unless the total

exceeds *3 points*. In Table 4.3, we establish the equivalence used in our examples in the identification of degree of infestation, infection level, EPG value, number of L_3 infective larvae on small intestine, and the use of the points system; further details can be found in [2, 123].

Table 4.3. Degree of infestation, infection level, number of L_3 infective larvae on small intestine and EPG value. A guide to interpretation for *Nematodirus* spp.

Degree of infestation	Level of infection (m)	Points system	No. of L_3 infective larvae on small intestine	EPG value
Null	0	0	$[0, 1000)$	$[0, 50)$
Light	1	0	$[1000, 2000)$	$[50, 100)$
Light	2	0	$[2000, 3000)$	$[100, 150)$
Light	3	0	$[3000, 4000)$	$[150, 200)$
Moderate	4	1	$[4000, 5000)$	$[200, 250)$
Moderate	5	1	$[5000, 6000)$	$[250, 300)$
Moderate	6	1	$[6000, 7000)$	$[300, 350)$
Moderate	7	1	$[7000, 8000)$	$[350, 400)$
High	8	2	$[8000, 9000)$	$[400, 450)$
High	9	2	$[9000, 10000)$	$[450, 500)$
High	10	2	$[10000, 11000)$	$[500, 550)$
High	11	2	$[11000, 12000)$	$[550, 600)$
Heavy	-1	$\{3, 4, ...\}$	$[12000, \infty)$	$[600, \infty)$

4.3.2 Identifying age-dependent patterns

We construct the mathematical model in terms of *levels of infection*. Thus, we let the random variable $M(t)$ record the infection level at time t. This means that, by Table 4.3, the degree of infestation is *null* if $M(t) = 0$, *light* if $M(t) = m$ with $m \in \{1, 2, 3\}$, *moderate* if $M(t) = m$ with $m \in \{4, 5, 6, 7\}$, *high* if $M(t) = m$ with $m \in \{8, 9, 10, 11\}$, and *heavy* if $M(t) = -1$; see e.g. [2, 123]. In the setting of GI nematode parasitism, the value $M_0 = 11$ amounts to a critical level that does not permit the host to develop immunity to the nematode infection, in such a way that an eventual intervention is assumed to be ineffective as the degree of infestation is heavy. Therefore, we let $M(t) = -1$ be equivalent to the degree heavy of infestation or the death of the host. Let $\mathcal{S}$ denote the set of infection levels $\{0, 1, ..., M_0\}$.

It is assumed that the number of acquired parasites does not allow the level $M(t)$ of infection to increase more than one unit at any acquisition instant, which is a plausible assumption in our examples where increments in the number of L_3 infective larvae on the small intestine are registered at daily intervals. Owing to infective larvae cannot reproduce directly within the host, it is assumed that $\lambda_m^*(t) = 0$ for every level $m \in \{-1\} \cup \mathcal{S}$. As a result, we have that $\lambda_m(t) = \lambda(t)$ for $t \in [0, \tau_0)$, where $\lambda(t)$ is derived from Figure 4.10 (broken line) and Table 4.3 by translating increments in the number of L_3 infective larvae into levels of infection. To be concrete, we first specify the value $\lambda(n)$ at the nth day as

$$\frac{p(n) \times i(n) \times pr}{l},$$

where $p(n)$ is the number of L_3 infective larvae of *Nematodirus* spp. on pasture, $i(n)$ is the DM intake at the nth day (i.e., 6% of BW), pr is the establishment proportion (i.e., $pr = 0.55$), and l is the interval length used in Table 4.3 to define infection levels m in terms of numbers of infective larvae on the small intestine; i.e., $l = 1000$ for $m \in \mathcal{S}$. The age-dependent rate $\lambda(t)$ is then defined to be the piecewise linear function formed by connecting the points $(n, \lambda(n))$ in order, by line segments.

A reasonable assumption for the death rates of parasites in $[\tau_0, \tau]$ is given by

$$\eta_m(t) = m\eta(t), \tag{4.10}$$

for infection levels m ranging between 1 and $M_0 = 11$, where $\eta(t)$ reflects the therapeutic efficacy of a concrete anthelmintic over time. We use in Subsections 4.3.3 and 4.3.4 empirical data of [90], where the efficacy of three anthelmintics against GI nematodes is investigated. More concretely, forty weaner sheep having naturally acquired infestation of GI nematodes were selected for the study in [90], and randomly divided into four groups termed A, B, C and D, of ten animals each. Animals of groups B, C and D were orally administered *ivermectin* (0.2 mg kg^{-1} BW), *fenbendazole* (5.0 mg kg^{-1} BW) and *albendazole* (7.5 mg kg^{-1} BW), respectively, and animals of group A served as control. Faecal samples were collected from each animal at day 0 immediately before administering the

drug, and thereafter on day 3, 7, 14, 21 and 28 (post-treatment), and EPG values of samples were appropriately determined.

In our approach, the vaccination instant τ_0 corresponds to the day 0 in [90] and, for a concrete anthelmintic treatment (termed B, C and D), the underlying age-dependent function $\eta(t)$ in (4.10) is defined as the polyline connecting the points $(\tau_n, \eta(\tau_n))$ where instants τ_n are given by τ_0, $\tau_1 = \tau_0 + 3$, $\tau_2 = \tau_0 + 7$, $\tau_3 = \tau_0 + 14$, $\tau_4 = \tau_0 + 21$ and $\tau_5 = \tau_0 + 28$. Values $\eta(\tau_n)$ with $n \in \{0, ..., 4\}$ are derived from [90, Table 1] as

$$\frac{p'(\tau_n)}{lev(\tau_n)(\tau_{n+1} - \tau_n)l'} \left(1 + \frac{p'_A(\tau_{n+1}) - p'_A(\tau_n)}{p'_A(\tau_n)} - \frac{p'(\tau_{n+1})}{l'}\right), \tag{4.11}$$

where $p'(t)$ and $lev(t)$ record the EPG value and the infection level at time t, respectively, and l' is the interval length used in Table 4.3 to define levels of infection in terms of EPG values. Since $l' = 50$ for levels $m \in \mathcal{S}$, $lev(\tau_n)$ is given by $[(l')^{-1}p'(\tau_n)]$. Note that EPG values in group A, denoted by $p'_A(\cdot)$ in (4.11), allow us to estimate the effect of larvae established on the small intestine in the interval $(\tau_n, \tau_{n+1}]$. In order to reflect the end of the therapeutic period, it is assumed that $\eta(t) = 0$ if $t \geq \tau_5$. As the reader may readily verify, the functions $\tilde{R}^j_m(\tau_0; t)$ in (4.8) and (4.9) can be evaluated from

$$\tilde{R}^j_{m-j}(\tau_0; t) = \binom{m}{j+1} \left(1 - e^{-H(\tau_0;t)}\right)^{j+1},$$

where $H(\tau_0; t) = \int_{\tau_0}^{t} \eta(u)du$. Values for $H(\tau_0; t)$, which are related to the area under the polyline, can be computed as a function of the length $t - \tau_0$.

We conclude the model construction with the selection $\delta_m(t) = \delta(t) = \delta'(t)$, for every $m \in \mathcal{S}$. In accordance to the points system (Table 4.3), this implies that the parasite-induced death of the host is negligible, except as the total exceeds 3 points (i.e., $m = -1$). In our examples, it is assumed that $\delta(t) = \delta'(t) = e^{-10.0t}$, from which it follows that the probability that, in absence of any parasite burden, the host dies in the interval $[0, \tau]$ with $\tau = 1$ year equals 9.5162%. Thus, the conditional probability that the host death occurs within the first 24 hours, given that it dies in the interval $[0, \tau]$, equals 99.9995%.

4.3.3 Grazing strategy TI

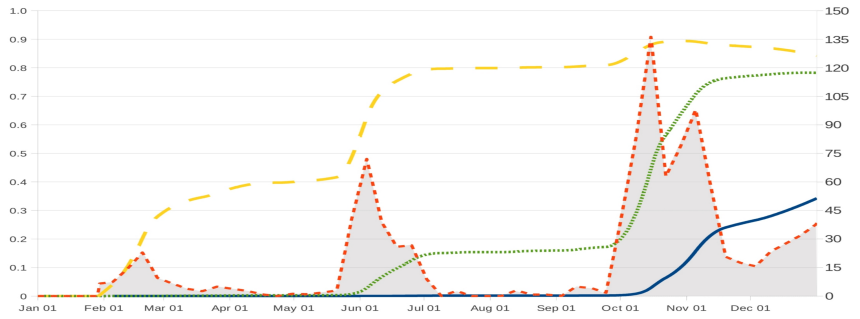

Fig. 4.11. The age-dependent probability $P_{\geq m'}(t)$ as a function of t for $m' = 1$ (*broken* line), 4 (*dotted* line) and 8 (*solid* line), and increments in the number of L_3 infective larvae on the small intestine (*shaded* area, *right* vertical axis). Parasite: *Nematodirus* spp.

To begin with, we define the grazing strategy TI in the following manner:

Strategy TI: *The host is treated with anthelmintics and isolated (that is, moved to an uninfected area) at age* τ_0. The resulting process $\mathcal{Z}$ can be thought of as an age-dependent pure birth process with killing in $[0, \tau_0)$ with rates $\lambda_m(t) = \lambda(t) + \lambda^*_m(t)$ and $\delta_m(t) = \delta(t) + \gamma_m(t)$, and an age-dependent pure death process with killing in $[\tau_0, \tau]$ with rates $\eta_m(t) = \eta'_m(t)$ and $\delta_m(t) = \delta'(t) + \gamma'_m(t)$. In particular, for the sets of empirical data in [90, 128], we have $\lambda^*_m(t) = 0$, $\gamma_m(t) = 0$, $\gamma'_m(t) = 0$, and $\delta(t) = \delta'(t)$.

Let $\pi^{TI}_m(t)$ and $\pi^{TI}_m(\tau_0; t)$ be the probabilities derived from Equations (4.3) and (4.4) for $t \in [0, \tau_0)$, and (4.6) and (4.7) for $t \in [\tau_0, \tau]$, respectively, by using the age-dependent rates $\lambda(t)$ and $\eta(t)$, related to [90, 128], and $\delta(t) = e^{-10.0t}$. In applying Criteria 1 and 2 to the resulting model, we first determine the set $I_{\geq m'}$ of potential vaccination instants with $m' = 4$ (i.e., measurable presence of worms in accordance to the points system) and a predetermined probability $p \in (0, 1)$. We may note that, by Figure 4.11, only values of p ranging between 0 and $P_{\geq 4}(\tau)$ lead us to non-empty sets $I_{\geq 4}$, since $P_{\geq 4}(t)$ appears to be a non-decreasing

Table 4.4. Vaccination instants τ_0 versus p and p_1 for $m' = 4$. Anthelmintic treatments B, C and D. Application of Criterion 1 with $\pi_{-1}^{TI}(t;\tau)$ (*cost of vaccination)* and $\sum_{m=0}^{3}\pi_m^{TI}(t;\tau)$ (*effectiveness*). Parasite: *Nematodirus* spp.

p	$I_{\geq 4}$	p_1	$J_{\geq 4}^{1,B}$	τ_0^B	$J_{\geq 4}^{1,C}$	τ_0^C	$J_{\geq 4}^{1,D}$	τ_0^D
0.1	[170,365)	0.75	[170,295]	170	[170,317]	170	[170,311]	170
		0.70	[170,303]	170	[170,340]	170	[170,330]	170
		0.65	[170,308]	170	[170,343]	170	[170,341]	170
0.2	[274,365)	0.75	[274,295]	274	[274,317]	274	[274,311]	274
		0.70	[274,303]	274	[274,340]	274	[274,330]	274
		0.65	[274,308]	274	[274,343]	274	[274,341]	274
0.3	[281,365)	0.75	[281,295]	281	[281,317]	281	[281,311]	281
		0.70	[281,303]	281	[281,340]	281	[281,330]	281
		0.65	[281,308]	281	[281,343]	281	[281,341]	281
0.4	[286,365)	0.75	[286,295]	286	[286,317]	286	[286,311]	286
		0.70	[286,303]	286	[286,340]	286	[286,330]	286
		0.65	[286,308]	286	[286,343]	286	[286,341]	286
0.5	[290,365)	0.75	[290,295]	290	[290,317]	290	[290,311]	290
		0.70	[290,303]	290	[290,340]	290	[290,330]	290
		0.65	[290,308]	290	[290,343]	290	[290,341]	290
0.6	[298,365)	0.75	—	—	[298,317]	298	[298,311]	298
		0.70	[298,303]	298	[298,340]	298	[298,330]	298
		0.65	[298,308]	298	[298,343]	298	[298,341]	298
0.7	[308,365)	0.75	—	—	[308,317]	308	[308,311]	308
		0.70	—	—	[308,340]	308	[308,330]	308
		0.65	[308,308]	308	[308,343]	308	[308,341]	308

function of $t \in (0, \tau)$. Thus, we next determine sets $I_{\geq 4}$ for values $p \in \{0.1, 0.2, ..., 0.7\}$, and apply Criteria 1 and 2 with probabilities $p_1 \in \{0.65, 0.7, 0.75\}$ and $p_2 \in \{0.15, 0.2, 0.25\}$, respectively. In Figure 4.11, we also consider values $m' = 1$ (i.e., the host is alive, but infected), and 8 (i.e., the degree of infestation is high or heavy); note that, for example, $p = 0.4$ yields the empty set $I_{\geq m'}$ as $m' = 8$.

Values of τ_0 are listed in Tables 4.4 and 4.5 for the anthelmintic treatments B, C and D, and are denoted by τ_0^B, τ_0^C and τ_0^D. The effectiveness and cost of vaccination in these tables are measured in terms of $\sum_{m=0}^{3}\pi_m^{TI}(t;\tau)$ (i.e., the degree of infestation is null or light) and $\pi_{-1}^{TI}(t;\tau)$ (i.e., the degree of infestation is heavy), respectively. An examination of the resulting instants τ_0 reveals three important observations: (i) for every anthelmintic treatment and fixed value p, Criteria 1 and 2

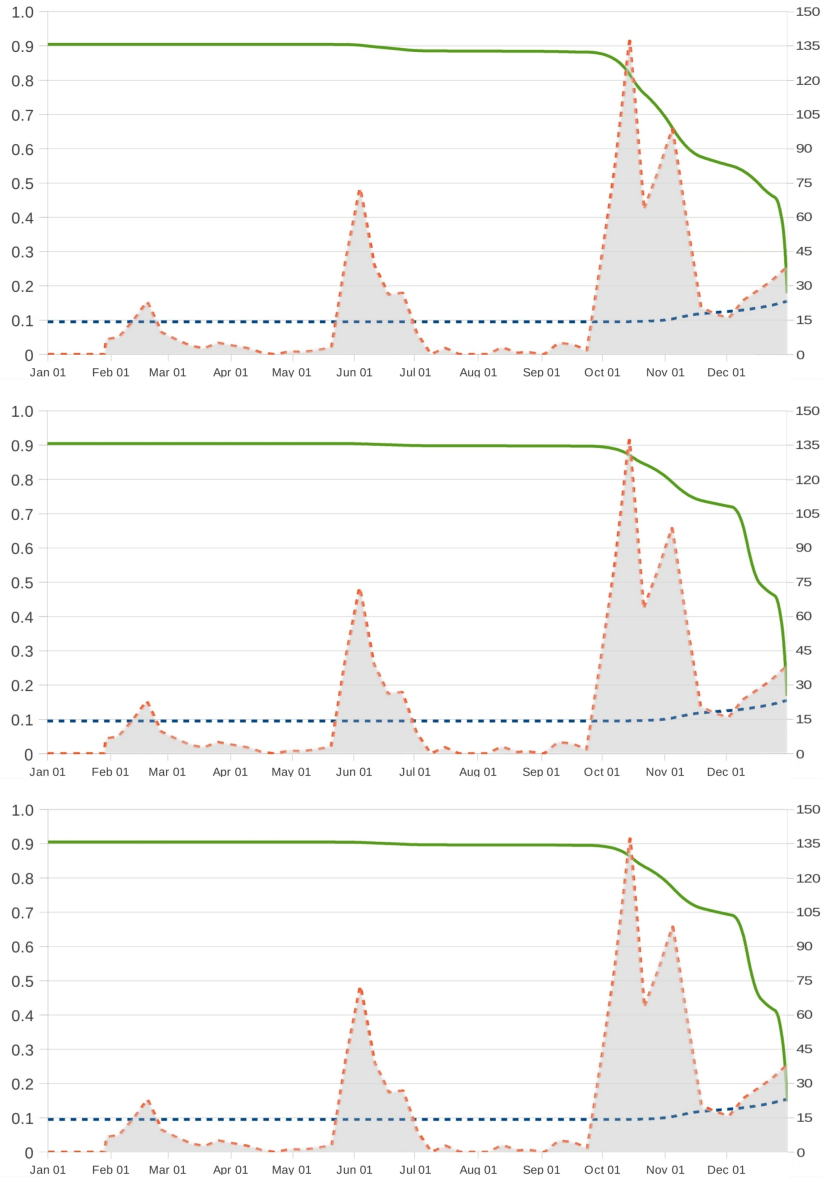

Fig. 4.12. The age-dependent probabilities $\pi_{-1}^{TI}(\tau_0;\tau)$ (*broken* line) and $\sum_{m=0}^{3}\pi_m^{TI}(\tau_0;\tau)$ (*solid* line) versus the vaccination instant τ_0 for $\tau = 1$ year, and increments in the number of L_3 infective larvae on the small intestine (*shaded* area, *right* vertical axis). Anthelmintic treatments B, C and D (*from top to bottom*). Parasite: *Nematodirus* spp.

Table 4.5. Vaccination instants τ_0 versus p and p_2 for $m' = 4$. Anthelmintic treatments B, C and D. Application of Criterion 2 with $\pi_{-1}^{TI}(t;\tau)$ (*cost of vaccination*) and $\sum_{m=0}^{3}\pi_m^{TI}(t;\tau)$ (*effectiveness*). Parasite: *Nematodirus* spp.

p	$I_{\geq 4}$	p_2	$J_{\geq 4}^{2,B}$	τ_0^B	$J_{\geq 4}^{2,C}$	τ_0^C	$J_{\geq 4}^{2,D}$	τ_0^D
0.1	[170,365)	0.25	[170,365)	170	[170,365)	170	[170,365)	170
		0.20	[170,365)	170	[170,365)	170	[170,365)	170
		0.15	[170,360]	170	[170,360]	170	[170,360]	170
0.2	[274,365)	0.25	[274,365)	274	[274,365)	274	[274,365)	274
		0.20	[274,365)	274	[274,365)	274	[274,365)	274
		0.15	[274,360]	274	[274,360]	274	[274,360]	274
0.3	[281,365)	0.25	[281,365)	281	[281,365)	281	[281,365)	281
		0.20	[281,365)	281	[281,365)	281	[281,365)	281
		0.15	[281,360]	281	[281,360]	281	[281,360]	281
0.4	[286,365)	0.25	[286,365)	286	[286,365)	286	[286,365)	286
		0.20	[286,365)	286	[286,365)	286	[286,365)	286
		0.15	[286,360]	286	[286,360]	286	[286,360]	286
0.5	[290,365)	0.25	[290,365)	290	[290,365)	290	[290,365)	290
		0.20	[290,365)	290	[290,365)	290	[290,365)	290
		0.15	[290,360]	290	[290,360]	290	[290,360]	290
0.6	[298,365)	0.25	[298,365)	298	[298,365)	298	[298,365)	298
		0.20	[298,365)	298	[298,365)	298	[298,365)	298
		0.15	[298,360]	298	[298,360]	298	[298,360]	298
0.7	[308,365)	0.25	[308,365)	308	[308,365)	308	[308,365)	308
		0.20	[308,365)	308	[308,365)	308	[308,365)	308
		0.15	[308,360]	308	[308,360]	308	[308,360]	308

yield identical vaccination instants with the exception of the pairs $(p, p_1) \in \{(0.6, 0.75), (0.7, 0.7), (0.7, 0.75)\}$ for treatment B; (ii) for every anthelmintic treatment, the vaccination instant τ_0 increases with increasing values of p, regardless of the control criterion; and (iii) in applying Criterion 1 (respectively, Criterion 2), values of $p_1 \in \{0.65, 0.7, 0.75\}$ (respectively, $p_2 \in \{0.15, 0.2, 0.25\}$) result in identical vaccination instants τ_0, irrespectively of the anthelmintic treatment. These consequences can be easily explained from the monotone behaviors of the age-dependent probabilities $\pi_{-1}^{TI}(\tau_0;\tau)$ and $\sum_{m=0}^{3}\pi_m^{TI}(\tau_0;\tau)$ shown in Figure 4.12. On the one hand, it is shown in Figure 4.12 that the probability $\pi_{-1}^{TI}(\tau_0;\tau)$ appears to behave as a constant function for vaccination instants τ_0 ranging between 0 and 300 (October 28), and it becomes an increasing function for instants τ_0 ranging between 300 and 365. On the other hand, it is seen that the probability $\sum_{m=0}^{3}\pi_m^{TI}(\tau_0;\tau)$ essen-

Table 4.6. Values of $\pi_{-1}^{TI}(\tau_0;\tau)$ and $\sum_{m=0}^{3}\pi_m^{TI}(\tau_0;\tau)$. Anthelmintic treatments B, C and D. Parasite: *Nematodirus* spp.

τ_0	Treatment	$\pi_{-1}^{TI}(\tau_0;\tau)$	$\sum_{m=0}^{3}\pi_m^{TI}(\tau_0;\tau)$
170	B	0.09516	0.89296
	C	0.09516	0.90104
	D	0.09516	0.89999
274	B	0.09517	0.87534
	C	0.09517	0.89480
	D	0.09517	0.89218
281	B	0.09521	0.85437
	C	0.09521	0.88681
	D	0.09521	0.88230
286	B	0.09540	0.82248
	C	0.09540	0.87372
	D	0.09540	0.86636
290	B	0.09592	0.78717
	C	0.09592	0.85808
	D	0.09592	0.84758
298	B	0.09763	0.73694
	C	0.09763	0.83380
	D	0.09763	0.81895
308	B	0.10415	0.65801
	C	0.10415	0.79063
	D	0.10415	0.76935

tially behaves as a constant function within the interval $(0, 275)$, with only a small decrease at day 175 (June 25). The variability of $\sum_{m=0}^{3}\pi_m^{TI}(\tau_0;\tau)$ is very significant for instants τ_0 ranging between 275 and 365, which is closely related to the occurrence of maximum increments in the number of L_3 infective larvae on the small intestine; such as maximum increments are registered at days 287 and 308, that is, by October-November. It is also remarkable to observe that, by Table 4.6, *fenbendazole* administered to animals of Group C is found the most effective drug since the highest values of $\sum_{m=0}^{3}\pi_m^{TI}(\tau_0;\tau)$ are associated with treatment C for every vaccination instant τ_0 in Tables 4.4 and 4.5. Moreover, the selection $\tau_0^C = 170$ (June 19, derived with $p = 0.1$) results simultaneously in the minimum cost of vaccination, $\pi_{-1}^{TI}(\tau_0^C;\tau) = 0.09516$, and the maximum effectiveness, $\sum_{m=0}^{3}\pi_m^{TI}(\tau_0^C;\tau) = 0.90104$, and consequently it can be seen as optimal for our purposes. In Figure 4.13, we compare the distribution of the parasite load $M(\tau)$ when

the host is free living up to age τ (that is, there is no intervention) and when the host is treated and isolated at age $\tau_0 = 170$.

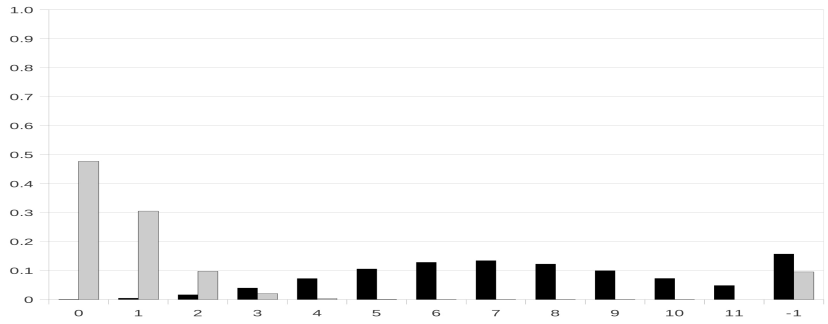

Fig. 4.13. The mass functions of the parasite burden $M(\tau)$ for $\tau = 1$ year when the host is free living up to age τ (*left*), and when it is transferred to the uninfected area and treated with *albendazole* at age $\tau_0 = 170$ (*right*). Parasite: *Nematodirus* spp.

4.3.4 Grazing strategies TI+S, UM, TS and TM

An important feature of the analysis in the previous sections is that the underlying processes, recording the number of parasites infesting the host at an arbitrary time t, can be thought of as age-dependent versions of a pure birth process with killing, and a pure death process with killing, which are both defined on a finite state space. We complement the treatment of control strategies applied to GI nematode burden we have started by focusing here on strategies that are not based on isolation of the host, but on movement to safe paddocks where the acquisition of parasites by the host is reduced but not removed. This implies that the processes used hereinafter to describe the parasite load will be no longer formulated as pure birth/death processes with killing.

In analyzing the process $\mathcal{Z} = \{M(t) : 0 \leq t \leq \tau\}$, we distinguish again between the free-living interval $[0, \tau_0)$, and the post-intervention interval $[\tau_0, \tau]$. For a host that has survived at age t with $t < \tau_0$, the possible transitions are as in Figure 4.1, and the probabilities $\pi_m(t) = P(M(t) = m|M(0) = 0)$, for levels $m \in \{-1\} \cup \mathcal{S}$, satisfy Equations (4.1) and (4.2), so that they are obtained by taking $\lambda_m(t) = \lambda(t)$ in (4.3) and (4.4).

Next, we focus on three grazing strategies that are defined in terms of the intervention instant τ_0. This implies that, at post-intervention ages $t \in (\tau_0, \tau]$, the rates $\lambda(t)$, $\delta(t)$ and $\gamma_m(t)$ are replaced by functions $\lambda'(t)$, $\delta'(t)$ and $\gamma'_m(t)$, respectively. The functions $\lambda'(t)$, $\delta'(t)$ and $\gamma'_m(t)$ appropriately reflect the use of a paddock with safe pasture and/or the efficacy of an anthelmintic treatment, in accordance with the following grazing strategies:

Strategy UM: *The host is left untreated but moved to a paddock with safe pasture at age* τ_0. The resulting process $\mathcal{Z}$ can be thought of as an age-dependent pure birth process with killing, whose birth rates are given by $\lambda_m(t) = \lambda(t)$ if $t \in [0, \tau_0)$, and $\lambda'(t)$ if $t \in [\tau_0, \tau]$, and killing rates are defined by $\delta_m(t) = \delta(t) + \gamma_m(t)$ if $t \in [0, \tau_0)$, and $\delta'(t) + \gamma'_m(t)$ if $t \in [\tau_0, \tau]$, for $m \in \mathcal{S}$.

Strategy TS: *The host is treated with anthelmintics and set-stocked at age* τ_0. Let $\eta'_m(t)$ be the death rate of parasites when the infection level of the host is $m \in \mathcal{S}$ at time t with $t > \tau_0$. In this case, $\mathcal{Z}$ can be seen as an age-dependent birth and death process with killing. The birth and death rates are defined by $\lambda_m(t) = \lambda(t)$ if $t \in [0, \tau]$, and $\eta_m(t) = 0$ if $t \in [0, \tau_0)$, and $\eta'_m(t)$ if $t \in [\tau_0, \tau]$, for $m \in \mathcal{S}$, respectively. Killing rates are defined identically to the rates $\delta_m(t)$ in strategy UM.

Strategy TM: *The host is treated with anthelmintics and moved to safe pasture at age* τ_0. In a similar manner to strategy TS, the process $\mathcal{Z}$ may be formulated as an age-dependent birth and death process with killing. Birth, death and killing rates are identical to those in strategy TS with the exception of $\lambda_m(t)$ for time instants $t \in [\tau_0, \tau]$, which has the form $\lambda_m(t) = \lambda'(t)$.

The age-dependent rates $\lambda_m(t)$, $\delta_m(t)$, and $\eta'_m(t)$ defining grazing strategies UM, TS and TM are directly obtained from Subsection 4.3.2. To reflect the use of a paddock with safe pasture in grazing strategies UM and TM, it is assumed that $\lambda'(t) = 0.2\lambda(t)$ for ages $t \in (\tau_0, \tau]$.

For the sake of completeness, we introduce the term *scenario US* to reflect *no intervention*, that is, the host is left untreated

Table 4.7. Age-dependent rates of the process $\mathcal{Z}$ for scenario US, and strategies UM, TS, TI, and TM. Parasite: *Nematodirus* spp.

Strategy	Rate	$t \in [0, \tau_0]$	$t \in [\tau_0, \tau]$
US	$\lambda_m(t)$	$\lambda(t)$	$\lambda(t)$
	$\eta_m(t)$	0	0
	$\delta_m(t)$	$\delta(t)$	$\delta(t)$
UM	$\lambda_m(t)$	$\lambda(t)$	$\lambda'(t)$
	$\eta_m(t)$	0	0
	$\delta_m(t)$	$\delta(t)$	$\delta(t)$
TS	$\lambda_m(t)$	$\lambda(t)$	$\lambda(t)$
	$\eta_m(t)$	0	$\eta'_m(t)$
	$\delta_m(t)$	$\delta(t)$	$\delta(t)$
TI	$\lambda_m(t)$	$\lambda(t)$	0
	$\eta_m(t)$	0	$\eta'_m(t)$
	$\delta_m(t)$	$\delta(t)$	$\delta(t)$
TM	$\lambda_m(t)$	$\lambda(t)$	$\lambda'(t)$
	$\eta_m(t)$	0	$\eta'_m(t)$
	$\delta_m(t)$	$\delta(t)$	$\delta(t)$

and set-stocked. Note that scenario US has been already used in Figure 4.13. In scenario US, the process $\mathcal{Z}$ is an age-dependent pure birth process with killing, and its birth and killing rates are specified by $\lambda_m(t) = \lambda(t)$ and $\delta_m(t) = \delta(t) + \gamma_m(t)$ if $t \in [0, \tau]$, for $m \in \mathcal{S}$. It follows then that the transient distribution of $\mathcal{Z}$ is given by (4.3) and (4.4) for time instants t with $0 \leq t \leq \tau$. A summary of the underlying age-dependent rates used in this section is given in Table 4.7.

A slight modification of our arguments in Section 4.1 allows us to derive explicit expressions for the transient solution at post-intervention instants $t \in (\tau_0, \tau]$ in grazing strategy UM. For time instants $t \in [\tau_0, \tau]$, we introduce probabilities $\pi_m^{UM}(\tau_0; t) = P(M(t) = m)$ and initial conditions $\pi_m^{UM}(\tau_0; \tau_0) = \pi_m(\tau_0)$, for $m \in \{-1\} \cup \mathcal{S}$, which are obtained from (4.3) and (4.4) with $\lambda_m(t) = \lambda(t)$.

Then, the transient solution at time instants $t \in (\tau_0, \tau]$ can be readily expressed as

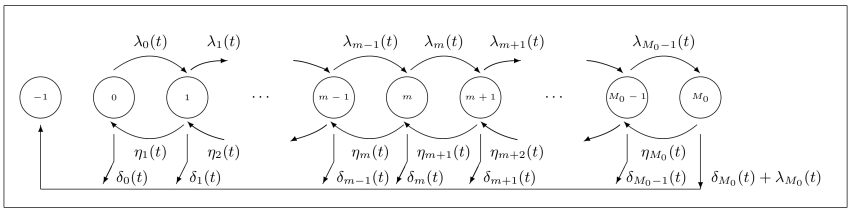

Fig. 4.14. State space and transitions at post-intervention instants $t \in [\tau_0, \tau]$. Grazing strategies TS and TM

$$\pi_m^{UM}(\tau_0;t) = e^{-\Lambda'(\tau_0;t)-\Delta'_m(\tau_0;t)}\left(\pi_m^{UM}(\tau_0;\tau_0) + (1-\delta_{0,m})\sum_{j=0}^{m-1}\pi_j^{UM}(\tau_0;\tau_0)K_{m-1}^{UM,j}(\tau_0;t)\right), \tag{4.12}$$

where $\Lambda'(\tau_0;t) = \int_{\tau_0}^{t}\lambda'(u)du$ and $\Delta'_m(\tau_0;t) = \int_{\tau_0}^{t}(\delta'(u)+\gamma'_m(u))du$. Starting from

$$K_{m-1}^{UM,m-1}(\tau_0;t) = \int_{\tau_0}^{t}\lambda'(u)e^{\tilde{\Delta}'_{m-1}(\tau_0;u)}du,$$

the functions $K_{m-1}^{UM,j}(\tau_0;t)$, for values $0 \le j \le m-2$, are iteratively computed as

$$K_{m-1}^{UM,j}(\tau_0;t) = \int_{\tau_0}^{t}\lambda'(u)e^{\tilde{\Delta}'_{m-1}(\tau_0;u)}K_{m-2}^{UM,j}(\tau_0;u)du,$$

with $\tilde{\Delta}'_{m-1}(\tau_0;t) = \Delta'_m(\tau_0;t) - \Delta'_{m-1}(\tau_0;t)$.

For grazing strategies TS and TM, the transient solution at time instants $t \in (\tau_0, \tau]$ can be numerically derived by using splitting techniques [53]. In a unifying manner, we may observe that, for a host that has survived at age t with $\tau_0 < t < \tau$ and $M(t) = m \in \mathcal{S}$, the possible transitions (in both strategies TS and TM) are as follows (Figure 4.14):

(i) $m \to m+1$ at rate $\lambda_m(t)$, for levels $m \in \{0, 1, ..., M_0 - 1\}$;
(ii) $m \to m-1$ at rate $\eta_m(t)$, for levels $m \in \{1, 2, ..., M_0\}$;
(iii) $m \to -1$ at rate $\delta_m(t)$, for levels $m \in \{0, 1, ..., M_0 - 1\}$;

(iv) $M_0 \to -1$ at rate $\delta_{M_0}(t) + \lambda_{M_0}(t)$.

Then, if we select a certain grazing strategy s with $s \in \{TS, TM\}$, the resulting probabilities $\pi_m^s(\tau_0; t) = P(M(t) = m)$, for $m \in \{-1\} \cup \mathcal{S}$ and time instants $t \in [\tau_0, \tau]$, satisfy the equality

$$\pi_{-1}^s(\tau_0; t) = 1 - \sum_{m=0}^{M_0} \pi_m^s(\tau_0; t), \quad \tau_0 \le t \le \tau,$$

and the time-dependent linear system of differential equations

$$\frac{d}{dt}\mathbf{\Pi}^s(\tau_0; t) = \mathbf{B}(t)\mathbf{\Pi}^s(\tau_0; t), \quad \tau_0 \le t \le \tau, \tag{4.13}$$

where $\mathbf{\Pi}^s(\tau_0; t) = (\pi_0^s(\tau_0; t), \pi_1^s(\tau_0; t), ..., \pi_{M_0}^s(\tau_0; t))^T$, and $\mathbf{B}(t)$ is a tri-diagonal matrix with entries

$$(\mathbf{B}(t))_{i,j} = \begin{cases} -(\lambda_i(t) + \delta_i(t) + (1 - \delta_{0,i})\eta_i(t)), & \\ & \text{if } 0 \le i \le M_0,\ j = i, \\ \eta_{i+1}(t), & \text{if } 0 \le i \le M_0 - 1,\ j = i + 1, \\ \lambda_{i-1}(t), & \text{if } 1 \le i \le M_0,\ j = i - 1, \\ 0, & \text{otherwise.} \end{cases}$$

Needless to say, initial conditions in (4.13) are given by $\mathbf{\Pi}^s(\tau_0; \tau_0) = (\pi_0(\tau_0), \pi_1(\tau_0), ..., \pi_{M_0}(\tau_0))^T$ where the values for $\pi_m(\tau_0)$ with $m \in \mathcal{S}$ are given by (4.4), regardless of the grazing strategy. Further details on how to solve (4.13) by using Strang-Marchuk splitting techniques are presented in Appendix.

For grazing strategies UM, TS and TM, we follow the methodology in Subsections 4.2.1 and 4.2.2, and define a control strategy by means of an age τ_0 and a concrete infection level $m' \in \{1, 2, ..., M_0\}$, such that $P_{\ge m'}(t) \ge p$ for a predetermined probability $p \in (0, 1)$. This procedure leads us to a set $I_{\ge m'}$ of potential intervention instants. In carrying out our examples, we select the threshold $m' = 4$ and values $p \in \{0.1, 0.2, ..., 0.7\}$. Then, for each resulting set $I_{\ge m'}$ of potential intervention instants, the problem is to find a single instant $\tau_0 \in I_{\ge m'}$ that appropriately balances the effectiveness and cost of intervention in the grazing strategy under consideration. Then, we apply Criteria 1 and 2 with effectiveness measured in terms of

Table 4.8. Intervention instants τ_0 versus p and the probabilities p_1 (Criterion 1) and p_2 (Criterion 2) for $m' = 4$. Grazing strategy UM. Parasite: *Nematodirus* spp.

p	$I_{\geq 4}$	p_1	$J^1_{\geq 4}$	τ_0^1	p_2	$J^2_{\geq 4}$	τ_0^2
0.1	[170,365)	0.70	—	—	0.25	[170,299]	170
		0.60	—	—	0.20	[170,290]	170
		0.50	[170,194]	170	0.15	[170,282]	170
0.2	[274,365)	0.70	—	—	0.25	[274,299]	274
		0.60	—	—	0.20	[274,290]	274
		0.50	—	—	0.15	[274,282]	274
0.3	[281,365)	0.70	—	—	0.25	[281,299]	281
		0.60	—	—	0.20	[281,290]	281
		0.50	—	—	0.15	[281,282]	281
0.4	[286,365)	0.70	—	—	0.25	[286,299]	286
		0.60	—	—	0.20	[286,290]	286
		0.50	—	—	0.15	—	—
0.5	[290,365)	0.70	—	—	0.25	[290,299]	290
		0.60	—	—	0.20	[290,290]	290
		0.50	—	—	0.15	—	—
0.6	[298,365)	0.70	—	—	0.25	[298,299]	298
		0.60	—	—	0.20	—	—
		0.50	—	—	0.15	—	—
0.7	[308,365)	0.70	—	—	0.25	—	—
		0.60	—	—	0.20	—	—
		0.50	—	—	0.15	—	—

$$\sum_{m=0}^{3} \pi_m^s(\tau_0;\tau),$$

that is, the probability that the degree of infestation at age τ is null or light as the intervention is prescribed at age τ_0 in accordance with the grazing strategy s with $s \in \{UM, TS, TM\}$. In contrast, we make the cost of intervention depend on the probability

$$\sum_{m=8}^{11} \pi_m^s(\tau_0;\tau) + \pi_{-1}^s(\tau_0;\tau)$$

that either the host does not survive or its degree of infestation is high at age τ. Values of τ_0 are listed in Table 4.8 for grazing strategy UM and denoted by τ_0^1 and τ_0^2 as they are derived by applying Criteria 1 and 2, respectively. In Tables 4.9 and 4.10, values of τ_0 are listed for grazing strategies TS and TM, and the

anthelmintic treatments B (*ivermectin*), C (*fenbendazole*) and D (*albendazole*), which are denoted by t_0^B, t_0^C and τ_0^D, respectively. An examination of the resulting instants τ_0 in Tables 4.8-4.10 reveals the following important consequences:

(i) For every anthelmintic treatment and fixed value p, Criteria 1 and 2 applied to grazing strategy TM yield identical intervention instants τ_0, with the exception of those pairs (p, p_1) for treatment B leading us to empty subsets $J_{\geq 4}^{1,B}$.

(ii) In applying Criterion 1 (respectively, Criterion 2) to grazing strategy TM, values of $p_1 \in \{0.5, 0.6, 0.7\}$ (respectively, $p_2 \in \{0.15, 0.2, 0.25\}$) result in identical intervention instants τ_0, irrespectively of the anthelmintic treatment, with the exception of the case $p = 0.1$.

(iii) For every anthelmintic treatment, the intervention instant τ_0 derived in grazing strategy TM behaves as an increasing function of p, regardless of the control criterion.

(iv) For every anthelmintic treatment and fixed value p_1, the intervention instant τ_0 in grazing strategy TS appears to be constant as a function of p.

(v) In contrast to grazing strategies TS and TM, the values $p_1 \in \{0.5, 0.6, 0.7\}$ for grazing strategy UM lead us to empty subsets $J_{\geq 4}^{1}$ of potential intervention instants, with the exception of the pair $(p, p_1) = (0.1, 0.5)$.

In Table 4.11, we list the value of effectiveness $\sum_{m=0}^{3} \pi_m^s(\tau_0; \tau)$ and the cost of intervention $\sum_{m=8}^{11} \pi_m^s(\tau_0; \tau) + \pi_{-1}^s(\tau_0; \tau)$ for those intervention instants τ_0 derived in Tables 4.8-4.10 for grazing strategies UM, TS and TM; in scenario US, these values are replaced by the probabilities $\sum_{m=0}^{3} \pi_m^{US}(\tau)$ and $\sum_{m=8}^{11} \pi_m^{US}(\tau) + \pi_{-1}^{US}(\tau)$, respectively. It can be noticed that the selection $\tau_0 = 273$ (October 1), which is related to $p = 0.1$ in the case TM with the anthelmintic treatment C (*fenbendazole*), results in the minimum cost of intervention (0.09589, instead of 0.49951 in scenario US) and the maximum effectiveness (0.79086, instead of 0.06072 in scenario US), and it can be thus taken as optimal for our purposes. Moreover, the anthelmintic treatment C is found the most effective drug since the highest values of $\sum_{m=0}^{3} \pi_m^s(\tau_0; \tau)$ and the smallest values of $\sum_{m=8}^{11} \pi_m^s(\tau_0; \tau) + \pi_{-1}^s(\tau_0; \tau)$ are observed in Table 4.11

Table 4.9. Intervention instants τ_0 versus p and p_1 (Criterion 1) for $m' = 4$. Grazing strategies TS and TM; anthelmintic treatments B, C and D. Parasite: *Nematodirus* spp.

p	$I_{\geq 4}$	p_1		$J^{1,B}_{\geq 4}$	τ_0^B	$J^{1,C}_{\geq 4}$	τ_0^C	$J^{1,D}_{\geq 4}$	τ_0^D
0.1	[170,365)	0.70	TS	—	—	—	—	—	—
			TM	[170,278]	170	[170,319]	273	[170,308]	272
		0.60	TS	—	—	[336,339]	336	—	—
			TM	[170,301]	170	[170,344]	273	[170,342]	272
		0.50	TS	—	—	[308,344]	308	[313,343]	313
			TM	[170,343]	170	[170,348]	273	[170,346]	272
0.2	[274,365)	0.70	TS	—	—	—	—	—	—
			TM	[274,278]	274	[274,319]	274	[274,308]	274
		0.60	TS	—	—	[336,339]	336	—	—
			TM	[274,301]	274	[274,344]	274	[274,342]	274
		0.50	TS	—	—	[308,344]	308	[313,343]	313
			TM	[274,343]	274	[274,348]	274	[274,346]	274
0.3	[281,365)	0.70	TS	—	—	—	—	—	—
			TM	—	—	[281,319]	281	[281,308]	281
		0.60	TS	—	—	[336,339]	336	—	—
			TM	[281,301]	281	[281,344]	281	[281,342]	281
		0.50	TS	—	—	[308,344]	308	[313,343]	313
			TM	[281,343]	281	[281,348]	281	[281,346]	281
0.4	[286,365)	0.70	TS	—	—	—	—	—	—
			TM	—	—	[286,319]	286	[286,308]	286
		0.60	TS	—	—	[336,339]	336	—	—
			TM	[286,301]	286	[286,344]	286	[286,342]	286
		0.50	TS	—	—	[308,344]	308	[313,343]	313
			TM	[286,343]	286	[286,348]	286	[286,346]	286
0.5	[290,365)	0.70	TS	—	—	—	—	—	—
			TM	—	—	[290,319]	290	[290,308]	290
		0.60	TS	—	—	[336,339]	336	—	—
			TM	[290,301]	290	[290,344]	290	[290,342]	290
		0.50	TS	—	—	[308,344]	308	[313,343]	313
			TM	[290,343]	290	[290,348]	290	[290,346]	290
0.6	[298,365)	0.70	TS	—	—	—	—	—	—
			TM	—	—	[298,319]	298	[298,308]	298
		0.60	TS	—	—	[336,339]	336	—	—
			TM	[298,301]	298	[298,344]	298	[298,342]	298
		0.50	TS	—	—	[308,344]	308	[313,343]	313
			TM	[298,343]	298	[298,348]	298	[298,346]	298
0.7	[308,365)	0.70	TS	—	—	—	—	—	—
			TM	—	—	[308,319]	308	[308,308]	308
		0.60	TS	—	—	[336,339]	336	—	—
			TM	—	—	[308,344]	308	[308,342]	308
		0.50	TS	—	—	[308,344]	308	[313,343]	313
			TM	[308,343]	308	[308,348]	308	[308,346]	308

Table 4.10. Intervention instants τ_0 versus p and p_2 (Criterion 2) for $m' = 4$. Grazing strategies TS and TM; anthelmintic treatments B, C and D. Parasite: *Nematodirus* spp.

p	$I_{\geq 4}$	p_2		$J_{\geq 4}^{1,B}$	τ_0^B	$J_{\geq 4}^{1,C}$	τ_0^C	$J_{\geq 4}^{1,D}$	τ_0^D
0.1	[170,365)	0.25	TS	[286,363]	358	[268,363]	338	[270,363]	338
			TM	[170,363]	170	[170,363]	273	[170,363]	272
		0.20	TS	[299,362]	358	[279,362]	338	[281,361]	338
			TM	[170,362]	170	[170,362]	273	[170,362]	272
		0.15	TS	—	—	[290,346]	338	[292,344]	338
			TM	[170,350]	170	[170,350]	273	[170,348]	272
0.2	[274,365)	0.25	TS	[286,363]	358	[274,363]	338	[274,363]	338
			TM	[274,363]	274	[274,363]	274	[274,363]	274
		0.20	TS	[299,362]	358	[279,362]	338	[281,361]	338
			TM	[274,362]	274	[274,362]	274	[274,362]	274
		0.15	TS	—	—	[290,346]	338	[292,344]	338
			TM	[274,350]	274	[274,350]	274	[274,348]	274
0.3	[281,365)	0.25	TS	[286,363]	358	[281,363]	338	[281,363]	338
			TM	[281,363]	281	[281,363]	281	[281,363]	281
		0.20	TS	[299,362]	358	[281,362]	338	[281,361]	338
			TM	[281,362]	281	[281,362]	281	[281,362]	281
		0.15	TS	—	—	[290,346]	338	[292,344]	338
			TM	[281,350]	281	[281,350]	281	[281,348]	281
0.4	[286,365)	0.25	TS	[286,363]	358	[286,363]	338	[286,363]	338
			TM	[286,363]	286	[286,363]	286	[286,363]	286
		0.20	TS	[299,362]	358	[286,362]	338	[286,361]	338
			TM	[286,362]	286	[286,362]	286	[286,362]	286
		0.15	TS	—	—	[290,346]	338	[292,344]	338
			TM	[286,350]	286	[286,350]	286	[286,348]	286
0.5	[290,365)	0.25	TS	[290,363]	358	[290,363]	338	[290,363]	338
			TM	[290,363]	290	[290,363]	290	[290,363]	290
		0.20	TS	[299,362]	358	[290,362]	338	[290,361]	338
			TM	[290,362]	290	[290,362]	290	[290,362]	290
		0.15	TS	—	—	[290,346]	338	[292,344]	338
			TM	[290,350]	290	[290,350]	290	[290,348]	290
0.6	[298,365)	0.25	TS	[298,363]	358	[298,363]	338	[298,363]	338
			TM	[298,363]	298	[298,363]	298	[298,363]	298
		0.20	TS	[299,362]	358	[298,362]	338	[298,361]	338
			TM	[298,362]	298	[298,362]	298	[298,362]	298
		0.15	TS	—	—	[298,346]	338	[298,344]	338
			TM	[298,350]	298	[298,350]	298	[298,348]	298
0.7	[308,365)	0.25	TS	[308,363]	358	[308,363]	338	[308,363]	338
			TM	[308,363]	308	[308,363]	308	[308,363]	308
		0.20	TS	[308,362]	358	[308,362]	338	[308,361]	338
			TM	[308,362]	308	[308,362]	308	[308,362]	308
		0.15	TS	—	—	[308,346]	338	[308,344]	338
			TM	[308,350]	308	[308,350]	308	[308,348]	308

Table 4.11. Effectiveness measured in terms of $\sum_{m=0}^{3} \pi_m^s(\tau_0;\tau)$ and $\tau^{-1}eff^s(\tau_0)$, and cost of intervention measured in terms of $\sum_{m=8}^{11} \pi_m^s(\tau_0;\tau) + \pi_{-1}^s(\tau_0;\tau)$ and $\tau^{-1}cost^s(\tau_0)$. Scenario US, and grazing strategies UM, TS and TM; anthelmintic treatments B, C and D. Parasite: *Nematodirus* spp.

Strat.	Anth.	τ_0	Criterion	$\sum_{m=0}^{3} \pi_m^s(\tau_0;\tau)$	$\sum_{m=8}^{11} \pi_m^s(\tau_0;\tau) + \pi_{-1}^s(\tau_0;\tau)$	$\tau^{-1}eff^s(\tau_0)$	$\tau^{-1}cost^s(\tau_0)$
US		—	—	0.06072	0.49951	0.68645	0.14746
UM		170	1 & 2	0.54431	0.11049	0.79996	0.09726
		274	2	0.45540	0.12524	0.76629	0.09983
		281	2	0.38981	0.14216	0.74973	0.10267
		286	2	0.32115	0.16811	0.73306	0.10715
		290	2	0.26634	0.19763	0.72023	0.11233
		298	2	0.20886	0.24130	0.70769	0.11984
TS	B	358	2	0.41766	0.16608	0.69160	0.14217
	C	308	1	0.50340	0.12350	0.75871	0.10433
		336	1	0.60161	0.13144	0.71941	0.12421
		338	2	0.60604	0.13209	0.71613	0.12578
	D	313	1	0.50240	0.12842	0.74908	0.10793
		338	2	0.57385	0.13407	0.71312	0.12626
TM	B	170	1 & 2	0.73224	0.09721	0.86987	0.09525
		274	1 & 2	0.71025	0.09797	0.82480	0.09580
		281	1 & 2	0.69119	0.09877	0.81634	0.09602
		286	1 & 2	0.66653	0.10011	0.80686	0.09644
		290	1 & 2	0.64110	0.10197	0.79743	0.09713
		298	1 & 2	0.61142	0.10528	0.78209	0.09911
		308	1 & 2	0.56977	0.11374	0.76202	0.10372
	C	273	1 & 2	0.79086	0.09589	0.83891	0.09557
		274	1 & 2	0.79080	0.09589	0.83820	0.09558
		281	1 & 2	0.78559	0.09601	0.83107	0.09573
		286	1 & 2	0.77604	0.09636	0.82304	0.09605
		290	1 & 2	0.76467	0.09707	0.81476	0.09662
		298	1 & 2	0.75182	0.09895	0.79922	0.09852
		308	1 & 2	0.72721	0.10573	0.77734	0.10310
	D	272	1 & 2	0.78128	0.09605	0.83749	0.09558
		274	1 & 2	0.78102	0.09606	0.83605	0.09560
		281	1 & 2	0.77361	0.09623	0.82838	0.09576
		286	1 & 2	0.76132	0.09666	0.81971	0.09610
		290	1 & 2	0.74737	0.09747	0.81089	0.09671
		298	1 & 2	0.73134	0.09945	0.79492	0.09867
		308	1 & 2	0.70211	0.10641	0.77271	0.10336

for every grazing strategy $s \in \{TS, TM\}$ and fixed intervention instant τ_0.

An alternative manner to measure the effectiveness and cost of intervention at a certain age $\tau_0 < \tau$ is given by the respective values

$$\tau^{-1}eff^s(\tau_0) = \tau^{-1}\int_0^\tau \sum_{m=0}^{3} \tilde{\pi}_m^s(\tau_0;u)du,$$

$$\tau^{-1}cost^s(\tau_0) = \tau^{-1}\int_0^\tau \left(\sum_{m=8}^{11} \tilde{\pi}_m^s(\tau_0;u) + \tilde{\pi}_{-1}^s(\tau_0;u)\right) du,$$

where $\tilde{\pi}_m^s(\tau_0;u) = \pi_m^{US}(u)$ if $u \in (0,\tau)$ in scenario US, and $\tilde{\pi}_m^s(\tau_0;u) = \pi_m^s(u)$ if $u \in (0,\tau_0)$, and $\pi_m^s(\tau_0;u)$ if $u \in [\tau_0,\tau)$ in grazing strategy s with $s \in \{UM, TS, TM\}$. Values for $\tau^{-1}eff^s(\tau_0)$ and $\tau^{-1}cost^s(\tau_0)$ in Table 4.11 correspond to the expected proportions of time that the host infection level $M(t)$ remains in the subsets of levels $\{0,1,2,3\}$ and $\{8,9,10,11\} \cup \{-1\}$, respectively. It is remarkable to note that the maximum effectiveness $\tau^{-1}eff^s(\tau_0) = 0.86987$ (instead of 0.68645 in scenario US) and the minimum cost of intervention $\tau^{-1}cost^s(\tau_0) = 0.09525$ (instead of 0.14746 in scenario US) are both related to the selection $\tau_0 = 170$ (June 19) in grazing strategy TM with the anthelmintic treatment B (*ivermectin*).

4.3.5 Discussion

It should be noted that $\tau_0 = 170$ results in the longest post-intervention interval $[\tau_0,\tau]$ in our examples; similarly to the grazing strategy TI, the maintenance of stable safe-pasture conditions (or noninfectious conditions in the case TI) for a long period of time may often be difficult and highly expensive, so that the choice $\tau_0 = 170$ might be unsustainable for practical use. Thus, we investigate, in Tables 4.12-4.15 and Figure 4.15, a modified grazing strategy TI+S, which is specified by moving the host to its original paddock (set-stocking) after living for 28 days under noninfectious conditions. This means to distinguish between two free-living intervals $[0,\tau_0)$ and $[\tau_5,\tau]$, and an intermediate isolated-living interval $[\tau_0,\tau_5)$ with $\tau_5 = \tau_0 + 28$; see [90]. Solutions for $t \in [\tau_5,\tau]$ are readily derived in a similar way of those ones for $t \in [0,\tau_0)$. In applying Criteria 1 and 2, we use $\sum_{m=0}^{3}\pi_m^{TI+S}(t;\tau)$ to measure effectiveness, whereas the cost of vaccination is measured by $\pi_{-1}^{TI+S}(t;\tau)$ (i.e., the degree of infestation is heavy) and, alternatively, by $\sum_{m=8}^{11}\pi_m^{TI+S}(t;\tau)+\pi_{-1}^{TI+S}(t;\tau)$ (i.e., the degree of infestation is high or heavy), with the resulting vaccination instants denoted by $\bar{\tau}_0$ and $\hat{\tau}_0$, respectively. In contrast to Figure 4.12, the age-dependent probabilities $\pi_{-1}^{TI+S}(t;\tau)$, $\sum_{m=8}^{11}\pi_m^{TI+S}(t;\tau) + \pi_{-1}^{TI+S}(t;\tau)$ and $\sum_{m=0}^{3}\pi_m^{TI+S}(t;\tau)$ exhibit in Figure 4.15 non-monotone behaviors over time.

Tables 4.12-4.15 are themselves explanatory, whence we comment only on three remarkable observations. First, we empha-

Table 4.12. Vaccination instants τ_0 versus p and p_1 for $m' = 4$. Grazing strategy TI+S with anthelmintics B, C and D. Values $\bar{\tau}_0$ and $\hat{\tau}_0$ result from the application of Criterion 1 with $\pi_{-1}^{TI+S}(t;\tau)$ and $\sum_{m=8}^{11} \pi_m^{TI+S}(t;\tau) + \pi_{-1}^{TI+S}(t;\tau)$ (*cost of vaccination*), respectively, and $\sum_{m=0}^{3} \pi_m^{TI+S}(t;\tau)$ (*effectiveness*). Parasite: *Nematodirus* spp.

p	$I_{\geq 4}$	p_1	$J_{\geq 4}^{1,B}$	$\bar{\tau}_0^B$	$\hat{\tau}_0^B$	$J_{\geq 4}^{1,C}$	$\bar{\tau}_0^C$	$\hat{\tau}_0^C$	$J_{\geq 4}^{1,D}$	$\bar{\tau}_0^D$	$\hat{\tau}_0^D$
0.1	[170,365)	0.75	—		—	—		—	—		—
		0.70	—		—	[334,340]	334	334	—		—
		0.65	—		—	[284,306]∪[323,343]	284	287	[287,297]∪[330,341]	287	287
		0.60	—		—	[280,345]	280	287	[281,343]	281	287
		0.55	[282,296]	282	286	[276,347]	280	287	[277,345]	280	287
0.2	[274,365)	0.75	—		—	—		—	—		—
		0.70	—		—	[334,340]	334	334	—		—
		0.65	—		—	[284,306]∪[323,343]	284	287	[287,297]∪[330,341]	287	287
		0.60	—		—	[280,345]	280	287	[281,343]	281	287
		0.55	[282,296]	282	286	[276,347]	280	287	[277,345]	280	287
0.3	[281,365)	0.75	—		—	—		—	—		—
		0.70	—		—	[334,340]	334	334	—		—
		0.65	—		—	[284,306]∪[323,343]	284	287	[287,297]∪[330,341]	287	287
		0.60	—		—	[281,345]	281	287	[281,343]	281	287
		0.55	[282,296]	282	286	[281,347]	281	287	[281,345]	281	287
0.4	[286,365)	0.75	—		—	—		—	—		—
		0.70	—		—	[334,340]	334	334	—		—
		0.65	—		—	[286,306]∪[323,343]	286	287	[287,297]∪[330,341]	287	287
		0.60	—		—	[286,345]	286	287	[286,343]	286	287
		0.55	[286,296]	286	286	[286,347]	286	287	[286,345]	286	287
0.5	[290,365)	0.75	—		—	—		—	—		—
		0.70	—		—	[334,340]	334	334	—		—
		0.65	—		—	[290,306]∪[323,343]	290	290	[290,297]∪[330,341]	290	290
		0.60	—		—	[290,345]	290	290	[290,343]	290	290
		0.55	[290,296]	290	290	[290,347]	290	290	[290,345]	290	290
0.6	[298,365)	0.75	—		—	—		—	—		—
		0.70	—		—	[334,340]	334	334	—		—
		0.65	—		—	[298,306]∪[323,343]	298	298	[330,341]	330	330
		0.60	—		—	[298,345]	298	298	[298,343]	298	298
		0.55	—		—	[298,347]	298	298	[298,345]	298	298
0.7	[308,365)	0.75	—		—	—		—	—		—
		0.70	—		—	[334,340]	334	334	—		—
		0.65	—		—	[323,343]	323	323	[330,341]	330	330
		0.60	—		—	[308,345]	308	308	[308,343]	308	308
		0.55	—		—	[308,347]	308	308	[308,345]	308	308

size that there is no optimal vaccination instant τ_0 for strategy TI+S; see, for example, entries in Table 4.15 for $\pi_{-1}^{TI+S}(\tau_0;\tau)$ and $\sum_{m=0}^{3} \pi_m^{TI+S}(\tau_0;\tau)$ at ages $\tau_0 = 280$ and 337 and anthelmintic treatment C. Second, *fenbendazole* is also found the most effective drug as the length of 28 days is assumed for the isolated-living interval. Third, an interesting feature in applying Criteria 1 and 2 is that the intervention by anthelmintics is mostly prescribed at age 337 (December 4), thus implying that the second free-living interval $[\tau_5, \tau]$ becomes empty in the modified version. It should be noted that the selection $\tau_0 = 337$ in the modified control strategy does not contradict those conclusions derived from Table

Table 4.13. Vaccination instants τ_0 versus p and p_2 for $m' = 4$. Grazing strategy TI+S with anthelmintics B, C and D. Application of Criterion 2 with $\pi_{-1}^{TI+S}(t;\tau)$ (*cost of vaccination*) and $\sum_{m=0}^{3}\pi_m^{TI+S}(t;\tau)$ (*effectiveness*). Parasite: *Nematodirus* spp.

p	$I_{\geq 4}$	p_2	$J_{\geq 4}^{2,B}$	$\bar{\tau}_0^B$	$J_{\geq 4}^{2,C}$	$\bar{\tau}_0^C$	$J_{\geq 4}^{2,D}$	$\bar{\tau}_0^D$
0.1	[170,365)	0.25	[170,365)	286	[170,365)	337	[170,365)	337
		0.20	[170,365)	286	[170,365)	337	[170,365)	337
		0.15	[170,360]	286	[170,360]	337	[170,360]	337
0.2	[274,365)	0.25	[274,365)	286	[274,365)	337	[274,365)	337
		0.20	[274,365)	286	[274,365)	337	[274,365)	337
		0.15	[274,360]	286	[274,360]	337	[274,360]	337
0.3	[281,365)	0.25	[281,365)	286	[281,365)	337	[281,365)	337
		0.20	[281,365)	286	[281,365)	337	[281,365)	337
		0.15	[281,360]	286	[281,360]	337	[281,360]	337
0.4	[286,365)	0.25	[286,365)	286	[286,365)	337	[286,365)	337
		0.20	[286,365)	286	[286,365)	337	[286,365)	337
		0.15	[286,360]	286	[286,360]	337	[286,360]	337
0.5	[290,365)	0.25	[290,365)	290	[290,365)	337	[290,365)	337
		0.20	[290,365)	290	[290,365)	337	[290,365)	337
		0.15	[290,360]	290	[290,360]	337	[290,360]	337
0.6	[298,365)	0.25	[298,365)	337	[298,365)	337	[298,365)	337
		0.20	[298,365)	337	[298,365)	337	[298,365)	337
		0.15	[298,360]	337	[298,360]	337	[298,360]	337
0.7	[308,365)	0.25	[308,365)	337	[308,365)	337	[308,365)	337
		0.20	[308,365)	337	[308,365)	337	[308,365)	337
		0.15	[308,360]	337	[308,360]	337	[308,360]	337

4.5. More concretely, we may first observe that, for $p = 0.7$ and $p_2 \in \{0.15, 0.2, 0.25\}$, the sub-sets $J_{\geq 4}^{2,B}$, $J_{\geq 4}^{2,C}$ and $J_{\geq 4}^{2,D}$ of potential vaccination instants in Table 4.5 are identical to their counterparts in Table 4.13. However, though the values of $\sum_{m=0}^{3}\pi_m^s(\tau_0;\tau)$ in Figures 4.12 and 4.15, for $s \in \{TI, TI+S\}$, are clearly identical for ages τ_0 ranging between 337 and 365, the differences among values of the age-dependent probabilities $\sum_{m=0}^{3}\pi_m^s(\tau_0;\tau)$ in Figures 4.12 and 4.15 are significant for ages $\tau_0 < 337$, and particularly it is seen that $\sum_{m=0}^{3}\pi_m^{TI+S}(308;\tau) < \sum_{m=0}^{3}\pi_m^{TI+S}(337;\tau)$ for the modified control strategy.

With respect to grazing strategies UM, TS and TM, because of seasonal conditions a preliminary analysis of the probabilities $\sum_{m=0}^{3}\pi_m^s(\tau_0;\tau)$ and $\sum_{m=8}^{11}\pi_m^s(\tau_0;\tau)+\pi_{-1}^s(\tau_0;\tau)$ is required to determine values p_1 and p_2 in such a way that Criteria 1 and 2 lead

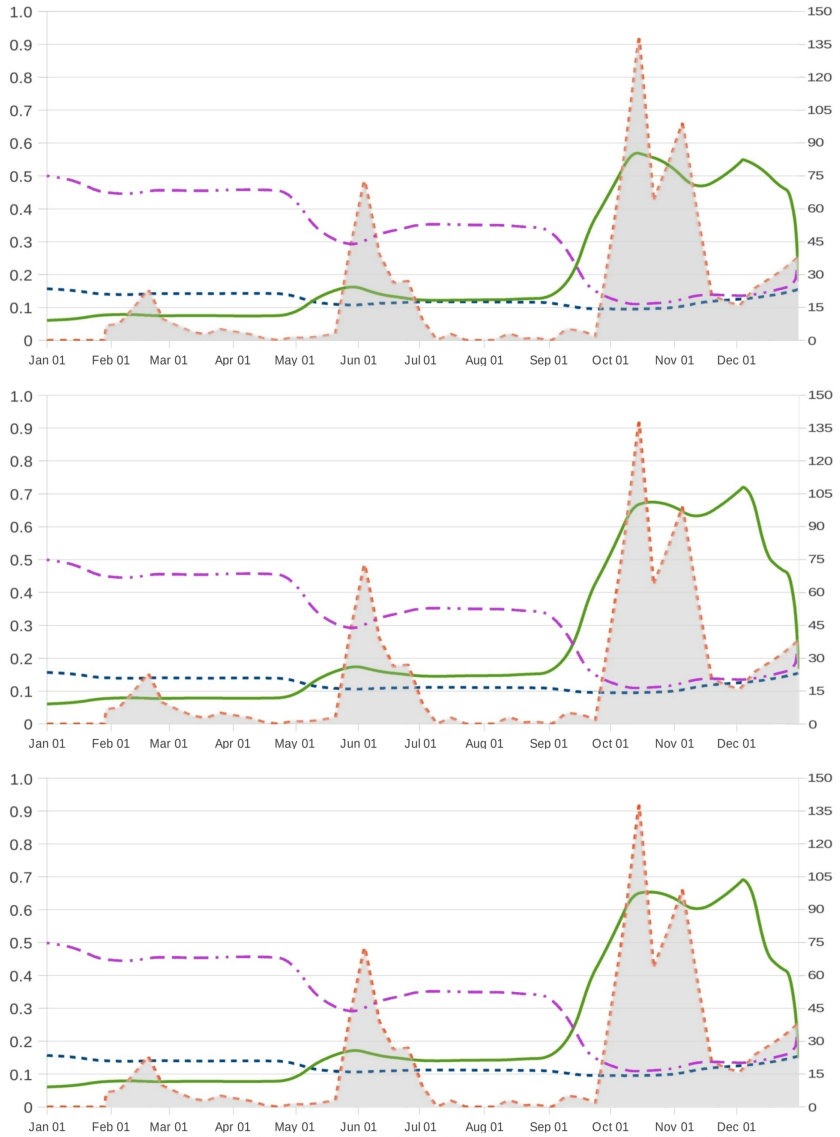

Fig. 4.15. The age-dependent probabilities $\pi_{-1}^{TI+S}(\tau_0;\tau)$ (*broken* line), $\sum_{m=8}^{11}\pi_m^{TI+S}(\tau_0;\tau)+\pi_{-1}^{TI+S}(\tau_0;\tau)$ (*dashed* line) and $\sum_{m=0}^{3}\pi_m^{TI+S}(\tau_0;\tau)$ (*solid* line) versus the vaccination instant τ_0 for $\tau = 1$ year, and increments in the number of L_3 infective larvae on the small intestine (*shaded* area, *right* vertical axis). Grazing strategy TI+S with anthelmintics B, C and D (*from top to bottom*). Parasite: *Nematodirus* spp.

Table 4.14. Vaccination instants τ_0 versus p and p_2 for $m' = 4$. Grazing strategy TI+S with anthelmintics B, C and D. Application of Criterion 2 with $\sum_{m=8}^{11} \pi_m^{TI+S}(t;\tau) + \pi_{-1}^{TI+S}(t;\tau)$ (*cost of vaccination*) and $\sum_{m=0}^{3} \pi_m^{TI+S}(t;\tau)$ (*effectiveness*). Parasite: *Nematodirus* spp.

p	$I_{\geq 4}$	p_2	$J_{\geq 4}^{2,B}$	$\hat{\tau}_0^B$	$J_{\geq 4}^{2,C}$	$\hat{\tau}_0^C$	$J_{\geq 4}^{2,D}$	$\hat{\tau}_0^D$
0.1	[170,365)	0.25	[255,363]	286	[251,363]	337	[252,363]	337
		0.20	[259,362]	286	[257,362]	337	[257,362]	337
		0.15	[266,352]	286	[262,352]	337	[263,349]	337
0.2	[274,365)	0.25	[274,363]	286	[274,363]	337	[274,363]	337
		0.20	[274,362]	286	[274,362]	337	[274,362]	337
		0.15	[274,352]	286	[274,352]	337	[274,349]	337
0.3	[281,365)	0.25	[281,363]	286	[281,363]	337	[281,363]	337
		0.20	[281,362]	286	[281,362]	337	[281,362]	337
		0.15	[281,352]	286	[281,352]	337	[281,349]	337
0.4	[286,365)	0.25	[286,363]	286	[286,363]	337	[286,363]	337
		0.20	[286,362]	286	[286,362]	337	[286,362]	337
		0.15	[286,352]	286	[286,352]	337	[286,349]	337
0.5	[290,365)	0.25	[290,363]	290	[290,363]	337	[290,363]	337
		0.20	[290,362]	290	[290,362]	337	[290,362]	337
		0.15	[290,352]	290	[290,352]	337	[290,349]	337
0.6	[298,365)	0.25	[298,363]	337	[298,363]	337	[298,363]	337
		0.20	[298,362]	337	[298,362]	337	[298,362]	337
		0.15	[298,352]	337	[298,352]	337	[298,349]	337
0.7	[308,365)	0.25	[308,363]	337	[308,363]	337	[308,363]	337
		0.20	[308,362]	337	[308,362]	337	[308,362]	337
		0.15	[308,352]	337	[308,352]	337	[308,349]	337

us to nonempty subsets $J_{\geq m'}^1$ and $J_{\geq m'}^2$ of potential intervention instants $\tau_0 \in I_{\geq m'}$, for a predetermined threshold m'. Thus, similarly to strategy TI, a graphical representation of $\sum_{m=0}^{3} \pi_m^s(\tau_0;\tau)$ and $\sum_{m=8}^{11} \pi_m^s(\tau_0;\tau) + \pi_{-1}^s(\tau_0;\tau)$ can help in measuring allowable values for the minimum value of effectiveness and the maximum cost of intervention in terms of concrete values for p_1 and p_2, respectively. Figures 4.16 and 4.17 show how $\sum_{m=0}^{3} \pi_m^s(\tau_0;\tau)$ and $\sum_{m=8}^{11} \pi_m^s(\tau_0;\tau) + \pi_{-1}^s(\tau_0;\tau)$ behave in terms of τ_0 for grazing strategies UM, TS and TM. We recall here that, in scenario US, the effectiveness (respectively, cost of intervention) is given by $\sum_{m=0}^{3} \pi_m^{US}(\tau)$ (respectively, $\sum_{m=8}^{11} \pi_m^{US}(\tau) + \pi_{-1}^{US}(\tau)$), which is a constant as a function of τ_0. It is worth noting that the value $\sum_{m=0}^{3} \pi_m^{US}(\tau)$ (respectively, $\sum_{m=8}^{11} \pi_m^{US}(\tau) + \pi_{-1}^{US}(\tau)$) results in a lower bound (respectively, upper bound) to the corresponding val-

Table 4.15. Values of $\pi_{-1}^{TI+S}(\tau_0;\tau)$, $\sum_{m=8}^{11}\pi_m^{TI+S}(\tau_0;\tau)+\pi_{-1}^{TI+S}(\tau_0;\tau)$ and $\sum_{m=0}^{3}\pi_m^{TI+S}(\tau_0;\tau)$. Grazing strategy TI+S with anthelmintics B, C and D. Parasite: *Nematodirus* spp.

τ_0	Treatment	$\pi_{-1}^{TI+S}(\tau_0;\tau)$	$\sum_{m=8}^{11}\pi_m^{TI+S}(\tau_0;\tau)+\pi_{-1}^{TI+S}(\tau_0;\tau)$	$\sum_{m=0}^{3}\pi_m^{TI+S}(\tau_0;\tau)$
280	B	—	—	—
	C	0.09524	—	0.61241
	D	0.09525	—	0.59796
281	B	—	—	—
	C	0.09524	—	0.62559
	D	0.09525	—	0.61074
282	B	0.09533	—	0.55290
	C	—	—	—
	D	—	—	—
284	B	—	—	—
	C	0.09530	—	0.65477
	D	—	—	—
286	B	0.09547	0.10772	0.56927
	C	0.09541	—	0.66563
	D	0.09542	—	0.64831
287	B	—	—	—
	C	—	0.10012	0.66852
	D	0.09551	0.10113	0.65056
290	B	0.09600	0.10869	0.56314
	C	0.09594	0.10024	0.67312
	D	0.09594	0.10131	0.65342
292	B	—	—	—
	C	—	—	—
	D	0.09631	—	0.65392
293	B	—	—	—
	C	0.09649	—	0.67475
	D	—	—	—
298	B	0.09770	—	0.54469
	C	0.09764	0.10181	0.67148
	D	0.09765	0.10301	0.64877
308	B	—	—	—
	C	0.10416	0.10899	0.64554
	D	0.10416	0.11057	0.61845
323	B	—	—	—
	C	0.11948	0.12269	0.65152
	D	—	—	—
330	B	—	—	—
	C	—	—	—
	D	0.12295	0.12561	0.65263
334	B	—	—	—
	C	0.12485	0.12598	0.70327
	D	—	—	—
337	B	0.12629	0.13310	0.54949
	C	0.12629	0.12700	0.71988
	D	0.12629	0.12745	0.69110

ues of effectiveness (respectively, cost of intervention) in grazing strategies UM, TS and TM.

As intuition tells us, grazing strategy TM results in the most effective procedure for every time instant τ_0, regardless of the anthelmintic treatment. In Figures 4.16 and 4.17, it is also seen that grazing strategy UM is preferred to grazing strategy TS when in-

tervention is prescribed at ages $\tau_0 < 293$ (October 21), 285 (October 13) and 286 (October 14) as the respective anthelmintic treatments B, C and D are used in the case TS; on the contrary, the latter is preferred to the former at intervention instants $\tau_0 > 293$, 285 and 286. This behavior is also noted in Figures 4.18 and 4.19, where we make the effectiveness and cost of intervention depend on $\tau^{-1}eff^s(\tau_0)$ and $\tau^{-1}cost^s(\tau_0)$, respectively. For example, if we focus on anthelmintic treatment C, grazing strategy UM is preferred to grazing strategy TS for intervention instants $\tau_0 < 278$ (October 6), and the latter is preferred to the former in the case of intervention instants $\tau_0 > 281$ (October 9). For grazing strategy TS, it is seen in Figure 4.16 (respectively, Figure 4.17) that the probability $\sum_{m=0}^{3} \pi_m^{TS}(\tau_0;\tau)$ (respectively, $\sum_{m=8}^{11} \pi_m^{TS}(\tau_0;\tau)+\pi_{-1}^{TS}(\tau_0;\tau)$) appears to behave as an increasing (respectively, decreasing) function of the intervention instant τ_0 as $\tau_0 < 346$ (December 13) and 338 (December 5) if the anthelmintic treatment B and anthelmintic treatments C or D are administered to the host (respectively, $\tau_0 < 309$ (November 6), 308 (November 5) and 339 (December 6) if anthelmintic treatments B, C and D are used); moreover, its variation over time seems to be more apparent in agreement with the three periods of maximum pasture contamination; that is, with 42.0 L_3 kg^{-1} DM (by mid-February), 68.0 L_3 kg^{-1} DM (by June 2) and 80.0 L_3 kg^{-1} DM (between October and November) as maximum values of infective larvae on herbage. Figure 4.16 (respectively, Figure 4.17) allows us to remark that, in comparison with the case TS, these periods of maximum pasture contamination influence in an opposite manner on the effectiveness (respectively, cost of intervention) in grazing strategies UM and TM.

An interesting question concerns the comparative analysis between the mass functions $\{\pi_m^s(\tau_0;\tau) : m \in \{-1\} \cup \mathcal{S}\}$ of the parasite burden at age $\tau = 1$ year in grazing strategies UM, TS and TM, and the corresponding mass function $\{\pi_m^{US}(\tau) : m \in \{-1\} \cup \mathcal{S}\}$ in the case of no intervention (see also Figure 4.13, which is related to the case TI). In Figure 4.20, we first focus on this question as intervention is prescribed at age $\tau_0 = 170$ in grazing strategies UM, TS and TM, with the anthelmintic treatment B (*ivermectin*) in the cases TS and TM. We may note that the

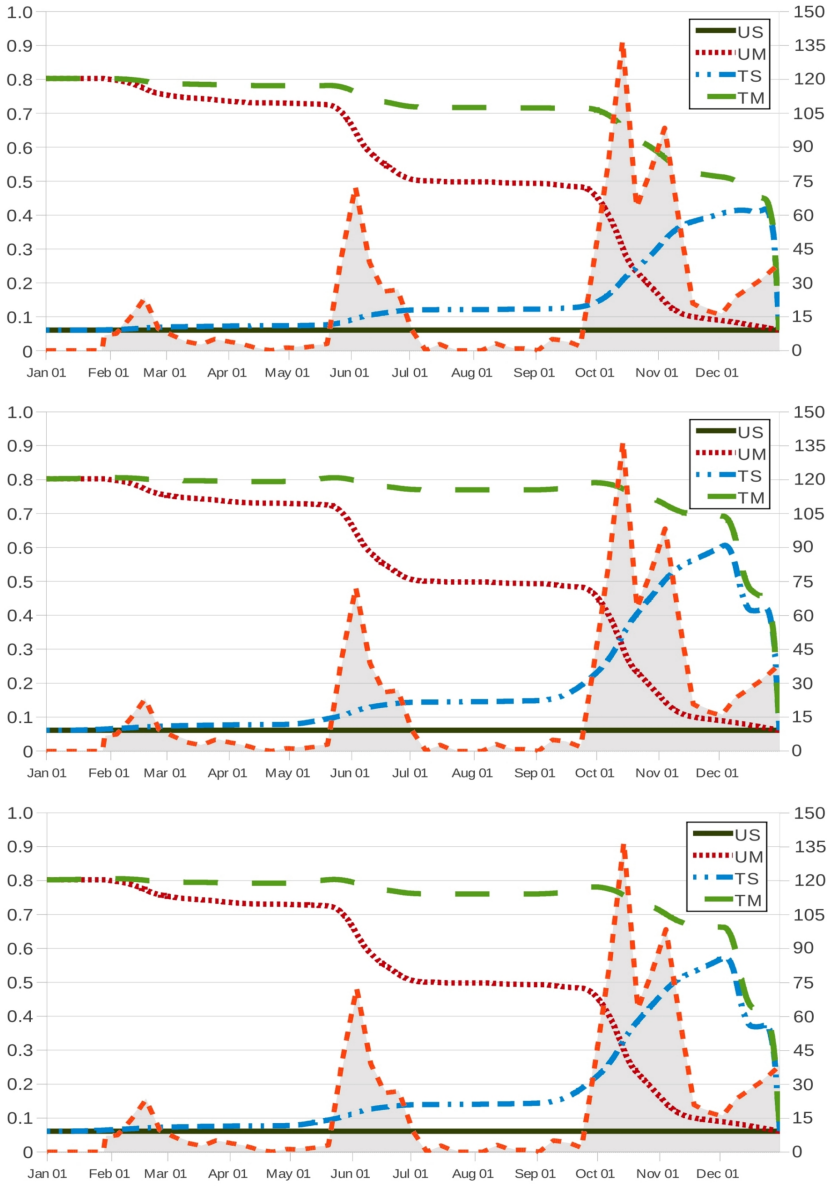

Fig. 4.16. The age-dependent probability $\sum_{m=0}^{3} \pi_m^s(\tau_0;\tau)$ as a function of τ_0 for $\tau = 1$ year, and increments in the number of L_3 infective larvae on the small intestine (*shaded* area, *right* vertical axis). Scenario US, and grazing strategies UM, TS and TM; anthelmintic treatments B, C and D (*from top to bottom*). Parasite: *Nematodirus* spp.

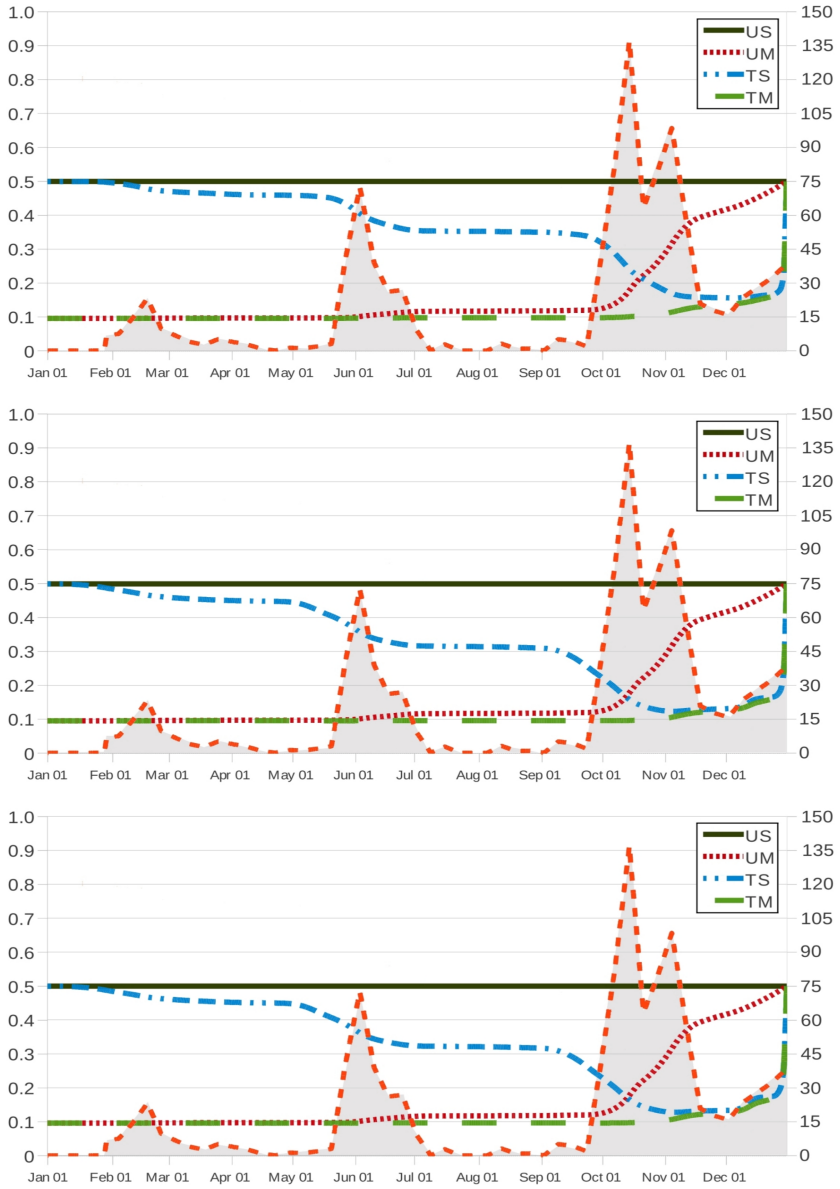

Fig. 4.17. The age-dependent probability $\sum_{m=8}^{11} \pi_m^s(\tau_0;\tau)+\pi_{-1}^s(\tau_0;\tau)$ as a function of τ_0 for $\tau = 1$ year, and increments in the number of L_3 infective larvae on the small intestine (*shaded* area, *right* vertical axis). Scenario US, and grazing strategies UM, TS and TM; anthelmintic treatments B, C and D (*from top to bottom*). Parasite: *Nematodirus* spp.

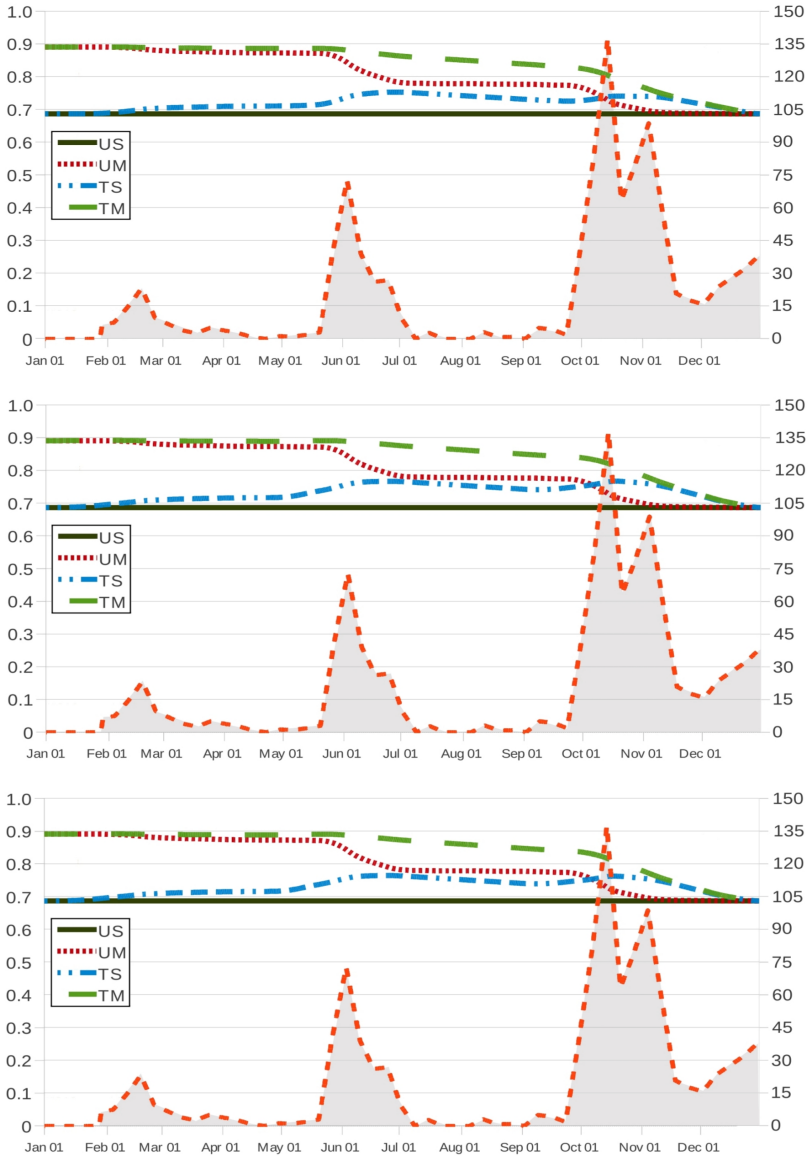

Fig. 4.18. The expected proportions $\tau^{-1}eff^s(\tau_0)$ as a function of τ_0 for $\tau = 1$ year, and increments in the number of L_3 infective larvae on the small intestine (*shaded* area, *right* vertical axis). Scenario US, and grazing strategies UM, TS and TM. Anthelmintic treatments B, C and D (*from top to bottom*). Parasite: *Nematodirus* spp.

intervention instant $\tau_0 = 170$ is derived for probabilities $p_1 = 0.5$ (Criterion 1) and $p_2 \in \{0, 15, 0.2, 0.25\}$ (Criterion 2) in grazing strategy UM with $p = 0.1$ (Table 4.8), and for $p_1 \in \{0.5, 0.6, 0.7\}$ (Criterion 1) and $p_2 \in \{0.15, 0.2, 0.25\}$ (Criterion 2) in grazing strategy TM with $p = 0.1$ (Tables 4.9 and 4.10). However, the selection $\tau_0 = 170$ is not feasible for values $p_1 \in \{0.5, 0.6, 0.7\}$, $p_2 \in \{0.15, 0.2, 0.25\}$ and $p \in \{0.1, 0.2, ..., 0.7\}$ in grazing strategy TS, which is closely related to the apparent similarity between the values $\pi_m^{US}(\tau)$ and $\pi_m^{TS}(\tau_0; \tau)$ for every infection level $m \in \{-1\} \cup \mathcal{S}$.

In Figure 4.21, we plot the mass function of the parasite burden $M(\tau)$ at age $\tau = 1$ year in scenario US versus its counterpart in grazing strategy TM, when animals are treated with *ivermectin*, *fenbendazole* and *albendazole* at ages $\tau_0 = 170$, 273 and 272, respectively. By Tables 4.9 and 4.10, ages $\tau_0 = 170$, 273 and 272 are all feasible intervention instants, which leads us to mass functions that are essentially comparable in magnitude. On the contrary, shape and magnitudes of the mass function in grazing strategy TM are dramatically different form the shape and magnitudes in scenario US, where no intervention is prescribed, irrespectively of the anthelmintic product.

4.4 Conclusions

Seasonal changes are usually cyclic and arguably represent the strongest and most ubiquitous source of external variation influencing population dynamics; see [6, 55] and their references. We refer the reader to [69, Chapter 5] for a good summary of models in a range of infectious diseases that show how seasonally varying parameters act as a forcing mechanism, and their dynamical consequences. Despite the pervasive nature of seasonality, exploring its consequences poses a challenge for biologists and ecologists because empirical seasonal fluctuations often generate complex stochastic mathematical models. In the present thesis, we contribute to the subject by investigating the effects of seasonal variations upon the distribution of the parasite load of a single host. We use nonhomogeneous Poisson patterns to model the stochastic processes governing the acquisition of parasites, the natural and parasite-induced host mortality, and the reproduction and death

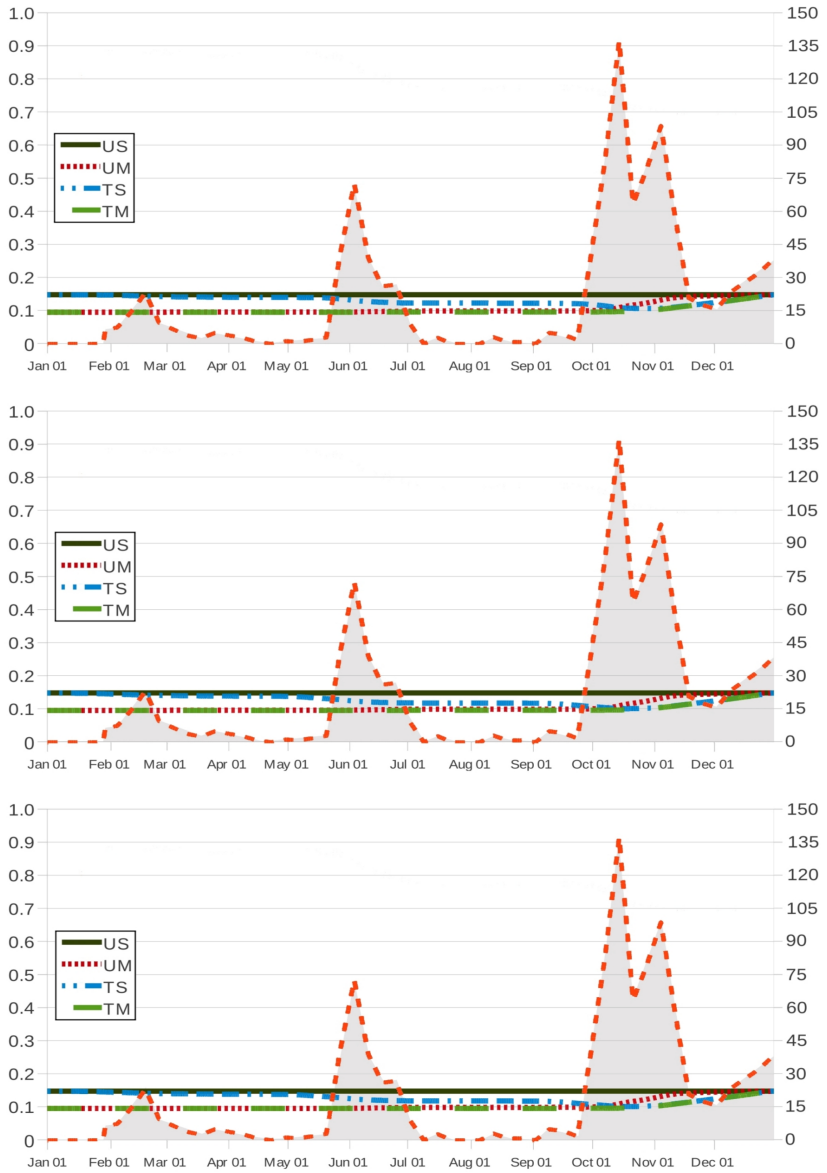

Fig. 4.19. The expected proportions $\tau^{-1} cost^s(\tau_0)$ as a function of τ_0 for $\tau = 1$ year, and increments in the number of L_3 infective larvae on the small intestine (*shaded* area, *right* vertical axis). Scenario US, and grazing strategies UM, TS and TM. Anthelmintic treatments B, C and D (*from top to bottom*). Parasite: *Nematodirus* spp.

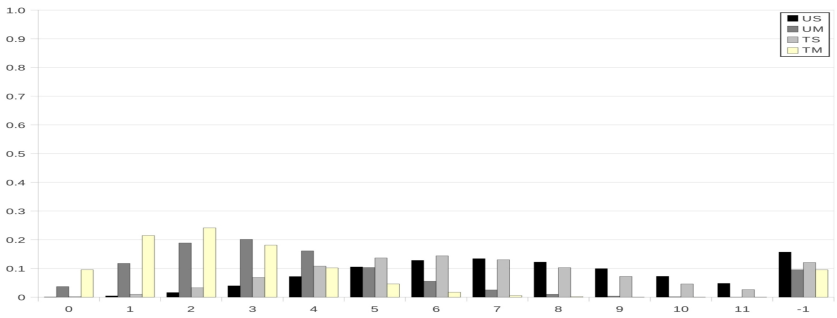

Fig. 4.20. The mass function of the parasite burden $M(\tau)$ at age $\tau = 1$ year. Scenario US, and grazing strategies UM, TS and TM (*from left to right*); anthelmintic treatment B. Intervention instant $\tau_0 = 170$. Parasite: *Nematodirus* spp.

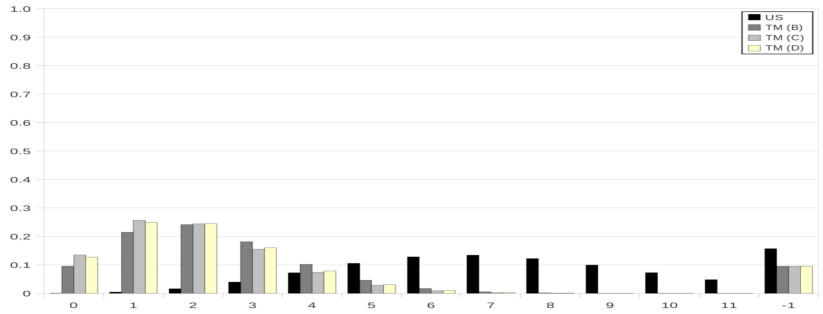

Fig. 4.21. The mass function of the parasite burden $M(\tau)$ at age $\tau = 1$ year. Scenario US, and grazing strategy TM with anthelmintic treatments B, C and D (*from left to right*). Intervention instants $\tau_0 = 170$, 273 and 272 for grazing strategy TM with anthelmintic treatments B, C and D, respectively. Parasite: *Nematodirus* spp.

of parasites within the host. As in early work by Herbet and Isham [61], and Isham [68], exact algebraic results are possible. An important feature of the analysis in the basic model (Section 4.1) is that the underlying processes $\mathcal{X}$ and $\mathcal{Y}$, recording the number $M(t)$ of parasites infecting the host at an arbitrary time $t \in [0, \tau_0) \cup [\tau_0, \tau]$, can be thought of as age-dependent versions of a pure birth process with killing, and a pure death process with killing, respectively, which are both defined on a finite state space $\{-1\} \cup \mathcal{S}$.

For practical use, a fixed value of τ might amount to the periodic occurrence of a certain event, such as an annual inspection. In such a case, the time instant $t = 0$ does not necessarily correspond

to the host birth instant, and the initial parasite burden might be positive, instead of null. Our approach then requires the solution of (4.1) and (4.2) under the assumption of initial conditions with $\pi_0(0) < 1$, in a similar manner to the solution derived in Section 4.3 for the second free-living interval $[\tau_5, \tau]$. In the absence of inter-inspection preventive actions, the outcome most likely to succeed is frequently the death of the host, or a parasite load that will not permit the host to develop immunity to the parasite infection. It is therefore important to define control strategies based intervention at a certain age $\tau_0 < \tau$. Intervention in Subsection 4.3.3 means isolation and vaccination of the host, whereas it means either movement to a paddock with safe pasture or anthelmintic treatment of the host in Subsection 4.3.4. For the resulting strategies (TI, TI+S, UM, TS, and TM) the selection of τ_0 implies to distinguish between the free-living interval $[0, \tau_0)$ and the post-intervention interval $[\tau_0, \tau]$, which are related to changes in the susceptibility of the host to the natural and parasite-induced mortality, as well as in the stochastic processes that govern the acquisition of parasites, and the reproduction and death of parasites within the host. From an applied perspective, periodical variations in the biology of hosts and parasites suggest that, in devising an evasive strategy [21, Section 2.2], the selection of the age τ_0 should rely on probabilistic principles that incorporate the role of seasonality into the mathematical model.

In a first step, we use in Section 4.2 a simple probabilistic principle to identify a set $I_{\geq m'}$ of potential vaccination instants. The set $I_{\geq m'}$ reflects a plausible level of intervention, and it results from concrete specifications of the threshold m' and the probability $p \in (0, 1)$. In a second step, we present two lines of reasoning to determine the time instant $t_0 \in I_{\geq m'}$ that adequately balances the effectiveness and cost of vaccination. Effectiveness and cost of vaccination are measured in Section 4.2 in terms of the probability $\pi_0(\tau_0; \tau)$ that the host is alive and parasite free, and the probability $\pi_{-1}(\tau_0; \tau)$ that the host does not survive, respectively, at age τ. This means that we should translate the minimum level of effectiveness and the maximum cost of vaccination into certain probabilities p_1 and p_2. For illustrative purposes, we consider

in Section 4.2 a simple host-parasite model defined by sinusoidal functions, in a similar manner to [6, 55].

The problem of how empirical data can lead us to concrete specifications of the age-dependent rates $\lambda_m(t)$, $\delta_m(t)$ and $\eta_m(t)$ is addressed in Section 4.3, where control strategies and criteria are applied to the development of GI nematode infection in growing lambs. The degree of nematode infection acquired by the grazing animal is determined by a number of factors, which are to some extent inter-related. These factors include the direct and indirect effect of seasonal conditions, which determine the availability of both infection and physiological state of the animal. The effects of parasite infection may be modified by nutrition but are nevertheless directly related to the number of parasites present, which since each worm must be separately ingested, broadly reflects the number of infective larvae on pasture, and vice versa.

It is of fundamental importance in the development of GI nematode infection in sheep to understand the role of grazing management in reducing anthelmintic use and improving helminth control. With empirical data of [90, 128], we present a valuable modeling framework for better understanding the host-macroparasite interaction under fluctuations in time, which arguably represents the most realistic setting for assessing the impact of seasonal changes in the parasite burden of a growing lamb. Grazing strategies UM, TI, TI+S, TS and TM in Section 4.3 are defined in terms of movement to safe/uninfected pasture and/or chemotherapeutic treatment of the host at a certain age $\tau_0 \in (0, \tau)$. For a suitable choice of τ_0, we suggest to use two criteria that adequately balance the effectiveness and cost of intervention at age τ_0 by using simple stochastic principles. Specifically, each intervention instant τ_0 in Tables 4.6, 4.11 and 4.15 yields an individual-based grazing strategy for a lamb that is born, parasite-free, at time $t = 0$ (January 1, in our examples). The individual-based grazing strategies UM, TI, TI+S, TS and TM can be also thought of as *group-based* grazing strategies in the case of a flock consisting of young lambs, essentially homogeneous in age. In such a case, intervention at age τ_0 is prescribed (in accordance with a predetermined grazing strategy) by applying our methodology to a *typical* lamb that is assumed to be born, parasite-free, at a certain *average* day t'. Then, re-

sults are routinely derived by handling the set of empirical data in [128] starting from the day t', instead of day 0, since intervention at time instant $t' + \tau_0$ amounts to age τ_0 of the typical lamb in the paddock. From an applied perspective, the descriptive model in this chapter becomes a prescriptive model as the set of empirical data [128, Figure 2] is appropriately replaced by a set of data derived by taking the average of annual empirical data from historical records.

Appendix

Operator splitting techniques

In analyzing grazing strategies TS and TM in Subsection 4.3.4, we use a variant of the Strang-Marchuk splitting approach discussed by Faragó et al. [53], which suggests to split the original problem (4.13) into several *subsystems* that are solved cyclically one after the other. The approach in [53, Section 1.3] is of particular interest when, for a certain splitting $\mathbf{B}(t) = \mathbf{U}(t) + \mathbf{V}(t)$, the time-dependent linear systems of differential equations

$$\frac{d}{dt}\mathbf{\Pi}^s(\tau_0; t) = \mathbf{U}(t)\mathbf{\Pi}^s(\tau_0; t), \quad \tau_0 \le t \le \tau,$$
$$\frac{d}{dt}\mathbf{\Pi}^s(\tau_0; t) = \mathbf{V}(t)\mathbf{\Pi}^s(\tau_0; t), \quad \tau_0 \le t \le \tau,$$

can be accurately and efficiently solved, which is our case here.

We consider the splitting $\mathbf{B}(t) = \mathbf{U}(t) + \mathbf{V}(t)$, where $\mathbf{U}(t)$ is given by

$$\begin{pmatrix} -(\lambda_0(t) + \delta_0(t)) & & & & \\ \lambda_0(t) & -(\lambda_1(t) + \delta_1(t)) & & & \\ & \ddots & \ddots & & \\ & & & \lambda_{M_0-1}(t) & -(\lambda_{M_0}(t) + \delta_{M_0}(t)) \end{pmatrix},$$

and

$$\mathbf{V}(t) = \begin{pmatrix} 0 & \eta_1(t) & & & \\ -\eta_1(t) & \eta_2(t) & & & \\ & \ddots & \ddots & & \\ & & -\eta_{M_0-1}(t) & \eta_{M_0}(t) & \\ & & & -\eta_{M_0}(t) & \end{pmatrix},$$

and we evaluate numerically the transient solution $\pi_m^s(\tau_0;t)$ at instants $t \in \{\tau_0, \tau_0+1, ..., \tau\}$ by solving a sequence of four time-dependent linear subsystems of differential equations.

In order to determine the probabilities $\pi_m^s(\tau_0;\tau_0+1)$ for levels $m \in \mathcal{S}$ and a certain grazing strategy s with $s \in \{TS, TM\}$, we first select the splitting time-step as $\Delta t = N^{-1}$ with $N = 10^3$, and introduce the notation

$$a_n = \tau_0 + (n-1)\Delta t, \quad n \in \{1, 2, ..., N+1\}, \tag{4.14}$$

$$b_n = \tau_0 + (n-0.5)\Delta t, \quad n \in \{1, 2, ..., N\}. \tag{4.15}$$

At step n with $n \in \{1, 2, ..., N\}$, we solve the subsystems $(S_1)_n$, $(S_2)_n$, $(S_3)_n$ and $(S_4)_n$ cyclically on successive intervals of length Δt, using the solution of one subsystem as the initial condition of the other one as follows:

$$\text{Subsystem } (S_1)_n \equiv \begin{cases} \frac{d}{dt}\boldsymbol{\Pi}_1^s(a_n;t) = \mathbf{U}(t)\boldsymbol{\Pi}_1^s(a_n;t), \ a_n \le t \le b_n, \\ \\ \boldsymbol{\Pi}_1^s(a_n;a_n) = \begin{cases} \boldsymbol{\Pi}^s(\tau_0;\tau_0), & \text{if } n=1, \\ \boldsymbol{\Pi}_4^s(b_{n-1};a_n), & \text{if } 2 \le n \le N. \end{cases} \end{cases}$$

$$\text{Subsystem } (S_2)_n \equiv \begin{cases} \frac{d}{dt}\boldsymbol{\Pi}_2^s(a_n;t) = \mathbf{V}(t)\boldsymbol{\Pi}_2^s(a_n;t), \ a_n \le t \le b_n, \\ \\ \boldsymbol{\Pi}_2^s(a_n;a_n) = \boldsymbol{\Pi}_1^s(a_n;b_n). \end{cases}$$

$$\text{Subsystem } (S_3)_n \equiv \begin{cases} \frac{d}{dt}\boldsymbol{\Pi}_3^s(b_n;t) = \mathbf{V}(t)\boldsymbol{\Pi}_3^s(b_n;t), \ b_n \le t \le a_{n+1}, \\ \\ \boldsymbol{\Pi}_3^s(b_n;b_n) = \boldsymbol{\Pi}_2^s(a_n;b_n). \end{cases}$$

$$\text{Subsystem } (S_4)_n \equiv \begin{cases} \frac{d}{dt}\boldsymbol{\Pi}_4^s(b_n;t) = \mathbf{U}(t)\boldsymbol{\Pi}_4^s(b_n;t), \ b_n \le t \le a_{n+1}, \\ \\ \boldsymbol{\Pi}_4^s(b_n;b_n) = \boldsymbol{\Pi}_3^s(b_n;a_{n+1}). \end{cases}$$

This procedure results in the solution at $t = \tau_0 + 1$, which is given by $\boldsymbol{\Pi}^s(\tau_0;t) = \boldsymbol{\Pi}_4^s(b_N;a_{N+1})$ since $a_{N+1} = \tau_0 + 1$. Then, we may proceed similarly in the numerical evaluation of the transient solution at subsequent time instants $t = \tau_0 + k$ with $k \ge 2$ and $\tau_0 + k \le \tau$, by replacing τ_0 by $\tau_0 + k$ in Equations (4.14) and (4.15), so that the solution of the previous subsystems at time instant $t = \tau_0 + k - 1$ is now used as initial condition in the subsystem $(S_1)_n$ at step $n = 1$. We refer the reader to [53] for qualitative properties of the operator splitting approach and convergence order.

Solutions to $(S_1)_n$, $(S_2)_n$, $(S_3)_n$ and $(S_4)_n$

For grazing strategy $s \in \{TS, TM\}$, the entries $\pi_m^s(a_n;t)$, for levels $m \in \mathcal{S}$, of the vector $\boldsymbol{\Pi}_1^s(a_n;t)$ are given by Equation (4.12) for time instants $t \in [a_n, b_n]$, with τ_0 replaced by a_n, and the function $\lambda'(t)$ replaced by $\lambda(t)$ in the case TS.

The solution $\boldsymbol{\Pi}_2^s(a_n;t)$ at time instants $t \in [a_n, b_n]$ has entries

$$\pi_m^s(a_n;t) = e^{-H_m(a_n;t)}\Big(\pi_m^s(a_n;a_n) + (1-\delta_{m,M_0})\sum_{j=m+1}^{M_0} \pi_j^s(a_n;a_n) K_{m+1}^{s,M_0-j}(a_n;t)\Big), \tag{4.16}$$

where $H_m(a_n;t) = (1-\delta_{0,m})\int_{a_n}^t \eta_m(u)du$ and, starting from

$$K_{m+1}^{s,M_0-(m+1)}(a_n;t) = \int_{a_n}^t \eta_{m+1}(u) e^{\tilde{H}_{m+1}(a_n;u)} du,$$

the functions $K_{m+1}^{s,M_0-j}(a_n;t)$, for $m+2 \le j \le M_0$, can be iteratively evaluated as

$$K_{m+1}^{s,M_0-j}(a_n;t) = \int_{a_n}^t \eta_{m+1}(u) e^{\tilde{H}_{m+1}(a_n;u)} K_{m+2}^{s,M_0-j}(a_n;u) du,$$

with $\tilde{H}_m(a_n;t) = H_{m-1}(a_n;t) - H_m(a_n;t)$.

In a similar manner, the solution $\boldsymbol{\Pi}_3^s(b_n;t)$ at time instants $t \in [b_n, a_{n+1}]$ has the form of Equation (4.16), with a_n replaced by b_n. The entries $\pi_m^s(b_n;t)$, for levels $m \in \mathcal{S}$, of the solution $\boldsymbol{\Pi}_4^s(b_n;t)$ are given by Equation (4.12) for time instants $t \in [b_n, a_{n+1}]$, with τ_0 replaced by b_n, and $\lambda'(t)$ replaced by $\lambda(t)$ in the case TS.

References

1. Abate J, Whitt W (1995) Numerical inversion of Laplace transforms of probability distributions. ORSA Journal on Computing 7:36-43.
2. Abbott KA, Taylor MA, Stubbings LA (2012) Sustainable worm control strategies for sheep, fourth edition. A technical manual for veterinary surgeons and advisers. SCOPS.
3. Ali SW, Cosner C (1995) Models for the effects of individual size and spatial scale on competition between species in heterogeneous environments. Mathematical Biosciences 127:45-76.
4. Allen EJ (1999) Stochastic differential equations and persistence time for two interacting populations. Dynamics of Continuous, Discrete and Impulsive Systems 5:271-281.
5. Allen LJS (2003) An introduction to stochastic processes with applications to biology. Pearson Education, New Jersey.
6. Altizer S, Dobson A, Hosseini P, Hudson P, Pascual M, Rohani P (2006) Seasonality and the dynamics of infectious diseases. Ecology Letters 9:467-484.
7. Amador J, Artalejo JR (2013) Modeling computer virus with the BSDE approach. Computer Networks 57:302-316.
8. Anderson RM, May RM, Gupta S (1989) Non-linear phenomena in host-parasite interactions. Parasitology 99:S59-S79.
9. Anderson RM, May RM (1992) Infectious diseases of humans: dynamics and control. Oxford University Press, Oxford.
10. Anderson WJ (1991) Continuous-time Markov chains. An applications-oriented approach. Springer-Verlag, New York.
11. Artalejo JR, Economou A, López-Herrero MJ (2010) The maximum number of infected individuals in SIS epidemic models: computational techniques and quasi-stationary distributions. Journal of Computational and Applied Mathematics 233:2563-2574.
12. Artalejo JR, Gómez-Corral A (2010) A state-dependent Markov-modulated mechanism for generating events and stochastic models. Mathematical Methods in the Applied Sciences 33:1342-1349.
13. Artalejo JR, Gómez-Corral A, He QM (2010) Markovian arrivals in stochastic modelling: a survey and some new results. SORT - Statistics and Operations Research Transactions 34:101-144.

14. Artalejo JR (2011) On the transient behavior of the maximum level length in structured Markov chains. In: Pardo L, Balakrishnan N, Gil MA (eds) Modern mathematical tools and techniques in capturing complexity. Springer Series in Synergetics, Berlin, pp. 332-342.
15. Bailey JN, Kahn LP, Walkden-Brown SW (2009) Availability of gastrointestinal nematode larvae to sheep following winter contamination of pasture with six nematode species on the Northern Tablelands of New South Wales. Veterinary Parasitology 160:89-99.
16. Bailey NTJ (1964) The elements of stochastic processes. John Wiley & Sons, New York.
17. Bailey NTJ (1975) The mathematical theory of infectious diseases, second edition. Griffin, London.
18. Ballyk MM, Wolkowicz GSK (2011) Classical and resource-based competition: a unifying graphical approach. Journal of Mathematical Biology 62:81-109.
19. Barbour AD (1976) Quasi-stationary distributions in Markov population processes. Advances in Applied Probability 8:296-314.
20. Barger IA (1989) Genetic resistance of hosts and its influence on epidemiology. Veterinary Parasitology 32:21-35.
21. Barger IA (1997) Control by management. Veterinary Parasitology 72:493-506.
22. Barger IA (1999) The role of epidemiological knowledge and grazing management for helminth control in small ruminants. International Journal for Parasitology 29:41-47.
23. Barger IA, Le Jambre LF, Georgi JR, Davies HI (1985) Regulation of *Haemonchus contortus* populations in sheep exposed to continuous infection. International Journal of Parasitology 15:529-533.
24. Bartlett MS (1956) Deterministic and stochastic models for recurrent epidemics. In: Neyman J (ed) Proceedings of the third Berkeley symposium on mathematical statistics and probability, volume IV: contributions to biology and problems of health. University of California Press, Berkeley, pp. 81-109.
25. Bartlett MS (1960) Stochastic population models in ecology and epidemiology. John Wiley & Sons, New York.
26. Bean NG, Bright L, Latouche G, Pearce CEM, Pollett PK, Taylor PG (1997) The quasi-stationary behavior of quasi-birth-and-death processes. The Annals of Applied Probability 7:134-155.
27. Bean NG, Pollett PK, Taylor PG (2000) Quasistationary distributions for level-dependent quasi-birth-and-death processes. Stochastic Models 16:511-541.
28. Bhattacharya S, Martcheva M (2010) Oscillations in a size-structured prey-predator model. Mathematical Biosciences 228:31-44.
29. Billard L (1974) Competition between two species. Stochastic Processes and their Applications 2:391-398.
30. Bjørn H, Monrad J, Nansen P (1991) Anthelmintic resistance in nematode parasites of sheep in Denmark with special emphasis on levamisole resistance in *Ostertagia circumcincta*. Acta Veterinaria Scandinavica 32:145-154.
31. Boa ME, Thamsborg SM, Kassuku AA, Bøgh HO (2001) Comparison of worn control strategies in grazing sheep in Denmark. Acta Veterinaria Scandinavica 42:57-69.

32. Bottomley C, Isham V, Basáñez MG (2007) Population biology of multispecies helminth infection: competition and coexistence. Journal of Theoretical Biology 244:81-95.
33. Briggs CJ, Hoopes MF (2004) Stabilizing effects in spatial parasitoid-host and predator-prey models: a review. Theoretical Population Biology 65:299-315.
34. Brockwell PJ (1985) The extinction time of a birth, death and catastrophe process and of a related diffusion model. Advances in Applied Probability 17:42-52.
35. Choudhury GL, Lucantoni DM, Whitt W (1994) Multidimensional transform inversion with applications to the transient $M/G/1$ queue. Annals of Applied Probability 4:719-740.
36. Chung KL (1960) Markov chains with stationary transition probabilities. Springer, Berlin.
37. Cobbold CA, Lewis MA, Lutscher F, Roland J (2005) How parasitism affects critical patch-size in a host-parasitoid model: application to the forest tent caterpillar. Theoretical Population Biology 67:109-125.
38. Cobbold CA, Roland J, Lewis MA (2009) The impact of parasitoid emergence time on host-parasitoid population dynamics. Theoretical Population Biology 75:201-215.
39. Conlan AJK, Grenfell BT (2007) Seasonality and the persistence and invasion of measles. Proceedings of the Royal Society B 274:1133-1141.
40. Cornell SJ (2005) Modelling nematode populations: 20 years of progress. Trends in Parasitology 21:542-545.
41. Cornell SJ (2010) Modelling stochastic transmission processes in helminth infections. In: Michael E and Spear RC (eds) Modelling parasite transmission and control. Landes Bioscience and Springer Science+Business Media, LLC, New York, pp. 66-78.
42. Cushing JM (1980) Two species competition in a periodic environment. Journal of Mathematical Biology 10:385-400.
43. Darroch JN, Seneta E (1965) On quasi-stationary distributions in absorbing discrete-time finite Markov chains. Journal of Applied Probability 2:88-100.
44. Darroch JN, Seneta E (1967) On quasi-stationary distributions in absorbing continuous-time finite Markov chains. Journal of Applied Probability 4:192-196.
45. Dietz K (1976) The incidence of infectious diseases under the influence of seasonal fluctuations. Lectures Notes in Biomathematics 11:1-15.
46. Dobson RJ, Waller PJ, Donald AD (1990) Population dynamics of *Trichostrongylus colubriformis* in sheep: the effect of infection rate on the establishment of infective larvae and parasite fecundity. International Journal for Parasitology 20:347-352.
47. Edelstein-Keshet L (2005) Mathematical models in biology. SIAM, Philadelphia.
48. Ellner S (1989) Convergence to stationary distributions in two-species stochastic competition models. Journal of Mathematical Biology 27:451-462.
49. Elton CS (1924) Periodic fluctuations in the numbers of animals: their causes and effects. British Journal of Experimental Biology 2:119-163.
50. Entrocasso C, Alvarez L, Manazza J, Lifschitz A, Borda B, Virkel G, Mottier L, Lanusse C (2008) Clinical efficacy assessment of the albendazole-

ivermectin combination in lambs parasited with resistant nematodes. Veterinary Parasitology 155:249-256.
51. Eysker M, Bakker N, Kooyman FNJ, Ploeger HW (2005) The possibilities and limitations of evasive grazing as a control measure for parasitic gastroenteritis in small ruminants in temperate climates. Veterinary Parasitology 129:95-104.
52. Eysker M, Bakker N, Kooyman FNJ, van der Linden D, Schrama C, Ploeger HW (2005) Consequences of the unusually warm and dry summer of 2003 in The Netherlands: poor development of free living stages, normal survival of infective larvae and long survival of adult gastrointestinal nematodes of sheep. Veterinary Parasitology 133:313-321.
53. Faragó I, Havasi A, Horváth R (2011) On the order of operator splitting methods for time-dependent linear systems of differential equations. International Journal of Numerical Analysis and Modeling, Series B 2:142-154.
54. Gopalsamy K (1982) Age-specific coexistence in two-species competition. Mathematical Biosciences 61:101-122.
55. Grassly NC, Fraser C (2006) Seasonal infectious disease epidemiology. Proceedings of the Royal Society B 273:2541-2550.
56. Grennan EJ (1999) Lamb growth rate on pasture: effect of grazing management, sward type and supplementation. Teagasc Research Centre, Athenry, Co. Galway.
57. Gyllenberg M, Silvestrov DS (1994) Quasi-stationary distributions of a stochastic metapopulation model. Journal of Mathematical Biology 33:35-70.
58. Gyllenberg M, Silvestrov DS (2008) Quasi-stationary phenomena in nonlinearly perturbed stochastic systems. Walter de Gruyter GmbH & Co. KG, Berlin.
59. He QM, Neuts MF (1998) Markov chains with marked transitions. Stochastic Processes and their Applications 74:37-52.
60. Hein WR, Shoemaker CB, Heath ACG (2001) Future technologies for control of nematodes of sheep. New Zealand Veterinary Journal 49:247-251.
61. Herbert J, Isham V (2000) Stochastic host-parasite interaction models. Journal of Mathematical Biology 40:343-371.
62. Hitchcock SE (1986) Extinction probabilities in predator-prey models. Journal of Applied Probability 23:1-13.
63. Horn RA, Johnson CR (1985) Matrix analysis. Cambridge University Press, Cambridge.
64. Hsu SB, Hubbell SP (1979) Two predators competing for two species: an analysis of MacArthur's model. Mathematical Biosciences 47:143-171.
65. Hsu SB (1981) On a resource based ecological competition model with interference. Journal of Mathematical Biology 12:45-52.
66. Hunter JJ (1983) Mathematical techniques of applied probability. Volume 1: discrete time models, basic theory. Academic Press, New York.
67. Iglehart DL (1964) Multivariate competition processes. The Annals of Mathematical Statistics 35:350-361.
68. Isham V (1995) Stochastic models of host-macroparasite interaction. The Annals of Applied Probability 5:720-740.
69. Keeling MJ, Rohani P (2008) Modeling infectious diseases in humans and animals. Princeton University Press, Princeton.

70. Kemeny JG, Snell JL (1961) Potentials for denumerable Markov chains. Journal of Mathematical Analysis and Applications 6:196-260.
71. Kemeny JG, Snell JL, Knapp AW (1976) Denumerable Markov chains, second edition. Springer-Verlag, New York.
72. Kijima M (1997) Markov processes for stochastic modelling. Chapman & Hall, London.
73. Knox DP (2004) Technological advances and genomics in metazoan parasites. International Journal for Parasitology 34:139-152.
74. Kostova T, Li J, Friedman M (1999) Two models for competition between age classes. Mathematical Biosciences 157:65-89.
75. Lamperti J (1963) Criteria for stochastic processes. II. Passage-time moments. Journal of Mathematical Analysis and Applications 7:127-145.
76. Latouche G, Ramaswami V (1999) Introduction to matrix analytic methods in stochastic modeling. ASA-SIAM Series on Statistics and Applied Probability, Philadelphia.
77. Li B, Smith HL (2003) Periodic coexistence of four species competing for three essential resources. Mathematical Biosciences 184:115-135.
78. Li B, Smith HL (2007) Global dynamics of microbial competition for two resources with internal storage. Journal of Mathematical Biology 55:481-515.
79. Loman J (1988) A graphical solution to a one-predator, two-prey system with apparent competition and mutualism. Mathematical Biosciences 91:1-16.
80. Lotka AJ (1925) Elements of physical biology. Williams & Wilkins, Baltimore.
81. Mailleret L, Castel M, Montarry J, Hamelin FM (2012) From elaborate to compact seasonal plant epidemic models and back: is competitive exclusion in the details? Theoretical Ecology 5:311-324.
82. Maingi N, Bjørn H, Thamsborg SM, Bøgh HO, Nansen P (1996) Anthelmintic resistance in nematode parasites of sheep in Denmark. Small Ruminant Research 23:171-181.
83. Mangel M, Roitberg BD (1992) Behavioral stabilization of host-parasite population dynamics. Theoretical Population Biology 42:308-320.
84. May R, McLean A (eds) (2007) Theoretical ecology. Principles and applications. Oxford University Press, Oxford.
85. Michel JF (1985) Strategies for the use of anthelmintics in livestock and their implications for the development of drug resistance. Parasitology 90:621-628.
86. Moler C, Van Loan C (2003) Nineteen dubious ways to compute the exponential of a matrix, twenty-five years later. SIAM Review 45:1-46.
87. Moneim IA (2007) Seasonally varying epidemics with and without latent period: a comparative simulation study. Mathematical Medicine and Biology 24:1-15.
88. Murray JD (2002) Mathematical biology: I. An introduction, third edition. Springer-Verlag, New York.
89. Namba T (1986) Bifurcation phenomena appearing in the Lotka-Volterra competition equations: a numerical study. Mathematical Biosciences 81:191-212.
90. Nasreen S, Jeelani G, Sheikh FD (2007) Efficacy of different anthelmintics against gastro-intestinal nematodes of sheep in Kashmir Valley. VetScan 2, No. 1, article 13.

91. Neuts MF (1994) Matrix-geometric solutions in stochastic models: an algorithmic approach, second edition. Dover Publications, New York.
92. Nicholson AJ, Bailey VA (1935) The balance of animal populations. Part 1. Proceedings of the Zoological Society. London, pp. 551-598.
93. Nisbet RM, Gurney WSC (1982) Modelling fluctuating populations. John Wiley & Sons, New York.
94. Norris JR (2004) Markov chains. Cambridge University Press, Cambridge.
95. Pakes AG (1987) Limit theorems for the population size of a birth and death process allowing catastrophes. Journal of Mathematical Biology 25:307-325.
96. Pakes AG (1988) The supercritical birth, death and catastrophe process: limit theorems on the set of non-extinction. Journal of Mathematical Biology 26:405-420.
97. Pakes AG (1989) A complementary note on the supercritical birth, death and catastrophe process. Journal of Mathematical Biology 27:321-325.
98. Pakes AG, Pollett PK (1989) The supercritical birth, death and catastrophe process: limit theorems on the set of extinction. Stochastic Processes and Their Applications 32:161-170.
99. Parham PE, Michael E (2011) Outbreak properties of epidemic models: The roles of temporal forcing and stochasticity of pathogen invasion dynamics. Journal of Theoretical Biology 271:1-9.
100. Peeters F, Kerimoglu O, Straile D (2013) Implications of seasonal mixing for phytoplankton production and bloom development. Theoretical Ecology 6:115-129.
101. Pielou EC (1969) An introduction to mathematical ecology. Wiley-Interscience, New York.
102. Pitman JW (1977) Occupation measures for Markov chains. Advances in Applied Probability 9:69-86.
103. Pugliese A (2000) Coexistence of macroparasites without direct interactions. Theoretical Population Biology 57:145-165.
104. Renshaw E (1991) Modelling biological populations in space and time. Cambridge University Press, Cambridge.
105. Reuter GEH (1961) Competition processes. In: Neyman J (ed) Proceedings of the fourth Berkeley symposium on mathematical statistics and probability, volume II: contributions to probability theory. University of California Press, Berkeley, pp. 421-430.
106. Reynolds JJH, Sherratt JA, White A, Lambin X (2013) A comparison of the dynamical impact of seasonal mechanisms in a herbivore-plant defence system. Theoretical Ecology 6:225-239.
107. Ridler-Rowe CJ (1967) On a stochastic model of an epidemic. Journal of Applied Probability 4:19-33.
108. Ridler-Rowe CJ (1978) On competition between two species. Journal of Applied Probability 15:457-465.
109. Ridler-Rowe CJ (1988) Extinction times for certain predator-prey processes. Journal of Applied Probability 25:612-616.
110. Roozen H (1987) Equilibrium and extinction in stochastic population dynamics. Bulletin of Mathematical Biology 49:671-696.
111. Rosà R, Pugliese A, Villani A, Rizzoli A (2003) Individual-based vs. deterministic models for macroparasites: host cycles and extinction. Theoretical Population Biology 63:295-307.

112. Sayers G, Sweeney T (2005) Gastrointestinal nematode infection in sheep – a review of the alternatives to anthelmintics in parasite control. Animal Health Research Reviews 6:159-171.
113. Schreiber SJ (2006) Host-parasitoid dynamics of a generalized Thompson model. Journal of Mathematical Biology 52:719-732.
114. Shi DH, Guo J, Liu L (1996) SPH-Distributions and the rectangle-iterative algorithm. In: Chakravarthy SR, Alfa AS (eds) Matrix-analytic methods in stochastic models. Lecture notes in pure and applied mathematics, volume 183. Marcel Dekker, Inc., New York, pp. 207-224.
115. Silvestrov DS (1996) Recurrence relations for generalized hitting times for semi-Markov processes. The Annals of Applied Probability 6:617-649.
116. Sissay MM, Uggla A, Waller PJ (2007) Epidemiology and seasonal dynamics of gastrointestinal nematode infections of sheep in a semi-arid region of eastern Ethiopia. Veterinary Parasitology 143:311-321.
117. Stear MJ, Doligalska M, Donskow-Schmelter K (2007) Alternatives to anthelmintics for the control of nematodes in livestock. Parasitology 134:139-151.
118. Stone L, Olinky R, Huppert A (2007) Seasonal dynamics of recurrent epidemics. Nature 446:533-536.
119. Strom T (1975) On logarithmic norms. SIAM Journal on Numerical Analysis 12:741-753.
120. Sutherland IA, Moen IC, Leathwick DM (2002) Increased burdens of drug-resistant nematodes due to anthelmintic treatment. Parasitology 125:375-381.
121. Sutherland IA, Scott I (2010) Gastrointestinal nematodes of sheep and cattle. Biology and control. Wiley-Blackwell, Chichester.
122. Tang S, Xiao Y, Cheke RA (2008) Multiple attractors of host-parasitoid models with integrated pest management strategies: eradication, persistence and outbreak. Theoretical Population Biology 73:181-197.
123. Taylor MA, Coop RL, Wall RL (2007) Veterinary parasitology, third edition. Blackwell, Oxford.
124. Thompson WR (1924) La théorie mathématique de l'action des parasites entomophages et le facteur du hasard. Annales Faculte des Sciences de Marseille 2:69-89.
125. Tilman D (1982) Resource competition and community structure. Princeton University Press, New Jersey.
126. Trotter RF (1959) Products of semigroups of operators. Proceedings of the American Mathematical Society 10:545-551.
127. Turchin P (2003) Complex population dynsmics: a theoretical/empirical synthesis. Princeton University Press, Princeton.
128. Uriarte J, Llorente MM, Valderrábano J (2003) Seasonal changes of gastrointestinal nematode burden in sheep under an intensive grazing system. Veterinary Parasitology 118:79-92.
129. Valderrábano J, Delfa R, Uriarte J (2002) Effect of level of feed intake on the development of gastrointestinal parasitism in growing lambs. Veterinary Parasitology 104:327-338.
130. Volterra V (1931) Leçons sur la théorie mathématique de la lutte pour la vie. Gauthier-Villars, Paris.

131. Van Doorn EA, Pollet PK (2013) Quasi-stationary distributions for discrete-state models. European Journal of Operational Research. doi:10.1016/j.rjor.2013.01.032.
132. Walker DM (1998) The expected time until absorption when absorption is not certain. Journal of Applied Probability 35:812-823.
133. Waller PJ, Thamsborg SM (2004) Nematode control in 'green' ruminant production systems. Trends in Parasitology 20:493-497.
134. Wangersky PJ (1978) Lotka-Volterra population models. Annual Review of Ecology and Systematics 9:189-218.
135. White KAJ, Grenfell BT, Hendry RJ, Lejeune O, Murray JD (1996) Effect of seasonal host reproduction on host-macroparasite dynamics. Mathematical Biosciences 137:79-99.
136. Zeeman ML (1995) Extinction in competitive Lotka-Volterra systems. Proceedings of the American Mathematical Society 123:87-96.

Author Index

Subject Index

Summary

Introduction

Competition processes, as discussed by Iglehart [11] and Reuter [17], have been frequently used in biology to describe the dynamics of population models involving some kind of interaction among various species. This thesis deals with two types of interspecific relations (namely, the two-species competition and the host-parasite interactions) which are closely related to the competition process by Reuter [17]. In [17], a general stochastic framework is presented in order to reflect two-species interaction in terms of a time-homogeneous continuous-time Markov chain (CTMC) $\mathcal{X} = \{X(t) = (M(t), N(t)) : t \geq 0\}$ on the state space $\mathcal{S} = \mathbb{N}_0 \times \mathbb{N}_0$, where $M(t)$ and $N(t)$ are defined as the population sizes of two species coexisting in an ecosystem. Possible jumps of $\mathcal{X}$ from a given state (m, n) are only permitted to some adjacent states (m', n') in such a way that the possibly non-null transitions rates are given by

$$q_{(m,n),(m',n')} = \begin{cases} a_{(m,n)}, & \text{if } (m', n') = (m+1, n), \\ b_{(m,n)}, & \text{if } (m', n') = (m, n+1), \\ c_{(m,n)}, & \text{if } (m', n') = (m-1, n), \\ d_{(m,n)}, & \text{if } (m', n') = (m, n-1), \\ e_{(m,n)}, & \text{if } (m', n') = (m-1, n+1), \\ f_{(m,n)}, & \text{if } (m', n') = (m+1, n-1), \end{cases}$$

where $a_{(m,n)}$, $b_{(m,n)}$, $c_{(m,n)}$, $d_{(m,n)}$, $e_{(m,n)}$ and $f_{(m,n)}$ are non-negative constants for $(m, n) \in \mathcal{S}$. Moreover, the condition

$$\begin{aligned} q_{(m,n)} &= -q_{(m,n),(m,n)} \\ &= a_{(m,n)} + b_{(m,n)} + c_{(m,n)} + d_{(m,n)} + e_{(m,n)} + f_{(m,n)} \end{aligned}$$

results in a conservative infinitesimal generator $\mathbf{Q}$.

In this setting, the two-species competition process is presented by Reuter [17, Example 1] as an example of Type I process (i.e., states in the axes are absorbing states, and $\mathcal{C} = \mathbb{N} \times \mathbb{N}$ is an irreducible class of transient states), where transition rates are defined by

$$\begin{aligned} a_{(m,n)} &= \alpha m, \quad & b_{(m,n)} &= \beta n, \quad & c_{(m,n)} &= \gamma mn, \\ d_{(m,n)} &= \delta mn, \quad & e_{(m,n)} &= 0, \quad & f_{(m,n)} &= 0, \end{aligned} \tag{S.1}$$

for strictly positive constants α, β, γ and δ. Although this specification does not lead us to a Type I process (since states of the form $(m, 0)$ and $(0, n)$ are not absorbing), it is suggested in [17] to *freeze* states $(m, 0)$ and $(0, n)$ by making $q_{(m,0),(m',n')} = 0$ and $q_{(0,n),(m',n')} = 0$, for $(m', n') \in \mathcal{S}$ and $m, n \geq 0$. This means that the state space becomes $\mathcal{S} = \mathbb{N}_0 \times \mathbb{N}_0 - \{(0, 0)\}$, since the state $(0, 0)$ is accessible only from the positive axes. The resulting process was widely studied by Ridler-Rowe [18], and is related to an ecosystem where individuals of two different species compete either directly or indirectly for common resources. As the total size of the ecosystem increases, the maintenance of stable growth conditions becomes unsustainable because of the *environmental pressure* (by overcrowding) and, consequently, births and deaths in both species depend strongly on the population sizes of one or both of the species. Note that the ecosystem in [18] is closed, in the sense that no immigration or emigration is supposed to take place, that is, $e_{(m,n)} = f_{(m,n)} = 0$.

In analyzing the extinction time and the size of the surviving species, the quadratic terms in the transition rates of the process defined by (S.1) make the solution intractable from an analytical point of view; see [18, Section 2]. One way of analyzing the process is to approximate its behavior, as the initial population sizes become large, by an essentially deterministic motion with a random diffusion of smaller order superimposed upon it. The techniques used by Ridler-Rowe [18] yield the asymptotic distribution of the position at which the process first hits the subset of absorbing

states, and a limit result for the probability that a given species should survive the other.

A process modeling host-parasite interaction is presented by Hitchcock [10, Model 1] by using the transition rates

$$\begin{aligned} a_{(m,n)} &= 0, \quad b_{(m,n)} = \lambda n, \quad c_{(m,n)} = \beta m, \\ d_{(m,n)} &= 0, \quad e_{(m,n)} = 0, \quad f_{(m,n)} = \alpha mn, \end{aligned} \tag{S.2}$$

where α, β and λ are strictly positive constants, and transition rates $q_{(m,0),(m',n')} = q_{(0,n),(m',n')} = 0$, which means that the process is of Type I. More concretely, the interspecific interaction described in [10] by (S.2) belongs to a special subclass of host-parasite models where parasites are called *parasitoids*, since hosts that are successfully parasitized die. In (S.2), transitions from a given state (m, n) to state (m', n') with $(m', n') = (m - 1, n)$, $(m, n + 1)$ and $(m + 1, n - 1)$ amount to the death of a parasite, birth of a host, and parasitism, respectively.

Our interest is in the Hitchcock process [10], which is uniquely specified in terms of its transition rates $q_{(m,n),(m',n')}$ given by (S.2), and where time delays are ignored. The process is modeled by a time-homogeneous CTMC $\mathcal{X} = \{X(t) = (M(t), N(t)) : t \geq 0\}$ defined on $\mathcal{S} = \mathbb{N}_0 \times \mathbb{N}_0 - \{(0, 0), (1, 0)\}$, where $M(t)$ and $N(t)$ record the numbers of parasitoids and hosts alive at time t, respectively. By using criteria developed by Reuter [17], Hitchcock [10] showed that ultimate extinction of either parasitoids or hosts is certain and that, given initial numbers of m parasitoids and n hosts, the expected time $\tau_{(m,n)}$ to the first extinction is always finite. Based on the general epidemic model [3] where $M(t)$ and $N(t)$ amount to the numbers of infected and susceptible individuals alive at time t, respectively, an exact expression is derived in [10, Section 3] for the probability that the parasitoid population is the first to become extinct in the special case $\lambda = 0$. These probabilities are then used to derive power series approximations to extinction probabilities when the host birth rate λ is strictly positive, and a similar method of approximation is applied to estimate the mean number of events before the first extinction occurs; see [10, Sections 4 and 5]. By means of an alternative construction – using Reuter's criterion [17] together a simple minimization result – Ridler-Rowe [19] proved that the mean extinction time $\tau_{(m,n)}$ tends to zero as

the combined initial population of parasitoids and hosts $m + n$ becomes large.

Parasitism is one of the factors believed to have a major impact on competitive interactions, but parasites might exhibit a wide degree of variability between species in the level of harm or damage they cause to their hosts. Parasites are commonly classified (see [21]) in two groups: *microparasites*, such as viruses, bacteria or protozoa; and *macroparasites* (helminths). The main difference between them is that microparasites multiply directly within their host, whereas macroparasites grow within their host but multiply by producing infective stages which are released into the environment to infect new hosts. For macroparasites, the burden of worms in an individual host is the unit of study.

As a variant of the standard host-parasite interaction, we deal with host-macroparasite interactions that can be modeled by birth and death processes with killing with rates varying throughout time. Unlike the Ridler-Rowe process [18] and the Hitchcock process [10] where $\mathcal{X}$ is a bivariate time-homogeneous CTMC, we shall consider now the univariate time-inhomogeneous CTMC $\mathcal{X} = \{M(t) : 0 \leq t \leq \tau\}$ where $M(t)$ records the number of parasites within the host (for practical use, the infection level of the host, which is caused by the presence of parasites), and τ might amount to the periodic occurrence of a certain event, such as an annual inspection. The CTMC $\mathcal{X}$ is defined on $\{-1\} \cup \mathcal{S}$ with $\mathcal{S} = \{0, \ldots, M_0\}$, where state -1 represents that the host is dead (or its level of infection is unacceptable) and state M_0 amounts to a critical value that means the impossible recovery of the host if that level of infection M_0 is exceeded. Seasonal conditions in our model are reflected by means of state-dependent nonhomogeneous Poisson processes associated with the acquisition of parasites, the reproduction and death of parasites within the host, and the natural (no parasite-induced) and parasite-induced host mortality.

Objectives

In this thesis, we focus on the use of stochastic models in order to describe the two-species competition interaction and the

host-parasite relationship. Specifically, our aim is to apply matrix-analytic methods [13, 16] in order to study probabilistic descriptors of the Ridler-Rowe process (Chapter 2), the Hitchcock process (Chapter 3), and the host-macroparasite interaction arising in the development of gastrointestinal (GI) nematode infection in sheep (Chapter 4).

Here is a list of specific objectives:

(i) To characterize the distribution of the maximum population size in the Ridler-Rowe process and the Hitchcock process. In addition, to compare the dynamics of the model during an extinction cycle and during a fixed time interval.

(ii) To use absorbing Markov chains defined on a finite state space in order to approximate the joint distribution of the extinction time, the identity of the species becoming extinct and the size of the surviving species in the Ridler-Rowe process, as well as other related measures such as the numbers of births and deaths, and the survival of a certain individual. In addition, to propose a criterion for the selection of the state space cardinality in terms of the maximum population size distribution.

(iii) To incorporate more realistic distributional assumptions in the Hitchcock process by dealing with events generated by non-exponential correlated flows, but keeping the dimensionality of the underlying Markov chain model tractable.

(iv) To investigate structural properties of the Hitchcock process and its BSDE variants, such as regularity, classification of states and extinction times.

(v) To reflect seasonal conditions in host-macroparasite models by means of state-dependent nonhomogeneous Poisson processes associated with the acquisition of parasites, the reproduction and death of parasites within the host, and the natural and parasite-induced host mortality.

(vi) To specify control criteria that appropriately balance effectiveness and cost of intervention and, from an applied perspective, to apply these criteria to the seasonal changes of GI nematode burden in growing lambs.

(vii) To develop algorithmic techniques allowing us to compute the resulting solutions in an efficient and accurate manner.

(viii) To develop a wide range of numerical experiments to analyze the main features of the two-species competition interaction, and the host-parasite and host-macroparasite relationships, as well as to compare the resulting solution with existing results and results obtained by simulation.

Research contents: Results and conclusions

In Chapter 1, we briefly comment on the existing literature on competition processes. By means of the general framework by Reuter [17], we present the two-species competition process, the prey-predator relation, the host-parasite interaction and epidemic models as particular cases.

In Chapter 2, the two-species competition process is the process under study. We consider the distribution of the extinction times, as well as the joint distribution of the identity of the species becoming extinct and the size of the surviving species. Our approach is mainly based on the replacement of the underlying absorbing Markov chain $\mathcal{X}$, which is a random walk in the quarter plane $\mathcal{S} = \mathbb{N}_0 \times \mathbb{N}_0 - \{(0,0)\}$, by a suitably defined finite Markov chain $\mathcal{X}(K)$, which is defined on those states $(m,n) \in \mathcal{S}$ such that the combined population of individuals $m+n$ is not greater than the value K. This means that, for a large enough value of K, we examine the process $\mathcal{X}$ till absorption under the taboo that sates (m,n) verifying $m+n > K$ are not accessible. The truncating process is based on the selection of K as a percentile K_q of the distribution of the maximum number X_{max} of individuals in the ecosystem during an extinction cycle. This simple truncating principle permits us to approximate a countable phase (PH) distribution (related to the extinction time) by a finite PH distribution in such a way that the probability q can be seen as a measure of global error control. To support our selection criterion, we carry out a wide range of numerical examples, which allow us to remark that the Normal result in [18] and the approximating process $\mathcal{X}(K_q)$ lead to significantly different results. In view of our numerical work, we conclude that we expect higher accuracy for moderate initial population sizes when, instead of the asymptotic solution [18], we

use the approximating process $\mathcal{X}(K_q)$. One of the main advantages of $\mathcal{X}(K_q)$ is related to the fact that it allows us to approximate the joint distribution of the extinction time T, the identity of the species becoming extinct and the number of individuals alive in the surviving species at time T, as well as to deal with non-degenerate probability distributions for initial population sizes. However, it is clear that, from a computational point of view, the Normal solution yields a simpler formula. The limit result in [18] is close enough to the true mass function of $X(T)$ when the initial population sizes become large, but it does not depend on the birth rates α and β. On the other hand, the solution based on $\mathcal{X}(K_q)$ does depend on the birth rates α and β, but it is defined on a finite state space $\mathcal{S}(K_q)$. The incidence of the finiteness of $\mathcal{S}(K_q)$ on the resulting solution is attenuated by a suitable selection of the level K_q, which is based on a key descriptor X_{max} that appropriately describes the effects of overpopulation on the ecosystem.

Our approximation method is also applied to the study of the number of births and deaths happening until extinction, and the survival of a certain individual. First, we derive the joint distribution of the extinction time $T^{(M,N)}$, and the numbers of births $B_1^{(M,N)}$ and $B_2^{(M,N)}$, and of deaths $D_1^{(M,N)}$ and $D_2^{(M,N)}$ occurring during an extinction cycle, provided that the extinction cycle starts from an initial population size $X(0) = (M, N)$. Then, the effects of the killing strategy on the survival of an individual are analyzed under various random and age-dependent assumptions. Our results are illustrated and the accuracy of our solution is tested with reference to simulated data. Numerical examples are presented to show the influence of the numbers of births and deaths on the dynamics of the two-species competition process and the survival of an individual. In the numerical work, our interest is in 12 scenarios where the per capita birth and death rates in each species are comparable in magnitude. These scenarios yield small and moderate levels of K_q in our solution, even if the value $q = 0.999$ is selected. The algorithms we present are seen to work well both regard to numerical accuracy and speed for moderate initial population sizes. However, if the *birth drift* of the process $\mathcal{X}$ (suitably defined from the birth rates α and β) is noticeably greater than its *death* counterpart (defined in terms of the death rates γ and

δ), a larger cardinality of the set $\mathcal{S}(K_q)$ of states will imply more demanding memory requirements. The use of quasi-stationary vectors, as initial probability distribution over $\mathcal{S}(K_q)$, results in an increase of the execution times, since general-purpose numerical procedures to evaluate eigenvectors have to be implemented. In analyzing the survival probabilities in the age-dependent models, we must record the age of the marked individual, which implies more demanding memory requirements when the resulting systems of equations are numerically solved by general-purpose algorithms; for instance, our numerical work indicates that LU-decomposition techniques applied to the computation of inverse matrices fail to give satisfactory results as K increases. It is advisable thus to write a driver routine by implementing our recursive procedures derived for different age-dependent models.

In Chapter 3, our interest is in the Hitchcock process. First, we study the maximum number $Z(t_0)$ of individuals alive during a fixed time interval $[0, t_0]$, which is an alternative descriptor to that in Chapter 2 related to an extinction cycle. We derive a matrix exponential form for the probability distribution function of $Z(t_0)$ in a community starting from strictly positive numbers m of parasitoids and n of hosts. The matrix exponential solution is an exact solution, but it needs to be complemented with algorithmic tools allowing us to compute the exponential of the matrix $\mathbf{T}(x)t_0$ in an accurate and efficient manner for a suitably defined matrix $\mathbf{T}(x)$ of infinitesimal rates. We present an approach which is strongly based on splitting methods and the use of eigenvalues and eigenvectors. In terms of a certain condition termed Condition (A), we assume simple conditions on the per capita rates α, β and δ of change of population sizes for the resulting matrix exponential to be explicit or amenable to numerical calculation. Condition (A) is a technical requirement to guarantee that the underlying eigenvalues are distinct for every $x \geq m+n$, but it can be thought of as sufficiently general to be applied in actual biological situations. Under Condition (A), the solution is explicitly specified in the special case $\beta = 0$, that is, if the process governing the death of parasitoids is not relevant. A particularly appealing feature of the resulting expression for $\exp\{\mathbf{T}(x)t_0\}$ is that it allows us to evaluate $\exp\{\mathbf{T}(x)t_0\}$ and, consequently, $P(Z(t_0) \leq x|X(0) = (m, n))$

for each value $x \geq m + n$, in an iterative manner by starting with $\exp\{\mathbf{T}(2)t_0\} = e^{-(\alpha+\lambda)t_0}$. In the general setting $\beta > 0$, we suggest to approximate the matrix exponential solution, as accurately as possible, by using the Trotter product based on the decomposition $\mathbf{T}(x) = \mathbf{U}(x) + \mathbf{V}(x)$. Specifically, we first analyze two splitting proposals (i.e., Approximations 1 and 2 with $\mathbf{U}_i(x) + \mathbf{V}_i(x)$, for $i \in \{1, 2\}$) for the underlying matrix $\mathbf{T}(x)$, and we then study practical qualities as each concrete splitting is combined with the spectral norm $||\cdot||_S$ (Criterion I) and the maximum row sum matrix norm $||\cdot||_\infty$ induced by the l_∞ vector norm (Criterion II). The first term $\mathbf{U}_i(x)$, for $i \in \{1, 2\}$, in Approximations 1 and 2 is a block bi-diagonal matrix. Similarly to the case $\beta = 0$, this means that, under Condition (A), the matrix exponential $\exp\{\mathbf{U}_i(x)t\}$ can be iteratively computed, by starting with $\exp\{\mathbf{U}_i(2)t\} = e^{-(\alpha+\beta+\lambda)t}$. The second term $\mathbf{V}_i(x)$, for $i \in \{1, 2\}$, in Approximations 1 and 2 has a single non-null block diagonal, and it is thus nilpotent. As a result, the exponential of the matrix $\mathbf{V}_i(x)t$, for $i \in \{1, 2\}$, can be written in explicit form, and it can be readily expressed in terms of the matrix exponential $\exp\{\mathbf{V}_i(x-1)t\}$. Thus, the resulting explicit expressions lead us to iterative schemes for computing $\exp\{\mathbf{V}_i(x)t\}$, regardless of Condition (A). The Trotter product formula given by the expression $\exp\{\mathbf{T}(x)t_0\} \simeq (\exp\{\mathbf{U}(x)t\}\exp\{\mathbf{V}(x)t\})^{p_0}$, with $t = p_0^{-1}t_0$, implies the selection of an integer p_0. For a suitable choice of p_0, we suggest the use of the splitting $\mathbf{T}(x) = \mathbf{U}_2(x) + \mathbf{V}_2(x)$ combined with the $||\cdot||_\infty$-norm. More particularly, we derive bounds for the accuracy of our solution when a concrete splitting $\mathbf{T}(x) = \mathbf{U}_i(x) + \mathbf{V}_i(x)$ is combined with the $||\cdot||_S$-norm and the $||\cdot||_\infty$-norm, for $i \in \{1, 2\}$. For both splitting proposals, it is seen that the $||\cdot||_\infty$-norm allows us to obtain global error control in terms of an arbitrary small value $\varepsilon > 0$.

We specify conditions under which the descriptor $Z(t_0)$ is preferred to its extinction-cycle version $Z(T)$. These conditions concern with the length t_0 of the interval and the expected length $\tau_{(m,n)}$ of an extinction cycle, and the number $m + n$ of individuals in the initial community. Our conclusions cannot be extrapolated to other host-parasitoid models since they are essentially explained by noting three facts, which are closely related to the model de-

fined by (S.2): (i) the ultimate extinction of either parasitoids or hosts is certain, given any initial numbers of m parasitoids and n hosts; (ii) the expected time $\tau_{(m,n)}$ to the first extinction is always finite; and (iii) the mean extinction time $\tau_{(m,n)}$ tends to zero as the combined initial number $m+n$ becomes large. In analyzing the descriptors $Z(t_0)$ and $Z(T)$ in other host-parasitoid models, we stress that, unlike the random variable $Z(t_0)$ whose distribution is always nondefective, the distribution of $Z(T)$ might be defective (i.e., $P(Z(T)<\infty|X(0)=(m,n))<1$) if the ultimate extinction is not certain.

In Chapter 3, we are also concerned with versions of the Hitchcock process that can exhibit correlation tendencies in the underlying processes generating events. We apply a block-structured state-dependent (BSDE) approach [1,2] that provides a methodological tool to model state-dependent transitions operating in the presence of phases. In a general setting, its goal in stochastic modeling is the possibility of dealing with events generated by non-exponential correlated flows, but keeping the dimensionality of the underlying Markov chain model tractable. This means that the dimensionality L in the BSDE host-parasitoid model remains constant, while it increases with increasing values of the combined number $m+n$ of parasitoids and hosts in the case of Markov-modulated models based on the replacement of the exponential lifetimes of the individuals by, for example, PH random variables. The BSDE approach turns the Hitchcock model into a CTMC allowing correlated and non-exponentially generated events. In the BSDE version of $\mathcal{X}$, we are concerned with an *augmented* CTMC $(\mathcal{X},\mathcal{Y})=\{(X(t),Y(t)):t\geq 0\}$ defined on the state space $\mathcal{S}_{(\mathcal{X},\mathcal{Y})}=\mathcal{C}_0\cup\mathcal{C}^*$, where $\mathcal{C}_0$ is the subset of absorbing states in the basic process $\mathcal{X}$, $\mathcal{C}^*=\cup_{k=2}^{\infty}l^*(k)$ and $l^*(k)=\{(m,n,y):m+n=k,m>0,n>0,1\leq y\leq L\}$. The random variable $Y(t)$ is called *phase*, and the augmented process $(\mathcal{X},\mathcal{Y})$ is regular, time-homogeneous, and irreducible in a similar manner to the basic process $\mathcal{X}$.

The basic state (m,n) is updated in the light of the observed value of a random vector $(Z_1,Z_2)|_{(m,n)}$, which records the events taking place when the sojourn time that $\mathcal{X}$ spends in (m,n) expires. The resulting basic state (m',n') is of the form

$$(m', n') = f\left((m, n), (Z_1, Z_2)|_{(m,n)}\right),$$

where the basic state function is defined as $f((m, n), (z_1, z_2)) = (m + z_1, n + z_2)$ for pairs $(m, n) \in \mathcal{C}$ and $(z_1, z_2) \in \{(0, 0), (1, -1), (-1, 0), (0, 1)\}$. The pairs $(z_1, z_2) = (1, -1)$, $(-1, 0)$ and $(0, 1)$ amount to parasitism, a parasitoid death and a host birth, respectively, in the basic host-parasitoid model and their occurrence may imply a jump in the phase variable; on the contrary, the pair $(z_1, z_2) = (0, 0)$ means a transition between phases, but it does not correspond to any event in the process $\mathcal{X}$.

For the derivation of the infinitesimal generator $\mathbf{Q}^*$ of the augmented process $(\mathcal{X}, \mathcal{Y})$, we introduce a family

$$\mathcal{F} = \bigcup_{(m,n)\in\mathcal{C}} \left\{\mathbf{C}_{(m,n)}(z_1, z_2) : (z_1, z_2) = (0, 0), (1, -1), (-1, 0), (0, 1)\right\}$$

of (possibly infinitely many) square matrices of order L, where $\mathbf{C}_{(m,n)}(z_1, z_2)$ with $(z_1, z_2) \in \{(1, -1), (-1, 0), (0, 1)\}$ are nonnegative, $\mathbf{C}_{(m,n)}(0, 0)$ has nonnegative off-diagonal elements and strictly negative diagonal elements, and $\mathbf{C}_{(m,n)} \equiv \mathbf{C}_{(m,n)}(0, 0) + \mathbf{C}_{(m,n)}(1, -1) + \mathbf{C}_{(m,n)}(-1, 0) + \mathbf{C}_{(m,n)}(0, 1)$ defines an irreducible infinitesimal generator. Roughly speaking, each basic state (m, n) in $\mathcal{X}$ translates into a set $\{(m, n, y) : 1 \leq y \leq L\}$ of augmented states in $(\mathcal{X}, \mathcal{Y})$, and the transition rates αmn, βm and λn in (S.2) are replaced by matrices $\mathbf{C}_{(m,n)}(1, -1)$, $\mathbf{C}_{(m,n)}(-1, 0)$ and $\mathbf{C}_{(m,n)}(0, 1)$ of infinitesimal rates, respectively. Then, the augmented process $(\mathcal{X}, \mathcal{Y})$ can be thought of as the *state-dependent* version of a marked Markovian arrival process.

An interesting question concerns the comparative analysis between the basic model $\mathcal{X}$ and its BSDE version $(\mathcal{X}, \mathcal{Y})$. Thus, we illustrate the theoretical work by carrying out numerical results for various BSDE scenarios, which are defined in terms of Markovian arrival processes (MAPs). Six scenarios are defined by replacing a single Poisson stream governing events in the basic process $\mathcal{X}$ (i.e., parasitism, a parasitoid death or a host birth) by a MAP with positive or negative correlation. This particular way of generalization may be seen as elementary, but it shows –under simple circumstances– a significant influence of the underlying Markovian stream on the number of remaining parasitoids, and the expected extinction times. The initial numbers of parasitoids and of hosts

are selected meaningfully to emphasize that certain BSDE versions yield noticeably different results from the basic model, even in the case of initial dominance of parasitism on the death of a parasitoid and the birth of a host.

In Chapter 4 our interest is in host-macroparasite interactions, where the acquisition of parasites by a single host is studied. We examine nonlinear stochastic models for the parasite load of the host, where the age-dependent rates represent seasonal conditions. More concretely, seasonal conditions are reflected by means of state-dependent nonhomogeneous Poisson processes associated with the acquisition of parasites, the reproduction and death of parasites within the host, and the natural and parasite-induced host mortality. We first present a basic model representing a host that, at a certain age τ_0, is isolated and treated with chemotherapeutic (anthelmintic) products. This means that the host is free living in a seasonal environment, and it is transferred to an uninfected area at age τ_0. In the uninfected area, the host does not acquire new parasites, undergoes an anthelmintic treatment to decrease the parasite load, and varies in its susceptibility to parasite-induced mortality and natural mortality. We then present two criteria (termed Criteria 1 and 2) based on stochastic principles that permit us to select an optimal intervention instant τ_0. The underlying problem is to find a time instant τ_0 that adequately balances the effectiveness and cost of vaccination, where effectiveness can be measured in terms of the probability that the host is alive and parasite-free and, in contrast, cost of vaccination depends on the probability that the host does not survive at a certain age τ, provided that it is transferred to the uninfected area at age $\tau_0 < \tau$. In the spirit of control systems discussed by Barger [4], our approach concerns with the role of grazing management in reducing anthelmintic use and improving helminth control. The problem of selecting the age τ_0 became established in the applied veterinary parasitology jargon with the epithet of *evasive* strategy; see the references [5, 6, 7], among others. Evasive strategies can be seen as variations of the dose-and-move procedure devised by Michel [14] for the control of GI nematodes in calves, which relies on removal of a moderate existing infection by chemotherapeutic treatment, allied with a movement of the treated host to a safe pasture, just

before the population of infective larvae on the original pasture rose to dangerously high concentrations. An application of our model is shown to the development of GI nematode infection in sheep. Our interest is in the parasite *Nematodirus* spp. with *Nematodirus battus*, *Nematodirus filicollis* and *Nematodirus spathiger* as main species. Grazing strategies are appropriately defined in terms of the intervention instant τ_0 as follows:

Strategy TI: *The host is treated with anthelmintics and isolated (that is, moved to an uninfected area) at age* τ_0.

Strategy TI+S: *The host is treated with anthelmintics and isolated at age* τ_0. *After treatment, the host is moved to the original paddock (set-stocked).*

Strategy UM: *The host is left untreated but moved to a paddock with safe pasture at age* τ_0.

Strategy TS: *The host is treated with anthelmintics and set-stocked at age* τ_0.

Strategy TM: *The host is treated with anthelmintics and moved to safe pasture at age* τ_0.

In analyzing these grazing strategies, we use age-dependent pure birth processes with killing at pre-intervention instants $t \in [0, \tau_0]$. At post-intervention instants $t \in [\tau_0, \tau]$, we use age-dependent pure death processes with killing in the cases TI and TI+S, pure birth processes with killing in the case UM, and birth-death processes with killing in the cases TS and TM. As in early work by Herbert and Isham [9], and Isham [12], exact algebraic results are possible. Specifically, in the case of the pure birth and pure death processes with killing, the transient solution is iteratively derived in terms of simple integral expressions. On the contrary, the underlying time-dependent linear system of differential equations in strategies TS and TM is solved by using Strang-Marchuk splitting techniques [8, Section 1.3], which imply to solve four time-dependent subsystems cyclically on successive intervals of a certain small length, using the solution of one subsystem as the initial condition of the other one.

In our application, we construct the mathematical model in terms of levels of infection. Results are related to the study conducted by Uriarte et al. [20], which was designed to describe the monthly fluctuations of nematode burden in sheep raised under

irrigated conditions in Ebro Valley (Spain) by using worm-free tracer lambs and monitoring the faecal excretion of eggs by ewes. Empirical data in [20] are appropriately combined with those derived in [15] on the clinical efficacy assessment of three anthelmintics (*ivermectin*, *fenbendazole* and *albendazole*) in lambs parasitized with nematode infective larvae.

Bibliography

1. Artalejo JR, Gómez-Corral A (2010) A state-dependent Markov-modulated mechanism for generating events and stochastic models. Mathematical Methods in the Applied Sciences 33:1342-1349.
2. Artalejo JR, Gómez-Corral A, He QM (2010) Markovian arrivals in stochastic modelling: a survey and some new results. SORT - Statistics and Operations Research Transactions 34:101-144.
3. Bailey NTJ (1975) The mathematical theory of infectious diseases, second edition. Griffin, London.
4. Barger IA (1997) Control by management. Veterinary Parasitology 72:493-506.
5. Barger IA (1999) The role of epidemiological knowledge and grazing management for helminth control in small ruminants. International Journal for Parasitology 29:41-47.
6. Eysker M, Bakker N, Kooyman FNJ, Ploeger HW (2005) The possibilities and limitations of evasive grazing as a control measure for parasitic gastroenteritis in small ruminants in temperate climates. Veterinary Parasitology 129:95-104.
7. Eysker M, Bakker N, Kooyman FNJ, van der Linden D, Schrama C, Ploeger HW (2005) Consequences of the unusually warm and dry summer of 2003 in The Netherlands: poor development of free living stages, normal survival of infective larvae and long survival of adult gastrointestinal nematodes of sheep. Veterinary Parasitology 133:313-321.
8. Faragó I, Havasi A, Horváth R (2011) On the order of operator splitting methods for time-dependent linear systems of differential equations. International Journal of Numerical Analysis and Modeling, Series B 2:142-154.

9. Herbert J, Isham V (2000) Stochastic host-parasite interaction models. Journal of Mathematical Biology 40:343-371.
10. Hitchcock SE (1986) Extinction probabilities in predator-prey models. Journal of Applied Probability 23:1-13.
11. Iglehart DL (1964) Multivariate competition processes. The Annals of Mathematical Statistics 35:350-361.
12. Isham V (1995) Stochastic models of host-macroparasite interaction. The Annals of Applied Probability 5:720-740.
13. Latouche G, Ramaswami V (1999) Introduction to matrix analytic methods in stochastic modeling. ASA-SIAM Series on Statistics and Applied Probability, Philadelphia.
14. Michel JF (1985) Strategies for the use of anthelmintics in livestock and their implications for the development of drug resistance. Parasitology 90:621-628.
15. Nasreen S, Jeelani G, Sheikh FD (2007) Efficacy of different anthelmintics against gastro-intestinal nematodes of sheep in Kashmir Valley. VetScan 2, No. 1, article 13.
16. Neuts MF (1994) Matrix-geometric solutions in stochastic models: an algorithmic approach, second edition. Dover Publications, New York.
17. Reuter GEH (1961) Competition processes. In: Neyman J (ed) Proceedings of the fourth Berkeley symposium on mathematical statistics and probability, volume II: contributions to probability theory. University of California Press, Berkeley, pp. 421-430.
18. Ridler-Rowe CJ (1978) On competition between two species. Journal of Applied Probability 15:457-465.
19. Ridler-Rowe CJ (1988) Extinction times for certain predator-prey processes. Journal of Applied Probability 25:612-616.
20. Uriarte J, Llorente MM, Valderrábano J (2003) Seasonal changes of gastrointestinal nematode burden in sheep under an intensive grazing system. Veterinary Parasitology 118:79-92.
21. White KAJ, Grenfell BT, Hendry RJ, Lejeune O, Murray JD (1996) Effect of seasonal host reproduction on host-macroparasite dynamics. Mathematical Biosciences 137:79-99.

Resumen

Introducción

Los procesos de competición de Iglehart [11] y Reuter [17] han sido usados con frecuencia en Biología para describir las dinámicas de modelos de población involucrando algún tipo de interacción entre especies. Esta tesis trata con dos tipos de relaciones interespecíficas (de competición entre dos especies, y entre un parásito y su receptor) que están estrechamente relacionadas con los procesos de competición de Reuter [17]. En [17], se presenta un marco estocástico general para reflejar la interacción entre dos especies en términos de una cadena de Markov en tiempo continuo (CTMC) homogénea en el tiempo $\mathcal{X} = \{X(t) = (M(t), N(t)) : t \geq 0\}$ sobre el espacio de estados $\mathcal{S} = \mathbb{N}_0 \times \mathbb{N}_0$, donde $M(t)$ y $N(t)$ son los tamaños poblacionales de las dos especies coexistiendo en el ecosistema. Las posibles transiciones en $\mathcal{X}$ desde un estado (m, n) se producen sólo hacia algunos estados adyacentes de tal modo que las tasas de transición que pueden ser no nulas vienen dadas por

$$q_{(m,n),(m',n')} = \begin{cases} a_{(m,n)}, & \text{if } (m', n') = (m+1, n), \\ b_{(m,n)}, & \text{if } (m', n') = (m, n+1), \\ c_{(m,n)}, & \text{if } (m', n') = (m-1, n), \\ d_{(m,n)}, & \text{if } (m', n') = (m, n-1), \\ e_{(m,n)}, & \text{if } (m', n') = (m-1, n+1), \\ f_{(m,n)}, & \text{if } (m', n') = (m+1, n-1), \end{cases}$$

donde $a_{(m,n)}$, $b_{(m,n)}$, $c_{(m,n)}$, $d_{(m,n)}$, $e_{(m,n)}$ y $f_{(m,n)}$ son constantes no negativas para $(m, n) \in \mathcal{S}$. Además, la condición

$$\begin{aligned} q_{(m,n)} &= -q_{(m,n),(m,n)} \\ &= a_{(m,n)} + b_{(m,n)} + c_{(m,n)} + d_{(m,n)} + e_{(m,n)} + f_{(m,n)} \end{aligned}$$

conduce a un generador infinitesimal $\mathbf{Q}$ conservativo.

En este contexto, el proceso de competición entre dos especies es presentado por Reuter [17, Ejemplo 1] como ejemplo de proceso de Tipo I (es decir, los estados de los ejes son absorbentes, y $\mathcal{C} = \mathbb{N}\times\mathbb{N}$ es una clase irreducible de estados transitorios), donde las tasas de transición se definen como

$$\begin{aligned} a_{(m,n)} = \alpha m, \quad b_{(m,n)} &= \beta n, \quad c_{(m,n)} = \gamma mn, \\ d_{(m,n)} = \delta mn, \quad e_{(m,n)} &= 0, \qquad f_{(m,n)} = 0, \end{aligned} \tag{S.1}$$

para constantes estrictamente positivas α, β, γ y δ. Aunque esta especificación no da lugar a un proceso de Tipo I (los estados de la forma $(m, 0)$ y $(0, n)$ no son absorbentes), se sugiere en [17] *congelar* los estados $(m, 0)$ y $(0, n)$ tomando $q_{(m,0),(m',n')} = 0$ y $q_{(0,n),(m',n')} = 0$, para $(m', n') \in \mathcal{S}$ con $m, n \geq 0$. Esto significa que el espacio de estados se transforma en $\mathcal{S} = \mathbb{N}_0 \times \mathbb{N}_0 - \{(0, 0)\}$, puesto que el estado $(0, 0)$ sólo es accesible desde los semiejes positivos. El proceso resultante fue ampliamente estudiado por Ridler-Rowe [18] y se refiere a un ecosistema donde los individuos pertenecientes a dos especies compiten directa e indirectamente por los recursos comunes. Conforme el tamaño total del ecosistema crece, el mantenimiento de condiciones estables de crecimiento pasa a ser insostenible debido a la *presión medioambiental* (debida a sobrepoblación) y, por tanto, los nacimientos y muertes de ambas especies dependen fuertemente de los tamaños poblacionales de una o ambas especies. Nótese que el ecosistema en [18] es cerrado en el sentido de que no se permite inmigración o emigración entre especies, es decir, $e_{(m,n)} = f_{(m,n)} = 0$.

Al analizar el tiempo hasta la extinción y el tamaño de la especie que sobrevive, los términos cuadráticos en las tasas de transición del proceso definido por (S.1) hacen la solución intratable desde un punto de vista analítico; véase [18, Sección 2]. Una manera de analizar el proceso es aproximar su comportamiento, conforme los tamaños de población iniciales tienden a infinito, con un movimiento esencialmente determinista con una difusión aleatoria. Las técnicas usadas por Ridler-Rowe [18] dan lugar a una

distribución asintótica para el estado en el cual el proceso alcanza por primera vez el subconjunto de estados absorbentes, y un resultado límite para la probabilidad de que una especie sobreviva a la otra.

Un proceso que modeliza la interacción receptor-parásito es presentado por Hitchcock [10] mediante el uso de las tasas de transición

$$\begin{aligned} a_{(m,n)} &= 0, \quad b_{(m,n)} = \lambda n, \quad c_{(m,n)} = \beta m, \\ d_{(m,n)} &= 0, \quad e_{(m,n)} = 0, \quad f_{(m,n)} = \alpha mn, \end{aligned} \tag{S.2}$$

donde α, β y λ son constantes estrictamente positivas, y donde $q_{(m,0),(m',n')} = q_{(0,n),(m',n')} = 0$, lo que significa que el proceso es de Tipo I. En concreto, la relación interespecífica descrita en [10] por (S.2) pertenece a una subclase especial de modelos receptor-parásito donde los parásitos son llamados *parasitoides*, puesto que los receptores mueren si son exitosamente parasitados. En (S.2), las transiciones desde un estado dado (m, n) hacia estados (m', n') con $(m', n') = (m-1, n)$, $(m, n+1)$ y $(m+1, n-1)$ se corresponden con la muerte de un parásito, el nacimiento de un receptor y parasitismo, respectivamente.

Nuestro interés está en el proceso de Hitchcock [10], que viene especificado en términos de sus tasas de transición $q_{(m,n),(m',n')}$ dadas por (S.2), y donde los retrasos temporales son ignorados. El proceso es modelizado mediante una CTMC homogénea en el tiempo $\mathcal{X} = \{X(t) = (M(t), N(t)) : t \geq 0\}$ sobre el espacio de estados $\mathcal{S} = \mathbb{N}_0 \times \mathbb{N}_0 - \{(0,0), (1,0)\}$, donde $M(t)$ y $N(t)$ representan los números de parasitoides y receptores vivos en el instante t, respectivamente. Mediante criterios dados por Reuter [17], Hitchcock [10] mostró que la extinción bien de los parasitoides o de los receptores es segura y que, dados los números iniciales de parásitos m y de receptores n, el tiempo esperado $\tau_{(m,n)}$ hasta dicha extinción es siempre finito. Basándose en el modelo general de epidemias [3] donde $M(t)$ y $N(t)$ representan los números de individuos infectados y susceptibles en el instante t, respectivamente, se deriva en [10, Sección 3] una expresión exacta para la probabilidad de que la población de parasitoides sea la primera en extinguirse en el caso especial $\lambda = 0$. Esas probabilidades son entonces utilizadas para derivar aproximaciones en series de potencias para las proba-

bilidades de extinción cuando la tasa de nacimiento de receptores λ es estrictamente positiva, y un método similar de aproximación es aplicado para estimar el número medio de eventos antes de la extinción; véase [10, Secciones 4 y 5]. Por medio de una construcción alternativa – usando el criterio de Reuter [17] junto con un simple resultado de minimización – Ridler-Rowe [19] probó que el tiempo medio hasta la extinción $\tau_{(m,n)}$ tiende a cero cuando la población conjunta de parasitoides y receptores $m + n$ tiende a infinito.

El parasitismo es uno de los factores que se considera que tiene mayor impacto en las interacciones de competición, aunque los parásitos pueden mostrar un amplio rango de variabilidad entre distintas especies en lo relativo al nivel de daño que causan a los receptores. Los parásitos son comúnmente clasificados (véase [21]) en dos grupos: *microparásitos*, tales como virus, bacterias o protozoos; y *macroparásitos* (helmintos). La principal diferencia entre ellos es que los microparásitos se multiplican directamente en el interior del receptor, mientras que los macroparásitos crecen dentro del receptor pero se multiplican produciendo larvas infecciosas que son expulsadas al exterior para extender la infección en nuevos receptores. En la interacción receptor-macroparásito, la variable de estudio es el número de parásitos albergados en un único receptor.

Como una variante de la interacción receptor-parásito, tratamos con interacciones receptor-macroparásito que pueden ser modelizadas mediante procesos de nacimiento y muerte con catástrofes, con tasas variando a lo largo del tiempo. A diferencia de los procesos de Ridler-Rowe [18] y Hitchcock [10], debemos considerar en este caso una CTMC unidimensional no homogénea en el tiempo $\mathcal{X} = \{M(t) : 0 \leq t \leq \tau\}$ donde $M(t)$ denota el número de parásitos dentro del receptor (para un uso práctico, el nivel de infección del receptor, causado por la presencia de parásitos) y τ puede representar la ocurrencia periódica de cierto evento, tal como una inspección anual. La CTMC $\mathcal{X}$ está definida sobre $\{-1\} \cup \mathcal{S}$ con $\mathcal{S} = \{0, \ldots, M_0\}$, donde el estado -1 equivale a la muerte del receptor (o a un nivel inaceptable de infección) y el estado M_0 representa un valor crítico por encima del cual se considera imposible la recuperación del receptor. Las condiciones estacionales en nuestro modelo son reflejadas en términos de procesos de Poisson no homogéneos dependientes del estado asociados con

la adquisición de parásitos, la reproducción y muerte de parásitos dentro del receptor, así como la muerte natural del receptor y la muerte del receptor inducida por los parásitos.

Objetivos

En esta tesis, nos centramos en el uso de modelos estocásticos con el objetivo de describir la interacción de competición entre dos especies, así como la relación receptor-parásito. Específicamente, nuestro objetivo es aplicar métodos analítico-matriciales [13, 16] para estudiar descriptores probabilísticos relativos al proceso de Ridler-Rowe (Capítulo 2), el proceso de Hitchcock (Capítulo 3), y la interacción receptor-macroparásito que surge en el desarrollo de infección por nematodos gastrointestinales (GI) en ovejas (Capítulo 4).

Presentamos a continuación una lista de objetivos específicos:

(i) Caracterizar la distribución del tamaño máximo de la población en los procesos de Ridler-Rowe y de Hitchcock. Además, comparar las dinámicas del modelo durante un ciclo de extinción y durante un intervalo de tiempo fijo.

(ii) Usar cadenas de Markov absorbentes definidas sobre un espacio de estados finito para aproximar la distribución conjunta del tiempo hasta la extinción, la identidad y el tamaño de la especie que sobrevive en el proceso de Ridler-Rowe, así como otras medidas relacionadas tales como el número de nacimientos y muertes, y la supervivencia de un individuo concreto. Además, proponer un criterio para la selección de la cardinalidad del espacio de estados en términos de la distribución del tamaño máximo de la población.

(iii) Incorporar hipótesis distribucionales más realistas en el proceso de Hitchcock mediante la incorporación de eventos generados por flujos no exponenciales correlados, pero manteniendo tratable la dimensionalidad de la cadena de Markov subyacente.

(iv) Investigar propiedades estructurales en el proceso de Hitchcock y sus variantes BSDE, tales como regularidad, clasificación de estados y tiempos hasta la extinción.

(v) Reflejar condiciones estacionales en modelos receptor-macroparásito en términos de procesos de Poisson no homogéneos dependientes del estado asociados con la adquisición de parásitos, la reproducción y muerte de parásitos dentro del receptor, y la mortalidad del receptor por causas naturales y producida por los parásitos.

(vi) Especificar criterios de control que equilibren adecuadamente la eficacia y el coste de la intervención y, desde una perspectiva aplicada, aplicar estos criterios a las fluctuaciones estacionales de la carga de nematodos en corderos.

(vii) Desarrollar técnicas algorítmicas que permitan computar las soluciones resultantes de una manera eficiente y precisa.

(viii) Desarrollar un amplio abanico de experimentos numéricos para analizar las principales características de la interacción de competición entre dos especies, y las relaciones receptor-parásito y receptor-macroparásito, así como comparar la solución resultante con soluciones existentes y soluciones obtenidas por simulación.

Contenidos de la investigación: Resultados y conclusiones

En el Capítulo 1, comentamos brevemente sobre la literatura existente acerca de los procesos de competición. Dentro del marco general de Reuter [17], presentamos el proceso de competición entre dos especies, la relación presa-depredador, la interacción receptor-parásito y los modelos de epidemias como casos particulares.

En el Capítulo 2, el proceso de competición entre dos especies es el proceso bajo estudio. Consideramos la distribución de los tiempos hasta la extinción, así como la distribución conjunta de la identidad y el tamaño de la especie que sobrevive. Nuestra aproximación está principalmente basada en el reemplazamiento de la cadena de Markov absorbente que subyace $\mathcal{X}$, que es un camino aleatorio sobre el primer cuadrante $\mathcal{S} = \mathbb{N}_0 \times \mathbb{N}_0 - \{(0,0)\}$, por una cadena de Markov $\mathcal{X}(K)$ convenientemente definida sobre aquellos estados $(m,n) \in \mathcal{S}$ tales que la población conjunta $m+n$ no supera el valor K. Esto significa que, para un valor suficientemente grande de K, examinamos el proceso $\mathcal{X}$ hasta la absorción bajo

la restricción de que los estados (m, n) verificando $m + n > K$ no son accesibles. El procedimiento de truncación está basado en la selección de K como un percentil K_q de la distribución del número máximo X_{max} de individuos en el ecosistema durante un ciclo de extinción. Este principio simple de truncación nos permite aproximar una distribución fase (PH) numerable (relativa al tiempo hasta la extinción) mediante una distribución PH finita de tal modo que la probabilidad q puede ser vista como una medida de control del error global. Para apoyar nuestro criterio de selección, desarrollamos un amplio rango de experimentos numéricos, que nos permiten remarcar que la aproximación Normal en [18] y el proceso aproximativo $\mathcal{X}(K_q)$ dan lugar a resultados significativamente diferentes. A la vista de los resultados numéricos, podemos concluir que es de esperar una mayor precisión para poblaciones iniciales moderadas cuando, en lugar de utilizar la solución asintótica [18], se utiliza el proceso aproximativo $\mathcal{X}(K_q)$. Una de las primeras ventajas de $\mathcal{X}(K_q)$ está relacionada con el hecho de que nos permite aproximar la distribución conjunta del tiempo hasta la extinción T, y la identidad y tamaño de la especie que sobrevive en el instante T, así como tratar con distribuciones iniciales no degeneradas. Sin embargo, es evidente que, desde un punto de vista computacional, la solución Normal da lugar a una fórmula más sencilla. El resultado límite en [18] es suficientemente cercano a la función de masa real de $X(T)$ cuando las poblaciones iniciales son grandes, pero no depende de las tasas de nacimiento α y β. Por otro lado, la solución basada en $\mathcal{X}(K_q)$ sí depende de las tasas de nacimiento α y β, pero está definida sobre un espacio de estados finito $\mathcal{S}(K_q)$. La incidencia de la finitud de $\mathcal{S}(K_q)$ en la solución resultante puede ser atenuada mediante una elección adecuada de K_q, que está basada en un descriptor X_{max} que apropiadamente describe los efectos de la sobrepoblación en el ecosistema.

Nuestro método de aproximación también es aplicado al estudio del número de nacimientos y muertes que ocurren hasta la extinción, y a la supervivencia de un individuo concreto. En primer lugar, derivamos la distribución conjunta del tiempo hasta la extinción $T^{(M,N)}$, y el número de nacimientos $B_1^{(M,N)}$ y $B_2^{(M,N)}$, y de muertes $D_1^{(M,N)}$ y $D_2^{(M,N)}$ registrados durante un ciclo de extinción, en el supuesto de que la población inicial viene dada por

$X(0) = (M, N)$. Entonces, el efecto en la supervivencia de un individuo causado por las estrategias de selección del individuo para morir es analizado bajo varias hipótesis dependientes de la edad. Nuestros resultados son ilustrados y la precisión de nuestra solución es testada mediante simulación. Son presentados ejemplos numéricos para mostrar la influencia del número de nacimientos y muertes en las dinámicas del proceso de competición entre dos especies y la supervivencia de un individuo. En el trabajo numérico, nuestro interés se centra en doce escenarios donde las tasas de nacimiento y muerte en cada especie son comparables en magnitud. Estos escenarios dan lugar a niveles pequeños y moderados de K_q en nuestra solución, incluso si el valor $q = 0.999$ es escogido. Los algoritmos presentados parecen funcionar bien en cuanto a precisión y velocidad para tamaños iniciales de población moderados. Sin embargo, si la *tendencia natal* del proceso $\mathcal{X}$ (convenientemente definida desde las tasas de nacimiento α y β) es significativamente mayor que su opuesta *mortal* (definida en términos de las tasas de muerte γ y δ), una mayor cardinalidad del espacio de estados $\mathcal{S}(K_q)$ implicará mayores requisitos de memoria. El uso de distribuciones cuasi-estacionarias como distribuciones iniciales sobre $\mathcal{S}(K_q)$ resulta en un incremento de los tiempos de ejecución, puesto que es necesario implementar procedimientos numéricos de propósito general para la obtención de autovectores. Al analizar las probabilidades de supervivencia en los modelos dependientes de la edad, debemos almacenar la edad del individuo en cuestión, lo cual implica de nuevo más requisitos de memoria cuando los sistemas de ecuaciones resultantes son resueltos numéricamente mediante algoritmos de propósito general; por ejemplo, nuestro trabajo numérico indica que la descomposición LU aplicada a la computación de matrices inversas no resulta satisfactoria conforme K se incrementa. Es recomendable entonces desarrollar rutinas que implementen nuestros procedimientos recursivos obtenidos para los diferentes modelos dependientes de la edad.

En el Capítulo 3, nuestro interés está en el proceso de Hitchcock. En primer lugar, estudiamos el número máximo $Z(t_0)$ de individuos vivos durante un intervalo de tiempo fijo $[0, t_0]$, que es un descriptor alternativo al relacionado con el ciclo de extinción en el Capítulo 2. Derivamos una solución en forma de exponencial ma-

tricial para la función de distribución de $Z(t_0)$ en una comunidad que comienza con cantidades positivas m de parasitoides y n de receptores. La solución exponencial matricial es una solución exacta, pero necesita ser complementada con herramientas algorítmicas que permitan la computación de la exponencial de la matriz $\mathbf{T}(x)t_0$ de manera precisa y eficiente, para una cierta matriz $\mathbf{T}(x)$ de tasas de transición convenientemente definida. Presentamos una aproximación basada en métodos *splitting* que hace uso de autovalores y autovectores. En términos de cierta condición, Condición (A), asumimos condiciones sencillas sobre las tasas α, β y δ de cambios en los tamaños de población para que la matriz exponencial matricial sea explícita o sea computable desde el punto de vista numérico. La Condición (A) es un requisito técnico que garantiza que los autovalores subyacentes sean distintos para todo valor $x \geq m+n$, pero puede ser considerada como suficientemente genérica para ser aplicada a situaciones biológicas reales. Bajo la Condición (A), la solución es explícita en el caso especial $\beta = 0$, es decir, si el proceso gobernando la muerte de parasitoides no es relevante. Una característica particularmente interesante de la expresión resultante para $\exp\{\mathbf{T}(x)t_0\}$ es que nos permite evaluar $\exp\{\mathbf{T}(x)t_0\}$ y, consecuentemente, $P(Z(t_0) \leq x|X(0) = (m,n))$ para cada valor $x \geq m+n$, de forma iterativa comenzando con $\exp\{\mathbf{T}(2)t_0\} = e^{-(\alpha+\lambda)t_0}$. En el caso general $\beta > 0$, sugerimos aproximar la solución exponencial matricial, de forma tan precisa como sea posible, usando el producto de Trotter basado en la descomposición $\mathbf{T}(x) = \mathbf{U}(x) + \mathbf{V}(x)$. Específicamente, en primer lugar analizamos dos propuestas de *splitting* (es decir, Aproximaciones 1 y 2 con $\mathbf{U}_i(x)+\mathbf{V}_i(x)$, para $i \in \{1,2\}$) para la matriz subyacente $\mathbf{T}(x)$, y entonces estudiamos las características prácticas de cada *splitting* concreto cuando éste es combinado con la norma espectral $||\cdot||_S$ (Criterio I) y la norma de la máxima suma por filas $||\cdot||_\infty$ inducida por la norma vectorial l_∞ (Criterio II). El primer término $\mathbf{U}_i(x)$, para $i \in \{1,2\}$, en las Aproximaciones 1 y 2 es una matriz bidiagonal por bloques. De manera similar al caso $\beta = 0$, esto significa que, bajo la Condición (A), la matriz exponencial $\exp\{\mathbf{U}_i(x)t\}$ puede ser iterativamente computada comenzando con $\exp\{\mathbf{U}_i(2)t\} = e^{-(\alpha+\beta+\lambda)t}$. El segundo término $\mathbf{V}_i(x)$, para $i \in \{1,2\}$, en las Aproximaciones 1 y 2 tiene una única diagonal de

bloques no nulos y es, por tanto, una matriz nilpotente. Como resultado, la exponencial de la matriz $\mathbf{V}_i(x)t$, para $i \in \{1, 2\}$, puede ser escrita de forma explícita y puede ser fácilmente expresada en términos de la matriz exponencial $\exp\{\mathbf{V}_i(x-1)t\}$. Por tanto, las expresiones explícitas resultantes dan lugar a esquemas iterativos para computar $\exp\{\mathbf{V}_i(x)t\}$, sin necesidad de que se verifique la Condición (A). La fórmula del producto de Trotter, dada por $\exp\{\mathbf{T}(x)t_0\} \simeq (\exp\{\mathbf{U}(x)t\} \exp\{\mathbf{V}(x)t\})^{p_0}$ con $t = p_0^{-1}t_0$, implica la elección de un valor p_0 entero. Para una conveniente elección de p_0, sugerimos usar el *splitting* $\mathbf{T}(x) = \mathbf{U}_2(x) + \mathbf{V}_2(x)$ combinado con la norma $||\cdot||_\infty$. En particular, derivamos cotas de error para la precisión de la solución cuando un *splitting* concreto $\mathbf{T}(x) = \mathbf{U}_i(x) + \mathbf{V}_i(x)$ es combinado con las normas $||\cdot||_S$ y $||\cdot||_\infty$, para $i \in \{1, 2\}$. Para los dos *splitting* propuestos, se puede observar que la norma $||\cdot||_\infty$ permite la obtención de un mejor control del error global en términos de un valor arbitrariamente pequeño $\varepsilon > 0$.

Especificamos condiciones bajo las cuales el descriptor $Z(t_0)$ es preferible a su versión $Z(T)$ relativa al ciclo del extinción. Estas condiciones se refieren a la longitud t_0 del intervalo y a la longitud esperada $\tau_{(m,n)}$ del ciclo de extinción, así como al número inicial $m+n$ de individuos en el ecosistema. Nuestras conclusiones no pueden ser extrapoladas a otros modelos receptor-parasitoide puesto que se basan en las tres características relacionadas con el proceso definido por (S.2) que siguen: (i) la extinción de una de las dos especies es segura, dados cualesquiera números iniciales m de parásitos y n de receptores; (ii) el tiempo esperado hasta la extinción es siempre finito; y (iii) el tiempo medio $\tau_{(m,n)}$ hasta la extinción tiende a cero conforme el tamaño total inicial de la población tiende a infinito. Al analizar los descriptores $Z(t_0)$ y $Z(T)$ en otros modelos receptor-parasitoide, puntualizamos que, a diferencia de la variable aleatoria $Z(t_0)$ cuya distribución es siempre no defectiva, la distribución de $Z(T)$ pudiera ser defectiva (es decir, $P(Z(T) < \infty | X(0) = (m, n)) < 1$) si la extinción no es segura.

En el Capítulo 3, nos centramos también en versiones del proceso de Hitchcock que incluyen tendencias de correlación en los procesos subyacentes que generan eventos. Aplicamos una aproxi-

mación estructurada por bloques y dependiente del estado (BSDE) [1,2] que proporciona un marco metodológico para modelizar transiciones dependientes del estado operando en presencia de fases. En un sentido amplio, la metodología BSDE permite la modelización estocástica de eventos desde flujos correlados no exponenciales, pero manteniendo tratable la dimensionalidad de la cadena de Markov que resulta. Esto significa que la dimensionalidad L en el modelo BSDE receptor-parasitoide permanece constante, mientras que ésta se incrementa conforme lo hace el tamaño total inicial de la población en el caso de modelos modulados de Markov basados en el reemplazamiento de los tiempos de vida exponenciales de los individuos por, por ejemplo, variables aleatorias PH. La aproximación BSDE convierte el proceso de Hitchcock en una CTMC que permite trabajar con eventos correlados y no generados bajo la hipótesis exponencial. En la versión BSDE de $\mathcal{X}$, consideramos una CTMC aumentada $(\mathcal{X}, \mathcal{Y}) = \{(X(t), Y(t)) : t \geq 0\}$ definida sobre el espacio de estados $\mathcal{S}_{(\mathcal{X},\mathcal{Y})} = \mathcal{C}_0 \cup \mathcal{C}^*$, donde $\mathcal{C}_0$ es el conjunto de estados absorbentes del proceso básico $\mathcal{X}$, $\mathcal{C}^* = \cup_{k=2}^{\infty} l^*(k)$ y $l^*(k) = \{(m, n, y) : m + n = k, m > 0, n > 0, 1 \leq y \leq L\}$. La variable aleatoria $Y(t)$ se denomina *fase*, y el proceso aumentado $(\mathcal{X}, \mathcal{Y})$ es regular, homogéneo en el tiempo e irreducible, de manera similar al proceso básico $\mathcal{X}$.

El estado fundamental (m, n) se actualiza en función del valor observado por un vector aleatorio $(Z_1, Z_2)|_{(m,n)}$, que representa los eventos teniendo lugar cuando el tiempo de permanencia de $\mathcal{X}$ en el estado (m, n) concluye. El estado fundamental resultante (m', n') es de la forma

$$(m', n') = f\left((m, n), (Z_1, Z_2)|_{(m,n)}\right),$$

donde la función del estado fundamental se define como $f((m, n), (z_1, z_2)) = (m + z_1, n + z_2)$ para parejas $(m, n) \in \mathcal{C}$ y $(z_1, z_2) \in \{(0, 0), (1, -1), (-1, 0), (0, 1)\}$. Las parejas $(z_1, z_2) = (1, -1)$, $(-1, 0)$ y $(0, 1)$ representan parasitismo, muerte de un parasitoide y nacimiento de un receptor, respectivamente, en el modelo receptor-parasitoide básico y su ocurrencia puede dar lugar o no a un salto en la variable fase; por el contrario, la pareja $(z_1, z_2) = (0, 0)$ representa una transición entre fases y no se corresponde con ningún evento en el proceso básico $\mathcal{X}$.

Para la obtención del generador infinitesimal $\mathbf{Q}^*$ del proceso aumentado $(\mathcal{X}, \mathcal{Y})$, introducimos una familia

$$\mathcal{F} = \bigcup_{(m,n)\in\mathcal{C}} \left\{ \mathbf{C}_{(m,n)}(z_1, z_2) : (z_1, z_2) = (0,0), (1,-1), (-1,0), (0,1) \right\}$$

de (posiblemente infinitas) matrices cuadradas de orden L, donde $\mathbf{C}_{(m,n)}(z_1, z_2)$ con $(z_1, z_2) \in \{(1,-1), (-1,0), (0,1)\}$ son matrices no negativas, $\mathbf{C}_{(m,n)}(0,0)$ tiene elementos estrictamente negativos en la diagonal y elementos no negativos fuera de ella, y $\mathbf{C}_{(m,n)} \equiv \mathbf{C}_{(m,n)}(0,0) + \mathbf{C}_{(m,n)}(1,-1) + \mathbf{C}_{(m,n)}(-1,0) + \mathbf{C}_{(m,n)}(0,1)$ define un generador infinitesimal irreducible. Informalmente hablando, cada estado fundamental (m,n) en $\mathcal{X}$ se transforma en un conjunto $\{(m,n,y) : 1 \leq y \leq L\}$ de estados aumentados en $(\mathcal{X}, \mathcal{Y})$, y las tasas de transición αmn, βm y λn en (S.2) son reemplazadas por matrices $\mathbf{C}_{(m,n)}(1,-1)$, $\mathbf{C}_{(m,n)}(-1,0)$ y $\mathbf{C}_{(m,n)}(0,1)$ de tasas de transición, respectivamente. Entonces, el proceso aumentado $(\mathcal{X}, \mathcal{Y})$ puede ser visto como una versión dependiente del estado de un proceso Markoviano de llegadas marcadas.

Una cuestión interesante es la relativa al análisis comparativo entre el modelo básico $\mathcal{X}$ y su versión BSDE $(\mathcal{X}, \mathcal{Y})$. Por ese motivo, ilustramos el trabajo teórico realizado mediante el desarrollo de resultados numéricos para distintos escenarios BSDE, los cuales son definidos mediante procesos Markovianos de llegadas (MAPs). Se definen seis escenarios reemplazando cada proceso de Poisson gobernando los eventos del proceso básico $\mathcal{X}$ (esto es, parasitismo, muerte de un parasitoide y nacimiento de un receptor) por un MAP con correlación positiva o negativa. Estas versiones BSDE podrían ser consideradas como elementales, pero muestran –bajo ciertas circunstancias sencillas– una influencia significativa de los flujos Markovianos en la extinción de cada especie y los tiempos medios hasta la extinción. Los números iniciales de parasitoides y receptores son seleccionados con la intención de enfatizar que ciertas versiones BSDE dan lugar a resultados significativamente diferentes a los obtenidos con el modelo básico, incluso en el caso de que haya una clara dominancia inicial del parasitismo sobre la muerte de un parasitoide y el nacimiento de un receptor.

En el Capítulo 4 nuestro interés está en las interacciones receptor-macroparásito, donde la adquisición de parásitos por un

único receptor es el objeto de estudio. Examinamos modelos estocásticos no lineales para la carga de parásitos en un receptor, donde las tasas dependientes de la edad representan las condiciones estacionales. En concreto, las condiciones estacionales son reflejadas mediante procesos de Poisson no homogéneos dependientes del estado asociados a la adquisición de parásitos, la reproducción y muerte de parásitos dentro del receptor, y la mortalidad del receptor por causas naturales o inducida por los parásitos. En primer lugar, presentamos un modelo sencillo representando un receptor que, en cierto instante τ_0, es aislado y tratado con productos terapéuticos (antihelmínticos). Esto se traduce en que el receptor vive libremente en un ambiente estacional hasta el instante τ_0, y es entonces transferido a un área de aislamiento. En el área de aislamiento, el receptor no adquiere nuevos parásitos, sigue un tratamiento para disminuir su carga de parásitos y varía su susceptibilidad en referencia a la mortalidad por causas naturales y la mortalidad inducida por los parásitos. Presentamos entonces dos criterios (Criterios 1 y 2) basados en principios estocásticos que nos permiten seleccionar un instante óptimo de intervención τ_0. El problema subyacente consiste en encontrar un instante de tiempo τ_0 que adecuadamente equilibre la efectividad y el coste de la intervención, donde la efectividad puede ser medida en términos de la probabilidad de que el receptor esté vivo y libre de parásitos y, por contra, el coste de la intervención puede ser medido mediante la probabilidad de que el receptor no haya sobrevivido a cierto instante τ, en el caso de ser aislado en el instante $\tau_0 < \tau$. En el espíritu de los sistemas de control discutidos por Barger [4], nuestra aproximación se refiere al papel que juega la gestión del pastoreo de rumiantes en reducir el uso de los antihelmínticos y en mejorar el control de los helmintos. El problema de seleccionar un instante τ_0 fue establecido en el contexto de la Parasitología Veterinaria bajo el término de estrategia *evasiva*; véanse las referencias [5, 6, 7], entre otras. Las estrategias de evasión pueden ser vistas como variaciones de los procedimientos *dose-and-move* dados en [14] para el control de nematodos en terneros, basados en la disminución moderada de la infección mediante un tratamiento terapéutico y la combinación con un movimiento del receptor hacia un pasto seguro, justo antes de que la población de larvas infec-

ciosas en el pasto original alcance concentraciones peligrosamente altas. Una aplicación de nuestro modelo viene dada por el desarrollo de infección por nematodos GI en ovejas. En este caso, nuestro interés está en el parásito *Nematodirus* spp. con *Nematodirus battus*, *Nematodirus filicollis* y *Nematodirus spathiger* como sus principales especies. Las estrategias de pastoreo se definen convenientemente en términos del instante de intervención τ_0 como sigue:

Estrategia TI: *El receptor es tratado con antihelmínticos y aislado (es decir, trasladado a un área no infectada) en el instante* τ_0.

Estrategia TI+S: *El receptor es tratado con antihelmínticos y aislado en el instante* τ_0. *Al concluir el tratamiento terapéutico, el receptor es trasladado al pasto original.*

Estrategia UM: *El receptor no es tratado pero sí es trasladado a pastos seguros en el instante* τ_0.

Estrategia TS: *El receptor es tratado con antihelmínticos en el instante* τ_0 *y mantenido en el pasto original.*

Estrategia TM: *El receptor es tratado con antihelmínticos y trasladado a pastos seguros en el instante* τ_0.

Al analizar las estrategias de pastoreo, usamos procesos de nacimiento puro con catástrofes dependientes del tiempo para los instantes pre-intervención $t \in [0, \tau_0]$. Para instantes post-intervención $t \in [\tau_0, \tau]$, usamos procesos de muerte pura con catástrofes para los casos TI y TI+S, procesos de nacimiento puro con catástrofes en el caso UM, y procesos de nacimiento y muerte con catástrofes para los casos TS y TM. Al igual que en los trabajos de Herbert e Isham [9], e Isham [12], es posible obtener resultados algebraicos exactos. En particular, en el caso de los procesos de nacimiento puro y de muerte pura con catástrofes, la solución transitoria es derivada iterativamente en términos de expresiones integrales sencillas. Por el contrario, el sistema lineal de ecuaciones diferenciales dependientes del tiempo referido a las estrategias TS y TM es resuelto mediante las técnicas *splitting* de Strang-Marchuk [8, Sección 1.3], que implican resolver cuatro subsistemas dependientes del tiempo de forma cíclica en intervalos sucesivos de longitud suficientemente pequeña, usando la solución de un subsistema como condición inicial del siguiente.

En nuestra aplicación, construimos un modelo matemático en términos de niveles de infección. Los resultados obtenidos están relacionados con el estudio desarrollado por Uriarte y otros [20], que se centra en la descripción de las fluctuaciones mensuales en la carga de nematodos en ovejas en el Valle del Ebro (España), mediante el uso de corderos indicadores y la monitorización de la excreción de huevos en las heces. Los datos empíricos de [20] son combinados de manera apropiada con aquéllos obtenidos en [15] concernientes a la eficacia clínica de tres antihelmínticos (*ivermectin*, *fenbendazole* y *albendazole*) en corderos infectados por nematodos.

Bibliografía

1. Artalejo JR, Gómez-Corral A (2010) A state-dependent Markov-modulated mechanism for generating events and stochastic models. Mathematical Methods in the Applied Sciences 33:1342-1349.
2. Artalejo JR, Gómez-Corral A, He QM (2010) Markovian arrivals in stochastic modelling: a survey and some new results. SORT - Statistics and Operations Research Transactions 34:101-144.
3. Bailey NTJ (1975) The mathematical theory of infectious diseases, second edition. Griffin, London.
4. Barger IA (1997) Control by management. Veterinary Parasitology 72:493-506.
5. Barger IA (1999) The role of epidemiological knowledge and grazing management for helminth control in small ruminants. International Journal for Parasitology 29:41-47.
6. Eysker M, Bakker N, Kooyman FNJ, Ploeger HW (2005) The possibilities and limitations of evasive grazing as a control measure for parasitic gastroenteritis in small ruminants in temperate climates. Veterinary Parasitology 129:95-104.
7. Eysker M, Bakker N, Kooyman FNJ, van der Linden D, Schrama C, Ploeger HW (2005) Consequences of the unusually warm and dry summer of 2003 in The Netherlands: poor development of free living stages, normal survival of infective

larvae and long survival of adult gastrointestinal nematodes of sheep. Veterinary Parasitology 133:313-321.
8. Faragó I, Havasi A, Horváth R (2011) On the order of operator splitting methods for time-dependent linear systems of differential equations. International Journal of Numerical Analysis and Modeling, Series B 2:142-154.
9. Herbert J, Isham V (2000) Stochastic host-parasite interaction models. Journal of Mathematical Biology 40:343-371.
10. Hitchcock SE (1986) Extinction probabilities in predator-prey models. Journal of Applied Probability 23:1-13.
11. Iglehart DL (1964) Multivariate competition processes. The Annals of Mathematical Statistics 35:350-361.
12. Isham V (1995) Stochastic models of host-macroparasite interaction. The Annals of Applied Probability 5:720-740.
13. Latouche G, Ramaswami V (1999) Introduction to matrix analytic methods in stochastic modeling. ASA-SIAM Series on Statistics and Applied Probability, Philadelphia.
14. Michel JF (1985) Strategies for the use of anthelmintics in livestock and their implications for the development of drug resistance. Parasitology 90:621-628.
15. Nasreen S, Jeelani G, Sheikh FD (2007) Efficacy of different anthelmintics against gastro-intestinal nematodes of sheep in Kashmir Valley. VetScan 2, No. 1, article 13.
16. Neuts MF (1994) Matrix-geometric solutions in stochastic models: an algorithmic approach, second edition. Dover Publications, New York.
17. Reuter GEH (1961) Competition processes. In: Neyman J (ed) Proceedings of the fourth Berkeley symposium on mathematical statistics and probability, volume II: contributions to probability theory. University of California Press, Berkeley, pp. 421-430.
18. Ridler-Rowe CJ (1978) On competition between two species. Journal of Applied Probability 15:457-465.
19. Ridler-Rowe CJ (1988) Extinction times for certain predator-prey processes. Journal of Applied Probability 25:612-616.
20. Uriarte J, Llorente MM, Valderrábano J (2003) Seasonal changes of gastrointestinal nematode burden in sheep under an intensive grazing system. Veterinary Parasitology 118:79-92.

21. White KAJ, Grenfell BT, Hendry RJ, Lejeune O, Murray JD (1996) Effect of seasonal host reproduction on host-macroparasite dynamics. Mathematical Biosciences 137:79-99.